Three-Flavor Color Superconductivity

vom Fachbereich Physik der Johann Wolfgang Goethe–Universität
als Dissertation angenommen.

Dekan: Prof. Dr. W. Aßmus

Gutachter: Prof. Dr. D.-H. Rischke, Prof. Dr. Adrian Dumitru

Datum der Disputation: Dezember 7, 2007.

Acknowledgements

I would like to express my special thanks to Prof. Dirk Rischke for all the generous supports that during my Ph.D thesis he gave mentally and practically to me. I learned a lot of things from him which will be certainly very useful for me in future as well. Without his helps and encouragements it would be difficult to come to the end of this thesis. Thank you Dirk!

I am also very grateful to Prof. Igor Shovkovy for very instructive discussions we had. He was the one who taught this stimulating field to me. Also, I had a lot of fun with him during lunch breaks and in other occasions.

Since I wanted to take ten watermelons with my tow hands, I needed to work harder. On other words, along my Ph.D thesis, I wanted to work on other fields as well, although the project were not published. I had great times when I was collaborating with Prof. Adrian Dumitru and Prof. Michael Strickland. I thank both of you for teaching me those fascinating topics. I also had a wonderful chance to talk to Prof. Robert Pisarski. I thank him as the person who encouraged me to continue working on this field and also as one of my referees. His kindness is very special.

I also thank Stefan Ruester, Andreas Schmitt, and Qun Wang for very fruitful discussions and collaborations. I always had great times with Andreas in many conferences, lots of joke and fun. Looking forward for other conferences.

I thank all my dear friends with whom I had always fun. Phillip Reuter for the time we shared the office, which were full of jokes and sometimes discussions. I thank him that gave me good times during lunches break, without his unique humor, which worked as a tasty sauce, it was impossible to enjoy German food in the Mensa. Thank you man! Additionally, my thanks go to Amir Haghighirad for his truly friendship, Jacquelyn Hostler for her kindness, Benjamin Koch for his unfinishable nice humor, Gregor Kaczor for repeating the timeless jokes which were sometimes very funny, Sophie Nahrwold with whom I hanged out anytime I wanted to, Jorge Noronha for funny times, imitating everybody starting from me and ending to Prof. Stöcker, Basil Sa'd for showing the cool side of life, and Nan Su for exhibiting the exciting part of life.

My thanks also go to the scientific administrator Dr. Joachim Reinhardt, to the system administrators Alexander Achenbach, and Gebhard Zeeb, to the secretaries Mrs. Walburga Bergmann, Mrs. Veronika Palade, Mrs. Laura Quist, and Mrs. Daniela Radulescu and to Joe Laperal-Gomez for their support.

My innumerable thanks of course are for my family. Maman, Baba, Roya, Lida, va Vida mamnun be khatere hame chiz.

I thank Frankfurt International Graduate School for Sciences for the financial supports.

Abstract

I investigate some of the inert phases in three-flavor, spin-zero color-superconducting quark matter: the CFL phase (the analogue of the B phase in superfluid ^{3}He), the A and A* phases, and the 2SC and sSC phases. I compute the pressure of these phases with and without the neutrality condition. Without the neutrality condition, after the CFL phase the sSC phase is the dominant phase. However, including the neutrality condition, the CFL phase is again the energetically favored phase except for a small region of intermediate densities where the 2SC/A* phase is favored. It is shown that the 2SC phase is identical to the A* phase up to a color rotation. In addition, I calculate the self-energies and the spectral densities of longitudinal and transverse gluons at zero temperature in color-superconducting quark matter in the CFL phase. I find a collective excitation, a plasmon, at energies smaller than two times the gap parameter and momenta smaller than about eight times the gap. The dispersion relation of this mode exhibits a minimum at some nonzero value of momentum, indicating a van Hove singularity.

Kurzfassung

In dieser Arbeit werden verschiedene inerte Phasen von Quarkmaterie mit drei verschiedenen Quarkarten (flavors) die sich in einem farbsupraleitenden Zustand mit Spin null befinden untersucht. Insbesondere werden die CFL Phase, die A, die A*, die 2SC und die sSC Phasen studiert. Für diese Phasen wird der Druck sowohl ohne eine Neutralitätsbedingung als auch mit einer Neutralitätsbedingung errechnet. Es zeigt sich, dass ohne die eine Neutralitätsbedingung die CFL und die sSC Phasen dominieren. Berücksichtigt man jedoch die Neutralität der Quarkmaterie, wird meist die CFL Phase energetisch favorisiert. Lediglich für eine kleine Teilmenge des Parameterraumes bei mittelgroßen Dichten sind die 2SC und die A* Phasen energetisch favorisiert. Es wird gezeigt, dass sich die 2SC und die A* Phasen abgesehen von einem konstanten Farbfaktor gleichen. Anschließend werden für die CFL Phase die Selbstenergien und spektralen Energiedichten longitudinaler und transversaler Gluonen bei einer Temperatur $T = 0$ in farbsupraleitender Quarkmaterie berechnet. Bei Energien, die kleiner sind als der doppelte Lückenparameter (gap) und bei Impulsen die kleiner sind als das Achtfache des Lückenparameters zeigt es sich, dass es eine kollektive Anregung (Plasmon) möglich ist. Die Dispersionsrelation dieser Anregung hat ein Minimum bei endlichem Impuls, was auf eine van Hove Singularität hinweist.

Contents

List of Figures

11

List of Tables

Chapter 1

Introduction

1.1 Superconductivity

Superconductivity was discovered in 1911 at Leiden laboratory. While studying the temperature dependence of the electric resistivity of mercury, H. Kamerlingh-Onnes realized that at a temperature T_c in the vicinity of $4K$ the resistance of the sample dropped suddenly to zero and remained immeasurable at all attainable temperatures below T_c (critical temperature) [1]. As the temperature decreased, the resistance disappeared instantly rather than gradually. Clearly the sample had undergone a transformation into a novel, as yet unknown, state characterised by zero electrical resistance. This phenomenon was named "superconductivity". On the other hand, it was found that superconductivity can be destroyed not only by heating the sample, but also by placing it in a relatively weak magnetic field, H_{cm}. Soon after the discovery of superconductivity in mercury, the same property was found in several other metals: tin, lead, indium, aluminium, niobium, and etc. Many alloys and intermetallic compounds also came out to be superconductors.

The key to the theory of superconductivity, presented by Bardeen, Cooper, and Schrieffer (BCS) in 1957 [2, 3], turned out to be the formation of "Cooper pairs", i.e., pairs of two electrons with opposite momentum k and spin projection σ, $(k \uparrow, -k \downarrow)$. These particular Cooper pairs are structureless objects, i.e., the two partners form a spin-singlet state in a relative s-wave orbital state. Cooper pairs may therefore be looked upon in a way as composite bosons, which all have the same pair wave function and are all in the same quantum-mechanical state. Hence, in this view the transition to the superconducting state corresponds to the formation of Cooper pairs that are automatically Bose-condensed; the condensate is characterised by macroscopic quantum coherence. Such a view requires some qualification, but is nevertheless very helpful for understanding many basic properties of superconductors.

While in free space an attractive force has to be sufficiently strong to bind two electrons, inside a metal the presence of the Fermi sea filled up with conducting electrons blocks the decay of a Cooper pair so that an arbitrarily small attractive interaction leads to the formation of stable Cooper pairs. The attractive interaction between the electrons of a Cooper pair in a conventional superconducting metal is due to the exchange of virtual phonons between the two electrons (electron-phonon interaction). If the phonon-mediated interaction is strong enough

to overcome the repulsive Coulomb interaction between two electrons, then, a transition into a superconducting state may occur. On the other hand, any other mechanism leading to attraction between electrons at the Fermi surface is equally well suited to cause superconductivity.

Since the total spin of a Cooper pair is zero, it represents a Bose particle and should obey Bose-Einstein statistics. Therefore, if the temperature of the system goes below T_c they can all gather at the lowest energy level. Furthermore, the larger the number of the particles that have accumulated at the ground state, the more difficult it is for one of them to leave this state. This process is called Bose condensation. All the particles in the condensate have the same wavefunction which is a function of a single spatial coordinate. The flow of such a condensate must be superfluid, that is, a dissipation-free liquid. It is not easy at all for one of the particles to be scattered by, say, an impurity atom or by any other defect of the crystal lattice. In order to become scattered, the particle would first have to overcome the resistance of the rest of the condensate. Also one should notice that the transition to the superconductivity is a virtually perfect second-order phase transition. This means that there is neither a latent heat nor a sharp finite discontinuity in the specific heat.

In the following we present some properties of superconductivity which were crucial for its development. After that we give a relatively detailed explanation on the microscopic theory of superconductivity.

1.1.1   Magnetic flux quantisation

An electric current in a superconducting ring can persist for an infinitely long time. For this phenomenon there is no need for an external power supply because the resistance of the ring is zero. As an experiment, place a ring in an external magnetic field and decrease the temperature to below T_c, where the material is a superconductor, and then switch off the magnetic field. Soon after the field is switched off, the magnetic flux through the ring decreases and according to Faraday's law of electromagnetic induction induces a current in the ring which is persistent from this moment on. The current prevents a further decrease of the magnetic flux through the ring. At a time the external magnetic field is set to zero, the current itself supports the flux through the ring at the initial level. If the ring had a finite resistance R, the flux through the ring would decay during the time of the order L/R, where L is the inductance of the ring. In a superconducting ring, since $R = 0$, it takes the flux infinite time to decay. This means that the magnetic flux becomes "frozen" while the ring carries a persistent current usually referred to as a superconducting current or a supercurrent.

At first sight it may seem that the frozen magnetic flux can have an arbitrary value. However, a number of experiments [4, 5] clarified that the magnetic flux through a hollow superconducting cylinder may only assume values that are integer multiples of $\phi = 2.07 \times 10^{-7}$ Gcm^2, which can be written as a combination of fundamental constants $\phi = \pi \hbar c / e$, where $\hbar$ is Planck's constant, c is the speed of light, and e is the electron charge [6]. This phenomenon is called flux quantization.
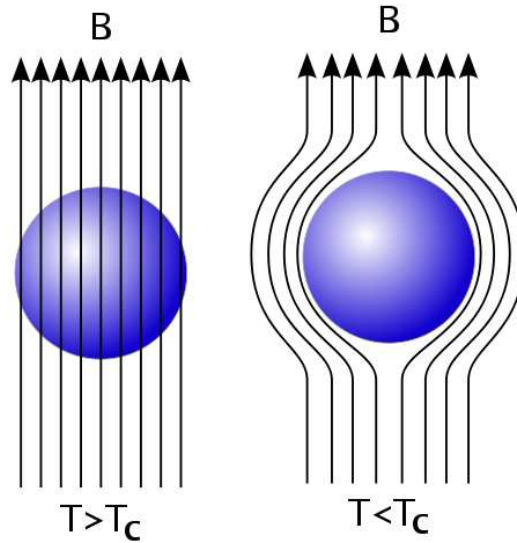
Figure 1.1: For an ideal conductor, its magnetic state at $T < T_c$, $H > 0$ depends on its history: (right) magnetic field applied to an ideal conductor at $T < T_c$; (left) field applied at $T > T_c$.

1.1.2 Meissner-Ochsenfeld effect

For 22 years after the discovery of the superconductivity, scientists believed that a superconductor was simply a form of an ideal conductor, that is, a piece of metal with zero resistance. The later studies, however, showed that this idea was not true.

Let us see what happens if we treat a superconductor as an ideal conductor. Suppose that initially an ideal conductor is cooled down below the critical temperature in zero external magnetic field. Afterwards, if an external magnetic field is switched on, from the general consideration, it is easy to show that the field does not penetrate the interior of the sample. In other words, immediately after the field penetrates the surface layer of the ideal conductor, an induced current is set up which, according to Lenz's law, generates a magnetic field in the direction opposite to that of the external field. Therefore, the total field in the interior of the specimen is zero.

The theoretical proof of the latter idea is given by Maxwell equations. As the induction **B** changes, according to

$$\nabla \times \mathbf{E} = -\frac{1}{c}\frac{\partial \mathbf{B}}{\partial t} \ , \tag{1.1}$$

an electric field **E** must be induced through the specimen. Since for an ideal conductor the resistivity is zero $\rho = 0$ and we know that $\mathbf{E} = \mathbf{j}\rho$, therefore, the electric field in the conductor must be zero $\mathbf{E} = 0$. Here **j** is the density of the induced current. The zero value for the electric field $\mathbf{E} = 0$ leads to a constant value for the induction $\mathbf{B} = \text{const}$. Taking into account that before applying the external field the induction is zero $\mathbf{B} = 0$, we arrive at $\mathbf{B} = 0$ also after the field is applied. Thus, at any point of an ideal conductor placed in an external magnetic field the induction vanishes $\mathbf{B} = 0$. However if one applies the external magnetic field to a

warm specimen $T > T_c$ and, afterwards, decreases temperature below the critical value $T < T_c$, electrodynamics predicts that the magnetic field remains inside the specimen even at the time it is in a superconducting phase. However, experiments showed that the truth in the real world is different from that in the theoretical world.

The experiment in 1933 by W. Meissner and R. Ochsenfeld revealed that at $T < T_c$ the field inside a superconducting specimen was always zero in the presence of an external field, independent of which procedure had been chosen to cool the specimen through until reaching to the superconducting state. Consequently, the zero induction can be treated as an intrinsic property of the superconducting state at $H < H_{cm}$, Fig. 1.1. In addition, it implies that we can treat a transition to the superconducting state as a phase transition and, therefore, we can apply all the might of the thermodynamic approach to examine the superconducting phase. It is now clear that the superconducting state obeys the equations

$$\rho = 0\,, \tag{1.2}$$
$$\mathbf{B} = 0\,. \tag{1.3}$$

Consequently, the Meissner effect cannot be explained by Maxwell equations for an ideal conductor.

1.1.3   London theory

The first theory that presented a successful description for the electrodynamics of superconductors was the London theory (1935) [7]. The theory introduces two equations in addition to Maxwell equations. The equations give a correct description of absolute diamagnetism and zero resistance to a DC current, which are two basic properties of a superconductor.

According to the London theory, electrons in a superconductor are a mixture of superconducting electrons n_s and normal electrons n_n. An increase in the temperature decreases the density number of the superconducting electrons n_s, so that n_s becomes zero at the critical temperature. On the other hand, at zero temperature, where the specimen is a perfect superconductor, the number density of the normal electrons is zero $n_n = 0$.

The behaviour of the superconducting component of the electronic liquid in both DC and AC electromagnetic fields can be described by the London equations. However, at the end of 1940s there was a contradiction between the London theory and the experiments. According to the London theory, the surface energy for an interface between adjacent normal and superconducting (NS) regions is negative, $\sigma_{NS} < 0$. If this accepted, the total energy of a superconductor in an external magnetic field can be decreased by turning into a mixture of alternating normal and superconducting regions. In contrast, the experiments showed that the surface energy of the interface is not negative.

The contradiction above was reconciled by a theory proposed by V. L. Ginzburg and L. D. Landau [8].

1.1.4   Ginzburg-Landau theory

The Ginzburg-Landau theory (GL) [8] introduced quantum mechanics into the theory of superconductivity. The theory considers the superconducting electrons as quantum mechanical

wavefunctions. The squared amplitude of the wavefunction $|\Psi|^2$ is proportional to n_s which is zero in the normal region, increases smoothly through the NS interface and finally reaches a certain value in the superconducting region. Therefore, the theory gives a nonzero value for the gradient of Ψ at the interface. At the same time, as it is well known from quantum mechanics, $|\nabla\Psi|^2$ is proportional to the density of the kinetic energy. Hence, by taking into account the quantum effects, the additional positive energy stored at the NS interface is regained. This leads to a positive value for the surface energy $\sigma_{NS} > 0$.

Since the theory assigns a wavefunction depending on a single spatial coordinate to the entire number of superconducting electrons, it establishes the coherent behaviour of all superconducting electrons. In quantum mechanics a single electron in the superconducting state is described by a function $\Psi(r)$. If we have n_s absolutely identical electrons and all the electrons behave coherently, it is then clear that the same wavefunction with the single parameter is sufficient to describe all of them. This idea was a breakthrough to explain the microscopic (quantum) as well as the macroscopic properties of superconductors. However, one should notice that the GL theory is based on the theory of second-order phase transitions (the Landau theory). Thus, the theory is valid only in the vicinity of the critical temperature, that is within the temperature range $T_c - T << T_c$.

Neither the London theory nor the GL theory could find a proper explanation for the superconducting electrons and everybody had to wait until 1957 for the microscopic theory of superconductivity proposed by J. Bardeen, L. Cooper, and J. Schrieffer (the BCS theory) [2]. Besides, in 1958, there was an important contribution from N. N. Bogoliubov who developed a mathematical method for the superconducting theory [9]. We do not explain the Bogolyubov approach in this thesis since we are not going to make use of it.

1.1.5 Cooper instability

The concept of pair correlations in interacting Fermi systems was first introduced in 1957 by Bardeen, Cooper and Schrieffer (BCS) to provide a microscopic understanding of superconductivity [2]. The theoretical explanation of the phenomenon was missing for more than 40 years. According to the modern interpretation, the salient feature of the BCS theory is the concept of spontaneously breaking of gauge symmetry, see Sec. 1.3, or, in other words, the fact that the pair-correlated state is described by a complex rather than a real-valued order parameter. This is related to the appearance of a gap in the single-particle excitation spectrum. The phase rigidity of the wavefunction (or order parameter) for the pair-correlated state is responsible for the property of superconductivity or superfluidity [10].

The theory is as follows. Consider a system of N non-interacting identical fermions of mass m and spin $1/2$ in the ground state (the "Fermi sea"). If we add two more particles, the ground state of the $N+2$ particles system is obtained by putting the two particles in the lowest available states at the Fermi energy. What happens if we now switch on an attractive interaction between the two particles added? This was answered by Cooper in 1956 [11] and became the preliminary stage for the development of the BCS theory.

The wavefunction of the system is given by an antisymmetrized product of a correlated pair wavefunction $\Phi(\vec{r}_1, \vec{r}_2; \alpha, \beta)$ and an N-particle Slater determinant describing the Fermi sea. The pair wavefunction in turn is a product of the centre-of-mass plane wave, the wavefunction

describing the relative motion $\psi(\vec{r}_1 - \vec{r}_2)$, and the spin function $\chi(\alpha, \beta)$

$$\Phi(\vec{r}_1, \vec{r}_2; \alpha, \beta) = \exp[\frac{1}{2}\mathrm{i}\,\vec{p}\cdot(\vec{r}_1 + \vec{r}_2)]\,\psi(\vec{r}_1 - \vec{r}_2)\,\chi(\alpha, \beta) \tag{1.4}$$

The important effect of the particles in the Fermi sea is to block the single-particle states below the Fermi energy. This can be well taken into account by working in momentum space,

$$\psi(\vec{r}) = \sum_k \mathrm{e}^{\mathrm{i}\vec{k}\cdot\vec{r}}\psi_{\vec{k}} = (2\pi)^{-3}\int \mathrm{d}^3\vec{k}\,\mathrm{e}^{\mathrm{i}\vec{k}\cdot\vec{r}}\psi_{\vec{k}}\;, \tag{1.5a}$$

$$V_{\vec{k}} = \int \mathrm{d}^3\vec{k}\,\mathrm{e}^{-\mathrm{i}\vec{k}\cdot\vec{r}}V(\vec{r})\;. \tag{1.5b}$$

Defining the quasiparticle energy

$$\xi_{\vec{k}} = \frac{\hbar^2 k^2}{2m} - \mu\;, \tag{1.6}$$

where μ is the chemical potential, the Schrödinger equation for the paired particles takes the form

$$(\xi_{\vec{k}+\vec{p}/2} + \xi_{\vec{k}-\vec{p}/2} - E)\psi_{\vec{k}} = -(2\pi)^{-3}\int_{\vec{k}' > \vec{k}_{\mathrm{F}}} \mathrm{d}^3\vec{k}'\,V_{\vec{k}-\vec{k}'}\psi_{\vec{k}'}\;. \tag{1.7}$$

The blocking effect has been taken into account via the sum over the intermediate states k'. In the following, it is useful to measure the single-particle energies from the Fermi level. Using Eq. (1.7) the lowest energy is obtained when the two particles have equal and oppositely directed momenta. We put $\vec{p} = 0$, because nonzero $\vec{p}$ corresponds to a trivial centre-of-mass motion of the pair with momentum $\hbar\vec{p}$.

Equation (1.7) can be separated into angular-momentum components owing to the spherical symmetry assumed for the interaction potential. By expanding $V_{\vec{k}-\vec{k}'}$ and $\psi_{\vec{k}}$ in terms of Legendre polynomials $P_l(\hat{k}, \hat{k}')$ and spherical harmonics $Y_{lm}(\hat{k})$, one has

$$V_{\vec{k}-\vec{k}'} = \sum_{l=0}^{\infty} (2l + 1)\,V_l(k, k')\,P_l(\hat{k}, \hat{k}')\;, \tag{1.8a}$$

$$\psi_{\vec{k}} = \sum_{lm} a_{lm}\psi_l(k)\,Y_{lm}(\hat{k})\;. \tag{1.8b}$$

The analytic solution of Eq. (1.7) is possible by setting $V_l(k, k')$ equal to a constant within a thin shell around the Fermi surface and zero elsewhere

$$V_l(k, k') = \begin{cases} V_l & (|\xi_{\vec{k}}|, |\xi_{\vec{k}'}| \leq \epsilon_{\mathrm{c}} \ll \epsilon_{\mathrm{F}})\;, \\ 0 & \text{otherwise}\;. \end{cases} \tag{1.9a}$$

Afterwards, Eq. (1.7) can be written in a relatively simple form,

$$(2\xi_{\vec{k}} - E)\psi_l(k) = -V_l\,N(0)\int_0^{\epsilon_{\mathrm{c}}} \psi_l(k')\,\mathrm{d}\xi_{\vec{k}'}\;, \tag{1.10}$$

where the density of states (for one spin species) $N(0)$ has been taken out of the integral. We see that Eq. (1.10) has essentially the same form as the Schrödinger equation for two particles in

two spatial dimensions. This is due to the fact that the effective density of the states is nonzero (and constant) above the Fermi energy and zero below, as exactly as in the case of the scattering of two particles in two dimensions. Inspecting Eq. (1.10), it becomes clear that for an attractive interaction ($V_l < 0$) the energy eigenvalue E is necessarily negative. Therefore, in the presence of the Fermi sea, the two particles form a bound state for arbitrarily weak attractive interaction. The bound state is formed with a relative orbital angular momentum l corresponding to the strongest attractive interaction parameter V_l. The correlated pair is called a "Cooper pair".

Cooper's problem is in contrast with the two-particle problem without blocking effect, where a bound state is formed only if the potential is sufficiently attractive,

$$\int |V(\vec{r})|^{3/2} \, \mathrm{d}^3\vec{r} > \frac{\pi^2}{4} \left(\frac{3\hbar^2}{2m} \right)^{3/2} \;, \tag{1.11}$$

and the lowest bound state is always an s-state.

1.1.6   BCS theory

If the formation of a bound pair is energetically advantageous in Cooper's problem, and if all particles interact with each other, the formation of the correlated pairs of particles with momenta $(\hbar b\vec{f}k, -\hbar b\vec{f}k)$ is still profitable. Then, it is expected that all particles in the vicinity of the Fermi surface should form pairs of some kind in order to lower the total energy. In order to minimise the system energy, it is believed that the particles all form identical pairs with the largest binding energy; just like the Bose-Einstein condensation in a Bose system. This idea led Bardeen *et al.* to postulate a correlated wavefunction $|\psi>$ for electrons in superconductors that is an antisymmetrized product of the pair wavefunctions [10],

$$|\psi> = \prod_k \prod_\alpha \left(u_{k\alpha\alpha} + \sum_\beta v_{k\alpha\beta} a^\dagger_{k\alpha} a^\dagger_{-k\beta} \right) |0> \;. \tag{1.12}$$

The operator $(a^\dagger_{k\alpha} a^\dagger_{-k\beta})$ acting on the vacuum state $|0>$ creates a pair of (quasi)particles in single-particle states $(\hbar b\vec{f}k, -\hbar b\vec{f}k)$. The probability amplitudes for the pair state to be occupied or empty are $v_{k\alpha\beta}$ and $u_{k\alpha\alpha}$ respectively. The state $|\psi>$ is not an eigenstate of the particle number operator N, i.e., the system is not gauge invariant. Moreover, the state $|\psi>$ is transformed under $a^\dagger_{k\alpha} \to \mathrm{e}^{\mathrm{i}\theta} a^\dagger_{k\alpha}$ into a state $|\psi(2\theta)>$. Therefore, the ground state is not unique but has a continuous degeneracy.

The Hamiltonian of the interacting quasiparticle system is given by

$$\begin{aligned}
\mathcal{H} - \mu N &= \sum_{k\alpha} \xi_{k\alpha} a^\dagger_{k\alpha} a_{k\alpha} \\
&+ \frac{1}{2} \sum_{kk'q} \sum_{\alpha\beta\alpha'\beta'} < -k\alpha, k+q\beta |V| k'\alpha', -k'+q\beta' > a^\dagger_{k'\alpha'} a^\dagger_{-k'+q\beta'} a_{-k\alpha} a_{k+q\beta} \;,
\end{aligned} \tag{1.13}$$

where $\xi_{k\alpha} = \xi_k - \alpha\mu_0 H$ for a magnetic field H and $\alpha = +1$ or -1 for spin $\uparrow$ or $\downarrow$, respectively. Within the pair wave function (1.12), only pairs with equal and opposite momenta are correlated.
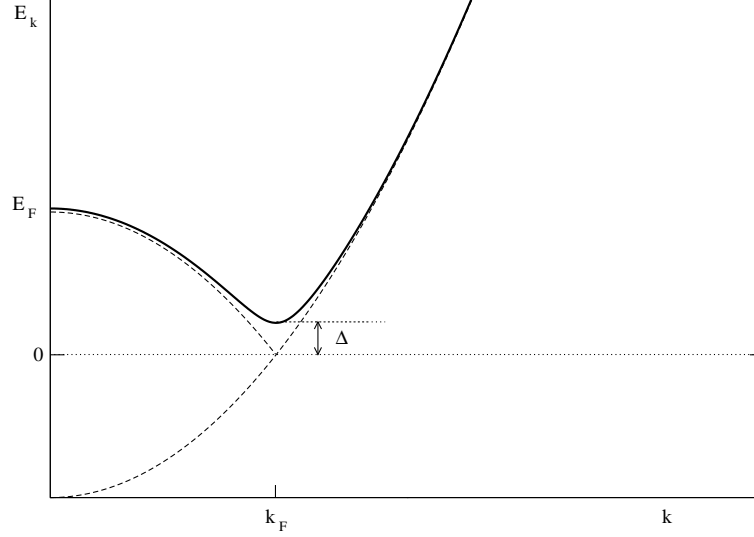
Figure 1.2: Energy spectrum of Bogoliubov quasiparticles.

The fact that the pair correlations are of dominant importance can be exploited to simplify the product of the field operators in the interaction term of Eq. (1.13). This is achieved by replacing one pair of operators, $a_k^\dagger a_{k'}^\dagger$ or $a_k a_{k'}$, by its expectation value. Thus, for a given pair, the other pairs act effectively as a kind of a mean field. The resulting mean-field Hamiltonian can be written as

$$\mathcal{H}_{MF} - \mu N = \sum_{k\alpha} \xi_{k\alpha} a_{k\alpha}^\dagger a_{k\alpha} + \frac{1}{2} \sum_{k\alpha\beta} \left(\Delta_{k\alpha\beta}^* a_{-k\beta} a_{k\alpha} + a_{k\alpha}^\dagger a_{-k\beta}^\dagger \Delta_{k\alpha\beta} - \Delta_{k\alpha\beta}^* F_{k\alpha\beta} \right) , \qquad (1.14)$$

where

$$F_{k\alpha\beta} = v_{k\alpha\beta} u_{k\beta\beta}^* = -F_{-k\beta\alpha} \qquad (1.15)$$

is referred to as the "pair amplitude". The off-diagonal energy or the off-diagonal mean-field $\Delta_{k\alpha\beta}$ is defined by

$$\Delta_{k\alpha\beta} = \sum_{k'\alpha'\beta'} <-k\alpha, k\beta|V|k'\alpha', -k'\beta'> F_{k'\alpha'\beta'} = -\Delta_{-k\beta\alpha} . \qquad (1.16)$$

The mean-field Hamiltonian (1.13) is a bilinear form in the quasiparticle field operators and can be diagonalized by a canonical transformation, i.e., the effects of the off-diagonal terms $a_{-k\beta} a_{k\alpha}$ and $a_{k\alpha}^\dagger a_{-k\beta}^\dagger$ can be absorbed into the diagonal terms [9]. After some calculation, one finally obtains

$$\mathcal{H}_{MF} - \mu N = \sum_{k\alpha} \left[\frac{1}{2} (\Delta_k \Delta_k^\dagger)_{\alpha\alpha} \left(\frac{1}{2E_{k\alpha}} - \frac{1}{\xi_{k\alpha} + E_{k\alpha}} \right) + E_{k\alpha} b_{k\alpha}^\dagger b_{k\alpha} \right] , \qquad (1.17)$$

where

$$E_{k\alpha} \;=\; \left[\, \xi_{k\alpha}^2 + (\Delta_k \Delta_k^\dagger)_{\alpha\alpha} \right]^{1/2} , \tag{1.18}$$

and

$$b_{k\alpha} \;=\; \sum_\beta (u_{k\alpha\beta} a_{k\beta} - v_{k\alpha\beta} a_{-k\beta}^\dagger) , \tag{1.19a}$$

$$b_{k\alpha}^\dagger \;=\; \sum_\beta (u_{k\alpha\beta}^* a_{k\beta}^\dagger - v_{k\alpha\beta}^* a_{-k\beta}) . \tag{1.19b}$$

As the operator $b^\dagger b$ is positive, the ground state $|\Psi\!>$ is characterised by the condition

$$b_{k\alpha}|\Psi\!>= 0 . \tag{1.20}$$

Excited states are obtained by the action of $b_{k\alpha}^\dagger$ on $|\Psi\!>$. The state defined by

$$|\Psi; k\alpha\!>= b_{k\alpha}^\dagger |\Psi\!> \tag{1.21}$$

describes a single elementary excitation, so-called Bogoliubov quasiparticle. It is a momentum eigenstate with eigenvalue $\hbar\vec{\mathbf{k}}$. From Eq. (1.17) the single-particle excitation energy is found to be

$$E_{k\alpha} = \left[\left(\frac{\hbar^2 k^2}{2m^*} - \mu \right)^2 + \sum_\beta \Delta_{k\alpha\beta} \Delta_{k\alpha\beta}^* \right]^{1/2} . \tag{1.22}$$

At the Fermi surface where $\hbar^2 k^2 / 2m^* = \mu$, the excitation energy does not tend to zero as in the normal state, but rather remains finite, i.e., the energy spectrum has a gap depending, in general, on the direction $\hat{k}$ in the momentum space. The off-diagonal mean-field $\Delta_{k\alpha\beta}$ is therefore referred to as the "gap parameter", cf. Fig. 1.2.

Until 1987 everything for superconductivity seemed to have settled down. Then the critical temperature made a quantum leap. J. Bednorz and K. A. Müller discovered the first high-T_c superconductor (LaBaCuO$_4$, T_c 40 K). Subsequently, there were found materials which raise T_c up to 130 K, e.g., HgBa$_2$Ca$_2$Cu$_3$O$_8$. The classic BCS theory failed to account for many properties of the high-T_c materials. The electron-phonon mechanism became questionable. Further studies on this hot topic, high-T_c superconductivity, are not within the scope of this thesis.

Since some phases of color superconductivity have superfluid properties, which for some part of this thesis we have made use of, in the next section we give an elementary introduction to the properties of superfluids ^{4}He and ^{3}He. For detailed studies, one can refer to many text books like [10].

1.2 Superfluidity

Superfluity is the property of a liquid flowing through capillaries without any viscosity. This is a quantum phenomenon. In classical physics, interactions of a liquid with capillary walls always

cause the liquid velocity to decrease,

$$E \equiv \frac{M\,v^2}{2} \rightarrow E' \equiv \frac{M\,v'^2}{2} < E, \;\; \text{if} \;\; v' < v \,, \tag{1.23}$$

where $E(E')$, $v(v')$ are respectively the initial (final) energy and the velocity of a liquid with a mass M. In classical physics, such a process is never forbidden by energy-momentum conservation.

In quantum physics, the situation is different. Let us consider the flow in a coordinate system moving with the liquid. The key point in the Landau consideration was that the interactions of the liquid with the walls of the capillary (moving with velocity $-v$ in this frame) cannot initiate movement of the liquid as a whole. The interaction initially lead to the appearance of "elementary excitations" in the liquid.

An elementary excitation appears with momentum $\vec{\mathbf{k}}$ and energy $\epsilon(\vec{\mathbf{k}})$. Therefore the energy E'_0 of the liquid becomes equal to $\epsilon(\vec{\mathbf{k}})$ and its momentum $\vec{\mathbf{P}}'_0 = \vec{\mathbf{k}}$. Transforming the liquid onto the coordinate system where the capillary is at rest, we find

$$\begin{aligned}
E' &= E'_0 + \vec{\mathbf{P}}'_0 \cdot \vec{\mathbf{v}} + \frac{m\,v^2}{2} = \epsilon(k) + \vec{\mathbf{k}} \cdot \vec{\mathbf{v}} + E \,, \\
\vec{\mathbf{P}}'_0 &= \vec{\mathbf{k}} + M\vec{\mathbf{v}} \,.
\end{aligned} \tag{1.24}$$

Since the energy of the liquid must decrease as a result of the appearance of the elementary excitation, consequently

$$\epsilon(k) + \vec{\mathbf{k}} \cdot \vec{\mathbf{v}} \leq 0 \tag{1.25}$$

The minimum of this relation comes with antiparallel $\vec{\mathbf{k}}$ and $\vec{\mathbf{v}}$, thus,

$$v > \frac{\epsilon(k)}{k} \tag{1.26}$$

is the critical value for which superfluidity can take place; this is known as Landau criterion. Hence, superfluidity cannot be explained within classical mechanics.

As an elementary excitation in a classical liquid, one can consider a small piece of a liquid with mass $m \ll M$ and, thus, with energy $\epsilon(k) = k^2/2m$. Using Eq. (1.26), the Landau criterion is upheld at any v provided $k < 2mv$, consequently superfluidity is impossible in a classical liquid. However, one can show that an almost ideal Bose gas is superfluid [12].

Experimentally, helium-4 and hydrogen are well-known superfluids with a long history for their discovery. The existence of ^{4}He had already been established indirectly in 1871 by its characteristic line in the solar spectrum. Then in 1895 Ramsey succeeded in obtaining an actual sample of ^{4}He gas be heating the uranium ore cleveite.

In addition, there exists another rather well-known superfluid, helium-3. Since ^{3}He has spin half, it obeys Fermi-Dirac statistics. The transition of ^{3}He liquid to superfluid, which is a manifestation of Bose-Einstein condensation, is very interesting in comparison to what happens in superconductivity. The discovery and identification of the lighter isotope, ^{3}He, was only made much later by Oliphant *et al.* [13].

From a microscopic point of view, helium atoms are structureless spherical particles interacting via a two-body potential that is already well understood. The attractive part of the

potential, arising from weak van der Waals-type dipole (or higher multipole) forces, causes helium gas to condense into a liquid state at normal pressure at the temperature 3.2 K and 4.2 K for ^{3}He and ^{4}He, respectively. Decreasing the temperature one finds that the helium liquid, unlike all other known liquids, does not solidify unless a pressure around 30 bar is applied. This is the first remarkable indication of macroscopic quantum effects in this systems. The strikingly different behaviours of ^{3}He and ^{4}He at even lower temperatures come again from quantum effects. Whereas ^{4}He undergoes a second-order phase transition into a superfluid phase, no such transition is observed in liquid ^{3}He at the same temperature range. It is only at the temperature roughly one thousandth of the transition temperature of ^{4}He that ^{3}He also becomes superfluid. At this stage, there are several superfluid phases, each of which has a much more complex structure than that of superfluid ^{4}He.

Given the success of the BCS theory to explain superconductivity, it was rational to ask whether a similar mechanism works for ^{3}He. Since there is no underlying crystal lattice in the liquid that can mediate the attractive force, the attraction must be an intrinsic property of one-component ^{3}He liquid itself. The main feature of the interatomic ^{3}He potential is the strong repulsive component at short distances, and the weak van der Waals attraction at medium and long distances. It soon became clear that, in order to avoid the hard repulsive core and thus make optimal use of the attractive part of the potential, ^{3}He atoms have to form Cooper pairs in a state of nonzero relative angular momentum l. In this case the Cooper-pair wave function vanishes at zero relative distance, thus cutting out the most strongly repulsive part of the potential. In a pair revolving about the centre of gravity, the atoms are kept away from each other by the centrifugal force. After this, everything was similar to that of the theory of superconductivity. There is an attractive force between the fermions and decreasing the temperature there must be a Bose condensation.

There were plenty of failed theories to estimate the transition temperature for Cooper pairs with large relative angular-momentum quantum number, bound by the long-range tail of the van der Waals attraction. As more experimental data on liquid ^{3}He became available, it was soon realized that the system is a strongly interacting system. The entities forming the Cooper pairs are not the bare ^{3}He atoms but are rather the quasiparticles of Landau's theory. These quasiparticles are single-particle excitations, which are sometimes viewed as particles surrounded by a polarised cloud of other particles. In fact, the effective mass of each quasiparticle may be as much as six times the bare atomic mass. Similarly, the interaction between quasiparticles was found to be very strong. It is then not surprising that the bare atomic potential bears little resemblance to the effective quasiparticle potential.

Furthermore, it is interesting to know that the property of superfluidity was indeed first discovered experimentally in a Fermi system [14]. The superfluidity of ^{4}He was found more than 25 years later.

1.2.1   Quasiparticle concept

The quasiparticle concept was used for the first time to describe the low-energy properties of an interacting many-body system. A quasiparticle is a type of low-lying excited state of the system that is known as an elementary excitation. In other words, most of the low-lying excited states can be viewed as states in which multiple quasiparticles are present. It turns out that the

interactions between quasiparticles becomes negligible at sufficiently low temperatures, in which case we can obtain a great amount of information about the system as a whole, including the flow properties and heat capacity, by investigating the properties of individual quasiparticles.

The energy eigenstates of the noninteracting (spin $\frac{1}{2}$) Fermi gas are specified by the number of particles $N_{\mathbf{p}\alpha}(= 0, 1)$ in each of the single-particle states with momentum $\hbar\mathbf{p}$ and spin projection σ. In order to describe macroscopic properties, it is sufficient to introduce a smoothed distribution function $n_{\mathbf{p}\alpha}$ $(0 \leq n_{\mathbf{p}\alpha} \leq 1)$ in place of the highly discontinuous occupation number $N_{\mathbf{p}\alpha}$ by averaging $N_{\mathbf{p}\alpha}$ over a group of neighbouring states. In the ground state all single-particle states with momentum less than the Fermi momentum $\hbar p_F$ are occupied, $(n_{\mathbf{p}\alpha} = 1)$, and all other states are empty, $(n_{\mathbf{p}\alpha} = 0)$. Employing the periodic boundary condition in a unit volume, p_F is related to the particle density n by

$$n = \sum_{\mathbf{k}\alpha} n_{\mathbf{k}\alpha} = \frac{p_F^3}{3\pi^2} \ . \tag{1.27}$$

Let us assume that the interaction between the particles is turned on adiabatically. In this case, if the single-particle energy spectrum of the interacting system is in one-to-one correspondence with the Fermi-gas spectrum and if the ground state has the full symmetry of the Hamiltonian, then the system is referred to as "normal". In contrast, in a superfluid state the mentioned one-to-one correspondence does not exist, owing to the condensation of degrees of freedom into a macroscopic quantum state. Obviously the state of a normal Fermi liquid is still completely characterised by the distribution function $n_{\mathbf{p}\alpha}$ of the corresponding noninteracting system. This is true at least as long as any collective excitations that are introduced by the interaction are negligible. The elementary excitations of a normal Fermi-liquid correspond to the particle and hole excitations of the perfect Fermi gas and are referred to as "quasiparticles" and "quasiholes" [10].

In this thesis the quasiparticle concept as the basis of the Fermi liquid is used to describe the weakly interacting quark matter.

1.2.2   Fermi liquids

In the temperature range from well below the Fermi temperature $T_F (\approx 1K)$ down to the transition temperature T_c of the superfluid phases, the properties of liquid ^{3}He can be described by so called Landau-Fermi liquid model. Starting from the perfect gas, this model introduces the effects of the interactions between the atoms in phenomenological way [15]. It is based on the concept of elementary excitations, according to which the low-energy properties of an interacting many-body system can be described in terms of a rarefied gas of elementary excitations or "quasiparticles". After all, in liquid ^{3}He the interparticle distance is of the same order as the range of the interatomic potential, and therefore interaction effects between the hard-sphere atoms are expected to be very important.

As will become clear in Sec.1.4, according to asymptotic freedom [16, 17], the force between quarks becomes arbitrarily weak as the characteristic momentum scale of their interaction grows larger. Therefore, at sufficiently high densities and low temperatures, matter will consist of a Fermi sea of essentially free quarks whose behaviour is dominated by the freest of them all: the

high-momentum quarks that live at the Fermi surface. In consequence, it is relevant for us to study the Fermi liquid in more details.

The Lagrangian for a non-relativistic fermionic system with short-range interactions is introduced as

$$\mathcal{L}_0 = \psi^\dagger \left(i\partial_0 + \frac{\nabla^2}{2m} \right) \psi - \frac{C_0}{2} \left(\psi^\dagger \psi \right)^2 \;, \tag{1.28}$$

where the coupling constant C_0 is related to the scattering length, $C_0 = 4\pi a/m$, $C_0 > 0$ corresponds to a repulsive interaction, and $C_0 < 0$ to an attractive interaction. Since the Lagrangian is invariant under the $U(1)$ transformation $\psi \to e^{i\phi}\psi$, the fermion number

$$N = \int d^3x \, \psi^\dagger \psi \tag{1.29}$$

is conserved. At nonzero density we use the grand canonical partition function,

$$Z(\mu, \beta) = \text{Tr} \left[e^{-\beta(H-\mu N)} \right] \;, \tag{1.30}$$

where μ is the chemical potential conjugated to the fermion number N, H is the Hamiltonian associated with the Lagrangian $\mathcal{L}$, and $\beta = 1/T$. The trace runs over all possible states of the system. At zero temperature, the chemical potential is by definition the energy required to add or remove a particle from the system. In order to write the partition function as a time evolution operator, it is sufficient to replace β with it,

$$Z = \int D\psi D\psi^\dagger \exp \left(- \int_0^\beta d\tau \int d^3x \, \mathcal{L}_E \right) \;, \tag{1.31}$$

where we have also absorbed the chemical potential into the Lagrangian,

$$\mathcal{L}_E = \psi^\dagger \left(\partial_\tau - \mu - \frac{\nabla^2}{2m} \right) \psi + \frac{C_0}{2} \left(\psi^\dagger \psi \right)^2 . \tag{1.32}$$

From Eq. (1.32), the fermion propagator reads

$$S^0_{\alpha\beta}(p) = \frac{\delta_{\alpha\beta}}{ip_4 + \mu - \vec{p}^2/2m}, \tag{1.33}$$

where α and β are spin labels. Then one can write the fermion propagator in Minkowskian space as

$$S^0_{\alpha\beta}(p) = \frac{\delta_{\alpha\beta}}{p_0 - \epsilon_p + i\delta \text{sgn}(\epsilon_p)} = \delta_{\alpha\beta} \left\{ \frac{\Theta(p - p_F)}{p_0 - \epsilon_p + i\delta} + \frac{\Theta(p_F - p)}{p_0 - \epsilon_p - i\delta} \right\}, \tag{1.34}$$

where $\epsilon_p = E_p - \mu$, $E_p = \vec{p}^2/(2m)$ and $\delta \to 0^+$. The surface defined by $p_F = \sqrt{2m\mu}$ is called the Fermi surface. The Θ functions in Eq. (1.34) determine the occupied or the empty states at zero temperature and nonzero density. All states with $p < p_F$ are occupied, while all states with $p > p_F$ are empty. The excitations happen either for particles above the Fermi surface, $p > p_F$, or for holes below the Fermi surface, $p < p_F$. Using the particle density defined by

$$\rho = \langle \psi^\dagger \psi \rangle = \int \frac{d^4p}{(2\pi)^4} S^0_{\alpha\alpha}(p) \, e^{ip_0\eta} \Big|_{\eta \to 0^+} = 2 \int \frac{d^3p}{(2\pi)^3} \Theta(p_F - p) = \frac{p_F^3}{3\pi^2} \;, \tag{1.35}$$

a)   b)   c)

$$p_F^5 \qquad\qquad p_F^5\,(p_Fa) \qquad\qquad\qquad p_F^5\,(p_Fa)^2$$
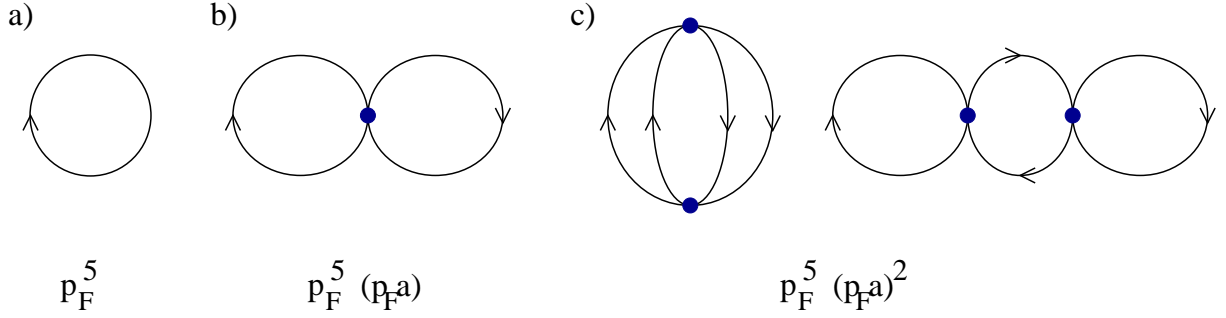
Figure 1.3: Leading-order Feynman diagrams for the ground state energy of a dilute gas of fermions interacting via a short range potential [18].

the energy density as a function of the fermion density for free fermions is found to be

$$\mathcal{E} = 2 \int \frac{d^3p}{(2\pi)^3} E_p \Theta(p_F - p) = \frac{3}{5}\, \rho\, \frac{p_F^2}{2m}\ . \tag{1.36}$$

With this expression we can compute the first correction to the ground state due to the interaction $\frac{1}{4}C_0(\psi^\dagger\psi)^2$, which is a two-loop diagram with one insertion of C_0, Fig. 1.3,

$$\mathcal{E}_1 = C_0 \left(\frac{p_F^3}{6\pi^2} \right)^2 . \tag{1.37}$$

Adding up the first two terms in the energy density, we have

$$\mathcal{E} = \rho\frac{p_F^2}{2m} \left(\frac{3}{5} + \frac{2}{3\pi}(p_Fa) + \dots \right), \tag{1.38}$$

where a is the hard-sphere diameter which can be looked upon as the scattering length. Comparing the second term in (1.38) with what we have already found in Eq.(1.37) indicates that C_0 is the first term in an expansion in p_Fa which is an small value for a dilute, weakly interacting Fermi gas [19, 20]. Using the effective Lagrangian, one can also derive the fermion propagator near the Fermi surface,

$$S_{\alpha\beta} = \frac{Z\delta_{\alpha\beta}}{p_0 - v_F(|\vec{p}| - p_F) + i\delta\mathrm{sgn}(|\vec{p}| - p_F)}. \tag{1.39}$$

Here Z is the wavefunction renormalization and $v_F = p_F/m^*$ is the Fermi velocity. Z and m^* can be worked out order by order in (p_Fa), see Ref. [21, 22]. It is interesting to note that even taking the interactions into account, the structure of the propagator is unchanged. The low energy excitations are quasi-particles and holes, and near the Fermi surface the lifetime of a quasi-particle is infinite. This is the basis of Fermi-liquid theory. We should however note that for nuclear systems the (p_Fa) expansion is not particularly useful since the nucleon-nucleon scattering length is very large. It is worthwhile to mention that Eq. (1.38) is of interest for trapped dilute Fermi gases.

1.2.3 Order parameter

In general, the order parameter is a quantity used to distinguish between two different states of a matter. By definition, it has a nonzero value below T_c and is zero above T_c. The phase transition to the normal liquid is of second order. The more common example of such a phase transition is the transition from a paramagnetic to a ferromagnetic state of a metal when cooled below the Curie temperature. In the paramagnetic state, for $T > T_c$, the spins of the particles point randomly in all possible directions. Below the transition temperature $T < T_c$, where we have a ferromagnetic state, the spins are more or less perfectly aligned.

There are different ways to specify an order parameter for a phenomenon. For the above mentioned example, the transition from a paramagnetic state to a ferromagnetic state, one can define the average spin $< \mathbf{S} >$ as an order parameter. In the paramagnetic phase the ground state of the system is left unchanged if all spins are rotated with the same angle around a single axis; it is invariant under spin rotations. In the ferromagnetic state, below T_c, this is no longer true. In this case a rotation of all spins leads to a perceptible change in the ground state. Since the original symmetry of the system is broken by the system itself without any external influence, it is said that the symmetry is "spontaneously broken". Note that at this stage the system is not able to pick out any particular preferred direction, it is yet undetermined. Therefore the average spin $< \mathbf{S} >$, when taken over many ensembles, is still zero as in the paramagnetic state. This implies that the ground state of the system is degenerate, i.e., it costs no energy to turn all the spins into some direction. This prepares the ground for a collective excitation of the spins in the ferromagnetic state with energy $\hbar\omega = 0$ and a wavevector $\mathbf{q} = 0$, which rotates all the spins. In any system that has experienced continuous global symmetry breaking, such a mode is called a "Goldstone mode". In the case of short-range interactions, there is, in such a system, a gapless spin-zero excitation, a so-called "Goldstone boson". Hence, in a ferromagnetic system, the Goldstone mode is a spin wave connected with the spontaneously broken spin-rotation symmetry.

In the ferromagnetic state, the degeneracy of the system can be destroyed by the influence of even infinitesimally small effects that lack the symmetry under spin rotation, for example due to the interaction in the system or via an external magnetic field. In this case the Goldstone mode will no longer be a $\omega = 0$ mode but will acquire an energy gap proportional to the coupling strength of the interaction. Once a preferred direction has been chosen, the average $< \mathbf{S} >$ is no longer zero and the system has a nonzero magnetisation $\mathbf{M} \propto < \mathbf{S} >$. Therefore we can choose $\mathbf{M}$ as the order parameter of the system, which is zero above T_c and nonzero below T_c.

The same concept applies to a pair-correlated state, i.e., to superconductors and the superfluid ^{3}He. In these cases the new order parameter is associated with the formation of Cooper pairs below the critical temperature T_c. In analogy to ferromagnets this order parameter may be expressed mathematically by introducing a correlation function which involves two Cooper pairs (CP) at position $\mathbf{r}$ and $\mathbf{r}'$, respectively,

$$C^{\mathrm{CP,CP}}(\mathbf{r} - \mathbf{r}') = < \psi_\uparrow^+(\mathbf{r})\psi_\downarrow^+(\mathbf{r})\psi_\downarrow(\mathbf{r}')\psi_\uparrow(\mathbf{r}') > , \qquad (1.40)$$

with the creation and annihilation operators, $\psi_\sigma^+(\mathbf{r})$ and $\psi_\sigma(\mathbf{r})$, respectively, for an electron with spin σ at position $\mathbf{r}$. In the superconducting state the correlation function is nonzero even at

infinite separation limit

$$\lim_{|\mathbf{r}-\mathbf{r}'|\to\infty} C^{\mathrm{CP,CP}}(\mathbf{r}-\mathbf{r}') \neq 0. \tag{1.41}$$

This is in contrast to the normal state, where this quantity is zero. Furthermore, it shows that the off-diagonal elements of the two-particle density matrix in the position space representation have a long-range order. This is indeed the case for Bose-Einstein condensate, which is the simplest example of off-diagonal long-range order.

1.3 Spontaneous symmetry breaking

The concept of the spontaneous symmetry breaking (SSB) is very helpful to understand some quantum mechanical phenomena, e.g. superconductivity, superfluidity etc. SSB takes place when a system which is symmetric with respect to some symmetry group goes into a vacuum state that does not have the same symmetry.

As a simple example consider a ball sitting on top of a hill. The ball is in a completely symmetric state. However, the ball is not in a stable state as it can easily roll down the hill. At some point, the ball spontaneously rolls down the hill in one direction. In this case, the symmetry is broken since the ball has chosen a direction which has been singled out from other directions.

Group theory can be used very well to give a better understanding of the concept of "broken symmetry" and to formalise the connection between the order parameter structure and its symmetry. From a group-theoretical point of view, "broken symmetry" means that below the transition the lowest state of the system is no longer invariant under the full symmetry group of transformation G, as it was above the transition. Some symmetries are "broken", such that the new state is only invariant under a subgroup H of the original symmetry group G [10].

In most systems of condensed matter physics that exhibit a broken symmetry, the symmetry corresponds to rotations about an axis or three-dimensional rotations. Rotations about an axis may be described by the Abelian group $U(1)$, the unitary group of rotations about a single axis. Equivalently, they can be represented by the group $SO(2)$, the special orthogonal group of rotations in a plane with determinant $+1$, having real elements, therefore $U(1)\hat{=}SO(2)$. For example, the order parameter in a BCS superconductor is a single complex parameter $\psi = \psi_0\, e^{\mathrm{i}\phi}$ with amplitude ψ_0 and phase ϕ. Above T_c the system is invariant under an arbitrary change of the phase $\phi \to \phi'$, i.e., under a gauge transformation. The invariance is equivalent to a $U(1)$ symmetry, $G = U(1)$. Below T_c a particular value of ϕ is spontaneously preferred; the symmetry is completely broken.

In the following we explain SSB in some physical systems.

1.3.1 SSB in condensed matter

In general, SSB occurs when the action of a dynamical system is invariant under some symmetry transformation but the ground state or vacuum of the system is not assigned to a singlet representation of the symmetry group. The latter point plus the idea that in the case of SSB the group generators commute with the Hamiltonian reveal that the vacuum must be degenerate.

The Lagrangian density for an ideal Bose gas of particles with mass m is

$$\mathcal{L} = i\psi^\dagger \frac{\partial}{\partial t}\psi - \frac{1}{2m}\frac{\partial \psi^\dagger}{\partial x^i}\frac{\partial \psi}{\partial x^i} . \tag{1.42}$$

In a finite volume the solution of the Lagrangian is as follows

$$\psi(x,t) = V^{-1/2}\sum_{\mathbf{k}} a_{\mathbf{k}}\exp\left(-i\epsilon(k)t + i\mathbf{k}\cdot\mathbf{x}\right) \quad\text{with}\quad \epsilon(k) = \frac{\mathbf{k}^2}{2m} \equiv \frac{k^2}{2m} , \tag{1.43}$$

where $a_{\mathbf{k}}$ and $a_{\mathbf{k}}^\dagger$ are annihilation and creation operators with which the Hamiltonian H and the particle number operator $\hat{N}$ read

$$H = \sum_{\mathbf{k}} \epsilon(k)\, a_{\mathbf{k}}^\dagger a_{\mathbf{k}} \quad,\quad \hat{N} = \sum_{\mathbf{k}} a_{\mathbf{k}}^\dagger a_{\mathbf{k}} . \tag{1.44}$$

Since $[H, \hat{N}] = 0$, the particle number of the system is a conserved quantity.

When we study the infinite volume limit, $V \to \infty$, it is appropriate to consider the particle number density instead,

$$n = \frac{N}{V} . \tag{1.45}$$

As $V \to \infty$, fixed number density n=const requires an infinite particle number N. The symmetry that is broken by condensation is associated with particle number conservation,

$$\psi \to e^{-i\theta}\psi \quad,\quad \psi^\dagger \to e^{i\theta}\psi^\dagger . \tag{1.46}$$

Under this symmetry the Lagrangian density (1.42) is invariant. The ground state of the N-particle system

$$|N> = \frac{(a_0^\dagger)^N}{\sqrt{N!}}|0> \quad\text{where}\quad a_0^\dagger \equiv a_{\mathbf{k}}^\dagger\Big|_{\mathbf{k}=0} \tag{1.47}$$

is an eigenvalue of the operator $\hat{N}$, and therefore in the ideal Bose gas with the mentioned vacuum the $U(1)$ symmetry (1.46) is explicitly realized.

To show SSB of the system in an infinite volume we have to consider the coherent states defined by

$$|\theta>_0 \equiv \exp\left(-N/2\right)\exp\left(N^{1/2}e^{i\theta}a_0^\dagger\right)|0> . \tag{1.48}$$

With the unitary operator of the $U(1)$ symmetry

$$U_\theta = \exp\left(i\theta N\right) \tag{1.49}$$

the coherent states $|\theta>_0$ transform as

$$|\theta>_0 \to U_{\theta'}|\theta>_0 = |\theta + \theta'>_0 . \tag{1.50}$$

Since $H|\theta>_0 = 0$, all the states have the same energy $E = 0$. Furthermore, it can be shown that

$$_0<\theta|\hat{N}|\theta>_0 = N . \tag{1.51}$$

Moreover, using the Baker-Hausdorff formula,

$$\exp\left(\alpha a\right)\exp\left(\beta a^{\dagger}\right) = \exp\left(\beta a^{\dagger}\right)\exp\left(\alpha a\right)\exp\left(\alpha\beta\right), \tag{1.52}$$

and since $n = N/V$ is fixed, $|\theta >_0$-states become orthogonal,

$$_0 < \theta'|\theta >_0 = \exp\left\{N[\cos(\theta - \theta') - 1 + i\sin(\theta - \theta')]\right\}\Big|_{N\to\infty} = \delta_{\theta\theta'}. \tag{1.53}$$

Here, the important point is that all vectors from the Fock space F_θ with vacuum $|\theta >_0$ are orthogonal to vectors from the space $F_{\theta'}$, $\theta' \neq \theta$, as $V \to \infty$.

Introducing the particle number density operator $\hat{n} = \lim_{V\to\infty} \hat{N}/V$ we can calculate the dispersion of the density for the states $|\theta >_0$,

$$\begin{aligned}
\mathcal{D} &= \left[_0 < \theta|\hat{n}^2|\theta >_0 - (_0< \theta|\hat{n}|\theta >_0)^2\right]^{1/2} \\
&= V^{-1}\left[_0 < \theta|(a_0^{\dagger}a_0)^2|\theta >_0 - (_0< \theta|a_0^{\dagger}a_0|\theta >_0)^2\right]^{1/2} \\
&= V^{-1}N^{1/2} = nN^{-1/2},
\end{aligned} \tag{1.54}$$

where at $V \to \infty$ limit goes to zero. We see that the fluctuations of the density in these states are completely suppressed. In other words, in an infinite volume and with an infinite particle number, there is a continuum set of different states with the same number density n and the same energy $E = 0$.

Consequently, the transition to the Bose-Einstein condensation phase is a manifestation of the SSB phenomenon. While the Lagrangian (1.42) is invariant under the unitary transformation (1.46), the vacua $|\theta >_0$ of the system are not [12].

Now let us go one step forward and study the weakly interacting gas, $a\,n^{1/3} \ll 1$, where a is the scattering length. The Hamiltonian of the system is

$$\hat{H} = \sum_{\mathbf{k}} \frac{k^2}{2m} a_{\mathbf{k}}^{\dagger}a_{\mathbf{k}} + \frac{U_0}{2V}\sum_{\text{all }\mathbf{k}_i,\mathbf{k}_i'} \delta_{(\mathbf{k}_1+\mathbf{k}_2),(\mathbf{k}_1'+\mathbf{k}_2')} a_{\mathbf{k}_1'}^{\dagger}a_{\mathbf{k}_2'}^{\dagger}a_{\mathbf{k}_1}a_{\mathbf{k}_2}. \tag{1.55}$$

The system is almost similar to an ideal Bose gas. The vacua $|\theta >_0$ of the ideal Bose gas should be good approximations for the vacua $|\theta >$ of the Hamiltonian (1.55). Following the method used for the ideal Bose gas, the explicit representations of the vacua $|\theta >$ are of the form

$$|\theta >= \exp\left(-N/2\right)\exp\left(N_0^{1/2}e^{i\theta}a_0^{\dagger}\right)\prod_{\mathbf{k}\neq 0}(1 - L_k^2)^{1/4}\exp\left(\frac{1}{2}e^{2i\theta}L_k\,a_{\mathbf{k}}^{\dagger}a_{-\mathbf{k}}^{\dagger}\right)|0 >, \tag{1.56}$$

where

$$L_k = \frac{1}{mu^2}[\,\epsilon(k) - \frac{k^2}{2m} - mu^2\,], \tag{1.57}$$

with

$$\epsilon(k) = [\,u^2k^2 + (\frac{k^2}{2m})^2\,]^{1/2}\quad,\quad u = \left(\frac{4\pi aN}{m^2V}\right)^{1/2}. \tag{1.58}$$

The scattering length is defined as $a = mU_0/4\pi$. In addition, we have

$$N_0 = N \left[1 - \frac{8}{3} \left(\frac{Na^3}{\pi V} \right)^{1/2} \right] , \qquad (1.59)$$

where

$$a_0 = N^{1/2}e^{i\theta} \quad , \quad a_0^\dagger = N^{1/2}e^{-i\theta} . \qquad (1.60)$$

Under the unitary transformation (1.46), the vacua transform as

$$|\theta> \;\rightarrow\; U_{\theta'}|\theta> = |\theta + \theta' > \;. \qquad (1.61)$$

Therefore SSB of the $U(1)$ symmetry takes place in the system. Since U_θ commutes with the Hamiltonian, the vacua $|\theta>$ have the same energy. The degeneracy of the vacuum in this case is connected with the presence of a gapless mode with $\epsilon(k) \simeq uk$ at small k (phonon excitations). The above studied system, an almost ideal gas, can be considered as a system for a superfluid. Therefore, superconductivity can be considered as the superfluidity of a charged fermion gas or liquid. The Landau criterion (1.26) for superfluidity is applicable to superconductivity as well.

In an ideal Fermi gas, with the dispersion law $\epsilon(p) = p^2/2m$, superconductivity is impossible. Hence the phenomenon of superconductivity implies as an essential alternation the form of the spectrum in a superfluid Fermi gas [12]. The key underlying the BCS theory is the creation of an energy gap near the Fermi surface in the spectrum of one-fermion excitations. The gap appears as a result of the interactions of electrons with phonon. Although the presence of the gap implies the validity of the Landau criterion (1.26) for fermion excitations (if the velocity v of the fermion gas is sufficiently low), it is not sufficient to realize superconductivity. In fact, an energy gap is present on the electron spectrum of an insulator in which there is even no electric conductivity. *The essence of superconductivity is the generation of the superconducting gap which is related to the spontaneous (dynamical) breakdown of the $U(1)$ gauge symmetry that generates the superconducting current analogous to the superfluid current.*

1.3.2 SSB in relativistic quantum field theory

We consider a relativistic system at zero temperature and zero particle density. One might think of such a system as an *empty* state containing *nothing*. This view is related to the idea that the vacuum must be invariant under Lorentz transformations (if one does not consider the possibility of spontaneous Lorentz symmetry breaking). At first sight it is rather unbelievable to have another *empty* medium which is the same in all Lorentz frames.

On the other hand, when the spontaneous symmetry breaking takes place, the invariance of the action is no longer the invariance of its vacuum. It is again difficult to understand how the *empty* state can have a lower symmetry than the action.

The problem was unsolved until Nambu suggested the first and most important example of SSB in particle physics - chiral symmetry breaking, intimately connected with the dynamics generating masses for elementary particles [12]. In the following we point out the most important concepts of SSB which are employed in this thesis.

1.3.3 Goldstone modes

The Goldstone model first suggested for a real scalar field with the Lagrangian density

$$\mathcal{L} = \frac{1}{2}\partial_\mu\phi\,\partial^\mu\phi - U(\phi) , \tag{1.62}$$

where

$$U(\phi) = \frac{\mu^2}{2}\phi^2 + \frac{\lambda}{4!}\phi^4 \; ; \;\; \lambda > 0 . \tag{1.63}$$

The Lagrangian density is invariant under the discrete transformation $\phi \to -\phi$. Using Eq. (1.62) one can find the energy density of the system,

$$\mathcal{H} = \frac{1}{2}(\partial_0\,\phi)^2 + \frac{1}{2}(\nabla\phi)^2 + U(\phi) , \tag{1.64}$$

Restricting to the classical limit in which the field ϕ is a c-number field implies that a solution with the lowest energy density must be x-independent, i.e., $\phi = $ const.. In this case

$$\mathcal{H} = U(\phi) , \tag{1.65}$$

so that the field ϕ for which the potential assumes extrema is calculated via

$$\frac{dU}{d\phi} = \mu^2\phi + \frac{\lambda}{6}\phi^3 = 0 . \tag{1.66}$$

When $\mu^2 > 0$, the potential $U(\phi)$ has only one minimum at $\phi = 0$. On the other hand, when $\mu^2 < 0$, the form of the potential changes drastically, cf. Fig. 1.4. In this case the trivial solution $\phi = 0$ corresponds to its maximum and there are two nontrivial solutions corresponding to the two minima

$$\phi = \pm\left(-\frac{6\mu^2}{\lambda}\right)^{1/2} \equiv \pm v . \tag{1.67}$$

The trivial solution is however invariant under the transformation, $\phi \to -\phi$. Note that when $\mu^2 > 0$, the discrete symmetry is the symmetry both of the action and of the vacuum solution. Instead, when $\mu^2 < 0$, the solution is not invariant under the transformation above,

$$\phi_+ \equiv \left(-\frac{6\mu^2}{\lambda}\right)^{1/2} \;\; , \;\;\; \phi_- \equiv -\left(-\frac{6\mu^2}{\lambda}\right)^{1/2} . \tag{1.68}$$

In this case the symmetry of the vacuum solution is lower than the symmetry of the action. Therefore the spontaneous breakdown of the discrete symmetry takes place. Since the Hamiltonian of the system is invariant under the stated transformation, the energy density is the same

$$\mathcal{H}(\phi_\pm) = -3\mu^4/2\lambda , \tag{1.69}$$

hence the vacua ϕ_+ and ϕ_- are degenerate.

The mass of the field ϕ in the case $\mu^2 > 0$ is μ. To find the mass in the other case, $\mu^2 < 0$, we have to introduce a new field,

$$\phi' = \phi - v , \tag{1.70}$$
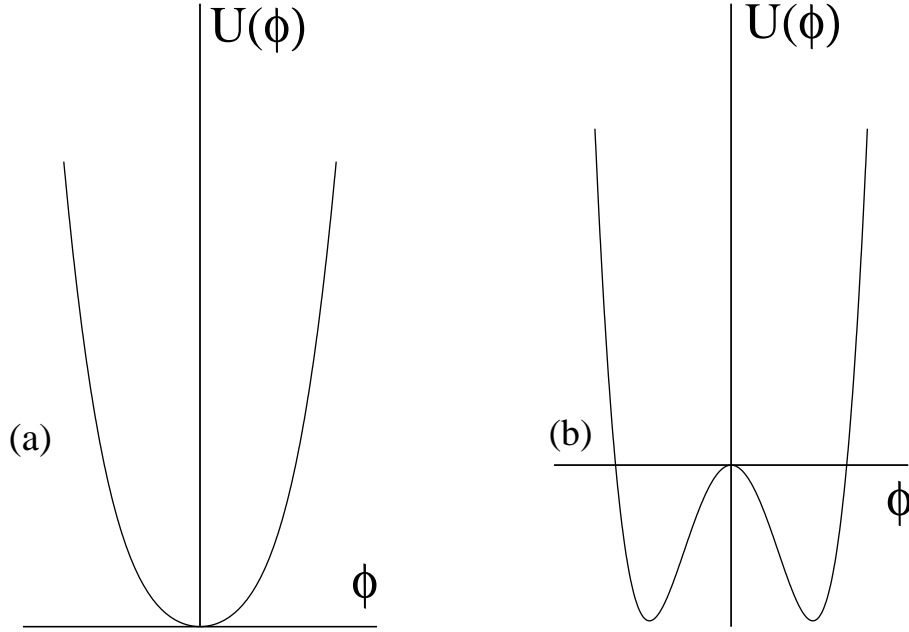
Figure 1.4: Potential $U(\phi)$ as a function of ϕ, (a) for $\mu^2 > 0$, and (b) for for $\mu^2 < 0$.

with which we have

$$U(\phi) = \frac{\lambda v^2}{6}\phi'^{\,2} + \frac{\lambda v}{6}\phi'^{\,3} + \frac{\lambda}{4!}\phi'^{\,4} - \frac{\lambda}{24}v^{\,4} \,. \tag{1.71}$$

Consequently the parameter $\lambda v^2/3$ is the mass squared of the field ϕ'.

A model for the Goldstone mode is introduced for a complex scalar field when a continuous symmetry is spontaneously broken. The Lagrangian for this case can be for instance

$$\mathcal{L} = \partial_\mu \phi^\dagger \partial^\mu \phi - U(\phi^\dagger \phi) \,, \tag{1.72}$$

where

$$U(\phi^\dagger \phi) = \mu^2 \phi^\dagger \phi + \frac{\lambda}{3!}\left(\phi^\dagger \phi\right)^2 \,. \tag{1.73}$$

Clearly the Lagrangian is invariant under the continuous $U(1)$ symmetry,

$$\phi \to \exp\left(i\theta\right)\phi \;, \quad \phi^\dagger \to \exp\left(-i\theta\right)\phi^\dagger \,. \tag{1.74}$$

Similar to the previous case, when $\mu^2 > 0$ the minimum of the potential is at $\phi = 0$, but when $\mu^2 < 0$, the minimum lies on a circle with the radius

$$2\phi^\dagger \phi = \phi_1^2 + \phi_2^2 = v^2 = -6\mu^2/\lambda \,, \tag{1.75}$$

where $\phi = (\phi_1 + \phi_2)/\sqrt{2}$. The minimum corresponds to a continuum set of degenerate vacua.

To determine the mass of the fields one shifts the fields around one particular vacuum, e.g. $(\phi_1, \phi_2) = (v, 0)$,

$$\phi_1' = \phi_1 - v \ , \quad \phi_2' = \phi_2 \ . \tag{1.76}$$

Therefore the potential is

$$U(\phi_1, \phi_2) = \frac{\lambda}{4!}(\phi_1'^{\,2} + \phi_2'^{\,2} + 2v\phi_1')^2 \ , \tag{1.77}$$

which describes two real scalar fields, ϕ_1' with mass $\mu_1 = \sqrt{\lambda v^2/3}$, and a massless field ϕ_2', $\mu_2 = 0$. One can show that there is always a massless field even if we expand around another vacuum state. The massless particles are called Nambu-Goldstone (NG) particles.

1.3.4 Higgs mechanism

The Higgs mechanism was originally proposed by the British physicist Peter Higgs based on a suggestion by Philip Anderson [23]. The theory clarifies the fate of the Goldstone model for gauge theories.

The Lagrangian density for a model when scalar fields interact with an Abelian gauge field is

$$\mathcal{L} = -\frac{1}{4}F^{\mu\nu}F_{\mu\nu} + \mathcal{L}_s\left(\phi, \phi^\dagger, D_\mu\phi, D_\mu\phi^\dagger\right) \ , \tag{1.78}$$

where

$$F_{\mu\nu} = \partial_\mu A_\nu - \partial_\nu A_\mu \ , \quad \mathcal{L}_s = D_\mu\phi^\dagger D^\mu\phi - U(\phi^\dagger, \phi) \ . \tag{1.79}$$

The covariant derivatives and the potential are defined as

$$D_\mu\phi = \partial_\mu\phi + i\,g\,A_\mu\phi \ , \quad D_\mu\phi^\dagger = \partial_\mu\phi^\dagger - i\,g\,A_\mu\phi \ , \quad U(\phi^\dagger, \phi) = \mu^2\phi^\dagger\phi + \frac{\lambda}{3!}\left(\phi^\dagger\phi\right)^2 \ ; \ \lambda \geq 0 \ , \tag{1.80}$$

and the minimum of the potential is given by

$$\phi^\dagger\phi = -\frac{3\mu^2}{\lambda} = \frac{v^2}{2} \ . \tag{1.81}$$

Rewriting the fields in terms of new variables

$$\phi = \frac{1}{\sqrt{2}}\,\rho\exp\left(i\,\theta\right) \ , \quad \phi^\dagger = \frac{1}{\sqrt{2}}\,\rho\exp\left(-i\,\theta\right) , \tag{1.82}$$

the Lagrangian density (1.78) takes a new form,

$$\begin{aligned}
\mathcal{L} =\ & -\frac{1}{4}\left(\partial_\mu A_\nu - \partial_\nu A_\mu\right)\left(\partial^\mu A^\nu - \partial^\nu A^\mu\right) + \frac{1}{2}\partial_\mu\rho'\,\partial^\mu\rho' \\
& + \frac{1}{2}(\rho' + v)^2(\partial_\mu\theta + gA_\mu)(\partial^\mu\theta + gA^\mu) - U(\rho' + v) \ ,
\end{aligned} \tag{1.83}$$

where $\rho' = \rho - v$. Obviously the Lagrangian is invariant under local $U(1)$ gauge transformations

$$\begin{aligned}
\phi &\rightarrow \exp\left(i\,\omega(x)\right)\phi \ , \quad \phi \rightarrow \exp\left(-i\,\omega(x)\right)\phi^\dagger \ , \\
A_\mu &\rightarrow A_\mu - g^{-1}\partial_\mu\omega(x) \ .
\end{aligned} \tag{1.84}$$

Under the transformation the field θ transforms as

$$\theta(x) \rightarrow \theta(x) + \omega(x) \ . \tag{1.85}$$

One can always choose a gauge in which

$$\theta(x) = 0 \ . \tag{1.86}$$

Therefore, there are a massive scalar boson with $M_{\rho'} = \sqrt{\lambda v^2/3}$ and a massive vector boson with $M_A = gv$; there is no NG boson in the spectrum.

The Lagrangian density (1.78) is the relativistic analogue of the Ginzburg-Landau model [8] in the presence of an external magnetic field. In fact, the Higgs phenomenon is the relativistic analogue of the Meissner effect in superconductors. As in the case of the Meissner effect, the Higgs mechanism can be interpreted as a transformation of the NG boson to the longitudinal component of the massive vector field.

In the non-Abelian model, there is in addition a term mixing vector fields A_μ^a and scalar fields ϕ_a' which can be, however, removed by a specific choice of the gauge. Also in this case, one can realize that NG bosons are transformed into longitudinal components of massive vector bosons [12].

1.4   Strong interactions

Historically, quantum chromodynamics (QCD) originated as a development of the quark model. In the early sixties it was established that hadrons could be classified according to the representations of what today we call flavor $SU(3)_F$ [24, 25]. This classification implied that, first of all, only a few specific representations occurred so that they built a representation of a group $SU(6)$ obtained by joining the group of spin rotations $SU(2)$ to the internal symmetry group $SU(3)_F$. However, neither for $SU(3)_F$ nor for $SU(6)$ did the fundamental representations (3 and $\bar{3}$ for $SU(3)_F$) appear to be realized in nature. This led Gell-Mann and Zweig in 1964 to postulate that physical hadrons are composite objects, made of three *quarks* (baryons) and quark-antiquark pairs (mesons). The three quarks are now widely known as the three *flavors*, u (up), d (down), and s (strange), where the first two carry the quantum number of isospin and the third strangeness. It was precisely found that only those representations of $SU(3)_F$ can occur that are obtained by reducing the products $3 \times 3 \times 3$ (baryons) or 3×3 (mesons). When the spin 1/2 of the quarks is taken into account, the $SU(6)$ scheme is completed. In addition, the mass differences of the hadrons may be understood by assuming

$$m_d - m_u \approx 4\,\mathrm{MeV} \ \ , \ \ m_s - m_d \approx 150\,\mathrm{MeV} \ , \tag{1.87}$$

together with possible electromagnetic radiative corrections. The electric charges of the quarks, in unit of the proton charge, are

$$Q_u = \frac{2}{3} \ \ , \ \ Q_d = Q_s = -\frac{1}{3} \ . \tag{1.88}$$

The idea that hadrons are composite objects was also a welcome hypothesis on another ground. For example, it was known that the magnetic moment of the proton is $\mu_p = 2.79 \times$

$e\hbar/2m_p$, instead of the value $\mu_p = e\hbar/2m$ expected if they were elementary. The values of the magnetic moments calculated with the quark model are, on the other hand, in reasonable agreement with experimental results.

These achievements led to a massive search for quarks that still goes on. As a result, c, b, and t quarks were discovered. The idea can be challenged at least on two grounds. First, the fundamental state of a composite system is the one in which all relative angular momenta vanish. Thus, the Δ^{++} resonance at relative rest had to be interpreted as made up of

$$(u\uparrow, u\uparrow, u\uparrow) \,, \tag{1.89}$$

where the arrows stand for spin components. This is preposterous because being spin one-half objects, quarks should obey Fermi-Dirac statistics and their states should be antisymmetric, which is certainly not the case in (1.89). Second, one can use current algebra techniques to calculate m_s/m_d with the result

$$m_s/m_d \approx 20 \,, \tag{1.90}$$

which is in contrast with (1.87) for quarks with a few GeV mass.

With respect to the first objection, a possible solution was proposed by Greenberg in 1964. He assumed that quarks obey parastatistics of rank three. It is known that such parastatistics can be composed by taking ordinary Fermi-Dirac statistics and introducing a new internal quantum number which was called by then "color". Therefore, each species of quark may come in any of the three colors $i = x(\text{red}), y(\text{green}), z(\text{blue})$. Using this model, the Δ^{++} can be interpreted as

$$\sum \epsilon^{ijk}(u^i\uparrow, u^j\uparrow, u^k\uparrow) \tag{1.91}$$

which is perfectly antisymmetric. In addition, the absence of states with, say, two or four quarks (so called "exotic") could be explained by postulating that all physical hadrons are colorless, i.e., they are singlets under rotations in color space

$$q^i \to \sum_k U_c^{ik} q^k \quad, \quad U_c^\dagger U_c = 1 \,. \tag{1.92}$$

If we take these transformations to have determinant 1 so as to eliminate a trivial overall phase, they build a new group, color $SU_c(3)$. Now the singlet representation only appears in $3_c \times 3_c \times 3_c$ (baryon) or $3_c \times \bar{3}_c$ (mesons) [26].

The Lagrangian of QCD is given by

$$\mathcal{L}_{QCD} = -\frac{1}{2}\text{tr}\, G^{\mu\nu}G_{\mu\nu} + \sum_{f=u,\ldots,t} \bar{q}_f(i\slashed{D} - m)q_f \,, \tag{1.93}$$

where

$$
\begin{aligned}
G_{\mu\nu} &= \partial_\mu A_\nu - \partial_\nu A_\mu - i\,[A_\mu, A_\nu] \,, \\
D_\mu &= \partial_\mu - i\,g\,A_\mu \,, \\
A_\mu &= \sum_{a=1}^{8} \frac{\lambda^a}{2}\,A_\mu^a \,.
\end{aligned}
\tag{1.94}
$$
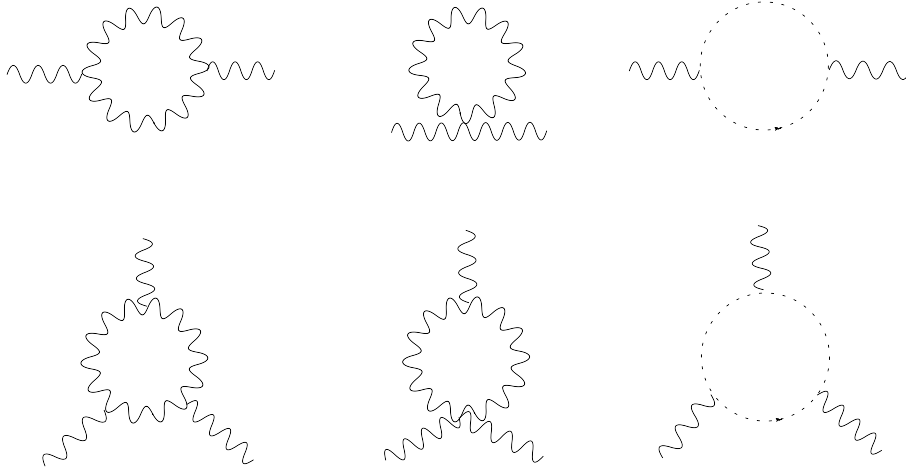
Figure 1.5: One loop contribution to the gluon self-energy and vertex functions. Both of them contribute to the β function. Here the wavy lines represent gluons while the dashed lines are ghost fields.

Here λ^a are the Gell-Mann matrices. The color $SU_c(3)$ gauge theory requires gauge invariance under the following gauge transformations

$$
\begin{aligned}
q_f & \rightarrow & U(\theta)\, q_f \;, \\
A_\mu & \rightarrow & U(\theta)\, A_\mu\, U^\dagger(\theta) + \frac{i}{g} U(\theta)\, \partial_\mu\, U^\dagger(\theta) \\
& = & U(\theta)\, (A_\mu + \frac{i}{g}\partial_\mu)\, U^\dagger(\theta) \;,
\end{aligned}
\tag{1.95}
$$

where $U(\theta) = \exp(i\,\lambda^a\theta_a)$. One can show that the covariant derivatives $\not{D}$ and the field tensor $G_{\mu\nu}$ transform in the same way

$$
\not{D} \rightarrow U\not{D}\,U^\dagger \;, \; G \rightarrow U\,G\,U^\dagger \;.
\tag{1.96}
$$

Furthermore, the mass matrix is diagonal in the flavor space

$$
m = \mathrm{diag}(m_f) = (m_u, m_d, ..., m_t) \;.
\tag{1.97}
$$

However, as it was pointed out separately by Gross and Wilczek in 1973 and Politzer in 1973 [16, 17], QCD can be distinguished by asymptotic freedom and infrared slavery from the other theories of physics: weak interactions, quantum electrodynamics (QED), and gravitation. This unique property of QCD can be characterised by the momentum (scale) dependent coupling constant g when the theory is renormalised. By calculating the one-loop contributions to gluon self-energy and vertex as shown in Fig. 1.5, one can extract the β function

$$
\beta(g) = -\frac{1}{16\pi^2}(11 - \frac{2}{3}N_f)\, g^3 \equiv b\, g^3 \;.
\tag{1.98}
$$
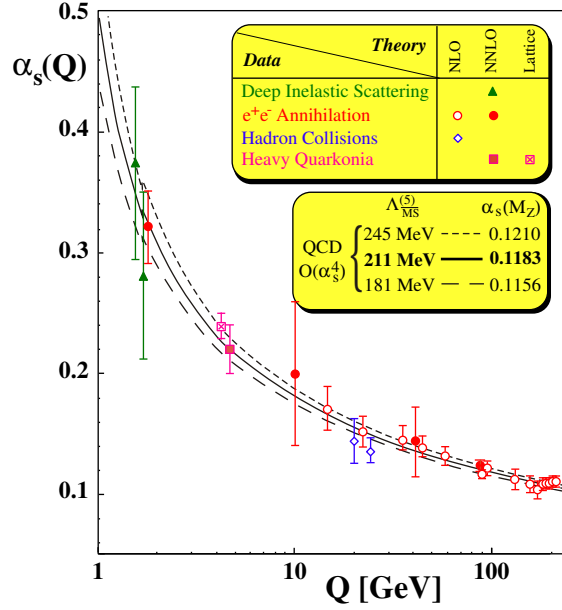
Figure 1.6: Summary of measurements of $\alpha_s(Q)$ [27].

For the renormalization group equation at one-loop level we have

$$\frac{dg}{dt} = -bg^3 \ . \tag{1.99}$$

Here the scale parameter t is defined by scaling the momentum by a parameter λ,

$$p \ \rightarrow \ \lambda p \ , \ \ t = \ln \lambda \ . \tag{1.100}$$

The solution of Eq. (1.99) is

$$g^2(t) = \frac{g(0)^2}{1 + 2b\,g(0)^2\,t} \ . \tag{1.101}$$

Hence, defining $\lambda^2 = Q^2/\mu^2$ and $t = (1/2)\ln Q^2/\mu^2$, we obtain

$$\alpha(Q^2) = \frac{\alpha(\mu^2)}{1 + 4\pi b\,\alpha(\mu^2)\mathrm{ln}(Q^2/\mu^2)} \ , \tag{1.102}$$

and using $\ln \Lambda^2 = \mathrm{ln}\mu^2 - 1/(\alpha(\mu^2)4\pi b)$, we have

$$\alpha(Q^2) = \frac{4\pi}{(11 - (2/3)N_f)\mathrm{ln}(Q^2/\Lambda^2)} \ , \tag{1.103}$$

where Λ is the QCD scale parameter and N_f is the number of relevant flavors. The running of $\alpha(Q^2)$ is shown in Fig.1.6.

In short, the non-Abelian character of QCD exhibits several non-trivial features which are not present in Abelian gauge theories, like quantum electrodynamics. The most important ones are the following:

- $\mathcal{L}_{QCD}$ contains gluonic self-couplings (three- and four-gluon vertices), i.e., gluons carry color.

- QCD is an asymptotically free theory, i.e., the coupling becomes weak at short distances, or equivalently, at large Euclidean momenta Q.

- Since the coupling constant is large at low momenta Q, perturbative QCD is not applicable to describe hadrons with masses below ~ 2 GeV. This may or may not be related to the phenomenon of "confinement", i.e., to the empirical fact that colored objects, like quarks and gluons, do not exist as physical degrees of freedom in vacuum.

The structure of strongly interacting matter at (not asymptotically) high density and low temperature is largely unknown. In particular, there is practically no exact information about the density region just above the hadron-quark phase transition which might be relevant for the interiors of compact stars.

At extremely high densities models may play an important role in developing and testing new ideas on a semi-quantitative basis and checking the robustness of older ones. Since models are simpler than the fundamental theory (QCD) they often allow for studying more complex situations than accessible by the latter. The price for this is, of course, a reduced predictive power due to dependencies on model parameters or certain approximation schemes. The results should, therefore, always be confronted with model independent statements or empirical facts, as far as available. In turn, models can help to interpret the latter where no other theory is available. Also, model independent results are often derived by an expansion in parameters which are assumed to be small. Thus, although mathematically rigorous, they do not necessarily describe the real physical situation. Here models can give hints about the validity of these assumptions or even uncover further assumptions which are hidden.

In Sec. 1.6 we present the most important model used to describe the BCS mechanism for superconductivity.

1.5   Phase diagram of QCD

Thermodynamic properties of a system are most readily expressed in terms of a phase diagram in the space of thermodynamic parameters - in the case of QCD - as a $T - \mu_B$ phase diagram, where μ_B is baryon chemical potential. Each point on the diagram corresponds to a stable thermodynamic state, characterized by various thermodynamic functions, such as, e.g., pressure, baryon density, etc (as well as kinetic coefficients, e.g., diffusion or viscosity coefficients, or other properties of various correlation functions).

Depending on the temperature, T, and the quark chemical potential, μ, strongly interacting matter may occur in three distinct phases: the hadronic phase, the quark-gluon plasma phase (QGP), and color-superconducting quark matter.

For temperatures below ~ 160 MeV and quark chemical potentials below ~ 350 MeV (corresponding to net-baryon densities which are a few times the ground state density of nuclear matter), strongly interacting matter is in the hadronic phase. Quite similar to the liquid-gas transition, there is a line of first-order phase transitions which separates the hadronic phase from
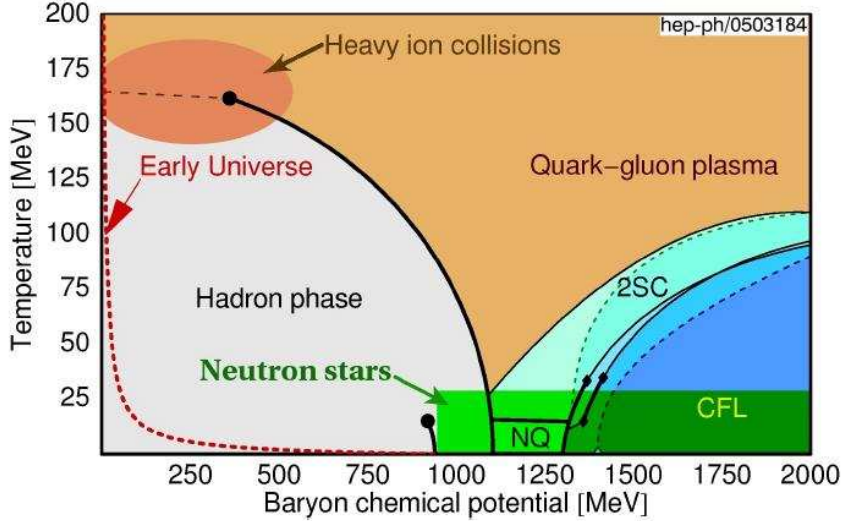
Figure 1.7: The phase diagram of QCD. [28].

the QGP and terminates in a critical endpoint where the transition is of second order. This endpoint is approximately at $(T, \mu) \sim (160, 240)$ MeV. For smaller quark chemical potentials (smaller net-baryon densities), the transition becomes crossover, and there is no real distinction between hadronic matter and the QGP. The position of the critical endpoint depends on the value of the quark masses.

In the hadronic phase, down-left part of Fig. 1.7, in the chiral limit - the idealized limit when 2 lightest quarks, u and d, are taken to be massless - the Lagrangian of QCD acquires chiral symmetry $SU(2)_L \times SU(2)_R$, corresponding to $SU(2)$ flavor rotations of (u_L, d_L) and (u_R, d_R) doublets independently. The ground state of QCD breaks the chiral symmetry spontaneously locking $SU(2)_L$ and $SU(2)_R$ rotations into a single vector-like $SU(2)_V$ (isospin) symmetry and generating 3 massless Goldstone pseudoscalar bosons - the pions. The breaking of the chiral symmetry is a non-perturbative phenomenon.

At sufficiently high temperature $T \gg \Lambda_{QCD}$, due to the asymptotic freedom of QCD, perturbation theory around the approximation of the gas of free quarks and gluons, QGP, should become applicable. In this regime chiral symmetry is not broken. Thus we must expect a transition from a broken chiral symmetry vacuum state to a chirally symmetric equilibrium state at some temperature $T_c \approx \Lambda_{QCD}$. Hence, the region of broken chiral symmetry on the $T - \mu_B$ phase diagram must be separated from the region of the restored symmetry. Therefore, for two massless quarks the transition can be either second or first order. As lattice and model calculations show, both possibilities are realised depending on the value of the strange quark mass m_s and/or the baryo-chemical potential μ_B. However, for three massless quarks, the transition must be of first order Ref. [29].

The point on the chiral phase transition line where the transition changes order is called

tricritical point. The location of this point is one of the unknowns of the QCD phase diagram with 2 massless quarks. In fact, even the order of the transition at $\mu_B = 0$ is still being questioned [30].

When the up and down quark masses are set to their observed finite values, the second order transition line is replaced by a crossover. In the absence of the exact chiral symmetry (broken by quark masses) the transition from low- to high-temperature phases of QCD need not proceed through a singularity. Lattice simulations do indeed show that the transition is a crossover for $\mu_B = 0$ [31].

In addition, the ground state of (infinite) nuclear matter is at $(T, \mu)_0 = (0, 308)$ MeV. From this point, a line of first-order phase transition emerges and terminates in a critical endpoint at a temperature of order ≈ 10 MeV. At this point, the transition is of second order. This phase transition is the nuclear liquid-gas transition [32]. To the left of the line nuclear matter is in the gaseous phase, and to the right in the liquid phase. Above the critical endpoint, there is no distinction between these two phases.

The early universe evolved close to the temperature axis in the phase diagram of strongly interacting matter. Matter in the core of compact stellar objects, like neutron stars, is close to the quark chemical potential axis, at values of μ around $400 - 500$ MeV. Nuclear collisions at bombarding energies around $E_{\text{Lab}} \approx 1$ AGeV explore a region of temperatures and quark chemical potentials around $(T, \mu) \approx (70, 250)$ MeV. Collisions at current RHIC energies of $\sqrt{s} = 200$ AGeV are expected to excite matter in a region around and above $(T, \mu) \approx (170, 10)$ MeV. Collision energies in between these two extremes cover the intermediate region and, in particular, may probe the critical endpoint [33].

Finally, at large quark chemical potential (large baryon density) and small temperature, quark matter becomes a color superconductor. There can be multitude of color-superconducting phases, depending on the symmetries of the order parameter for condensation of quark Cooper pairs. For very high densities, quark matter is in the so-called CFL phase and the so-called 2SC phase appears at the intermediate densities. However, for higher temperatures, the gapless phases occupy some part of the phase diagram [28]. Since this thesis is about color superconductivity, we give a detailed explanation of the color-superconducting phases in Chapter 2.

In the next section, we describe a model which is valid at very large baryon chemical potential, the NJL model.

1.6   NJL model

The Nambu-Jona-Lasinio model (NJL) was introduced to describe spontaneous chiral symmetry breaking in vacuum in analogy to the BCS mechanism for superconductivity [35, 36, 2]. The model was presented when QCD and even quarks were still unknown. In its original version, the NJL model was a model of interacting nucleons, and obviously, confinement was not the issue.

On the other hand, even in the pre-QCD era there were already indications for the existence of a (partially) conserved axial vector current (PCAC), i.e., chiral symmetry. Since (approximate) chiral symmetry implies (almost) massless fermions on the Lagrangian level, the problem was to find a mechanism which explains the large nucleon mass without destroying the symmetry. It was the pioneering idea of Nambu and Jona-Lasinio that the mass gap in the Dirac spectrum of
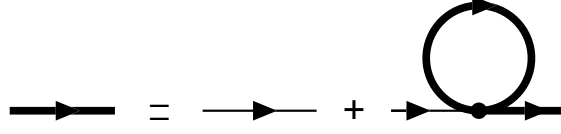
Figure 1.8: Dyson equation for the quark propagator in Hartree-Fock approximation. The bare (dressed) propagator is denoted by the thin (bold) line [37].

the nucleon can be generated quite analogously to the energy gap of a superconductor in BCS theory, which had been developed a few years earlier [2].

After the development of QCD, the NJL model was reinterpreted as a schematic quark model [38, 39, 40]. At that point, of course, the lack of confinement became a problem, severely limiting the applicability of the model. However, there are many situations where chiral symmetry is the relevant feature of QCD, confinement being less important. The most prominent example is again the Goldstone nature of the pion. In this aspect the NJL model is superior to the MIT bag model which fails to explain the low pion mass.

As one expects, the details of the results gained using the NJL model are model dependent. Although it seems to be quite natural that the four-point couplings are μ and T dependent quantities, just like the effective quark masses we compute, it is not clear whether the model parameters which are usually fitted to vacuum properties can still be applied at large densities.

The Lagrangian density of the model includes a quark field ψ with a point-like chirally symmetric four-fermion interaction,

$$\mathcal{L} = \bar{\psi}(i\partial\!\!\!/ - m)\psi + G\left\{(\bar{\psi}\psi)^2 + (\bar{\psi}i\gamma_5\vec{\tau}\,\psi)^2\right\} , \tag{1.104}$$

where m is the bare mass of the quark, $\vec{\tau}$ is the Pauli matrix acting in isospin space, and G a dimensionfull coupling constant.

Nambu and Jona-Lasinio calculated the quark self-energy which arises from the interaction term within Hartree-Fock approximation [35, 36]. The corresponding Dyson equation is shown in Fig. 1.8. The self-energy in this approximation is local and gives rise to a constant shift in the quark mass,

$$M = m + 2i\,G\int\frac{d^4p}{(2\pi)^4}\mathrm{Tr}\,S(p) , \tag{1.105}$$

where $S(p) = (p\!\!\!/ - M + i\epsilon)$ is the dressed quark propagator. Evaluating the trace over color, flavor, and Dirac space, we have

$$M = m + 8i\,GN_f\,N_c\int\frac{d^4p}{(2\pi)^4}\frac{M}{p^2 - M^2 + i\epsilon} . \tag{1.106}$$

Here N_f and N_c are the numbers of flavors and colors, respectively. For $N_f = 2$, $N_c = 3$ and sufficiently strong G there is a non-trivial solution in the chiral limit $m = 0$ which leads to an energy gap of $\Delta E = 2M$. Therefore, Eq.(1.106) is referred to as "gap equation" and M is known as "constituent quark mass". Moreover, the quark condensate is given by

$$< \bar{q}q > = -i\int\frac{d^4p}{(2\pi)^4}\,\mathrm{Tr}\,S(p) , \tag{1.107}$$
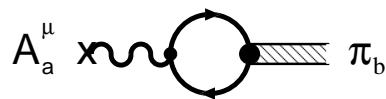
Figure 1.9: One-pion-to-vacuum matrix element in random phase approximation, giving rise to the weak pion decay: A pion with isospin index b is coupled via a quark loop to an axial current with isospin index a [37].

where q is the quark field. Hence, using (1.106), the condensate is expressed as

$$< \bar{q}q >= -\frac{M - m}{2G} . \tag{1.108}$$

The pion decay constant can be obtained from the one-pion-to-vacuum matrix element visualised in Fig. 1.9,

$$f_\pi \, q^\mu \, \delta_{ab} \; = \; g_{\pi qq} \int \frac{d^4p}{(2\pi)^4} \mathrm{Tr} \gamma^\mu \gamma_5 \frac{\tau_a}{2} \, S(p+q) \, i\gamma_5 \tau_b \, S(p) . \tag{1.109}$$

It is straightforward to show that in the chiral limit the generalised Goldberger-Treiman relation [41],

$$g_{\pi qq} \, f_\pi \; = \; M \; + \; \mathcal{O}(m) \tag{1.110}$$

holds. Furthermore, in first non-vanishing order in m, the pion mass satisfies the Gell-Mann-Oakes-Renner relation [42],

$$f_\pi^2 m_\pi^2 \; = \; -m \, < \bar{q}q > \; + \; \mathcal{O}(m^2) . \tag{1.111}$$

It is worthwhile to mention that the NJL model is not renormalizable. There are several regularisation methods which have been used in the literature, however, each of them has certain advantages and disadvantages. When the model is applied to thermodynamics, most authors prefer to regularise the integrals by a (sharp or smooth) 3-momentum cut-off. Besides being relatively simple, this has the advantage that it preserves the analytical structure, e.g., for the analytical continuation of functions given for imaginary Matsubara frequencies. Of course, 3-momentum cut-offs violate the Lorentz covariance of the model. It is often argued that this problem is less severe at nonzero temperature or density where the manifest covariance is anyway broken by the medium. Although this argument is questionable, since it makes a difference whether the symmetry is broken by physical effects or by hand, it is perhaps true that a 3-momentum cut-off has the least impact on the medium parts of the regularised integrals, in particular at $T = 0$ [37].

1.7 Nuclear astrophysics

Stars are born in primordial clouds of diffuse gases. They lead an active and ever changing life for millions of years as they synthesise their store of hydrogen into even heavier elements. Then they collapse and die. Their last gasp is an enormous explosion - a supernova - which lights the

day-time sky for months. From the primordial clouds, enriched by the elements of such stellar deaths, new stars are born [43].

Compact stars - broadly grouped as neutron stars and white dwarfs - are the ashes of luminous stars. Neutron stars or white dwarfs are the fate of most of the stars after tens of thousands of millions of years. Hyperon, hybrid, or strange quark stars are different forms of neutron stars. Among all of them, white dwarfs have different forms only in the dominant nuclear species. Black holes, on the other hand, are the fate of very massive stars.

Neutron stars were first discovered as pulsars. They are the smallest densest stars known, which are highly magnetised. Masses of neutron stars are as large as the sun mass and they are much smaller than the earth and some of them spin hundred times in a second. The high mass concentration and very rapid rotation of some pulsars warps the fabric of spacetime. In this view, neutron stars are fully relativistic objects.

Like all stars, neutron stars rotate as many as a few hundred times a second. A star having this frequency experiences a high centrifugal force that must be balanced by gravity to keep it rigid. Since we know gravitation quite well, consequently, we can estimate the lower density of a neutron star knowing its frequency. Some neutron stars are 10^{14} times denser than the earth. Some are in a binary orbit with a companion. Application of orbital mechanics allows an assessment of the masses in some cases. The mass of a neutron star is typically 1.5 solar masses. Knowing density and mass yield their radii about ten kilometres. Rotation and strong magnetic dipole fields are the means by which neutron stars can be detected.

1.7.1 Compact stars

The notion of a neutron star made of the ashes of a luminous star at end point of its evolution goes back to 1934 to the study of supernova explosions by Baade and Zwicky [44]. According to their theory, during the luminous life of a star, part of the original hydrogen is converted in fusion reactions to heavier elements by the heat produced by gravitational compression. When sufficient iron - the end point of exothermic fusion - is made, the core containing the heaviest ingredient (iron) collapses and an enormous energy is released in the explosion of the star. Baade and Zwicky guessed that the source of such a magnitude as makes these stellar explosions visible in daylight and for weeks must be gravitational binding energy.

Fusion reactions in the mother star (the luminous star) have reached the end point for energy release - the core has collapsed and the immense gravitational energy converted to the neutrinos has been carried away. Therefore, the star has no remaining energy source to excite the fermions. Only the Fermi and the short-range repulsion of the nuclear force sustain the neutron star against further gravitational collapse. At some cases where the mass is very concentrated the star becomes a black hole.

1.7.2 Compact stars and dense-matter physics

Neutron stars are bound by gravity, not by the nuclear force. The nuclear force is the strong force, but it is short-ranged and therefore acts only on its nearest neighbours. In contrast, the gravitational force is long-ranged and acts on all masses and for large and dense enough objects, it is thus the binding force. One can estimate the binding energy per nucleon due to gravity for a

canonical neutron star and finds a gravitation energy of ≈ 160 MeV/A compared to the binding energy of nuclear matter at its saturation density of ≈ 16 MeV/A. Hence, gravity compresses the matter of neutron stars so that the density lies far above the saturation density of nuclear matter. The nucleons feel repulsion from their neighbours. The energy required to compress nuclear matter to the density found at the centre of the most massive neutron stars is 200-300 MeV per nucleon. The compression energy reduces the net binding energy of neutron stars near the mass limit to about 100 MeV/A as compared to the energy of the nucleons dispersed to infinity. Therefore, the nuclear force contributes negatively to the binding of neutron stars [43].

There is still not a clear theory for describing the matter at supernuclear densities existing in the core of neutron stars. At the same time, it is not known clearly whether constituent matter of neutron stars experiences a phase transition from the confined phase in nucleons to the deconfined phase of quark matter.

Of a vastly different nature than neutron stars are strange stars. Like neutron stars they are, if they exist, very dense, of the same order as neutron stars. However, their existence hinges on a hypothesis that at first sight seems absurd. According to the hypothesis, sometimes referred to as the strange-matter hypothesis, quark matter - consisting of an approximately equal number of up, down, and strange quarks - has an equilibrium energy per nucleon that is lower than the mass of the nucleon or the energy per nucleon of the most bound nucleus, iron. In other words, under the hypothesis, strange quark matter is the absolute ground state of the strong interaction. The structure of strange stars is fascinating enough for study as are some of their properties. Special attention is placed on what sort of observation on pulsars would count as a virtually irrefutable proof of the strange-matter hypothesis.

1.7.3 Electrical neutrality of stars

Two particles carrying the same sign in charge experience the repulsive Coulomb force. This force is in competition with the gravitational attraction force in a star. The Coulomb force repels particles and the gravitational force attracts particles. The critical value for the net charge in a star above which a charged particle will be expelled comes from the following relations,

$$\frac{(Z_{net}e)e}{R^2} \leq \frac{GMm}{R^2} \leq \frac{G(Am)m}{R^2} \ , \tag{1.112}$$

where Z_{net}, R, M, are the net charge of the star, its radius, mass. m and e are the mass of a proton and its charge respectively. The number of baryons in the star is denoted by A, so that we have $M < Am$, that is, the mass of the star, because of its gravitational binding, is less than the mass of the baryons distributed to infinity. Hence,

$$Z_{net}/A < G(m/e)^2 \ . \tag{1.113}$$

This means that a net charge larger than the value above would not allow any additional charged particle of the same sign to be gravitationally bound. For example, in Natural units where $G = 1$, for a proton we have

$$(\frac{m}{e})^2 \approx \frac{(938 \, \text{MeV})^2}{1.44 \, \text{MeV fm}} \approx 10^{-36} \ , \tag{1.114}$$

consequently

$$Z_{net} < 10^{-36} A \; . \tag{1.115}$$

Similarly, this limit can be computed for a star having a net negative charge. Thus the net charge per nucleon (and therefore the average charge per nucleon on any star) must be very small, essentially zero. However, this is a global condition not a local one, i.e., this result places no restriction on the value of the charge density as a function of location in the star, so long as it integrates to the small value derived above.

1.7.4   Nuclear matter versus neutron star

Here we present a comparative discussion about the idealised matter made of nuclei and the matter of which neutron stars are made of. In both cases, matter is composed of baryons and the densities are the same within an order of magnitude or less. The differences arise from the facts that

i) It is gravity that binds the matter of neutron stars together in contrast to the isospin symmetric nuclear force that binds nuclei.

ii) Since in a neutron star the density is very high and its baryons have to obey the Pauli principle, nucleons at the top of the Fermi sea tend energetically to convert into baryons, to lower the Fermi energy. This includes strange stars (hyperons) as well. This transformation does not violate the strangeness conservation of the strong interaction because strangeness is conserved only on the strong interaction timescale, not on the weak interaction scale which causes the transformation of the nucleons to the baryons.

On the other hand, the properties of the hot,isospin symmetric, nonstrange matter produced in relativistic nuclear collisions and the cold, isospin asymmetric, charge neutral and strangeness-carrying matter of neutron stars are related in any comprehensive theory of matter. The connection between them can be made via the generalised relativistic nuclear field theory which incorporates nucleons and higher-mass baryon states interacting through the exchange of mesons. The coupling constant of the theory can be fixed by properties of symmetric nuclear matter. Also the theory describes numerous properties of nonzero nuclei and can be extended to finite temperature. The extrapolation to hot, dense matter and its composition (nucleons, deltas, and their excited baryon states) and to dense neutron matter have already been made in the literature [45, 46, 47, 48, 49].

1.7.5   Pion and kaon condensation

A few years ago, there were some studies of different condensation phenomena which might take place in neutron stars, like pion and kaon condensation. Since pions are lighter than kaons, pion condensation is more likely to occur. This happens when the pion energy becomes degenerate with the normal state. The crucial criteria for this is to have an attractive and sufficiently strong interaction.

In neutron stars charge neutrality favors pion condensation. The reason comes from the fact that neutrons at the top of the Fermi sea decay into protons and electrons. The electrons are fermions and their Fermi level increases with increasing density. When the electron chemical potential (Fermi energy) becomes equal to the effective pion mass in the medium, it will be

favorable for negative pions to play the role that the electrons had in preserving charge neutrality because they are bosons and can all condense in the lowest state. Consequently, while $\mu_e = \mu_n - \mu_p$ is essentially zero in symmetric matter, it is positive in neutron star matter, thus favoring π^- condensation since $\mu_{\pi^-} = \mu_e$. The other charged states of the pion are excluded since $\mu_{\pi^+} = -\mu_e$ and $\mu_{\pi^0} = 0$. The same scenario is valid for kaons, but its condensation, because of its larger mass, is less likely to occur.

The general form of the Euler-Lagrange equation for a meson field ϕ is

$$(\Box + m_\phi^2)\phi(x) = g_\phi \bar{\psi}(x)\Gamma_\phi \psi(x) . \tag{1.116}$$

In order to obtain this equation, a Yukawa potential has been included in the Lagrangian. The potential couples the scalar meson ϕ to the baryon scalar density $\bar{\psi}\psi$. The quantum numbers of the pion (spin-parity 0^-) and the kaon (which carries strangeness) are such that the ground state expectation value of the current source on the right-hand side vanishes identically in the mean-field approximation. The off-diagonal current source term on the right-hand side of (1.116) for the kaon vanishes in the normal ground state. In this case the meson field $< \phi >$ vanishes as well, yielding the lowest energy for the system. However, there might be a different configuration for the fermion state for which the source is nonzero. Such a case referred to as a condensate. The threshold for condensation is the lowest fermion density at which the fermion state has undergone a structural change from the normal ground state that endows $< \phi >$ with a nonzero value. At threshold we have

$$[-k_0^2 + \mathbf{k}^2 + m_\phi^2 + \Pi_\phi(k_0, \mathbf{k})] < \phi >= 0 , \tag{1.117}$$

where the self-energy is given by

$$\Pi_\phi(k_0, \mathbf{k}) = - \lim_{<\phi> \to 0} \frac{< J >}{< \phi >} . \tag{1.118}$$

The current is defined by $J = \bar{\psi}(x)\Gamma_\phi \psi(x)$. The brackets denote expectation values with respect to the fermion configuration, typically the ground state. The condition in Eq. (1.117) for a nonvanishing $< \phi >$ is that the quantity in the square brackets should vanish. The threshold for nonvanishing $< \phi >$ is the lowest density for which

$$-k_0^2 + \mathbf{k}^2 + m_\phi^2 + \Pi_\phi(k_0, \mathbf{k}) = 0 \tag{1.119}$$

has a solution for real $\mathbf{k}$ and $k_0 = \mu_\phi$.

1.7.6 Quark stars

Quark or hybrid neutron-quark stars are composed, in whole or in part, of quark matter. Such a state of matter was conceived soon after the realization that quarks, the constituents of nucleons, are asymptotically free. This means that at the extreme of asymptotic momentum transfer, density, or temperature, quarks are free of interaction. Under such circumstances the individuality of nucleons are lost, and the quarks of nuclear matter are free to explore a much larger "colorless" region of space referred to as quark matter [43].

According to the big-bang model, the universe has passed through the deconfined phase in the first few seconds. Furthermore, the high density of neutron stars may lead to a phase transition from ordinary hadronic matter (confined phase) to quark matter (deconfined phase). In this state, it is possible to have hybrid stars which are made of a quark matter in the central region and nuclear matter in the mantle. Also, it is feasible that the ground state of the strong interaction might be composed of strange quark matter rather than a state of nucleons and nuclei. If this is true, then, pulsars could be strange stars instead of neutron stars. All these arguments collect certainly sufficient motivation for astrophysicists to study the role of the deconfined phase in the formation of stars.

Besides all of this, nuclear astrophysics provides a ground for a new phenomenon called color superconductivity. In the following we give an introduction to the color-superconducting state of matter and afterwards explain its potential impact on compact stars.

1.8   Color superconductivity

Strongly interacting particles like protons and neutrons, as well as all mesons and baryons may appear in dense matter. Their properties and the properties of dense baryonic matter are, in principle, described by the microscopic theory of strong interactions, QCD.

It is known that baryons are not point-like particles. They have a typical size of about $1\,\mathrm{fm} = 10^{-13}\,\mathrm{cm}$. In sufficiently dense matter baryons are forced to stay very close to one another so that they would overlap. At such densities, constituent quarks are shared by neighbouring baryons and, with increasing the density further, quarks eventually become mobile over large distances, i.e., deconfinement. In this case hadronic matter is transformed into quark matter.

Nowadays it is believed that quark matter may exist inside central regions of neutron stars [50, 51, 52, 53, 54, 55, 56, 57, 58]. Neutron stars are dense, neutron-packed remnants of massive stars that blew apart in supernova explosions, cf. Sec. 1.7. Almost a decade ago it was suggested that the core of neutron stars may be in a color-superconducting state [59, 60, 61, 62]. This possibility has renewed tremendous interest in the physics and astrophysics of quark matter.

1.8.1   Introduction

The core of neutron stars is composed of matter with a density a few times the nuclear ground state density. At such high densities asymptotic freedom [16, 17] suggests that quarks behave nearly freely and therefore form large Fermi surfaces. As we turn on the interactions between quarks, we realize that most of the important interquark scattering processes allowed by the conservation laws and Fermi statistics involve large momentum transfer and are weak at asymptotically high densities. Therefore, one could try to understand the thermodynamic properties of the corresponding ground state by first completely neglecting the interaction between quarks. Consequently, the matter will be made of a Fermi sea of essentially free quarks whose behaviour is dominated by the freest of them which are the high-momentum quarks living at the Fermi surface.

The Helmholtz free energy is $F = E - \mu N$, where E is the total energy of the system, μ is the chemical potential of the particles in the system, and N is the number of particles. At the Fermi surface $E_F = \mu N$ the free energy is minimised, so that adding or subtracting a single

particle costs no free energy. Therefore, in the presence of a weak attractive interaction, a pair of particles (or holes) is created without any cost in the free energy. In fact the system has a tendency for such interactions. In consequence, many such pairs are created in all modes near the Fermi surface, and these pairs, which are now bosonic particles, will form a condensate.

In condensed matter systems the dominant interaction is the repulsive electrostatic force. There are several cases, however, where the system contains attractive phonon-mediated interactions. According to the BCS theory, in the presence of attractive interactions the Fermi surface is unstable. Then, the true ground state of the system will be a complicated coherent state of pairs of particles and holes so-called Cooper pairs. The ground state will be a superposition of states with all possible numbers of pairs. Hence the electromagnetic gauge symmetry is broken by Cooper pairs of electrons, i.e., the fermion number symmetry is broken. Similar to any system which undergoes spontaneous symmetry breaking, this leads to a mass for the photon and, in consequence, to the Meissner effect.

In QCD the dominant interaction between quarks is itself attractive [61, 62, 63, 64, 65]. Gluons play the role of phonons in the lattice. The relevant degrees of freedom are those which involve quarks with momenta near the Fermi surface. Therefore, at sufficiently low temperature, everything is ready to create a superconducting phase with quarks. This kind of superconductivity is called "color superconductivity" (CSC). Thus, in color superconductivity the attractive interactions already arise from the primary strong interaction. As a consequence of this, the accurate form of these interactions can be calculated from first principles, using asymptotic freedom. Besides, at densities where the strong interaction is much stronger than the electromagnetic interactions, we expect the color superconductors themselves to be robust in the sense that the ratio of their gaps and critical temperatures to the Fermi energy is quite large [59].

Color superconductivity spontaneously breaks color and chiral symmetries. The spectrum of elementary excitations is quite different from that found in naive perturbation theory. Nominally, massless quarks and gluons become massive via the Higgs mechanism, new massless collective modes appear, and various quantum numbers get modified. All the elementary excitations carry integer electric charges. Altogether, one finds an uncanny resemblance between the properties one computes at asymptotic densities, directly from the microscopic Lagrangian, and the properties one expects to be valid at low density, based on the known phenomenology of hadrons. In particular, the traditional "mysteries" of confinement and chiral symmetry breaking are fully embodied in a controlled, fully microscopic, weak-coupling (but nonperturbative!) calculation, that accurately describes a physical and intrinsically interesting regime [66, 67].

It was known for a long time that dense quark matter should be a color superconductor [63, 65, 68]. In many studies, however, this fact was commonly ignored. To large extent, this was triggered by the observation in Ref. [61, 62] that the value of the color-superconducting gap could be as large as $100 \, \mathrm{MeV}$ at baryon densities existing in the central regions of compact stars, i.e., at densities which are a few times larger than the normal nuclear density, $n_0 \simeq 0.15 \, \mathrm{fm}^{-3}$. This very natural estimate for the value of the gap in QCD, in which a typical energy scale itself is $200 \, \mathrm{MeV}$, opened a wide range of new theoretical possibilities, and the subject bursted with numerous studies. The main reason is that the presence of such a large energy gap in the quark spectrum may allow to extract clear signatures of the color-superconducting state of matter in observational data from compact stars.

As in electric superconductors, one of the main consequences of color superconductivity in

dense quark matter is the appearance of a nonzero energy gap in the one-particle spectrum,

$$\mathcal{E}_{\mathbf{k}} = \sqrt{(E_{\mathbf{k}} - \mu)^2 + \Delta^2},$$
(1.120)

where Δ is the gap. The presence of the gap in the energy spectrum should affect transport properties (e.g., conductivities and viscosities) of quark matter. Thus, if quark matter exists in the interior of compact stars, this will be reflected, for example, in the cooling rates and in the rotational slowing down of such stars. Also, a nonzero gap modifies thermodynamic properties, e.g., the specific heat and the equation of state. In application to stars, this could modify theoretical predictions for the mass-radius relations, or even suggest the existence of a new family of compact stars.

In general, it is of great phenomenological interest to perform a systematic study of all possible effects of color superconductivity in compact stars. Before this can be done, however, one needs to know the structure of the QCD phase diagram and properties of various color-superconducting phases in detail. Despite the recent progress in the field, such knowledge still remains patchy. While many different phases of quark matter have been proposed, there is no certainty that all possibilities have already been exhausted. This is especially so when additional requirements of charge neutrality and β equilibrium are imposed.

In some cases, for example, superconductivity may be accompanied by the baryon super-fluidity and/or the electromagnetic Meissner effect. If matter is superfluid, rotational vortices would be formed in the stellar core, and they would carry a portion of the angular momentum of the star. Because of the Meissner effect, the star interior could become threaded with magnetic flux tubes. In either event, the star evolution may be affected [69].

1.8.2 Gap equation

The condensation of fermions in the ground state can be understood via explicitly constructing a wavefunction with the appropriate pairing, using a many-body variational approach. Although the field-theoretical approach is less concrete, instead it is more general and we will briefly describe it here [70].

The one-particle irreducible (1PI) Green function of two quark fields gives the quark self-energy. The poles of the self-energy yield the gauge-invariant masses of the quasiquarks, the lowest energy of fermionic excitations around the quark Fermi surface. In order to know if any condensation (e.g. chiral condensation, flavor-singlet quark pairing, or whatever) occurs in some channels, one has to write a self-consistent equation, the "gap equation", for a self-energy. If it is zero, there is no condensation in that channel. If not, there can be condensation, but it may just be a local minimum of the free energy. There may be other solutions to the gap equation, and the one with the lowest free energy is the true ground state. In this view, the gap is the order parameter for condensation.

There are several possible choices for the interaction which can be used in the gap equation. We know that at asymptotically high densities QCD is weakly coupled, so one-gluon exchange is an appropriate approximation. However, the density regime of physical interest for neutron stars or heavy ion collisions is up to a few times nuclear density ($\mu \lesssim 500$ MeV) and weak-coupling calculations are unlikely to be trustworthy in that regime.
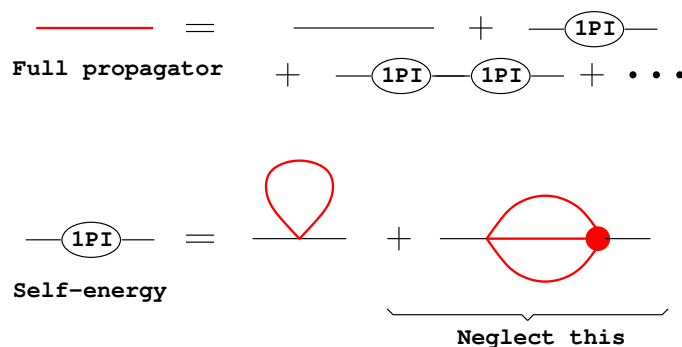
Figure 1.10: Mean-field Schwinger-Dyson (gap) equations [70]

.

In order to solve the problem we have to use some phenomenological interaction in the regime of interest. By renormalizing the interaction we can go to the low-energy physics such as the chiral condensate and afterwards extrapolate to the associated chemical potential. It was already shown in [61, 62, 74, 75] that in two-flavor theories the instanton vertex is a natural choice because it is a four-fermion interaction. For three flavors, the one-gluon exchange vertex must be taken into account [65, 66, 76]. However, both have the same results, to within a factor of about 2. The single-gluon-exchange interaction is symmetric under $U(1)_A$, in consequence, there is no distinction between condensates of the form $< qCq >$ and $< qC\gamma_5 q >$. When instantons are included the parity-even condensate $< qC\gamma_5 q >$ is favored [61, 62]. Thus in single-gluon-exchange calculations the parity-violating condensate is usually ignored.

The Schwinger-Dyson equation in the mean-field approximation is diagrammatically shown in Fig. 1.10. In the figure the relation between the full propagator and the self-energy is shown. In the mean-field approximation, only daisy-type diagrams are included in the resummation and vertex corrections are excluded. Using the diagrammatic rules, the equation corresponding to the self-energy takes the form

$$\Sigma(k) = -\frac{1}{(2\pi)^4} \int d^4q \, M^{-1}(q) D(k-q), \tag{1.121}$$

where M is the inverse fermion full propagator. The vertex is indicated by $D(k-q)$ which in the NJL model is independent of gluon momentum, but in weak-coupling QCD calculations include the gluon propagator and couplings. Similar to the case of chiral symmetry breaking where it is necessary to use 4-component Dirac spinors rather than 2-component Weyl spinors, even if there is no mass term in the action, here, we have to write the propagator in a way which allows the study of quark-quark condensation. Using Nambu-Gorkov 8-component spinors, $\Psi = (\psi, \bar{\psi}^T)$, the self-energy Σ includes a quark-quark pairing term Δ. The fermion matrix M then takes the form

$$M(q) = M_{\text{free}} + \Sigma = \begin{pmatrix} \slashed{q} + \mu\gamma_0 & \gamma_0\Delta\gamma_0 \\ \Delta & (\slashed{q} - \mu\gamma_0)^T \end{pmatrix}. \tag{1.122}$$

Equations (1.121) and (1.122) can be combined to give a self-consistent condition for the gap equation Δ. In the NJL model where the interaction is a point-like four-fermion interaction, the gap parameter is momentum-independent. Therefore, the analysis of different condensations is very simple.

Ttaking all this into account the gap equation reads

$$1 = K \int_0^\Lambda k^2 dk \, \frac{1}{\sqrt{(k - \mu)^2 + \Delta^2}}, \tag{1.123}$$

where K is the NJL four-fermion coupling. The approximation of small gaps simplifies the integral, so one finds

$$\Delta \sim \Lambda \exp\left(\frac{-\mathrm{const}}{K\mu^2}\right). \tag{1.124}$$

This shows the non-analytic dependence of the gap on the coupling K. Condensation is a nonperturbative effect that cannot be seen to any order in perturbation theory. The reason it can be seen in the diagrammatic Schwinger-Dyson approach is that there is an additional ingredient: an ansatz for the form of the self energy. This corresponds to guessing the from of the ground state wavefunction in a many-body variational approach. All solutions to gap equations therefore represent possible stable ground states, but to find the favored ground state their free energies must be compared with each other, and even then one can never be sure that the true ground state has been found, since there is always the possibility of another vacuum that solves the gap equation and has an even lower free energy [70].

In weak-coupling QCD calculations, where the full single-gluon-exchange vertex and the gluon propagator is accounted for, the gap equation takes the form [63, 64, 77, 78]

$$\Delta \sim \mu \frac{1}{g^5} \exp\left(-\frac{3\pi^2}{\sqrt{2}} \frac{1}{g}\right), \tag{1.125}$$

or, making the weak-coupling expansion in the QCD gauge coupling g more explicit,

$$\ln\left(\frac{\Delta}{\mu}\right) = -\frac{3\pi^2}{\sqrt{2}} \frac{1}{g} - 5\ln g + \mathrm{const} + O(g). \tag{1.126}$$

This gap equation has two interesting features. Firstly, it does not correspond to what we would naively expect from the NJL model of single-gluon exchange, in which the gluon propagator is discarded and $K \propto g^2$, yielding $\Delta \sim \exp(-1/g^2)$. The reason is that at high density the gluon propagator has an infrared divergence at very small angle scattering, because magnetic gluons are only Landau damped and are not screened [64, 77]. This divergence is regulated by the gap itself, weakening its dependence on the coupling.

Secondly, in (1.125) we did not specify the energy scale at which the coupling g is to be evaluated. Natural guesses would be μ or Δ. If we use $g(\mu)$ and assume it runs according to the one-loop formula $1/g^2 \sim \ln \mu$ then the exponential factor in (1.125) gives very weak suppression, and is in fact overwhelmed by the initial factor μ. Thus, the gap rises without limit at asymptotically high density. Although, in this case, Δ/μ shrinks to zero so that weak-coupling methods are still self-consistent, this however means that color superconductivity will inevitably

dominate the physics at sufficiently high densities.

Chapter 2

Three-flavor, spin-zero color superconductivity

2.1 Introduction

The interaction between electrons resulting from virtual exchange of phonons is attractive when the energy difference between the involved electrons is less than the phonon energy. There is a favorable attractive channel which dominates over the repulsive screened Coulomb interactions and produces superconductivity [3]. In cold and dense quark matter, due to asymptotic freedom [79], at quark chemical potentials $\mu \gg \Lambda_{QCD}$ single-gluon exchange is the dominant interaction between quarks and it is attractive in the color-antitriplet channel. This leads to the formation of quark Cooper pairs. This kind of condensation creates a new type of superconductivity which is called color superconductivity (CSC). The difference between this type of superconductivity compared and an ordinary electronic superconductor comes from the fact that quarks carry different flavors and non-Abelian color charges [61, 62, 65]. Then, CSC can appear in different phases depending on the various colors and flavors of the quarks which participate in Cooper pairing.

It has been found that at asymptotically large baryon number densities, where the masses of the u, d, and s quarks are much smaller than the chemical potential, the ground state of 3-flavor QCD is the color-flavor-locked (CFL) phase [66]. In this phase, quarks of all colors and flavors form Cooper pairs, and $SU(3)_c \otimes SU(3)_L \otimes SU(3)_R \otimes U(1)_B$ is spontaneously broken to a subgroup $SU(3)_{c+f} \otimes U(1)_{c+em}$. This phase is a superfluid but an electromagnetic superconductor. When the strange quark does not participate in pairing, the ground state is the so-called 2SC phase [61, 62]. The original symmetry $SU(3)_c \otimes SU(2)_L \otimes SU(2)_R \otimes U(1)_{em} \otimes U(1)_B$ breaks down to $SU(2)_c \otimes SU(2)_L \otimes SU(2)_R \otimes U(1)_{c+em} \otimes U(1)_{em+B}$. Unlike the CFL phase, the 2SC phase is not a superfluid.

In nature color superconductivity may exist in compact stars. The approximation of asymptotically large density is not valid then. Moreover, the matter in the bulk of compact stars is neutral with respect to color and electric charges. Besides, this matter should remain in β-equilibrium [80, 81, 82, 83, 84, 86, 87]. These conditions impose stress on the system. In contrast to the 2SC and the CFL phases at large densities, in this case the Fermi momenta of different

quark flavors participating in pairing cannot be equal. Therefore, the ground state is neither a pure CFL nor a pure 2SC state. There might appear phases in which the Cooper pairs carry nonzero total momenta and the system exhibits a crystalline structure due to a spatially varying energy gap. This kind of a superconductor was for first time studied by Larkin and Ovchinnikov [88] and Fulde and Ferrell [89], and is called LOFF superconductor. Alternately, there might be ungapped quasiparticle excitations with nonzero gap parameter for both the 2SC and CFL phases, giving rise to so-called gapless phases [83, 84, 90], but it has been shown that most of the gapless phases are unstable [91, 92, 93], the exceptions are pointed out in Ref. [94]. In Ref.[95, 96, 97, 98], the authors argued that the system may respond to this stress by forming a kaon condensate in the ground state. With this condensation the strange quark number density is decreased without a costly breaking of the pairs in the CFL background.

From the theoretical point of view, superfluidity is very similar to superconductivity. Both are states of interacting many-fermion systems that are distinguished from the normal matter by an order parameter. Among all possible phases of superfluid ^{3}He states only the so-called inert phases have been found in experiment. These phases play a crucial role in superconductivity due to Michel's theorem, cf. Ref. [99, 10]. It is known that the B phase is the dominant phase in a vast area of the phase diagram of superfluid ^{3}He, while the so-called A phase has a dominant pressure only in a tiny area of the diagram.

One-flavor CSC is similar to superfluid ^{3}He. The reason is that the order parameters are quite similar. In one-flavor CSC, the order parameter is a 3×3 matrix in color and spin spaces. For comparison, in superfluid ^{3}He, the order parameter is a 3×3 matrix in coordinate and spin space. It is natural to expect that one-flavor CSC has phases similar to the inert phases of superfluid ^{3}He [100].

In comparison, in three-flavor, spin-zero CSC the order parameter is a 3×3 matrix in color and flavor spaces. In this case, it was shown in Ref. [101] that there are 511 possible phases. However, using the symmetries present in the system this number could be lowered. Naturally, some of these are analogues of the inert phases encountered in one-flavor CSC and superfluid ^{3}He. The CFL phase is the analogue of the CSL phase in one-flavor CSC or the B phase in superfluid ^{3}He. The 2SC phase is the analogue of the polar phase in one-flavor CSC or superfluid ^{3}He. There is, however, also an analogue of the A phase of one-flavor CSC and superfluid ^{3}He, and a closely related phase, the A* phase which we discuss here for the first time. Finally, another inert phase is the sSC phase which is the complement of the 2SC phase in the sense that strange quarks pair with up and down quarks, but up and down quarks do not pair among themselves.

As it was mentioned earlier, at asymptotically large densities, it is known [66] that the CFL phase is the energetically favored phase. At intermediate densities, the 2SC phase may be energetically preferred over the CFL phase, depending on the value of the quark masses or the diquark coupling strength [61, 62]. The purpose of this chapter is to answer the question whether some of the inert phases, which have not been studied in three-flavor CSC yet, could be energetically favored over either the CFL or the 2SC phase at intermediate densities [102]. We go through this interesting question in two different schemes. First, we use QCD to calculate the pressure of each phase without imposing the neutrality condition which has to be taken into account in the study of neutron stars, Sec.1.7.3. Second, we employ the NJL model to find the ground state of color-superconducting matter in neutron stars which are color and electric

charge neutral.

This chapter is organised as follows. In the next section, we give a general expression for the pressure of the different phases without imposing the neutrality condition. Then, we compare the pressure of all phases to determine the ground state. In Sec.2.3, we calculate the pressure of the phases including the neutrality condition. In order to identify the chemical potentials that make the system color and charge neutral, we evaluate the tadpoles in each phase. At the end, we consider the symmetry breaking pattern.

Our units are $\hbar = c = k_B = 1$. The metric tensor is $g^{\mu\nu} = \text{diag}\,(+,-,-,-)$. We denote 4-vectors in energy-momentum space by capital letters, $K^\mu = (k_0, \mathbf{k})$. Absolute magnitudes of 3-vectors are denoted as $k \equiv |\mathbf{k}|$, and the unit vector in the direction of $\mathbf{k}$ is $\hat{\mathbf{k}} \equiv \mathbf{k}/k$.

2.2 Pressure without neutrality condition

In this section we calculate the pressure of CSC quark matter at zero temperature without the neutrality condition. In the absence of the neutrality condition, we use QCD. In consequence, first of all, we need to derive the gap equation for each phase of CSC.

In contrast, when we calculate the pressure applying the neutrality condition to the system, each quark obtains a specific chemical potential, consequently QCD will be very difficult to use. Therefore, in that case, we use a simplified model, the NJL model, see Sec.2.3.1.

2.2.1 Derivation of gap equation

In order to derive the gap equation, we follow the method used in Ref. [33] and refrain from repeating the details. The so-called "Cornwall-Jackiw-Tomboulis" (CJT) formalism [103] allows for a derivation of self-consistent Dyson-Schwinger equations from the QCD partition function,

$$\mathcal{Z} = \int \mathcal{D}A\,\mathcal{D}\bar{\psi}\mathcal{D}\psi \, \exp S \, , \tag{2.1}$$

where the action S is composed of three parts,

$$S = S_A + S_F + g \int_X \bar{\psi}(X)\gamma^\mu T_a \psi(X) A_\mu^a(X) \, . \tag{2.2}$$

Here $\mathcal{D}A$ is the gauge-invariant measure for the integration over the gauge fields A_a^μ. Therefore, $\mathcal{D}\bar{\psi}$ and $\mathcal{D}\psi$ denote the functional integration over the anti-quark $\bar{\psi}$ and quark fields ψ, respectively. These fields are $4N_c N_f$-component spinors that carry Dirac indices $\alpha = 1, \ldots, 4$, fundamental color indices $i = 1, \ldots, N_c$, and flavor indices $f = 1, \ldots, N_f$. In addition, γ^μ are the Dirac matrices, and $T_a = \lambda_a/2$ are the generators of $SU(N_c)$ for N_c quark colors. In QCD with $N_c = 3$, λ_a are the Gell-Mann matrices. The space-time integration is defined as $\int_x \equiv \int_0^{1/T} d\tau \int_V d^3\mathbf{x}$ and the QCD coupling constant is introduced via g. Note that, in this section, we restrict our discussion to the strong interaction which is responsible for the formation of Cooper pairs.

The first term in the action S is the gluon field part,

$$S_A = S_{F^2} + S_{gf} + S_{FPG} \, , \tag{2.3}$$

where

$$S_{F^2} = -\frac{1}{4} F_a^{\mu\nu} F_{\mu\nu}^a , \qquad (2.4)$$

is the gauge field part and $F_{\mu\nu}^a = \partial_\mu A_\nu^a - \partial_\nu A_\mu^a + g f^{abc} A_\mu^b A_\nu^c$ is the field strength tensor. When we calculate the gluon self-energy, we do not have to specify the gauge fixing, S_{gf}, and the Fadeev–Popov ghosts terms, S_{FPG}, because, as it will be clear later on, at zero temperature the contribution from these terms are suppressed compared to that from quarks.

The second term in Eq. (2.2) is the free fermion part in the presence of a chemical potential μ,

$$S_F = \int_X \bar{\psi}(X) \left(i\gamma \cdot \partial_X + \mu_f \gamma_0 - m \right) \psi(X) . \qquad (2.5)$$

Herethe matrix of quark masses m_f is denoted as $m \equiv \mathrm{diag}(m_1, m_2, \ldots, m_{N_f})$. Since we are not concerned with the neutrality condition, μ_f assumes equal value for all quark flavors, $\mu_f = \mu$. Thus, the $N_f \times N_f$ chemical potential matrix is diagonal, $\mu \equiv \mathrm{diag}(\mu_1, \mu_2, \ldots, \mu_{N_f})$. The term $\bar{\psi}\mu\gamma_0\psi$ is a measure for the energy of the excited states with respect to the vacuum at zero density. When the chemical potential goes to zero, $\mu_f = 0$, the ground state of the system lowers from the Fermi sea to the Dirac sea and the system is on the vacuum state. In this case, all negative energy states are occupied only by antiquarks and all positive energy states consisted of quarks are empty.

The third term in Eq. (2.2) describes the coupling between quarks and gluons. Such a term arises in any gauge theory where the requirement of gauge invariance leads to a covariant derivative including a gauge field.

In order to take into account color superconductivity effects, it is very convenient to employ Nambu-Gorkov spinors which give the possibility to implement a bilocal source term into the action. The spinors have the following form

$$\Psi = \begin{pmatrix} \psi \\ \psi_C \end{pmatrix} , \qquad \bar{\Psi} = (\bar{\psi}, \bar{\psi}_C) , \qquad (2.6)$$

where $\psi_C \equiv C\bar{\psi}^T$ is the charge conjugate spinor, with the charge conjugation matrix $C \equiv i\gamma^2\gamma_0$. We know that in $2N_c N_f$-dimensional Nambu-Gorkov space, the fermion action, Eq. (2.5), is written as

$$S_F = \frac{1}{2} \int_{X,Y} \bar{\Psi}(X) \, \mathcal{S}_0^{-1}(X,Y) \, \Psi(X) . \qquad (2.7)$$

The doubling of the degrees of freedom introduced by Nambu-Gorkov basis is accounted for by the additional factor $1/2$. The inverse free fermion propagator looks as follows,

$$\mathcal{S}_0^{-1} \equiv \begin{pmatrix} [G_0^+]^{-1} & 0 \\ 0 & [G_0^-]^{-1} \end{pmatrix} , \qquad (2.8)$$

where

$$[G_0^\pm]^{-1}(X,Y) \equiv -i \left(i\gamma \cdot \partial_X \pm \mu\gamma_0 - m \right) \delta^{(4)}(X-Y) . \qquad (2.9)$$

Moreover, in the current basis, the interaction term reads

$$g \int_X \bar{\psi}(X) \gamma^\mu T_a \psi(X) A_\mu^a(X) = \frac{1}{2} g \int_X \bar{\Psi}(X) \hat{\Gamma}_a^\mu \Psi(X) A_\mu^a(X) , \qquad (2.10)$$

where $\hat{\Gamma}_a^\mu$ is defined via

$$\hat{\Gamma}_a^\mu \equiv \begin{pmatrix} \gamma^\mu T_a & 0 \\ 0 & -\gamma^\mu T_a^T \end{pmatrix} . \tag{2.11}$$

Now we can add a bilocal source term

$$\mathcal{K} \equiv \begin{pmatrix} \sigma^+ & \varphi^- \\ \varphi^+ & \sigma^- \end{pmatrix} . \tag{2.12}$$

to the action. Consequently, the new form of the action (2.7) is given by

$$S[\mathcal{K}] = S + \int_{X,Y} \bar{\Psi}(X)\,\mathcal{K}(X,Y)\Psi(Y) . \tag{2.13}$$

The quantities that carry the superconductivity effect are the off-diagonal elements of $\mathcal{K}$, φ^+ and φ^-. Since they couple two (adjoint) quarks (while the diagonal elements σ^+ and σ^- couple quarks with adjoint quarks), a nonzero value of these elements is equivalent to a Cooper pair, or, in other words, to a nonvanishing diquark expectation value $\langle \psi\psi \rangle$. The entries of $\mathcal{K}$ are related via $\sigma^- = C[\sigma^+]^\dagger C^{-1}$ (due to charge conjugation invariance) and $\varphi^- = \gamma_0[\varphi^+]^\dagger\gamma_0$ (because the action must be real-valued). The new action $S[\mathcal{K}]$ yields a new form of the QCD partition function

$$\mathcal{Z}[\mathcal{K}] = \int \mathcal{D}A\,\mathcal{D}\bar{\Psi}\mathcal{D}\Psi \, \exp S[\mathcal{K}] . \tag{2.14}$$

Implementing the CJT formalism [103], the effective action is a functional only of two-point functions, namely the gauge boson and fermion propagators D_G and D_F,

$$\begin{aligned}
\Gamma[D_G, D_F] &= -\frac{1}{2}\mathrm{Tr}\,\ln D_G^{-1} - \frac{1}{2}\mathrm{Tr}(\Delta_0^{-1}D_G - 1) + \frac{1}{2}\mathrm{Tr}\,\ln D_F^{-1} \\
&\quad + \frac{1}{2}\mathrm{Tr}(\mathcal{S}_0^{-1}D_F - 1) + \Gamma_2[D_G, D_F] ,
\end{aligned} \tag{2.15}$$

where Δ_0^{-1} is the inverse free gluon propagator and the traces run over Nambu-Gorkov, Dirac, flavor, color, and momentum space. The functional $\Gamma_2[D_G, D_F]$ denotes the sum of all two-particle irreducible diagrams without external legs and with internal lines given by the gluon and quark propagators. The stationary points of the effective potential give the physical quantities. These points are obtained through taking the functional derivatives of the functional $\Gamma[D_G, D_F]$ with respect to the gluon and fermion propagators. Therefore, the associated set of equations for the stationary points $(D_G, D_F) = (\Delta, \mathcal{S})$ are as follows,

$$\Delta^{-1} = \Delta_0^{-1} + \Pi , \tag{2.16a}$$
$$\mathcal{S}^{-1} = \mathcal{S}_0^{-1} + \Sigma , \tag{2.16b}$$

where the gluon and fermion self-energies are defined as the functional derivatives of Γ_2 at the stationary point,

$$\Pi \equiv -2\left.\frac{\delta\Gamma_2}{\delta D_G}\right|_{(D_G,D_F)=(\Delta,\mathcal{S})} , \qquad \Sigma \equiv 2\left.\frac{\delta\Gamma_2}{\delta D_F}\right|_{(D_G,D_F)=(\Delta,\mathcal{S})} . \tag{2.17}$$
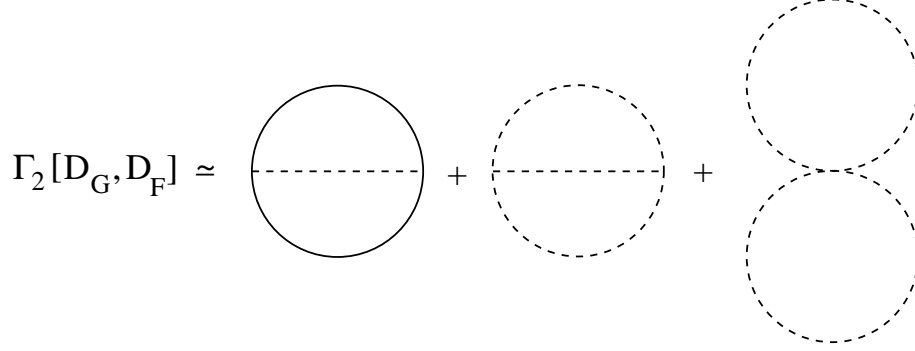
Figure 2.1: Two-loop approximation of $\Gamma_2[D_G, D_F]$ (without ghost contributions). Dashed lines represent the gluon propagator D_G while full lines represent the quark propagator D_F [100].

In order to find the full propagators, one has to solve the Dyson-Schwinger equations, Eqs. (2.16), self-consistently. Denoting the entries of the 2×2 fermion self-energy by

$$\Sigma \equiv \begin{pmatrix} \Sigma^+ & \Phi^- \\ \Phi^+ & \Sigma^- \end{pmatrix} , \tag{2.18}$$

and introducing the full quark propagator in the form

$$\mathcal{S} = \begin{pmatrix} G^+ & \Xi^- \\ \Xi^+ & G^- \end{pmatrix} , \tag{2.19}$$

we obtain the fermion propagators for quasiparticles and charge-conjugate quasiparticles,

$$G^{\pm} = \left\{ [G_0^{\pm}]^{-1} + \Sigma^{\pm} - \Phi^{\mp}([G_0^{\mp}]^{-1} + \Sigma^{\mp})^{-1}\Phi^{\pm} \right\}^{-1} , \tag{2.20}$$

and the so-called anomalous propagators,

$$\Xi^{\pm} = -([G_0^{\mp}]^{-1} + \Sigma^{\mp})^{-1}\Phi^{\pm}G^{\pm} . \tag{2.21}$$

In order to proceed, we have to use an approximate value for $\Gamma_2[D_G, D_F]$. In Fig. 2.1, all two-particle irreducible diagrams with two loops are shown. It is one of the important properties of the CJT formalism that even truncating the infinite set of diagrams contained in Γ_2 still yields a well-defined and self-consistent set of equations. The two-loop approximation of Γ_2 is equivalent to a one-loop approximation of the self-energies Π and Σ.

The derivative of Γ_2 with respect to the quark propagator, Eq. (2.17), is equivalent to cutting one quark line in the left diagram in Fig. 2.1. Consequently, the quark self-energy is given by

$$\Sigma(K) = -g^2 \int_Q \Gamma_a^\mu \, \mathcal{S}(Q) \, \Gamma_b^\nu \, \Delta_{\mu\nu}^{ab}(K - Q) . \tag{2.22}$$
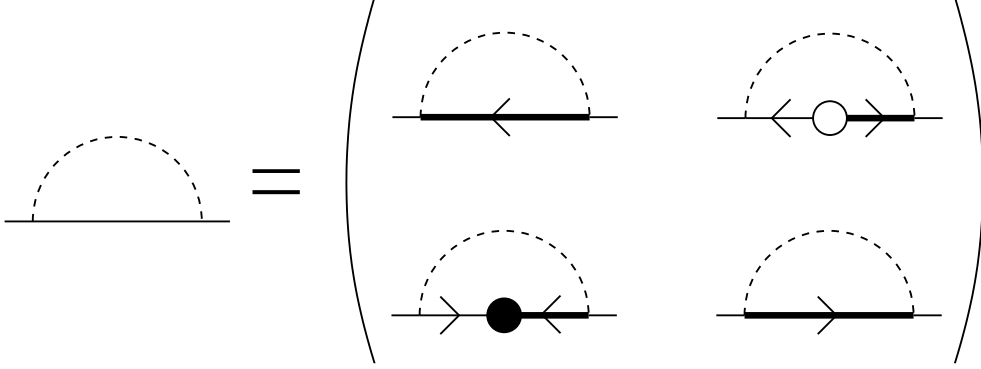
Figure 2.2: Diagrammatic representation of Eq. (2.22). The quark self-energy is shown as a 2×2 Nambu-Gorkov matrix (cf. also Eqs. (2.23)). Dashed lines correspond to the gluon propagator Δ. The normal full quasiparticle propagators G^+ and G^- are denoted by thick lines with an arrow pointing to the left and right, respectively. The anomalous propagators $\Xi^\pm$ are drawn according to their structure given in Eq. (2.21): Thin lines correspond to the term $([G_0^\mp]^{-1} + \Sigma^\mp)^{-1}$, while the full and empty circles denote the gap matrices Φ^+ and Φ^-, respectively [100].

Using this method together with Eqs. (2.18) and (2.19), we obtain the entries of the 2×2 fermion self-energy matrix

$$\Sigma^+(K) = -g^2 \int_Q \gamma^\mu T_a G^+(Q) \gamma^\nu T_b \Delta_{\mu\nu}^{ab}(K-Q) , \qquad (2.23a)$$

$$\Sigma^-(K) = -g^2 \int_Q \gamma^\mu T_a^T G^-(Q) \gamma^\nu T_b^T \Delta_{\mu\nu}^{ab}(K-Q) , \qquad (2.23b)$$

$$\Phi^+(K) = g^2 \int_Q \gamma^\mu T_a^T \Xi^+(Q) \gamma^\nu T_b \Delta_{\mu\nu}^{ab}(K-Q) , \qquad (2.23c)$$

$$\Phi^-(K) = g^2 \int_Q \gamma^\mu T_a \Xi^-(Q) \gamma^\nu T_b^T \Delta_{\mu\nu}^{ab}(K-Q) . \qquad (2.23d)$$

The diagrammatic form of these expressions is shown in Fig. 2.2. The dashed lines indicate the gluon propagator whereas the solid lines show the quark propagator. The full and empty circles stand for the gap matrices Φ^+ and Φ^-, respectively. Also,

$$\Phi^- = \gamma_0 [\Phi^+]^\dagger \gamma_0 . \qquad (2.24)$$

The gap equations $\Phi^\pm(K)$ are matrices in flavor, color, and Dirac space and a function of the quark four-momentum K.

Note that the gap matrices on the left-hand side of Eqs. (2.23c) and (2.23d) are hiding in the anomalous propagators $\Xi^\pm(Q)$ on the right-hand side. A complete self-consistent solution of the four coupled integral equations needs inevitably some approximations. In the next section, Sec. 2.2.2, we determine the structure of the quasiparticle excitation energies which follows from an ansatz for the gap matrix Φ^+ (without solving the gap equation).

2.2.2 Solution of gap equation

The main purpose of this section is to present a method to compute the value of the gap at the Fermi surface at zero temperature from the gap equation, Eqs. (2.23c) and (2.23d). To achieve this goal, we have to investigate the gap dependence of anomalous propagator $\Xi^{\pm}(Q)$. To this end, according to Eq. (2.21), we have to find a simple form for the full quasiparticle propagator $G^{\pm}(Q)$ in terms of the gap function.

In this section, we consider ultrarelativistic quarks, $m = 0$, because nonzero quark masses cause tremendous technical complications [104]. Therefore, restricting to Cooper pairing in the even-parity channel, the gap matrix can be written as

$$\Phi^{+}(K) = \sum_{e=\pm} \phi^{e}(K) \, \mathcal{M}_{\mathbf{k}} \, \Lambda_{\mathbf{k}}^{e} \, , \tag{2.25}$$

where $\phi^{e}(K)$ is the gap function, $\mathcal{M}_{\mathbf{k}}$ is a matrix defined by the symmetries of the color-superconducting condensate, and $\Lambda_{\mathbf{k}}^{e} = (1 + e\gamma_0 \boldsymbol{\gamma} \cdot \hat{\mathbf{k}})/2$ with $e = \pm$ are projectors onto states of positive or negative energy. In general, $\mathcal{M}_{\mathbf{k}}$ is a matrix in color, flavor, and Dirac space, and it can be chosen such that

$$[\mathcal{M}_{\mathbf{k}}, \Lambda_{\mathbf{k}}^{e}] = 0 \, . \tag{2.26}$$

The matrix $\mathcal{M}_{\mathbf{k}}$ depends implicitly on the order parameter Δ and the basis elements of the special representation of the underlying symmetry groups accounting for the (anti-)symmetry of the representation

$$\mathcal{M}^{-} = I_k \Delta_h^k J^h \gamma_5 \, , \tag{2.27}$$

with the following expressions,

$$I_k \equiv (I_{ij})_k \quad , \quad J^h \equiv (J^{fg})^h \tag{2.28}$$

which are completely antisymmetric 3×3 matrices, constructed from the Levi-Civita tensor $-i\,\epsilon_{ijk}$. In spin-zero CSC the matrix I_k is antisymmetric in color space and J^h is antisymmetric in flavor space. The k and h indices are for the associated color and flavor components respectively. The representation solely depends on the number of flavors, while the choice of the order parameter corresponds to a special phase. This will become more transparent below, when $\mathcal{M}_{\mathbf{k}}$ is specified for several numbers of flavors and several phases, cf. Eq. (2.69). In addition, note that the 4×4 Dirac structure is partially included into $\mathcal{M}_{\mathbf{k}}$ and partially explicitly written via the energy projectors. The Dirac structure of the gap matrix is studied in detail in Ref. [105].

In order to proceed, we write Eq. (2.20) in a simplified form,

$$\begin{aligned}
G^{+} &= ([G_0^{-}]^{-1} + \Sigma^{-}) \Big\{ ([G_0^{+}]^{-1} + \Sigma^{+})([G_0^{-}]^{-1} + \Sigma^{-}) \\
&\quad - \Phi^{-}([G_0^{-}]^{-1} + \Sigma^{-})^{-1}\Phi^{+}([G_0^{-}]^{-1} + \Sigma^{-}) \Big\}^{-1} \, ,
\end{aligned} \tag{2.29}$$

where the free fermion (charge-conjugate) propagator for massless quarks in momentum space is

$$G_0^{\pm}(K) = (\gamma^{\mu} K_{\mu} \pm \mu\gamma_0)^{-1} \, . \tag{2.30}$$

Following Ref. [106], in order to solve the gap equation to subleading order, we have to approximate the diagonal elements of the quark self-energy by

$$\Sigma(K) \equiv \Sigma^+(K) = \Sigma^-(K) \simeq \gamma_0 \, \bar{g}^2 \, k_0 \, \ln \frac{M^2}{k_0^2} \, , \qquad (2.31)$$

where

$$\bar{g} \equiv \frac{g}{3\sqrt{2}\pi} \quad , \quad M^2 \equiv \frac{3\pi}{4} m_g^2 \, , \qquad (2.32)$$

and where at zero temperature the gluon mass parameter (squared) is

$$m_g^2 \equiv \frac{N_f g^2 \mu^2}{6\pi^2} \, . \qquad (2.33)$$

Then, using the ansatz (2.25) for the gap matrix, the second term in curly brackets in Eq. (2.29) is

$$\Phi^-([G_0^-]^{-1} + \Sigma^-)^{-1} \Phi^+([G_0^-]^{-1} + \Sigma^-) = \sum_e |\phi^e(K)|^2 \, L_{\mathbf{k}}^+ \, \Lambda_{\mathbf{k}}^{-e} \, , \qquad (2.34)$$

where

$$L_{\mathbf{k}}^+ \equiv \gamma_0 \, \mathcal{M}_{\mathbf{k}}^\dagger \, \mathcal{M}_{\mathbf{k}} \, \gamma_0 \qquad \text{and} \qquad L_{\mathbf{k}}^- \equiv \mathcal{M}_{\mathbf{k}} \, \mathcal{M}_{\mathbf{k}}^\dagger \, . \qquad (2.35)$$

Moreover, we have

$$[L_{\mathbf{k}}^\pm, \Lambda_{\mathbf{k}}^{\pm e}] = 0 \, . \qquad (2.36)$$

Since $L_{\mathbf{k}}^\pm$ is hermitian, it has real eigenvalues and can be expanded in terms of a complete set of orthogonal projectors $\mathcal{P}_{\mathbf{k},r}^\pm$,

$$L_{\mathbf{k}}^\pm = \sum_r \lambda_r^\pm \, \mathcal{P}_{\mathbf{k},r}^\pm \, , \qquad (2.37)$$

where $\lambda_r^\pm$ are the eigenvalues of $L_{\mathbf{k}}^\pm$. The index r runs over different eigenvalues $\lambda_r^\pm$, i.e., the corresponding projectors $\mathcal{P}_{\mathbf{k},r}^\pm$ project onto $n_r^\pm$-dimensional eigenspaces, where $n_r^\pm \equiv \mathrm{Tr}\mathcal{P}_{\mathbf{k},r}^\pm$ is the degeneracy of the eigenvalue $\lambda_r^\pm$. In general, these eigenvalues depend on the direction of the quark 3-momentum $\mathbf{k}$. In consequence, we have

$$\mathcal{P}_{\mathbf{k},r}^\pm = \prod_{s \neq r}^n \frac{L_{\mathbf{k}}^\pm - \lambda_s^\pm}{\lambda_r^\pm - \lambda_s^\pm} \, , \qquad (2.38)$$

where n is the number of different eigenvalues, cf. Appendix A of [100].

The computation of the full quasiparticle propagator G^+ is now simpler. The fact that the $2n$ projectors $\mathcal{P}_{\mathbf{k},r}^\pm \Lambda_{\mathbf{k}}^\pm$ are orthogonal and form a complete set in color, flavor, and Dirac space leads us easily to invert the term in curly brackets in Eq. (2.29). Using Eqs. (2.29), (2.31), (2.34), and (2.37) we have

$$G^+(K) = \left([G_0^-(K)]^{-1} + \Sigma^-(K)\right) \sum_{e,r} \mathcal{P}_{\mathbf{k},r}^\pm \, \Lambda_{\mathbf{k}}^{-e} \, \frac{1}{[k_0/Z(k_0)]^2 - \left[\epsilon_{k,r}^e(\phi^e)\right]^2} \, , \qquad (2.39)$$

where

$$Z(k_0) \equiv \left(1 + \bar{g}^2 \, \ln \frac{M^2}{k_0^2}\right)^{-1} \qquad (2.40)$$

is the wave function renormalization factor [107]. Also, $\epsilon^e_{k,r}$ defined via

$$\epsilon^e_{k,r}(\phi^e) \equiv \left[(k - e\mu)^2 + \lambda^+_r |\phi^e|^2\right]^{1/2} \tag{2.41}$$

are the excitation energies for quasiparticles, $e = +$, or quasi-antiparticles, $e = -$. As we expect a zero value for the gap yields the excitation energy of the normal phase.

Having evaluated the propagator G^+, Eq. (2.39), we can now derive the gap equation $\Phi^+(K)$ for the gap function $\phi^e(K)$. For that, we have to first evaluate the anomalous propagators Eq. (2.21). Substituting Eq. (2.39) into Eq. (2.21) and using the gap matrix Φ^+ given in Eq. (2.25), we have

$$\Xi^+(K) = -\sum_{e,r} \gamma_0 \mathcal{M}_{\mathbf{k}} \gamma_0 \mathcal{P}^+_{\mathbf{k},r} \Lambda^{-e}_{\mathbf{k}} \frac{\phi^e(K)}{[k_0/Z(k_0)]^2 - \left[\epsilon^e_{k,r}(\phi^e)\right]^2} \; . \tag{2.42}$$

Inserting Eq. (2.42) into Eq. (2.23c), and then multiplying both sides from the right with $\mathcal{M}^\dagger_{\mathbf{k}} \Lambda^e_{\mathbf{k}}$, we evaluate the trace over color, flavor, and Dirac space. To subleading order in the gap equation, it is permissible to use the gluon propagator in the Hard-Dense-Loop (HDL) approximation [108], where it is diagonal in adjoint color space, $\Delta^{\mu\nu}_{ab} = \delta_{ab} \Delta^{\mu\nu}$. The result is

$$\phi^e(K) = g^2 \frac{T}{V} \sum_Q \sum_{e',s} \frac{\phi^{e'}(Q)}{[q_0/Z(q_0)]^2 - \left[\epsilon^{e'}_{q,s}(\phi^{e'})\right]^2} \Delta^{\mu\nu}(K - Q) \mathcal{T}^{ee',s}_{\mu\nu}(\mathbf{k}, \mathbf{q}) \; , \tag{2.43}$$

where the sum over s corresponds to the eigenvalues λ_s, and

$$\mathcal{T}^{ee',s}_{\mu\nu}(\mathbf{k}, \mathbf{q}) \equiv -\frac{\mathrm{Tr}\left[\gamma_\mu T^T_a \gamma_0 \mathcal{M}_{\mathbf{q}} \gamma_0 \mathcal{P}^+_{\mathbf{q},s} \Lambda^{-e'}_{\mathbf{q}} \gamma_\nu T_a \mathcal{M}^\dagger_{\mathbf{k}} \Lambda^e_{\mathbf{k}}\right]}{\mathrm{Tr}\left[\mathcal{M}_{\mathbf{k}} \mathcal{M}^\dagger_{\mathbf{k}} \Lambda^e_{\mathbf{k}}\right]} \; . \tag{2.44}$$

The form (2.43) of the gap equation holds for all cases considered in this thesis. The difference comes from the structure of the term $\mathcal{T}^{ee',s}_{\mu\nu}(\mathbf{k}, \mathbf{q})$. Here, the calculations are in the pure Coulomb gauge,

$$\Delta^{00}(P) = \Delta_\ell(P) \; , \;\; \Delta^{0i}(P) = 0 \; , \;\; \Delta^{ij}(P) = (\delta^{ij} - \hat{p}^i\hat{p}^j)\Delta_t(P) \; , \tag{2.45}$$

where Δ_ℓ and Δ_t are the longitudinal and transverse propagators, respectively, and $P \equiv K - Q$. This means that we only need the 00-component, $\mathcal{T}^{ee',s}_{00}(\mathbf{k}, \mathbf{q})$, and the transverse projection of the ij-components,

$$\mathcal{T}^{ee',s}_t(\mathbf{k}, \mathbf{q}) \equiv -(\delta^{ij} - \hat{p}^i\hat{p}^j)\mathcal{T}^{ee',s}_{ij}(\mathbf{k}, \mathbf{q}) \; , \tag{2.46}$$

The extra minus sign is included for the sake of notational convenience. The rest of the calculations are technical and beyond the scope of this text; the details are available in Ref. [100]. Finally, one finds the following zero-temperature result for the value of the gap ϕ_0 at the Fermi surface

$$\phi_0 = 2 \, b \, b'_0 \, \mu \, \exp\left(-\frac{\pi}{2\bar{g}}\right) \left(\langle\lambda_1\rangle^{a_1} \langle\lambda_2\rangle^{a_2} \langle\lambda_3\rangle^{a_3}\right)^{-1/2} \; , \tag{2.47}$$

where we have set $\lambda_i^+ = \lambda_i$. In this equation, a_1, a_2, and a_3 are positive constants defined by

$$a_s = \frac{n_s \lambda_s}{\sum_r n_r \lambda_r} \ . \tag{2.48}$$

They obey the constraint

$$\sum_s a_s = 1 \ . \tag{2.49}$$

The other constants in Eq. (2.47) are as follows,

$$\tilde{b} \equiv 256\pi^4 \left(\frac{2}{N_f g^2} \right)^{5/2} \quad , \quad b_0' \equiv \exp\left(-\frac{\pi^2 + 4}{8} \right) \quad , \quad b \equiv \tilde{b} \exp(-d) \ . \tag{2.50}$$

The constant d originates from subleading contributions to the gap equation. For spin-zero condensates, in this chapter, due to an accidental cancellation of some of the subleading terms arising from static electric and non-static magnetic gluon exchange, d is zero. In the spin-one cases, this cancellation does not occur and $d \neq 0$, cf. Ref. [109].

2.2.3 Pressure

In order to realise which phase of color-superconducting quark matter is the ground state, we have to calculate the effective potential V_{eff} of each phase. We expect the preferred color-superconducting state to minimise the effective potential. On the other hand, since the thermo-dynamic pressure is the negative of the effective potential (at its stationary point)

$$p = -V_{\text{eff}} \ , \tag{2.51}$$

this is equivalent to finding the state with the largest pressure. The effective action given in Eq. (2.15), cf. also Refs. [33, 110, 111], yields the effective potential as

$$V_{\text{eff}}[D_G, D_F] = -\frac{T}{V} \Gamma[D_G, D_F] \ . \tag{2.52}$$

Here, the two-loop approximation used for $\Gamma_2[D_G, D_F]$, which for the fermionic degrees of freedom, is equivalent to taking into account only the left diagram in Fig. 2.1, as it was in the derivation of the gap equation. If we omit the gluonic part we have

$$\Gamma_2[\Delta, \mathcal{S}] \simeq \frac{1}{4} \text{Tr}(\Sigma \mathcal{S}) \ . \tag{2.53}$$

The stationary point of the effective action $(D_G, D_F) = (\Delta, \mathcal{S})$ is given by the Dyson-Schwinger equations (2.16). Therefore, the fermionic part of the effective action at the stationary point is as follows,

$$\Gamma[\mathcal{S}] = \frac{1}{2} \text{Tr} \ln \mathcal{S}^{-1} - \frac{1}{4} \text{Tr}(1 - \mathcal{S}_0^{-1} \mathcal{S}) \ . \tag{2.54}$$

Performing the trace over Nambu-Gorkov space, we find

$$
\begin{aligned}
\Gamma[\mathcal{S}] &= \frac{1}{2} \text{Tr} \ln \left\{ ([G_0^+]^{-1} + \Sigma^+)\,([G_0^-]^{-1} + \Sigma^-) - \Phi^-\,([G_0^-]^{-1} + \Sigma^-)^{-1}\,\Phi^+\,([G_0^-]^{-1} + \Sigma^-) \right\} \\
&\quad + \frac{1}{4} \text{Tr} \left\{ 2 - G^+ [G_0^+]^{-1} - G^- [G_0^-]^{-1} \right\} \ .
\end{aligned} \tag{2.55}
$$

The regular quark self-energies are given in Eq. (2.31), and the full (charge-conjugate) quark propagators are introduced in Eq. (2.39) where we introduced two sets of projectors $\mathcal{P}_{\mathbf{k},r}^+$ and $\mathcal{P}_{\mathbf{k},r}^-$ which respectively project onto the eigenspaces of the matrices $L_{\mathbf{k}}^+$ and $L_{\mathbf{k}}^-$, respectively. Using the identity

$$[G_0^{\mp}]^{-1}[G_0^{\pm}]^{-1} = \sum_e [k_0^2 - (\mu - e\,k)^2]\Lambda_{\mathbf{k}}^{\pm e} \ , \tag{2.56}$$

the first term on the right-hand side of Eq. (2.55) is written as

$$
\begin{aligned}
\frac{1}{2}\mathrm{Tr}\ln\mathcal{S}^{-1} &= \frac{1}{2}\mathrm{Tr}\ln\sum_e \left[\frac{k_0^2}{Z^2(k_0)} - (\mu - ek)^2 - \phi_e^2 L_{\mathbf{k}}^+\right]\Lambda_{\mathbf{k}}^{-e} \\
&= \frac{1}{2}\sum_{e,r}\sum_K \mathrm{Tr}[\mathcal{P}_{\mathbf{k},r}^+\Lambda_{\mathbf{k}}^{-e}]\ln\left[\frac{k_0^2}{Z^2(k_0)} - (\epsilon_{k,r}^e)^2\right] \ .
\end{aligned}
\tag{2.57}
$$

Performing the Matsubara sum in terms of a contour integration in the complex plane gives

$$\sum_{k_0}\ln\frac{\epsilon_k^2 - k_0^2}{T^2} = \frac{\epsilon_k}{T} + 2\ln\left[1 + \exp\left(-\frac{\epsilon_k}{T}\right)\right] \ , \tag{2.58}$$

The proof of this relation has come in Appendix F of [100]. This relation together with $k_0 \to k_0/Z(k_0)$ yields

$$\frac{1}{2}\mathrm{Tr}\ln\mathcal{S}^{-1} = \frac{1}{2}\frac{V}{T}\sum_{e,r}\int\frac{d^3\mathbf{k}}{(2\pi)^3}\mathrm{Tr}[\mathcal{P}_{\mathbf{k},r}^+\Lambda_{\mathbf{k}}^{-e}]\left\{\tilde{\epsilon}_{k,r}^e + 2\,T\ln\left[1 + \exp\left(-\frac{\tilde{\epsilon}_{k,r}^e}{T}\right)\right]\right\} \ , \tag{2.59}$$

where the trace runs over color, flavor, and Dirac space. In addition, a modified notation for the excitation energy $\tilde{\epsilon}_{\mathbf{k},r}^e \equiv Z(\epsilon_{\mathbf{k},r}^e)\,\epsilon_{\mathbf{k},r}^e$ includes the effect of the regular quark self-energy.

For the second term on the right-hand side of Eq. (2.55) one obtains

$$\frac{1}{4}\mathrm{Tr}(1 - \mathcal{S}_0^{-1}\mathcal{S}) = -\frac{1}{4}\sum_{e,r}\sum_K \mathrm{Tr}[\mathcal{P}_{\mathbf{k},r}^+\Lambda_{\mathbf{k}}^e + \mathcal{P}_{\mathbf{k},r}^-\Lambda_{\mathbf{k}}^{-e}]\,Z^2(k_0)\frac{\lambda_r\,\phi_e^2}{k_0^2 - Z^2(k_0)\,[\epsilon_{k,r}^e]^2} \ . \tag{2.60}$$

In this case, the Matsubara sum can be performed with the help of the relation

$$\sum_{k_0}\frac{\varphi(k_0)}{k_0^2 - \epsilon_k^2} = -\frac{\varphi(\epsilon_k)}{2\epsilon_k}\tanh\frac{\epsilon_k}{2T} \ , \tag{2.61}$$

where φ is an even function of k_0. Therefore, one finds

$$
\begin{aligned}
\frac{1}{4}\mathrm{Tr}(1 - \mathcal{S}_0^{-1}\mathcal{S}) &= \frac{1}{4}\frac{V}{T}\sum_{e,r}\int\frac{d^3\mathbf{k}}{(2\pi)^3}\,\mathrm{Tr}[\mathcal{P}_{\mathbf{k},r}^+\Lambda_{\mathbf{k}}^e + \mathcal{P}_{\mathbf{k},r}^-\Lambda_{\mathbf{k}}^{-e}] \\
&\quad \times Z^2(\tilde{\epsilon}_{k,r}^e)\frac{\lambda_r\,\phi_e^2(\tilde{\epsilon}_{k,r}^e, k)}{2\,\tilde{\epsilon}_{k,r}^e}\tanh\frac{\tilde{\epsilon}_{k,r}^e}{2\,T} \ .
\end{aligned}
\tag{2.62}
$$

Moreover, regardless of the phase we consider, we can easily prove that in general the following relation is valid,

$$\frac{1}{2}\mathrm{Tr}[\mathcal{P}_{\mathbf{k}}^r] = \mathrm{Tr}[\mathcal{P}_{\mathbf{k},r}^+\Lambda_{\mathbf{k}}^e] = \mathrm{Tr}[\mathcal{P}_{\mathbf{k},r}^-\Lambda_{\mathbf{k}}^e] \ . \tag{2.63}$$

Using Eqs. (2.52), (2.54), (2.59) and (2.62), the final result for the pressure p is

$$p \;=\; \frac{1}{4} \sum_{e,r} \int \frac{d^3\mathbf{k}}{(2\pi)^3} \, \mathrm{Tr}[\mathcal{P}_\mathbf{k}^r] \left\{ \tilde\epsilon_{k,r}^e + 2\,T \ln \left[1 + \exp \left(-\frac{\tilde\epsilon_{k,r}^e}{T} \right) \right] \right.$$
$$\left. -Z^2(\tilde\epsilon_{k,r}^e) \, \frac{\lambda_r \, \phi_e^2(\tilde\epsilon_{k,r}^e, k)}{2 \, \tilde\epsilon_{k,r}^e} \, \tanh \frac{\tilde\epsilon_{k,r}^e}{2\,T} \right\} \; . \tag{2.64}$$

At zero temperature, $T = 0$, neglecting the effect of the regular quark self-energy, $Z^2 \simeq 1$, $\tilde\epsilon \simeq \epsilon$ and the antiparticle gap, $\phi_- \simeq 0$, the value of the pressure is calculated via

$$p = \frac{1}{4} \sum_r \int \frac{d^3\mathbf{k}}{(2\pi)^3} \, \mathrm{Tr}[\mathcal{P}_\mathbf{k}^r] \left[\epsilon_{k,r}^+ + \epsilon_{k,r}^- - \frac{\lambda_r \, \phi^2(\epsilon_{k,r}^+, k)}{2 \, \epsilon_{k,r}^+} \right] \; . \tag{2.65}$$

where $\phi \equiv \phi_+$. The integral over the absolute value of the quark momentum is evaluated using the approximation

$$\int_0^\delta d\xi \left(\sqrt{\xi^2 + \phi^2} - \frac{1}{2} \frac{\phi^2}{\sqrt{\xi^2 + \phi^2}} \right) = \frac{1}{2} \delta \sqrt{\delta^2 + \phi^2} = \frac{1}{2} \delta^2 + \frac{1}{4} \phi^2 + O\left(\frac{\phi^4}{\delta^2} \right) \; . \tag{2.66}$$

Eventually, the additional pressure of the color-superconducting phase compared to the normal-conducting phase is derived as

$$\Delta p = \frac{\mu^2}{16\,\pi^2} \phi_0^2 \, \mathrm{Tr}[L_\mathbf{k}^+] \; , \tag{2.67}$$

where ϕ_0 is the value of the gap at the Fermi surface for $T = 0$. In three-flavor, spin-zero color superconductivity the order parameter Δ_h^k, cf. Eq. (2.27), is a 3×3 matrix in color $(k = 1, 2, 3)$ and flavor $(h = 1, 2, 3)$ space. Different order parameters Δ_h^k lead to different gap matrices Φ^+, and thus to different physical states. From Eq. (2.67) we see that the value of the pressure is given in terms of $\mathrm{Tr}[L^+]$ and the value of the gap. Hence, different order parameters also produce in general different values for the pressure. In the following, after introducing the order parameter of each phase we calculate the respective pressure.

2.2.4 A phase

The order parameter of the so-called A phase has the following form, cf. Refs.[100, 10],

$$\Delta_h^k \;=\; \delta^{k3}(\delta_{h1} + i\delta_{h2}) \; . \tag{2.68}$$

where the upper index stands for color and the lower index for flavor, or in another form

$$\Delta = \begin{pmatrix} 0 & 0 & 0 \\ 0 & 0 & 0 \\ 1 & i & 0 \end{pmatrix} \; .$$

In this phase, as we see from the matrix, there is no contribution from blue quarks but all the other quark colors and flavors participate in pairing, i.e. the pairs are $(rd-gs), (rs-gd), (ru-gs),$

and $(rs - gu)$, where r, g, b, u, d, and s stand for $red, green, blue, up, down$, and $strange$ quark, respectively. Utilising the order parameter, the matrix $\mathcal{M}^-$ becomes

$$\mathcal{M}^- = I_3(J^1 + iJ^2)\gamma_5 . \tag{2.69}$$

Inserting this expression in Eq. (2.36) leads to

$$
\begin{aligned}
[L^+]_{ij}^{fg} &= (\delta_{ij} - \delta_{i3}\,\delta_{j3})(2\,\delta^{fg} - \delta^{f1}\,\delta^{g1} \\
&- \delta^{f2}\,\delta^{g2} - i\delta^{f2}\,\delta^{g1} + i\delta^{f1}\,\delta^{g2}) .
\end{aligned}
\tag{2.70}
$$

One should notice that because of the summation rule in Eq. (2.27), the role of the indices is interchanged, so that the upper index stands for flavor and the lower index for color. After some straightforward calculation, one finds that,

$$[L^+]^n = 2^{n-1}\,[L^+] . \tag{2.71}$$

The results for the eigenvalues λ_r come from the roots of the following equation,

$$\det(\lambda - L^+) = 0 , \tag{2.72}$$

The left-hand side of this equation can be rewritten in the form

$$\det(\lambda - L^+) = \exp\left\{\text{Tr}\left[\ln(\lambda - L^+)\right]\right\} . \tag{2.73}$$

which, after expanding the logarithm and making use of Eq. (2.71), gives

$$\lambda^5(\lambda - 2)^4 = 0 . \tag{2.74}$$

This equation yields two different eigenvalues for the A phase,

$$
\begin{cases}
\lambda_1 = 2 & (4 - \text{fold}) \quad \to a_1 = 1 , \\
\lambda_2 = 0 & (5 - \text{fold}) \quad \to a_2 = 0 .
\end{cases}
\tag{2.75}
$$

From Eqs. (2.47) and (2.67) we find the value of the pressure for this phase,

$$\Delta p_{\text{A}} = 4\,\alpha, \tag{2.76}$$

where α is defined as

$$\alpha = \frac{\mu^4}{4\pi^2}\,b^2\,b_0'^{\,2}\,\exp\left(-\frac{\pi}{\bar{g}}\right) . \tag{2.77}$$

2.2.5 A* phase

Here we define a new phase motivated by the order parameter of the A phase and we call it A* phase. This phase is not included in Ref.[100] but was introduced in Ref.[10]. The order parameter of this phase is a transposed form of that in the A phase, i.e., the roles of the color and flavor indices are interchanged,

$$\Delta_h^k = (\delta^{k1} + i\delta^{k2})\delta_{h3} . \tag{2.78}$$

The matrix form of this order parameter is

$$\Delta = \begin{pmatrix} 0 & 0 & 1 \\ 0 & 0 & i \\ 0 & 0 & 0 \end{pmatrix} .$$

In this case, $(gu - bd), (gd - bu), (ru - bd)$, and $(rd - bu)$ are the Cooper pairs making the color superconductivity and there is no contribution of strange quarks. By the same argument which led to this phase one realizes that the corresponding L^+ matrix can be derived by interchanging the color and flavor indices of the matrix L^+ in the A phase,

$$\begin{aligned} [L^+]_{ij}^{fg} &= (2\,\delta_{ij} - \delta_{i1}\,\delta_{j1} - \delta_{i2}\,\delta_{j2} - i\delta_{i2}\,\delta_{j1} \\ &+ i\delta_{i1}\,\delta_{j2})(\delta^{fg} - \delta^{f3}\,\delta^{g3}) . \end{aligned} \tag{2.79}$$

Therefore, one has the same expression for $[L^+]^n$ and the same eigenvalues $\lambda_{1,2}$ given for the A phase, cf. Eqs. (2.71) and (2.75) respectively. Considering Eqs. (2.47) and (2.67), the pressure of this phase is given by

$$\Delta\, p_{A^\star} = 4\,\alpha . \tag{2.80}$$

which is equal to the pressure of the A phase.

2.2.6   Planar or sSC phase

Another experimentally observed phase in superfluid ^{3}He is the so-called planar phase which has the following form for the order parameter

$$\Delta_h^k = \delta_h^k - \delta^{k3}\delta_{h3} , \tag{2.81}$$

where $\Delta_3^3 = 0$ and

$$\Delta = \begin{pmatrix} 1 & 0 & 0 \\ 0 & 1 & 0 \\ 0 & 0 & 0 \end{pmatrix} ,$$

which corresponds to pairings $(gd - bs), (gs - bd), (ru - bs)$, and $(rs - bu)$. As it is clear now, there is not any unpaired quark in this phase. This form of the order parameter is equivalent to the so-called sSC phase in three-flavor CSC, cf. Ref. [112], where the pressure of that phase was calculated including the neutrality condition. After some straightforward but tedious calculation the L^+ matrix for this phase is found to be

$$\begin{aligned} [L^+]_{ij}^{fg} &= 2\,\delta_{ij}\delta^{fg} - \delta^{fg}(\delta_{i1}\delta_{j1} + \delta_{i2}\delta_{j2}) \\ &- \delta_{ij}(\delta^{f1}\delta^{g1} + \delta^{f2}\delta^{g2}) \\ &+ (\delta_{i1}\delta^{f1} - \delta_{i2}\delta^{f2})(\delta_{j1}\delta^{g1} - \delta_{j2}\delta^{g2}) , \end{aligned} \tag{2.82}$$

which gives the following result

$$[L^+]^n = 2^{n-1}\,L^+ + (2^{n-1} - 1)\ell , \tag{2.83}$$

where ℓ is

$$
\begin{aligned}
[\ell]_{ij}^{fg} \;=\;& 2\,(\delta_{i1}\delta^{f1} - \delta_{i2}\delta^{f2})(\delta_{j1}\delta^{g1} - \delta_{j2}\delta^{g2}) \\
&- \delta^{fg}(\delta_{i1}\delta_{j1} + \delta_{i2}\delta_{j2}) \\
&- \delta_{ij}(\delta^{f1}\delta^{g1} + \delta^{f2}\delta^{g2})\,.
\end{aligned}
\tag{2.84}
$$

Then following the method introduced for calculating the eigenvalues of the A phase we derive

$$
\left\{
\begin{array}{llll}
\lambda_1 \;=\; 2 & (2-\text{fold}) & \to a_1 = 1/2\,, \\
\lambda_2 \;=\; 1 & (4-\text{fold}) & \to a_2 = 1/2\,, \\
\lambda_3 \;=\; 0 & (3-\text{fold}) & \to\; a_3 = 0\,.
\end{array}
\right.
\tag{2.85}
$$

The difference between the pressure of the sSC phase and normal conducting matter is found to be

$$
\Delta\, p_{\text{sSC}} \;=\; \frac{8}{2^{1/2}}\,\alpha\,.
\tag{2.86}
$$

2.2.7 Polar or 2SC phase

Analogous to the previous Sec. 2.2.6, the phase called the polar phase for superfluid ^{3}He is analogous to the 2SC phase in CSC,

$$
\Delta_h^k \;=\; \delta^{k3}\delta_{h3}\,,
\tag{2.87}
$$

which gives a zero value for the gaps Δ_1^1 and Δ_2^2 in the following form,

$$
\Delta = \left(
\begin{array}{ccc}
0 & 0 & 0 \\
0 & 0 & 0 \\
0 & 0 & 1
\end{array}
\right),
$$

In this case, there is no chance for blue and strange quarks to have any role in the pairings. The pairs are $(ru - gd)$ and $(rd - gu)$. In the sense that strange quarks do not pair, this phase is similar to the A* phase.. The L^+ matrix of this phase is

$$
[L^+]_{ij}^{fg} \;=\; (\delta_{ij} - \delta_{i3}\,\delta_{j3})(\delta^{fg} - \delta^{f3}\,\delta^{g3})\,,
\tag{2.88}
$$

and yields

$$
[L^+]^n \;=\; L^+\,,
\tag{2.89}
$$

so that with the same methods one arrives at

$$
\left\{
\begin{array}{llll}
\lambda_1 \;=\; 1 & (4-\text{fold}) & \to a_1 = 1\,, \\
\lambda_2 \;=\; 0 & (5-\text{fold}) & \to a_2 = 0\,,
\end{array}
\right.
\tag{2.90}
$$

with the pressure difference equal to

$$
\Delta\, p_{\text{2SC}} \;=\; 4\,\alpha\,.
\tag{2.91}
$$

2.2.8 CFL phase

To make a detailed comparison with the previous results we copy the results given for the CFL phase from Ref. [100]. The order parameter of the CFL phase is

$$\Delta_h^k = \delta_h^k \, , \tag{2.92}$$

The matrix form of this phase

$$\Delta = \begin{pmatrix} 1 & 0 & 0 \\ 0 & 1 & 0 \\ 0 & 0 & 1 \end{pmatrix}$$

clarifies that all quarks play some role in pairing, i.e. $(gd-bs), (gs-bd), (ru-bs), (rs-bu), (ru-gd)$ and $(rd-gu)$ and there is not any ungapped quark in the system. In this sense, this phase is very similar to the sSC phase. The L^+ matrix to calculate the pressure has the following form,

$$[L^+]_{ij}^{fg} = \delta_i^f \, \delta_j^g + \delta^{fg} \, \delta_{ij} \, , \tag{2.93}$$

with the following quantities,

$$\begin{cases} \lambda_1 = 4 & (1-\text{fold}) \quad \to a_1 = 1/3 \, , \\ \lambda_2 = 1 & (8-\text{fold}) \quad \to a_2 = 2/3 \, , \end{cases} \tag{2.94}$$

which are sufficient to find the pressure of this phase,

$$\Delta p_{\text{CFL}} = \frac{12}{2^{2/3}} \, \alpha \, . \tag{2.95}$$

Using all results, one can compare the pressure of the inert phases

$$P_{\text{CFL}} > P_{\text{sSC}} > P_{\text{A}} = P_{\text{A}^*} = P_{\text{2SC}} \, . \tag{2.96}$$

As we see, the pressure of the CFL phase is larger than the pressure of the other phases, i.e., the CFL phase is the dominant phase. Another interesting result is a larger value for the pressure of the sSC phase without the neutrality condition than that for the 2SC phase.

In the next section we calculate the pressure including the neutrality condition. As it was mentioned above, in this case the pressure for some of these inert phases (2SC, sSC, and CFL) was considered in the literature, cf. Ref. [28, 113]. Therefore, in the following we calculate the pressure of only those phases which were still left out, the A and A* phases.

2.3 Pressure including neutrality condition

It is widely believed that the central densities of compact stars are sufficiently hight so that their cores contain color-superconducting quark matter. In addition, it is understood that the bulk of compact stars must be neutral with respect to electric as well as color charges, otherwise the stars could not be bound by gravity which is much weaker than electromagnetism. Moreover, matter inside the stars should remain in β-equilibrium. This condition provides an equal rate in the processes such as $d \to u + e^- + \bar{\nu}_e, u + e^- \to d + \nu_e, s \to u + e^- + \bar{\nu}_e,$ and $u + e^- \to s + \nu_e.$

Therefore, in this section, when we calculate the pressure for the color-superconducting phases, we have to take into account these neutrality conditions.

At the moderate densities existing in the core of compact stars $n \lesssim 10n_0$, the use of the microscopic theory of strong interactions is very limited. In consequence, one has to rely on various effective models of QCD. A very simple type of such a model is the Nambu-Jona-Lasinio (NJL) model with a local four-fermion interaction, see Sec. 1.6. Within this model, in order to consider the neutrality condition, we have to specify the relevant chemical potentials of the system with which the neutrality conditions are satisfied.

The method is as follows. We have to calculate the tadpoles of the system because it is a nonvanishing tadpole that leads to violation of the neutrality of the system. Knowning which tadpoles do not vanish, we introduce the relevant chemical potentials in order to make them vanish [114, 115, 116, 117]. The sum of these chemical potentials together with the quark chemical potential is the relevant chemical potential for the system under color and electric charge neutrality condition. However, one should notice that this works only within the NJL model. In contrast, if we use QCD, the neutrality condition is dynamically realised due to the generation of the gluon condensate $\langle A_i^0 \rangle \neq 0$. In two-flavor CSC, it is found that $\langle A_8^0 \rangle \neq 0$ which is equivalent to having a nonzero value of the chemical potential $\mu_8 \sim g_s \langle A_8^0 \rangle$ [116]. Along this, in the CFL phase, we must also have $\langle A_3^0 \rangle \neq 0$ which means that $\mu_3 \sim g_s \langle A_3^0 \rangle$.

In the following, first, we give a short introduction to the NJL model for color superconductivity. Then, we will indicate how nonzero tadpoles in the system break the neutrality condition. We will calculate the tadpoles of the phases which we consider here. Adding them up to the quark chemical potential, we calculate the pressure of the system.

2.3.1 NJL model for CSC

Since in this work we are interested in physics at non-asymptotic densities, we cannot use weak-coupling methods. Working at zero temperature and high density keeps the fermion sign problem alive and the current methods of lattice QCD can therefore not be employed. For this reason, we need a model in which the interaction between quarks is simplified, while still respecting the symmetries of QCD. The natural choice is to model the interactions between quarks using a point-like four-fermion interaction, the NJL model, which we shall take to have the quantum numbers of single-gluon exchange. On the other hand, from the renormalization group point of view, this is a good approximation since only four-fermion operator are relatively close to the Fermi surface [118]. QCD is not perturbative at intermediate densities. Before improvements in lattice calculations, the NJL model is one of the few alternative models. However, it has several disadvantages. For instance, it fails to capture the dominance of the magnetic gluons and the asymptotic freedom of a gauge theory like QCD.

Originally, the NJL model was a model for interacting nucleons and the confinement was not its main issue, see Sec. 1.6. At the same time, there were indications for the existence of a partially conserved axial vector current meaning the system is chirally symmetric. Since this symmetry is a sign for massless fermions, there must be a theory to explain the large nucleon mass without destroying the symmetry. The idea of the mass gap in the Dirac spectrum in analogy to the energy gap of the superconductor in BCS theory is the solution for this problem which was suggested by Nambu and Jona-Lasinio. The Lagrangian for a quark field ψ with a

point-like, chirally symmetric four fermion-interaction is as following,

$$\mathcal{L} = \bar{\psi}(i\partial\!\!\!/ - m)\psi + G\left\{(\bar{\psi}\psi)^2 + (\bar{\psi}i\gamma_5\vec{\tau}\psi)^2\right\}, \tag{2.97}$$

where m is the bare quark mass, $\vec{\tau}$ is the Pauli matrix in isospin space, and G is a dimensionfull coupling constant. In the mid-eighties, after the developments in QCD, the NJL model was reinterpreted as a schematic model for QCD with point-like quark vertices without gluons [38, 39, 40], thereby, not covering the confinement. Nevertheless, there are many situations where chiral symmetry is the relevant feature of QCD, whereas confinement is less important such as the Goldstone nature of the pion.

The lack of gluons in the NJL model reflects that the $SU(3)_c$ color symmetry is global instead of the local (gauge) color symmetry. Furthermore, this model can be viewed as a result of integrating out heavy gluons from the QCD action. This is possible if the gluons obtain nonzero masses from nonperturbative effects. One arrives at an effective NJL model similar to that in Eq. (2.97) when the gauge fixing in QCD, needed to perform the integration, is consistent with the global color symmetry.

Nowadays, NJL-type models are used for the description of color-superconducting phases [37, 61, 62, 74, 75, 82, 119, 120, 132]. In two-flavor CSC, one of the simplest NJL models that respects the $SU(2)_L \times SU(2)_R$ global chiral symmetry (in the limit $m_i^{(0)} \to 0$), is defined by the following Lagrangian density [121]:

$$\begin{aligned}
\mathcal{L}_{\text{NJL}} &= \bar{\psi}_i^a\left(i\gamma^\mu\partial_\mu + \gamma^0\mu - m_i^{(0)}\right)\psi_i^a + G_S\left[(\bar{\psi}\psi)^2 + (i\bar{\psi}\gamma_5\vec{\tau}\psi)^2\right] \\
&+ G_D(i\bar{\psi}^C\varepsilon\epsilon^a\gamma_5\psi)(i\bar{\psi}\varepsilon\epsilon^a\gamma_5\psi^C).
\end{aligned} \tag{2.98}$$

The matrix C is defined so that $C\gamma_\mu C^{-1} = -\gamma_\mu^T$. Regarding the other notation, $\vec{\tau} = (\tau^1, \tau^2, \tau^3)$ are the Pauli matrices in the flavor space, while $(\varepsilon)^{ik} \equiv \varepsilon^{ik}$ and $(\epsilon^a)^{bc} \equiv \epsilon^{abc}$ are the antisymmetric tensors in flavor and color space, respectively. The dimensionfull coupling constant $G_S = 5.01\,\text{GeV}^{-2}$ and the momentum integration cutoff parameter $\Lambda = 0.65\,\text{GeV}$ (which appears only in loop calculations) are adjusted so that the values of the pion decay constant and the value of the chiral condensate take their standard values in vacuum QCD: $F_\pi = 93$ MeV and $\langle\bar{u}u\rangle = \langle\bar{d}d\rangle = (-250\,\text{MeV})^3$ [121]. The strength of the coupling constant G_D is taken to be proportional to the value of G_S as follows: $G_D = \eta G_S$ where η is a dimensionless parameter of order 1. Note that the value of η is positive which corresponds to having the antisymmetric diquark channel *attractive*. This is motivated by the microscopic QCD interaction, as well as by instanton models [61, 62].

The global color symmetry of the NJL model is broken in the 2SC phase. Then, because of the Goldstone theorem, five massless Nambu-Goldstone bosons should appear in the low-energy spectrum of such a theory. In QCD, however, there is no room for such Nambu-Goldstone bosons. The seeming contradiction is removed by noting that these Nambu-Goldstone bosons are not physical. Their appearance is an artifact of the gauge fixing. In particular, there exist a gauge choice in QCD, namely the unitary gauge, in which these bosons can be completely eliminated.

The gap equation in the NJL model in the mean field approximation looks as follows:

$$\Delta \simeq \frac{4G_D}{\pi^2}\int_0^\Lambda\left(\frac{\Delta}{\sqrt{(p-\mu)^2+\Delta^2}} + \frac{\Delta}{\sqrt{(p+\mu)^2+\Delta^2}}\right)p^2 dp. \tag{2.99}$$

This gap equation can be obtained from a Schwinger-Dyson equation similar to that in QCD in Eq. (2.16) after the gluon long-range interaction is replaced by a local interaction proportional to a constant.

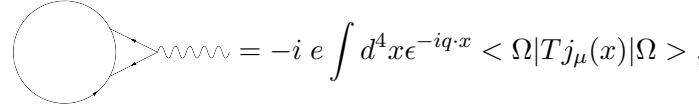The approximate solution to the gap equation in Eq. (2.99) reads

$$\Delta \simeq 2\sqrt{\Lambda^2 - \mu^2} \exp\left(-\frac{\pi^2}{8G_D\mu^2} + \frac{\Lambda^2 - 3\mu^2}{2\mu^2}\right). \tag{2.100}$$

This is very similar to the Bardeen-Cooper-Schrieffer solution in the case of low-temperature superconductivity in solid state physics [3]. As in the Bardeen-Cooper-Schrieffer theory, it has the same type of non-analytic dependence on the coupling constant and the same type of dependence on the density of quasiparticle states at the Fermi surface.

When the quark chemical potential μ takes a value in the range between $400\,\mathrm{MeV}$ and $500\,\mathrm{MeV}$, and the strength of the diquark pairing is $G_D = \eta G_S$ with η between 0.7 and 1, the value of the gap appears to be of order $100\,\mathrm{MeV}$ [61, 62].

2.3.2 Tadpoles

In QED, the tadpoles stand for the diagrams with a one-point function for photon. Note that the external photon must be attached to a QED vertex. Neglecting the external photon propagator we have

$$= -i\,e \int d^4x \epsilon^{-iq\cdot x} < \Omega|Tj_\mu(x)|\Omega >, \tag{2.101}$$

where $j_\mu = \bar{\psi}\gamma_\mu\psi$ is the electromagnetic current operator. In vacuum the expectation value of j_μ must vanish by Lorentz invariance, since otherwise it would be a preferred 4-vector. The photon one-point function also vanishes for a second reason: charge-conjugation invariance. Recall that C is a symmetry of QED, so $C|\Omega >= |\Omega >$. But $j_\mu(x)$ changes sign under charge conjugation, $CJ_\mu(x)C^\dagger = -j_\mu(x)$, so its vacuum expectation value must vanish,

$$< \Omega|Tj_\mu(x)|\Omega >=< \Omega|C^\dagger Cj_\mu(x)C^\dagger C|\Omega >= - < \Omega|Tj_\mu(x)|\Omega >= 0. \tag{2.102}$$

As we explained in the introduction of this chapter, bulk matter in neutron stars has to be neutral with respect to color (and electric) charges. This neutrality condition plays an important role in the determination of the phase structure of cold dense quark matter. In QCD, however, color neutrality is enforced automatically by the dynamics of the gluons [98, 114, 116]. The gluon field acquires a nonvanishing expectation value, which acts as an effective chemical potential for the color charge. This expectation value can be computed from the Yang-Mills equation [116],

$$\frac{\delta\Gamma}{\delta A_0^a}|_{A=\tilde{A}} \tag{2.103}$$

where Γ is the effective action, and $\tilde{A}$ is the expectation value of the gluon filed. On the other hand, $\tilde{A}$ can be computed perturbatively from the tadpole diagram

$$\mathcal{T}^a = \frac{\delta\Gamma}{\delta A_0^a}|_{A=0} \tag{2.104}$$
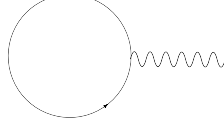
Figure 2.3: The tadpole diagram. Curly line is for gluon and solid line for quark.

by attaching and external gluon propagator.

In addition, using the NJL model, color neutrality has to be imposed as an external condition [80, 81, 83, 84, 85]. In fact, in a color superconductor the gluon field acquires a non-vanishing expectation value [98, 114, 116]. The leading order contribution to this expectation value can be computed from the one-loop gluon tadpole diagram Fig. 2.3.

In the following, we look for tadpoles of each phase. If we find any, therefore, we have to find also the relevant chemical potential via which the tadpole is vanished.

2.3.3 Calculation of tadpoles

In order to compute the tadpoles of a system we use Eq. (19) of Ref. [114],

$$\mathcal{T}^a = -\frac{g}{2} \int \frac{d^4 Q}{i(2\pi)^4} \mathrm{Tr}_{D,c,f}[\Gamma_0^a G^+(Q) + \bar{\Gamma}_0^a G^-(Q)] . \tag{2.105}$$

Here $\Gamma_0^a = \gamma_0 T^a$, $\bar{\Gamma}_0^a = -\gamma_0 (T^a)^T$ with $T^a = \lambda^a/2$ for $a = 1, \ldots, 8$ where λ^a are the Gell-Mann matrices in flavor space, and $G^{\pm}$ are the fermion propagators for quasiparticles and charge-conjugate quasiparticles,

$$G^{\pm}(Q) \equiv ([G_0^{\pm}]^{-1} - \Sigma^{\pm})^{-1} \ , \ \ \Sigma^{\pm} \equiv \mathcal{M}^{\mp} G_0^{\mp} \mathcal{M}^{\pm} . \tag{2.106}$$

In these equations, $\Sigma^{\pm}$ is the quark self-energy generated by exchanging particles or charge conjugate particles with the condensate. The role of different phases appears in the quark self-energy via the matrix $\mathcal{M}^{\mp}$, cf. Eq.(2.27). In the next subsections, 2.3.4 and 2.3.5, we insert the order parameter of each phase into $\mathcal{M}^{\mp}$ to find the tadpoles.

2.3.4 Tadpoles in A phase

In Eq.(2.105) we first evaluate the trace over color and flavor space, and afterwards the trace over the Dirac space. The inverse free fermion propagator for quarks $([G_0^{\pm}]^{-1})_{ij}^{fg}$ is given in Eq. (2.9) has the following color and flavor structure,

$$([G_0^{\pm}]^{-1})_{ij}^{fg} = (\gamma^{\mu} K_{\mu} \pm \hat{\mu}\gamma_0 - \hat{M})\delta^{fg}\delta_{ij} , \tag{2.107}$$

Using Eq. (2.69) yields

$$\begin{aligned}
(\Sigma^{\pm})_{ij}^{fg} &\equiv (\mathcal{M}^{\mp} G_0^{\mp} \mathcal{M}^{\pm})_{ij}^{fg} = \gamma_5 \frac{\Delta^2}{\gamma^{\mu} k_{\mu} \mp \hat{\mu}\gamma_0 - \hat{\mathcal{M}}} \\
&\times \gamma_5 (\delta^{fg} - \delta^{f3}\delta^{g3})(2\,\delta_{ij} - \delta_{i1}\delta_{j1} - \delta_{i2}\delta_{j2} \\
&\pm i\delta_{i2}\delta_{j1} \mp i\delta_{i1}\delta_{j2}) ,
\end{aligned} \tag{2.108}$$

where Δ is the value of the gap for this phase. After some algebraic calculation, one can find the color and flavor structure of the propagator $G^{\pm}(Q)$ as,

$$
\begin{aligned}
[G^{\pm}]_{ij}^{fg} &= ([G_0^{\pm}]^{-1} - 2\gamma_5 \, G^{\mp}\gamma_5\Delta^2)^{-1}(\delta^{fg} - \delta^{f3}\delta^{g3})\delta_{ij} \\
&+ [G_0^{\pm}]\delta^{f3}\delta^{g3}\delta_{ij} - ([G_0^{\pm}]^{-1} - 2\gamma_5 \, G^{\mp}\gamma_5\Delta^2)^{-1} \\
&\times (\gamma_5 \, G^{\mp}\gamma_5\Delta^2)[G_0^{\pm}](\delta^{fg} - \delta^{f3}\delta^{g3}) \\
&\times (\delta_{i1}\delta_{j1} + \delta_{i2}\delta_{j2} \pm i\delta_{i1}\delta_{j2} \mp i\delta_{i2}\delta_{j1}) \, .
\end{aligned}
\tag{2.109}
$$

Now one has to put these equations back into Eq. (2.105) and evaluate the traces. By doing so, it is revealed that all components of $\mathcal{T}^a$ are zero except for $a = 8$. This forces us to introduce a chemical potential μ_8 for the system to make the tadpole vanish and achieve color and electric charge neutrality.

2.3.5 Tadpoles in A* phase

Following the same procedure for calculating the tadpoles of the A phase, the color and flavor structure of the propagator $G^{\pm}(Q)$ is given by

$$
\begin{aligned}
[G^{\pm}]_{ij}^{fg} &= ([G_0^{\pm}]^{-1} - 2\gamma_5 \, G^{\mp}\gamma_5\Delta^2)^{-1}(\delta_{ij} - \delta_{i3}\delta_{j3})\delta^{fg} \\
&+ [G_0^{\pm}]\delta_{i3}\delta_{j3}\delta^{fg} - ([G_0^{\pm}]^{-1} - 2\gamma_5 \, G^{\mp}\gamma_5\Delta^2)^{-1} \\
&\times (\gamma_5 \, G^{\mp}\gamma_5\Delta^2)[G_0^{\pm}](\delta_{ij} - \delta_{i3}\delta_{j3}) \\
&\times (\delta^{f1}\delta^{g1} + \delta^{f2}\delta^{g2} \pm i\delta^{f1}\delta^{g2} \mp i\delta^{f2}\delta^{g1}) \, .
\end{aligned}
\tag{2.110}
$$

This form of the full fermion propagator yields a nonzero value for the $a = 2$ and $a = 8$ tadpoles. Hence, for this phase the chemical potential has to contain μ_2 and μ_8 to provide neutrality.

Now one is able to calculate the pressure.

2.3.6 Pressure

The QCD grand partition function can be written as

$$
\mathcal{Z} \equiv \mathrm{e}^{-\Omega V/T} = \int \mathcal{D}\bar{\psi}\mathcal{D}\psi \, \mathrm{e}^{i \int_X \left(\mathcal{L} + \bar{\psi}\hat{\mu}\gamma^0\psi\right)} \, ,
\tag{2.111}
$$

where we have slightly modified the function taking the chemical potential μ out of the Lagrangian. Here, $\mathcal{L}$ is the Lagrangian density for three-flavor quark matter again for a local NJL-type interaction

$$
\begin{aligned}
\mathcal{L} &= \bar{\psi}\left(i\slashed{\partial} - \hat{m}\right)\psi + G_S \sum_{a=0}^{8}\left[\left(\bar{\psi}\lambda_a\psi\right)^2 + \left(\bar{\psi}i\gamma_5\lambda_a\psi\right)^2\right] \\
&+ G_D \sum_{k,h}\left[\bar{\psi}_i^f i\gamma_5\epsilon^{ijk}\epsilon_{fgh}(\psi_C)_j^g\right]\left[(\bar{\psi}_C)_\rho^r i\gamma_5\epsilon^{\rho\sigma k}\epsilon_{rsh}\psi_\sigma^s\right] \\
&- K\left\{\det_F\left[\bar{\psi}\left(1 + \gamma_5\right)\psi\right] + \det_F\left[\bar{\psi}\left(1 - \gamma_5\right)\psi\right]\right\} \, ,
\end{aligned}
\tag{2.112}
$$

where the quark spinor field ψ_i^f carries color ($i = r, g, b$) and flavor ($f = u, d, s$) indices. The matrix of quark current masses is given by $\hat{m} = \mathrm{diag}_F(m_u, m_d, m_s)$ and $\lambda_0 \equiv \sqrt{2/3}\, b f 1_F$. Note that we include the 't Hooft interaction whose strength is determined by the coupling constant K. This term breaks the $U(1)$ axial symmetry.

The term in the second line of Eq. (2.112) describes a scalar diquark interaction in the color-antitriplet and flavor-antitriplet channel. For symmetry reasons there should also be a pseudoscalar diquark interaction with the same coupling constant but for the sake of simplicity we do not consider it here.

We use the following set of model parameters [122]:

$$m_{u,d} = 5.5\ \mathrm{MeV}\ , \tag{2.113}$$

$$m_s = 140.7\ \mathrm{MeV}\ , \tag{2.114}$$

$$G_S \Lambda^2 = 1.835\ , \tag{2.115}$$

$$K \Lambda^5 = 12.36\ , \tag{2.116}$$

$$\Lambda = 602.3\ \mathrm{MeV}\ . \tag{2.117}$$

Here, we study the regime of intermediate coupling strength with $G_D = \frac{3}{4} G_S$.

All quarks carry baryon charge $1/3$ and thus have a diagonal contribution $\mu \delta^{fg} \delta_{ij}$ to their matrix of chemical potentials. By definition $\mu = \mu_B/3$ with μ_B being the baryon chemical potential. In order to fulfil the neutrality condition one has to take into account the chemical potentials introduced in the previous sections, cf. 2.3.4 and 2.3.5. For the A phase one has

$$\mu_{ij}^{fg} = \left(\mu \delta^{fg} + \mu_Q Q_F^{fg} \right) \delta_{ij} + \mu_8 \left(T_8 \right)_{ij} \delta^{fg}\ , \tag{2.118}$$

and for the A* phase

$$\mu_{ij}^{fg} = \left(\mu \delta^{fg} + \mu_Q Q_F^{fg} \right) \delta_{ij} + \left(\mu_2 \left(T_2 \right)_{ij} + \mu_8 \left(T_8 \right)_{ij} \right) \delta^{fg}\ , \tag{2.119}$$

where μ_Q is the chemical potential of the electric charge and Q_F is the electric charge matrix $Q_F = \mathrm{diag}_F(\frac{2}{3}, -\frac{1}{3}, -\frac{1}{3})$.

In order to calculate the mean-field thermodynamic potential at temperature T, one has to linearise the interaction in the presence of the diquark condensates $\Delta_h^k \sim (\bar{\psi}_C)_i^f i \gamma_5 \epsilon^{ijk} \epsilon_{fgh} \psi_j^g$ and the quark-antiquark condensates $\sigma_\alpha \sim \bar{\psi}_\alpha^a \psi_\alpha^a$ (no sum over α). Then, integrating out the quark fields and neglecting the fluctuations of composite order parameters gives the following expression for the thermodynamic potential:

$$\begin{aligned}
\Omega = {}& \Omega_L + \frac{1}{4 G_D} \sum_{k,h=1}^3 \left| \Delta_h^k \right|^2 + 2 G_S \sum_{\alpha=1}^3 \sigma_\alpha^2 \\
& - 4 K \sigma_u \sigma_d \sigma_s - \frac{T}{2V} \sum_K \ln \det \frac{S^{-1}}{T}\ ,
\end{aligned} \tag{2.120}$$

Here we added the lepton contribution Ω_L. The inverse full quark propagator S^{-1} in the Nambu-Gorkov representation is

$$S^{-1} = \begin{pmatrix} [G_0^+]^{-1} & \mathcal{M}^- \\ \mathcal{M}^+ & [G_0^-]^{-1} \end{pmatrix}\ . \tag{2.121}$$

The constituent-quark mass matrix in the inverse propagator of quarks and charge-conjugate quarks, cf. Eq.(2.107), is defined as $\hat{M} = \text{diag}_F(M_u, M_d, M_s)$ with

$$M_\alpha = m_\alpha - 4G_S\sigma_\alpha + 2K\sigma_\beta\sigma_\gamma \, , \tag{2.122}$$

where the set of indices (α, β, γ) is a permutation of (u, d, s).

The off-diagonal components of the inverse propagator in Eq. (2.121) are given in Eq. (2.27) in terms of the diquark condensates Δ_h^k. The color- and flavor-symmetric condensates are neglected here because they are small and not crucial for the qualitative understanding of the phase diagram [87].

The inverse quark propagator is a 72×72 matrix. It was shown in the Appendix A of Ref. [28] that for a real-valued order parameter this matrix contains a two-fold spin and Nambu-Gorkov degeneracy. Then, it is sufficient to evaluate its 18 nondegenerate eigenvalues ϵ_i,

$$\det \frac{S^{-1}}{T} = \prod_{i=1}^{18} \left(\frac{\omega_n^2 + \epsilon_i^2}{T^2} \right)^2 \, . \tag{2.123}$$

However, for a complex-valued order parameter, which is the case for the A and A* phases, cf. Eqs. (2.68) and (2.78), one has to decompose the inverse propagator matrix into a real and an imaginary part to use the simplest numerical recipes. This doubles the dimension of the complex propagator matrix. Since one has to find the determinant of this matrix one can transform the matrix to a block-diagonal form without losing anything. After that, one separates the nondegenerate eigenvalues and follow the same procedure for a real-valued order parameter. We find the same degeneracies for the inverse quark propagator as in the case of real-valued order parameters. Therefore at the end, the number of the non-degenerate eigenvalues ϵ_i decreases again to 18. With $p \equiv -\Omega$ we find

$$
\begin{aligned}
p &= \frac{1}{2\pi^2} \sum_{i=1}^{18} \int_0^\Lambda \mathrm{d}k \, k^2 \left[|\epsilon_i| + 2T \ln \left(1 + \mathrm{e}^{-\frac{|\epsilon_i|}{T}} \right) \right] \\
&+ 4K\sigma_u\sigma_d\sigma_s - \frac{1}{4G_D} \sum_{k,h=1}^3 \left| \Delta_h^k \right|^2 - 2G_S \sum_{\alpha=1}^3 \sigma_\alpha^2 \\
&+ \frac{T}{\pi^2} \sum_{l=e,\mu} \sum_{\epsilon=\pm} \int_0^\infty \mathrm{d}k \, k^2 \ln \left(1 + \mathrm{e}^{-\frac{E_l - \epsilon\mu_l}{T}} \right) \, ,
\end{aligned}
\tag{2.124}
$$

where the contribution of electrons and muons with masses $m_e \approx 0.511$ MeV and $m_\mu \approx 105.66$ MeV are included. The expression for the pressure in Eq. (2.124) has a physical meaning only when the chiral and color-superconducting order parameters, σ_α and Δ_h^k, satisfy the following set of equations:

$$\frac{\partial p}{\partial \sigma_\alpha} = 0 \, , \tag{2.125}$$

$$\frac{\partial p}{\partial \Delta_h^k} = 0 \, . \tag{2.126}$$
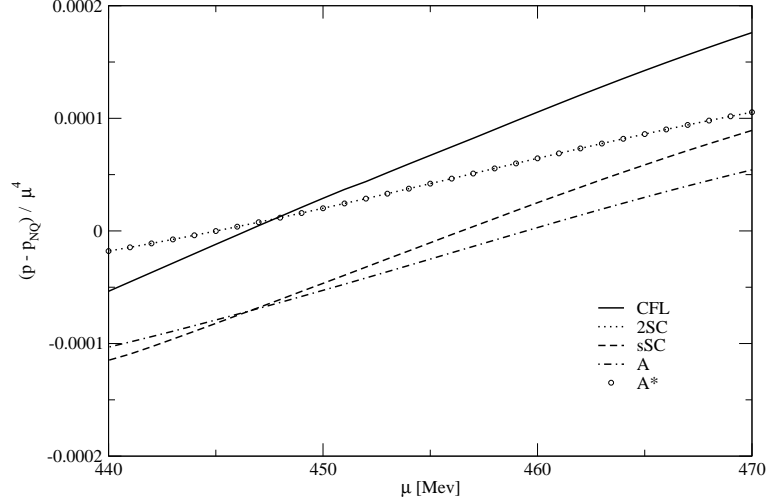
Figure 2.4: Pressure divided by μ^4 for the different neutral solutions of the gap equation at $T = 0$ as a function of the quark chemical potential μ. The diquark coupling strength is $G_D = \frac{3}{4} G_S$.

In order to enforce the condition of local charge neutrality in dense matter, for the A phase one has to require that

$$n_Q \equiv \frac{\partial p}{\partial \mu_Q} = 0 , \qquad (2.127)$$

$$n_8 \equiv \frac{\partial p}{\partial \mu_8} = 0 , \qquad (2.128)$$

and for the A* phase

$$n_Q \equiv \frac{\partial p}{\partial \mu_Q} = 0 , \qquad (2.129)$$

$$n_2 \equiv \frac{\partial p}{\partial \mu_2} = 0 , \qquad (2.130)$$

$$n_8 \equiv \frac{\partial p}{\partial \mu_8} = 0 . \qquad (2.131)$$

By these equations the chemical potentials μ_Q, μ_2, and μ_8 are fixed, but the quark chemical potential μ is left as a free parameter.

The difference between the pressure p of different phases and the pressure of normal quark matter p_{NQ} versus the chemical potential μ at zero temperature is depicted in Fig. 2.4. One observes that at large chemical potentials the pressure for the A and the A* phases is less than that for the CFL phase. Also the pressure of the sSC phase, which in the case that we did not enforce the neutrality condition was larger than that for the 2SC phase, is smaller in

this case. Therefore, in this circumstances the CFL phase is again the ground state of matter. Furthermore, the pressure of the A phase is smaller than that for the other phases. At smaller chemical potentials the 2SC/A* phase wins over the CFL phase.

Another interesting result comes from comparing the pressure of the 2SC and the A* phase. One observes that as before, cf. Eq. (2.96), their pressures are exactly equal for all values of the chemical potential. The question arises whether the A* phase is a different form of the 2SC phase? To answer that, one has to consider the order parameter of these phases and find a unitary transformation between these two phases. The order parameter in three-flavor, spin-zero color superconductivity is a 3×3 matrix in color and flavor space. Because of the different masses of the quark flavors one cannot find a unitary matrix in this space which transforms the A*(2SC) phase matrix into the 2SC (A*) phase matrix, but it is possible to investigate this in color space. The spinor fields in the Lagrangian, Eq. (2.112), are changed under a color transformation $U = \exp(-i\omega^\alpha \lambda^\alpha)$ as,

$$\psi \quad \rightarrow \quad U\,\psi \ , \tag{2.132}$$

$$\overline{\psi} \quad \rightarrow \quad \overline{\psi}\,U^\dagger \ , \tag{2.133}$$

$$\psi^c \quad \rightarrow \quad U^*\,\psi^c \ , \tag{2.134}$$

$$\overline{\psi^c} \quad \rightarrow \quad \overline{\psi^c}\,U^T \ , \tag{2.135}$$

with which the expression in the second line of Eq. (2.112),

$$\sum_{k,h} (\bar\psi_C)^r_\rho i\gamma_5 \epsilon^{\rho\sigma k}\epsilon_{rsh}\psi^s_\sigma \quad \equiv \quad (\bar\psi_C)^r_\rho i\gamma_5(\epsilon^{\rho\sigma 1} + i\epsilon^{\rho\sigma 2})\epsilon_{rs\,3}\psi^s_\sigma$$

$$= \quad (\bar\psi_C)^r_\rho i\gamma_5(\lambda_5 + i\lambda_7)^{\rho\sigma}\epsilon_{rs\,3}\psi^s_\sigma \ , \tag{2.136}$$

transforms into

$$(\bar\psi_C)^r_\rho i\gamma_5\, U^T\,(\lambda_5 + i\lambda_7)^{\rho\sigma}U\epsilon_{rs\,3}\psi^s_\sigma \ . \tag{2.137}$$

Hence, one has to find a unitary matrix U which changes the last expression to that in the 2SC phase,

$$(\bar\psi_C)^r_\rho i\gamma_5\,(\lambda_2)^{\rho\sigma}\,\epsilon_{rs\,3}\psi^s_\sigma \ . \tag{2.138}$$

The relevant matrix is

$$U = e^{i\pi(\lambda_5+\lambda_6)/2\sqrt{2}} \ , \tag{2.139}$$

by which one has

$$U^T\,(\lambda_5 + i\lambda_7)U \ \rightarrow \ i\sqrt{2}\lambda_2 \ . \tag{2.140}$$

Using Eq. (2.111) one observes that

$$\bar\psi\,U^\dagger\hat\mu^{A^*}\,U\gamma^0\psi \ \rightarrow \ \bar\psi\hat\mu^{2SC}\,\gamma^0\psi \ , \tag{2.141}$$

and the following results are derived,

$$\mu_2^{A^*} \quad \equiv \quad -\frac{\sqrt{3}}{2}\,\mu_8^{2SC} \ ,$$

$$\mu_8^{A^*} \quad \equiv \quad -\frac{1}{2}\,\mu_8^{2SC} \ . \tag{2.142}$$

We conclude that the A* phase is the same as the 2SC phase. This was not the case for superfluid ^{3}He, cf. Ref. [10].

In the next section we briefly mention the result derived for the symmetry pattern of the A* and 2SC phases and then investigate the generators of the symmetry groups for the A* phase in terms of those in the 2SC phase.

2.4 Pattern of symmetry breaking

The study of the order parameter of the A* phase reveals that just like the 2SC phase the strange quark does not participate in pairing. Thus, the A* phase is a two-flavor CSC phase. Without including the neutrality condition and in the case that all the quark masses are zero, the initial symmetry group for the A* phase is the same as the 2SC phase

$$G = SU(3)_c \otimes SU(2)_L \otimes SU(2)_R \otimes U(1)_B \otimes U(1)_{em} , \qquad (2.143)$$

where $SU(3)_c$ is the color gauge group and $SU(2)_L$ and $SU(2)_R$ are the representations of the flavor group. $U(1)_B$ and $U(1)_{em}$, respectively, are accounting for baryon number conservation symmetry and the electromagnetic gauge group. The order parameter Δ is an element of a representation of G. After pairing, the group G is spontaneously broken to a residual subgroup $H \subseteq G$ so that any transformation $g \in H$ leaves the order parameter invariant,

$$g(\Delta) = \Delta . \qquad (2.144)$$

To find all possible order parameters and the corresponding residual groups H one has to satisfy this invariance condition. Here we restrict the calculations to those which lead to the residual group of the A* phase. Using the method given in Ref. [10, 123] we find that

$$H_{A^*} = SU(2)_c \otimes SU(2)_L \otimes SU(2)_R \otimes \tilde{U}(1)_B \otimes \tilde{U}(1)_{em} , \qquad (2.145)$$

which is exactly the same residual group as for the 2SC phase. This result confirms the equivalence of the A* phase with the 2SC phase from this point of view. To complete this subsection, utilising the results of the previous section and knowing the generators for the residual group of the 2SC phase, we want to find the corresponding generators for the A* phase. In the 2SC phase the generator of baryon number conservation is

$$\tilde{B} = B - \frac{2}{\sqrt{3}} T_8 , \qquad (2.146)$$

and that for an unbroken $\tilde{U}(1)_{em}$ is

$$\tilde{Q} = Q - \frac{1}{\sqrt{3}} T_8 . \qquad (2.147)$$

Under the same color transformation for which the A* phase goes to the 2SC phase, Eq. (2.139), one finds the generators for the residual group of the A* phase,

$$\tilde{B}' = B + (T_2 + \frac{1}{\sqrt{3}} T_8) , \qquad (2.148)$$

$$\tilde{Q}' = Q + \frac{1}{2}(T_2 + \frac{1}{\sqrt{3}} T_8) , \qquad (2.149)$$

which is a linear combination of generators of the 2SC phase.

Chapter 3

Gluon self-energy in CFL phase

In the second chapter we calculated the pressure of the so-called inert phases in three-flavor color superconductivity in two different scenarios. First, using QCD we found that the CFL phase is the dominant phase for all values of μ at zero temperature. Second, we used the NJL model to find the ground state of matter in neutron stars. Since neutron stars have to be color and electric charge neutral, we had to impose the neutrality condition. Similarly, we realised that the CFL phase occupies a large area of the phase diagram of the matter in the color-superconducting state.

Knowing that, so far, the CFL phase is the most important phase of color superconductivity it is then very interesting to study the gluon self-energy in this state of matter [124]. Giving the ingredients needed for the explicit calculation of the self-energy, we proceed further to evaluate the relevant spectral densities and also dispersion relations.

3.1   Introduction

In the previous chapters, we presented many similarities between electric and color superconductors. There are, however, also fundamental differences between color and BCS superconductivity. First of all, the BCS superconductor requires the presence of an atomic lattice with phonons that cause electrons to form Cooper pairs. On the other hand, in QCD gluons themselves cause quarks to condense. Another difference is that in the BCS theory the zero-temperature gap depends on the BCS coupling constant G as $\phi_0 \sim \mu \exp(-c_{\mathrm{BCS}}/G^2)$ [125, 126], where μ is the chemical potential, and c_{BCS} =const., while in a color superconductor, $\phi_0 \sim \mu \exp(-c_{\mathrm{QCD}}/g)$ [77, 127], where g is the QCD coupling constant, and $c_{\mathrm{BCS}} \neq c_{\mathrm{QCD}} =$ const.

The physical reason for the change in the parametric dependence on the coupling constant c_{QCD} is that, because gluons are massless, gluon-mediated interactions are long-range, in contrast to the BCS theory, where phonon exchange is typically assumed to be a point-like interaction [125, 126]. The long-range nature of gluon exchange manifests itself in the infrared singular behaviour of the gluon propagator. This enhances the contribution of very soft, collinear gluons in the gap equations [78, 128], and causes the $1/g$ in the exponent, instead of a $1/g^2$ which would appear if gluons were massive [105], or gluon exchange a point-like interaction as assumed in the NJL-type approaches to color superconductivity.

The value of c_{QCD} depends on the form of the gluon propagator in the cold, dense quark medium. If one takes the gluon propagator in the standard "hard dense loop" (HDL) approximation [129], one obtains $c_{\mathrm{QCD}} = 3\,\pi^2/\sqrt{2}$ [77]. Within this approximation, the quarks inside the HDL's are assumed to be in the normal, and not the color-superconducting phase. Consequently, an important question that has to be addressed is how color superconductivity influences the propagation of gluons and whether this could change c_{QCD}.

In a two-flavor color superconductor, condensation of Cooper pairs in a channel of total spin $J = 0$ breaks $SU(3)_c$ to $SU(2)_c$. Then, the three gluons corresponding to the generators of the unbroken $SU(2)_c$ subgroup are expected to remain massless, while the other five should attain a mass through the Anderson–Higgs mechanism.

On the other hand, in a three-flavor color superconductor the color and flavor $SU(3)_c \times U(3)_V \times U(3)_A$ symmetry is broken to the diagonal subgroup $SU(3)_{c+V}$. This locks color and flavor rotations [66]. Out of 18 Goldstone bosons resulting from symmetry breaking, eight get "eaten" by the gluons, which consequently become massive.

Furthermore, similar to the mixing of weak and electromagnetic gauge bosons in the standard model, the electromagnetic field is mixed with the eighth gluon to form a modified photon, under which the color-superconducting condensate is electrically neutral. The mass of the modified eighth gluon becomes slightly larger than that of the other seven. However, the mixing angle as well as the increase in mass is determined by the ratio of electromagnetic and strong coupling constants and consequently quite small. Therefore, effects from electromagnetism will be neglected throughout the following.

Here we derive a general expression for the quark contribution to the gluon self-energy. For electric gluons, the limit where the gluon energy $p_0 = 0$ and the gluon momentum $p \to 0$ gives the Debye mass, while for magnetic gluons, it gives the Meissner mass. In comparison, the limit where $p_0 = 0$ but $p \gg \phi_0$ the gluon momentum is large enough to resolve individual quarks in a Cooper pair; consequently, the Debye masses approach their values in the normal phase and the Meissner effect vanishes.

Debye screening of static color-electric fields and the Meissner effect for static color-magnetic fields are in principle quite analogous to Debye screening and the Meissner effect for electromagnetic fields in ordinary superconductors [125, 126]. However, the somewhat more complicated color and flavor structure of a quark-quark condensate in comparison to an electron-electron condensate gives rise to an additional degree of complexity. While studying these effects in a color superconductor is interesting in itself, they might have, however, far greater implications for color superconductivity than the corresponding effects in ordinary superconductors: unlike photons, gluons themselves are responsible for condensation of quark pairs. The modification of the gluon self-energy in the superconducting phase directly enters the gap equation through the gluon propagator, and so might change the value for the gap. On the other hand, the influence of the photon self-energy on electron condensation is at best a higher order effect.

Although effects from quark condensation in the gluon propagator vanish for large gluon energies and momenta, one can *a priori* not exclude that they will not change the solution of the gap equations. For instance, to assess the importance of the Meissner effect, note that, in the HDL approximation, the main contribution to the gap equations comes from color-magnetic fields with momenta $p \sim (m_g^2\,\phi_0)^{1/3} \gg \phi_0$, where m_g is the gluon mass [77, 78, 128, 130]. As will be seen below, the Meissner effect is small, but not absent, at the same momentum scale. This

means that the Meissner effect can indeed influence the solution of the gap equation. A first estimate of this effect (neglecting the color-flavor structure of the condensate and considering only the dominant contribution to the gluon self-energy) was given in Ref. [131], and a reduction of the zero-temperature gap was found.

Furthermore, in a dense (or hot) medium, however, even *without* spontaneous breaking of the gauge symmetry the gauge bosons already have a longitudinal degree of freedom, the so-called *plasmon* mode [129]. Its appearance is related to the presence of gapless charged quasiparticles. Both transverse and longitudinal modes exhibit a mass gap, *i.e.*, the gluon energy $p_0 \to m_g > 0$ for momenta $p \to 0$. It is *a priori* unclear how the Nambu-Goldstone bosons interact with these longitudinal gluon modes. In particular, it is of interest to know whether coupling terms between these modes exist and, if yes, whether these terms can be eliminated by a suitable choice of ('t Hooft) gauge. The aim of this chapter is to address these questions. We shall show that the answer to both questions is "yes". Then, we proceed to find the spectrum of the imaginary and real part of gluon self-energy for a given momentum. Employing the results, we find the spectral densities and the dispersion relations.

3.2 Generating functional

As we explained in the second chapter, the generating functional for QCD with N_f quark flavors, suppressing the renormalization factors, is

$$\mathcal{Z}[J] \;=\; \int \mathcal{D}U[A] \, \exp\left[\int_x \left(\mathcal{L}_A + J^a_\mu A^\mu_a \right) \right] \, \mathcal{Z}[A] \; , \tag{3.1}$$

where

$$\mathcal{Z}[A] \;=\; \int \mathcal{D}\bar{\psi}\,\mathcal{D}\psi \, \exp\left\{ \int_x \left[\bar{\psi} \left(i\gamma^\mu \partial_\mu + \mu\gamma_0 - m + g\gamma^\mu A^a_\mu T_a \right) \psi \right] \right\} \; . \tag{3.2}$$

Here, the matrix of quark masses m_f is denoted as $m \equiv \mathrm{diag}(m_1, m_2, \ldots, m_{N_f})$, and because we are not concerned with the neutrality condition, μ_f has the same value for all quark flavors. Thus, the $N_f \times N_f$ chemical potential matrix is $\mu \equiv \mathrm{diag}(\mu_1, \mu_2, \ldots, \mu_{N_f})$. Moreover, the Lagrangian for the gauge fields in Eq. (3.1) contains three parts,

$$\mathcal{L}_A = \mathcal{L}_{F^2} + \mathcal{L}_{gf} + \mathcal{L}_{FPG} \; , \tag{3.3}$$

where

$$\mathcal{L}_F = -\frac{1}{4} F^{\mu\nu}_a F^a_{\mu\nu} \tag{3.4}$$

is the gauge field part, $F^a_{\mu\nu} = \partial_\mu A^a_\nu - \partial_\nu A^a_\mu + g f^{abc} A^b_\mu A^c_\nu$ is the field strength tensor. When we are calculating the gluon self-energy, we do not have to specify the gauge fixing, $\mathcal{L}_{\mathrm{gf}}$, and the Fadeev–Popov ghosts terms, $\mathcal{L}_{\mathrm{FPG}}$, because, as it will be clear in the following, the contribution from these terms are suppressed as compared to those from quarks.

There is a technique to remove the asymmetry caused by $\bar{\psi}\mu\gamma_0\psi$ via introducing a new particle which propagates like the other particle and interacts with the gluons of the system in the same way but has a negative chemical potential. This, however, creates a new degree of

freedom in the system as a cost to restore the symmetry. The technique is as following. First, we make M copies of the original quark fields. Then, we divide M by two and replace half of the fields by their charge-conjugate fields. At the end, after having computed N-point functions for this extended system, M is set equal to 1.

The change in Eq. (3.2), after making M copies of it, is as following,

$$\mathcal{Z}_M[A] \;\; = \;\; \left(\int \mathcal{D}\bar{\psi}\,\mathcal{D}\psi \, \exp\left\{ \int_x \left[\bar{\psi}\left(i\gamma^\mu \partial_\mu + \mu\gamma_0 - m + g\gamma^\mu A_\mu^a T_a \right)\psi \right] \right\} \right)^M . \qquad (3.5)$$

Now, it is the time to replace, in half of the M copies in Eq. (3.5), $\bar{\psi}$ and ψ by the charge conjugate spinors $\bar{\psi}_C$ and ψ_C respectively. Using the anticommutation property of the Grassmann-valued quark spinors, after an integration by parts, one obtains,

$$\begin{aligned}
\mathcal{Z}_M[A] \;\; = \;\; &\left(\int \mathcal{D}\bar{\psi}\,\mathcal{D}\psi\,\mathcal{D}\bar{\psi}_C\,\mathcal{D}\psi_C \; \exp\left\{ \int_x \left[\bar{\psi}\left(i\gamma^\mu \partial_\mu + \mu\gamma_0 - m + gA_\mu^a \Gamma_a^\mu \right)\psi \right.\right.\right. \\
&+ \;\; \left.\left.\left. \bar{\psi}_C\left(i\gamma^\mu \partial_\mu - \mu\gamma_0 - m + gA_\mu^a \bar{\Gamma}_a^\mu \right)\psi_C \right] \right\} \right)^{M/2} ,
\end{aligned} \qquad (3.6)$$

where

$$\Gamma_a^\mu \equiv \gamma^\mu T_a \quad , \quad \bar{\Gamma}_a^\mu \equiv C(\gamma^\mu)^T C^{-1} T_a^T \equiv -\gamma^\mu T_a^T . \qquad (3.7)$$

The generating functional (3.6) can be written in the compact form

$$\begin{aligned}
\mathcal{Z}_M[A] \;\; = \;\; &\int \prod_{r=1}^{M/2} \mathcal{D}\bar{\Psi}_r\,\mathcal{D}\Psi_r \; \exp\left\{ \sum_{r=1}^{M/2} \left[\int_{x,y} \bar{\Psi}_r(x)\,\mathcal{S}_0^{-1}(x,y)\,\Psi_r(y) \right.\right. \\
&+ \;\; \left.\left. \int_x \left(g\,\bar{\Psi}_r(x)\,A_\mu^a(x)\,\hat{\Gamma}_a^\mu\,\Psi_r(x) \right) \right] \right\} .
\end{aligned} \qquad (3.8)$$

where we have used the $8N_c N_f$-component (Nambu–Gorkov) spinors defined via Eq. (2.6). $\hat{\Gamma}_a^\mu$ is introduced in Eq. (2.11). In this notation, the $8N_c N_f \times 8N_c N_f$-dimensional inverse propagator is shown in Eq. (2.8). In Eq. (2.9), $[G_0^\pm]^{-1}(x.y)$ is the inverse propagator for non-interacting quarks (upper sign) or charge-conjugate quarks (lower sign), respectively. This form of the generating function, Eq. (3.8), absorbs all reference to the chemical potentials μ_f in the inverse propagator (2.8). Therefore, the generating functional for QCD, Eq. (3.1) together with (3.8), is formally identical to that at zero chemical potential. The asymmetry introduced by a nonzero chemical potential μ_f has been restored by introducing the charge-conjugate fields; the associated charge-conjugate propagator G_0^- appears on equal footing with the ordinary propagator G_0^+.

3.3   Gluon self-energy in normal phase

The gluon self-energy is defined via

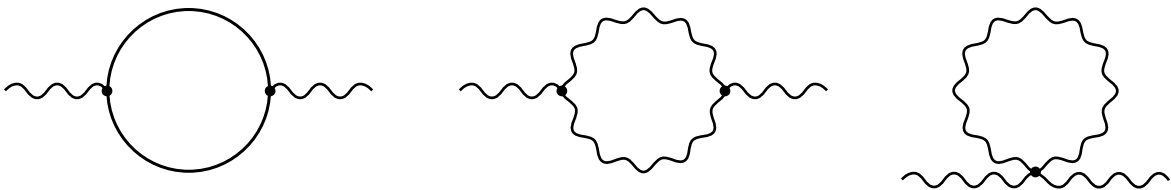$$\Pi \equiv \Delta^{-1} - \Delta_0^{-1} , \qquad (3.9)$$

Figure 3.1: The one-loop diagrams contributing to the gluon self-energy; possible ghost contributions are not shown [33].

where Δ^{-1} is the resummed and Δ_0^{-1} the free inverse gluon propagator. In the covariant gauge and in momentum space, the free inverse propagator Δ_0^{-1} has the following form,

$$[\Delta_0^{-1}]_{ab}^{\mu\nu}(P) = \delta_{ab}\left(P^2 g^{\mu\nu} + \frac{1-\alpha}{\alpha}\,P^\mu P^\nu\right)\,. \tag{3.10}$$

where P^μ is the four momentum of the gluon, $g^{\mu\nu}$ is the metric of space-time, and α is the gauge parameter. To one-loop order, there are contributions from gluon loops through the 3-gluon and 4-gluon vertices Π_g, ghost loops through the ghost-gluon vertex Π_{FPG}, and quark loops through the quark-gluon vertex Π_q to the gluon-self energy

$$\Pi = \Pi_g + \Pi_{FPG} + \Pi_q + O(g^3)\,. \tag{3.11}$$

The gluon and ghosts parts are independent of μ and the effects of the chemical potential appear only from the quark contribution Π_q. We have

$$\Pi_g\,,\ \Pi_{FPG} \sim g^2 T^2\quad,\quad \Pi_q \sim g^2(\mu^2 + a\,T^2)\,, \tag{3.12}$$

where a is a constant.

According to Ref. [78, 128], the critical temperature T_c when the superconducting condensate melts is $T_c \simeq 0.57\,\phi_0$, where ϕ_0 is the magnitude of the superconducting gap at $T = 0$. On the other hand, from Refs. [77, 78, 127, 128, 130, 133, 134, 135] we know that in the weak-coupling regime of QCD, $\phi_0 \sim \mu \exp(-c_{\mathrm{QCD}}/g) \ll \mu$, thus, to leading order, temperature-effects can be neglected. This means that, for the temperatures of interest in this work, the contributions from gluon and ghost loops to the gluon self-energy can be neglected, and only the quark contribution is taken into account, $\Pi \simeq \Pi_q$.

From Eq.(2.8) one can simply derive the quark contribution to the one-loop gluon self-energy using the general method. Without a superconducting condensate, the self-energy is

$$\Pi_{0\,ab}^{\mu\nu}(x,y) \equiv \frac{M}{2}\,g^2\,\mathrm{Tr}_{s,c,f,NG}\left[\hat{\Gamma}_a^\mu\,\mathcal{S}_0(x,y)\,\hat{\Gamma}_b^\nu\,\mathcal{S}_0(y,x)\right]\,. \tag{3.13}$$

where the trace is taken over 4-dimensional spinor space, N_c-dimensional color space, N_f-dimensional flavor space, and the 2-dimensional space of regular and charge-conjugate spinors (Nambu–Gorkov space). The factor $M/2$ comes from the fact that there are $M/2$ identical

species of quarks described by the spinors Ψ_r. Now we can set $M = 1$ in order to recover the original theory.

For convenience, we switch to momentum space. Implementing the Fourier transformation

$$\mathcal{S}_0(x) = \frac{T}{V} \sum_K e^{-iK \cdot x} \, \mathcal{S}_0(K) \tag{3.14}$$

the quark propagator in momentum space changes to

$$\mathcal{S}_0(K) \equiv \begin{pmatrix} G_0^+(K) & 0 \\ 0 & G_0^-(K) \end{pmatrix} \quad , \quad G_0^\pm(K) \equiv (\gamma^\mu K_\mu \pm \mu\gamma_0 - m)^{-1} \, . \tag{3.15}$$

Then, the gluon self-energy in momentum space becomes

$$\Pi_{0\,ab}^{\mu\nu}(P) = \frac{1}{2} \, g^2 \, \frac{T}{V} \sum_K \mathrm{Tr}_{s,c,f,NG} \left[\hat{\Gamma}_a^\mu \, \mathcal{S}_0(K) \, \hat{\Gamma}_b^\nu \, \mathcal{S}_0(K-P) \right] \, . \tag{3.16}$$

where we have employed translational invariance, $\mathcal{S}_0(x,y) \equiv \mathcal{S}_0(x-y)$ using Eq. (2.8), and

$$-i\,\delta^{(4)}(x) \quad \equiv \quad \delta^{(3)}(\mathbf{x})\,\delta(\tau) = \frac{T}{V} \sum_K e^{-iK \cdot x} \, , \tag{3.17}$$

$$\int_x e^{iK \cdot x} \quad = \quad \frac{V}{T} \, \delta_{K,0}^{(4)} \, , \tag{3.18}$$

where $\sum_K \equiv \sum_n V \int d^3\mathbf{k}/(2\pi)^3$. In the following, we first calculate the traces over color, flavor, and Nambu-Gorkov spaces and afterwards evaluate the self-energies versus energy p_0 for a certain value of the momentum p.

3.3.1 Nambu-Gorkov, flavor, and color spaces

Using Eqs. (2.8) and (2.11) and it is straightforward to find trace over the Nambu-Gorkov space,

$$\Pi_{0\,ab}^{\mu\nu}(P) = \frac{1}{2} \, g^2 \, \frac{T}{V} \sum_K \mathrm{Tr}_{s,c,f} \left[\Gamma_a^\mu \, G_0^+(K) \, \Gamma_b^\nu \, G_0^+(K-P) + \bar{\Gamma}_a^\mu \, G_0^-(K) \, \bar{\Gamma}_b^\nu \, G_0^-(K-P) \right] \, . \tag{3.19}$$

Since Γ_a^μ and $\bar{\Gamma}_a^\mu$ are diagonal in flavor space

$$(\Gamma_a^\mu)_{fg} = \delta_{fg} \, \Gamma_a^\mu \quad , \quad (\bar{\Gamma}_a^\mu)_{fg} = \delta_{fg} \, \bar{\Gamma}_a^\mu \, , \tag{3.20}$$

their role is only to change the flavor indices in the free propagators G_0^+ and G_0^-. On the other hand, since we are considering the system without the neutrality condition, all the chemical potentials are equal; this leads to a diagonal free propagator in flavor space,

$$\left(G_0^\pm \right)_{fg} = \delta_{fg} \, G_0^\pm \, . \tag{3.21}$$

Taking into account the last two expressions, the gluon self-energy assumes the following form

$$\Pi_{0\,ab}^{\mu\nu}(P) = \frac{1}{2} \, g^2 \, N_f \, \frac{T}{V} \sum_K \mathrm{Tr}_{s,c} \left[\Gamma_a^\mu \, G_0^+(K) \, \Gamma_b^\nu \, G_0^+(K-P) + \bar{\Gamma}_a^\mu \, G_0^-(K) \, \bar{\Gamma}_b^\nu \, G_0^-(K-P) \right] \, . \tag{3.22}$$

As for the flavor space, the free propagator is diagonal in color space too,

$$\left(G_0^\pm\right)_{ij} = \delta_{ij}\, G_0^\pm \; . \tag{3.23}$$

Hence, the self-energy reads

$$\Pi_{0\,ab}^{\mu\nu}(P) = \delta_{ab}\, \Pi_0^{\mu\nu}(P) \;, \tag{3.24a}$$

$$\Pi_0^{\mu\nu}(P) = \frac{1}{4}\, g^2\, N_f\, \frac{T}{V} \sum_K \mathrm{Tr}_s \left[\gamma^\mu\, G_0^+(K)\, \gamma^\nu\, G_0^+(K-P) \right.$$

$$\left. +\ \gamma^\mu\, G_0^-(K)\, \gamma^\nu\, G_0^-(K-P) \right] \;, \tag{3.24b}$$

where we have used the following identities

$$\mathrm{Tr}_c(T_a T_b) = \mathrm{Tr}_c(T_a T_b)^T = \mathrm{Tr}_c(T_a^T T_b^T) = \frac{1}{2}\, \delta_{ab} \; . \tag{3.25}$$

The quark propagator in Eq. (3.15), which appears in Eq. (3.24), does not show its own explicit dependence on spinor space. In the next subsection, we write the propagator in terms of the spin projectors and afterwards we will be able to perform the trace over spinor space. There, we have to utilise the mixed representations. The detailed description comes below.

3.3.2   Mixed Representation

Assuming that the quarks in the system are massless, $m = 0$, we can write the quark propagators in a different form

$$G_0^\pm(K) = \sum_{e=\pm} \frac{k_0 \mp (\mu - ek)}{k_0^2 - [\epsilon_{\mathbf{k}0}^e]^2}\, \Lambda_{\mathbf{k}}^{\pm e}\, \gamma_0 \;, \tag{3.26}$$

where

$$\epsilon_{\mathbf{k}0}^e \equiv |\mu - ek| \quad,\quad \Lambda_{\mathbf{k}}^e \equiv \frac{1}{2}\left(1 + e\gamma_0\, \gamma\cdot\hat{\mathbf{k}}\right) \;. \tag{3.27}$$

Mixed representations are used to include temperature effects into the system,

$$G_0^\pm(\tau,\mathbf{k}) \equiv T \sum_{k_0} e^{-k_0\tau}\, G_0^\pm(K) \quad,\quad G_0^\pm(K) \equiv \int_0^{1/T} d\tau\, e^{k_0\tau}\, G_0^\pm(\tau,\mathbf{k}) \;, \tag{3.28}$$

where the Matsubara sum is understood. The sum appears at nonzero temperature, where Euclidean time is a preferred coordinate. In Euclidean space all energies are discrete Matsubara frequencies on the imaginary energy axis. In order to determine the physical excitation spectrum, one has to analytically continue to real energies, $ik_{0\mathrm{n}} \to k_0 + i\eta$. Performing the Matsubara sum in terms of a contour integral in the complex k_0 plane in Eq. (3.28) leads to

$$G_0^+(\tau,\mathbf{k}) = -\sum_{e=\pm} \Lambda_{\mathbf{k}}^e\, \gamma_0 \left\{ (1 - n_{\mathbf{k}0}^e)\, [\theta(\tau) - N(\epsilon_{\mathbf{k}0}^e)]\, \exp(-\epsilon_{\mathbf{k}0}^e\tau) \right.$$

$$\left. -\ n_{\mathbf{k}0}^e\, [\theta(-\tau) - N(\epsilon_{\mathbf{k}0}^e)]\, \exp(\epsilon_{\mathbf{k}0}^e\tau) \right\} \;, \tag{3.29a}$$

$$G_0^-(\tau,\mathbf{k}) = -\sum_{e=\pm} \gamma_0\, \Lambda_{\mathbf{k}}^e \left\{ n_{\mathbf{k}0}^e\, [\theta(\tau) - N(\epsilon_{\mathbf{k}0}^e)]\, \exp(-\epsilon_{\mathbf{k}0}^e\tau) \right.$$

$$\left. -\ (1 - n_{\mathbf{k}0}^e)\, [\theta(-\tau) - N(\epsilon_{\mathbf{k}0}^e)]\, \exp(\epsilon_{\mathbf{k}0}^e\tau) \right\} \;, \tag{3.29b}$$

where $N(x) \equiv (e^{x/T} + 1)^{-1}$, and $n_{\mathbf{k}0}^e$ are the occupation numbers of particles ($e = +1$) or antiparticles ($e = -1$) at zero temperature defined through

$$n_{\mathbf{k}0}^e \equiv \frac{\epsilon_{\mathbf{k}0}^e + \mu - ek}{2\,\epsilon_{\mathbf{k}0}^e} \; . \tag{3.30}$$

Therefore, $1 - n_{\mathbf{k}0}^e$ corresponds to the occupation numbers for particle-holes or antiparticle-holes. The identity

$$G_0^{\pm}(-\tau, \mathbf{k}) = -\gamma_0\, G_0^{\mp}(\tau, \mathbf{k})\, \gamma_0 \tag{3.31}$$

together with $n_{\mathbf{k}0}^e \equiv \theta(\mu - ek)$ change the propagators (3.29) to

$$G_0^+(\tau, \mathbf{k}) = -\Lambda_{\mathbf{k}}^+\, \gamma_0\, \left[\theta(+\tau) - N_F^+(k)\right] e^{-(k-\mu)\tau} + \Lambda_{\mathbf{k}}^-\, \gamma_0\, \left[\theta(-\tau) - N_F^-(k)\right] e^{+(k+\mu)\tau} \;, \tag{3.32a}$$

$$G_0^-(\tau, \mathbf{k}) = +\gamma_0\, \Lambda_{\mathbf{k}}^+\, \left[\theta(-\tau) - N_F^+(k)\right] e^{+(k-\mu)\tau} - \gamma_0\, \Lambda_{\mathbf{k}}^-\, \left[\theta(+\tau) - N_F^-(k)\right] e^{-(k+\mu)\tau} \;. \tag{3.32b}$$

Here, $N_F^{\pm}(k) \equiv N(k \mp \mu)$ is the Fermi–Dirac distribution function for particles (antiparticles) and we used the Kubo–Martin–Schwinger relation for fermions

$$G_0^{\pm}\left(\frac{1}{T} - \tau, \mathbf{k}\right) = -G_0^{\pm}(-\tau, \mathbf{k}) \;, \tag{3.33}$$

which is valid for $0 \le \tau \le 1/T$ [129]. Using the conservation of momentum, $K_1 \equiv K$ and $K_2 \equiv K - P$, we have

$$
\begin{aligned}
T \sum_{k_0} \mathrm{Tr}_s \left[\gamma^\mu\, G_0^{\pm}(K_1)\, \gamma^\nu\, G_0^{\pm}(K_2)\right] &= T \sum_{k_0} \int_0^{1/T} d\tau_1\, d\tau_2\, e^{k_0 \tau_1 + (k_0 - p_0)\tau_2} \\
&\times\; \mathrm{Tr}_s \left[\gamma^\mu\, G_0^{\pm}(\tau_1, \mathbf{k}_1)\, \gamma^\nu\, G_0^{\pm}(\tau_2, \mathbf{k}_2)\right] \;.
\end{aligned}
\tag{3.34}
$$

The Matsubara sum over k_0 can be performed using the identity

$$T \sum_n e^{k_0 \tau} = \sum_{m=-\infty}^{\infty} (-1)^m\, \delta\left(\tau - \frac{m}{T}\right) \;, \tag{3.35}$$

where for fermions $k_0 = -i(2n+1)\pi T$. Since in Eq. (3.34) we have $0 \le \tau_1, \tau_2 \le 1/T$, the delta function in Eq. (3.35) supports only $m = 1$, *i.e.*, $\tau_2 = 1/T - \tau_1$. This information together with Eqs. (3.31) and (3.33), as well as $e^{p_0/T} = 1$ for bosonic Matsubara frequencies $p_0 = -i2n\pi T$, transform Eq.(3.34) into

$$T \sum_{k_0} \mathrm{Tr}_s \left[\gamma^\mu\, G_0^{\pm}(K_1)\, \gamma^\nu\, G_0^{\pm}(K_2)\right] = -\int_0^{1/T} d\tau\, e^{p_0 \tau}\, \mathrm{Tr}_s \left[\gamma^\mu\, G_0^{\pm}(\tau, \mathbf{k}_1)\, \gamma^\nu\, \gamma_0\, G_0^{\mp}(\tau, \mathbf{k}_2)\, \gamma_0\right] \tag{3.36}$$

Eventually, inserting (3.29) and integrating over τ gives the gluon self-energy:

$$\Pi_0{}^{\mu\nu}(P) = -\frac{1}{4}\, g^2\, N_f \int \frac{d^3\mathbf{k}}{(2\pi)^3} \sum_{e_1, e_2 = \pm} \left\{ \mathcal{T}_+^{\mu\nu}(\mathbf{k}_1, \mathbf{k}_2) \right.$$

$$
\times \quad \left[\left(\frac{n_1^0 \, (1 - n_2^0)}{p_0 + \epsilon_1^0 + \epsilon_2^0} - \frac{(1 - n_1^0) \, n_2^0}{p_0 - \epsilon_1^0 - \epsilon_2^0} \right) (1 - N_1^0 - N_2^0) \right.
$$

$$
+ \quad \left(\frac{(1 - n_1^0) \, (1 - n_2^0)}{p_0 - \epsilon_1^0 + \epsilon_2^0} - \frac{n_1^0 \, n_2^0}{p_0 + \epsilon_1^0 - \epsilon_2^0} \right) (N_1^0 - N_2^0) \right]
$$

$$
+ \quad \mathcal{T}_-^{\mu\nu}(\mathbf{k}_1, \mathbf{k}_2) \left[\left(\frac{(1 - n_1^0) \, n_2^0}{p_0 + \epsilon_1^0 + \epsilon_2^0} - \frac{n_1^0 \, (1 - n_2^0)}{p_0 - \epsilon_1^0 - \epsilon_2^0} \right) (1 - N_1^0 - N_2^0) \right.
$$

$$
+ \quad \left. \left(\frac{n_1^0 \, n_2^0}{p_0 - \epsilon_1^0 + \epsilon_2^0} - \frac{(1 - n_1^0) \, (1 - n_2^0)}{p_0 + \epsilon_1^0 - \epsilon_2^0} \right) (N_1^0 - N_2^0) \right] \bigg\} , \tag{3.37}
$$

where we have used the following notations

$$
\epsilon_i^0 \equiv \epsilon_{\mathbf{k}_i 0}^{e_i} \quad , \quad n_i^0 \equiv n_{\mathbf{k}_i 0}^{e_i} \quad , \quad N_i^0 \equiv N(\epsilon_i^0) , \tag{3.38}
$$

and

$$
\mathcal{T}_\pm^{\mu\nu}(\mathbf{k}_1, \mathbf{k}_2) \equiv \mathrm{Tr}_s \left(\gamma_0 \, \gamma^\mu \, \Lambda_{\mathbf{k}_1}^{\pm e_1} \, \gamma_0 \, \gamma^\nu \, \Lambda_{\mathbf{k}_2}^{\pm e_2} \right) . \tag{3.39}
$$

Employing $n_i^0 \equiv \theta(\mu - e_i k_i)$ one can show that

$$
n_i^0 \, (1 - N_i^0) \quad = \quad n_i^0 \left\{ \theta(e_i) \, N_F^+(k_i) + \theta(-e_i) \left[1 - N_F^-(k_i) \right] \right\} , \tag{3.40a}
$$

$$
(1 - n_i^0) \, N_i^0 \quad = \quad (1 - n_i^0) \left\{ \theta(e_i) \, N_F^+(k_i) + \theta(-e_i) \left[1 - N_F^-(k_i) \right] \right\} \tag{3.40b}
$$

$$
(1 - n_i^0) \, (1 - N_i^0) \quad = \quad (1 - n_i^0) \left\{ \theta(e_i) \left[1 - N_F^+(k_i) \right] + \theta(-e_i) \, N_F^-(k_i) \right\} , \tag{3.40c}
$$

$$
n_i^0 \, N_i^0 \quad = \quad n_i^0 \left\{ \theta(e_i) \left[1 - N_F^+(k_i) \right] + \theta(-e_i) \, N_F^-(k_i) \right\} . \tag{3.40d}
$$

These relations yield the self-energy in the normal phase,

$$
\Pi_0^{\mu\nu}(P) \quad = \quad \frac{1}{4} \, g^2 \, N_f \int \frac{d^3 \mathbf{k}}{(2\pi)^3} \sum_{e_1, e_2 = \pm} \left[\frac{\mathcal{T}_+^{\mu\nu}(\mathbf{k}_1, \mathbf{k}_2)}{p_0 - e_1 \, k_1 + e_2 \, k_2} - \frac{\mathcal{T}_-^{\mu\nu}(\mathbf{k}_1, \mathbf{k}_2)}{p_0 + e_1 \, k_1 - e_2 \, k_2} \right]
$$

$$
\times \quad \left\{ \theta(e_1) \left[1 - N_F^+(k_1) \right] + \theta(-e_1) \, N_F^-(k_1) - \theta(e_2) \left[1 - N_F^+(k_2) \right] \right.
$$

$$
- \quad \theta(-e_2) \, N_F^-(k_2) \bigg\} . \tag{3.41}
$$

It is relatively easy to compute the trace over spinor space. Separating the temporal and spatial components,

$$
\mathcal{T}_\pm^{00} \quad = \quad 1 + e_1 e_2 \, \hat{\mathbf{k}}_1 \cdot \hat{\mathbf{k}}_2 , \tag{3.42a}
$$

$$
\mathcal{T}_\pm^{0i} = \mathcal{T}_\pm^{i0} \quad = \quad \pm e_1 \, \hat{k}_1^i \pm e_2 \, \hat{k}_2^i \quad , \quad i = x, y, z , \tag{3.42b}
$$

$$
\mathcal{T}_\pm^{ij} \quad = \quad \delta^{ij} \left(1 - e_1 e_2 \, \hat{\mathbf{k}}_1 \cdot \hat{\mathbf{k}}_2 \right) + e_1 e_2 \left(\hat{k}_1^i \, \hat{k}_2^j + \hat{k}_1^j \, \hat{k}_2^i \right) \quad , \quad i, j = x, y, z , \tag{3.42c}
$$

the computation of the quark contribution to the gluon self-energy to one-loop in the normal phase is completed. In order to have a boundary condition for the self-energy in the color-superconducting phase, we calculate the self-energy at the hard-dense-loop (HDL) limit. At this limit the gluon energy p_0 and momenta p are much smaller than the quark chemical potential.

3.3.3 HDL limit

The HDL limit is obtained by taking p_0 and p to be of order $g\mu$ ("soft"), while k is of order μ ("hard") [129]. As the gluon self-energy (3.37) is already proportional to g^2, it is permissible to compute the integral in Eq. (3.37) to order $O(p^0)$. However, since some of the energy denominators are of order $O(p)$, one has to keep terms up to order $O(p)$ in the numerators as well. For the traces (3.42) one then obtains

$$\mathcal{T}_{\pm}^{00} \quad \simeq \quad 1 + e_1 e_2 + O\left(\frac{p^2}{k^2}\right) , \tag{3.43a}$$

$$\mathcal{T}_{\pm}^{0i} = \mathcal{T}_{\pm}^{i0} \quad \simeq \quad \pm(e_1 + e_2)\,\hat{k}^i \pm (e_1 - e_2)\left(\delta^{ij} - \hat{k}^i\,\hat{k}^j\right)\frac{p^j}{2\,k} + O\left(\frac{p^2}{k^2}\right) , \tag{3.43b}$$

$$\mathcal{T}_{\pm}^{ij} \quad \simeq \quad \delta^{ij}\left(1 - e_1 e_2\right) + 2\,e_1 e_2\,\hat{k}^i\,\hat{k}^j + O\left(\frac{p^2}{k^2}\right) . \tag{3.43c}$$

In order to derive the self-energies in the HDL limit, it is advantageous to shift the integration over 3-momentum in Eqs. (3.37) or (3.41), $\mathbf{k} \to \mathbf{k}+\mathbf{p}/2$, such that $\mathbf{k}_1 = \mathbf{k}+\mathbf{p}/2$ and $\mathbf{k}_2 = \mathbf{k}-\mathbf{p}/2$. Here, we cite the results from [129, 136] for those components of the imaginary part of the HDL polarisation function that we need and refrain from repeating the calculations,

$$\Pi_0{}^{00}(P) \quad \simeq \quad -3\,m_g^2 \int \frac{d\Omega}{4\pi}\left(1 - \frac{p_0}{p_0 + \mathbf{p}\cdot\hat{\mathbf{k}}}\right) , \tag{3.44a}$$

$$\Pi_0{}^{0i}(P) \quad \simeq \quad -3\,m_g^2 \int \frac{d\Omega}{4\pi}\frac{p_0\,\hat{k}^i}{p_0 + \mathbf{p}\cdot\hat{\mathbf{k}}} , \tag{3.44b}$$

$$\Pi_0{}^{ij}(P) \quad \simeq \quad 3\,m_g^2 \int \frac{d\Omega}{4\pi}\,\hat{k}^i\,\hat{k}^j\,\frac{p_0}{p_0 + \mathbf{p}\cdot\hat{\mathbf{k}}} . \tag{3.44c}$$

We use these results for comparison with the gluon self-energies in the CFL phase.

In the following, we calculate explicitly the gluon self-energy in the color superconducting phase for the quark propagator given by the mean-field approximation. The reason of employing this approximation comes from the point that the original partition function contains the current-current interaction which is biquadratic in the fermion fields. The biquadratic term prevents performing the integration over ψ and $\bar{\psi}$. To resolve this problem, we have to approximate the biquadratic term by a bilinear term times a fermion condensate, which then allows for integrating over ψ and $\bar{\psi}$ (see the details in Appendix-A of [105]).

3.4   Gluon self-energy in the superconducting phase

In the mean-field approximation, the gluon self-energy keeps its own original form (3.16), but with different quark propagators

$$\Pi_{ab}^{\mu\nu}(P) = \frac{1}{2}\,g^2\,\frac{T}{V}\sum_K \mathrm{Tr}_{s,c,f,NG}\left[\hat{\Gamma}_a^\mu\,\mathcal{S}(K)\,\hat{\Gamma}_b^\nu\,\mathcal{S}(K - P)\right] . \tag{3.45}$$

The calculation of the self-energy for two-flavor color superconductivity, the 2SC phase, was already done in Ref. [108]. Here we calculate the gluon polarisation tensor for three-flavor color superconductivity in the color-flavor-locked phase. For that, we first evaluate the trace over Nambu-Gorkov space. Then, to find the trace over color and flavor spaces, because of the locking between the color and flavor spaces, we have to write the gap matrix $\Phi^{\pm}$ in a new color and flavor basis. After performing the trace over color and flavor spaces, while we use the mixed representations, we calculate the trace over spinor space. At the end, we use the advantage of the similarity between the relations in the color-superconducting phase with that for the normal phase.

3.4.1 Nambu–Gorkov space

With Eqs. (2.9) and (2.19), the trace over the 2-dimensional Nambu–Gorkov space can be easily performed,

$$
\begin{aligned}
\Pi^{\mu\nu}_{ab}(P) &= \frac{1}{2}\,g^2\,\frac{T}{V}\sum_K \text{Tr}_{s,c,f}\left[\Gamma^\mu_a\,G^+(K)\,\Gamma^\nu_b\,G^+(K-P)+\bar\Gamma^\mu_a\,G^-(K)\,\bar\Gamma^\nu_b\,G^-(K-P)\right.\\
&\quad + \left.\Gamma^\mu_a\,\Xi^-(K)\,\bar\Gamma^\nu_b\,\Xi^+(K-P)+\bar\Gamma^\mu_a\,\Xi^+(K)\,\Gamma^\nu_b\,\Xi^-(K-P)\right]\;.
\end{aligned}
\tag{3.46}
$$

We see that when the temperature approaches the critical value, $T \to T_c$, the condensate melts, $\Phi^{\pm} \to 0$, *i.e.*, $\Xi^{\pm} \to 0$ and $G^{\pm} \to G_0^{\pm}$, and the gluon self-energy assumes the form of the normal phase, $\Pi^{\mu\nu}_{ab} \to \Pi_0{}^{\mu\nu}_{ab}$.

Note that the first line of Eq. (3.46) corresponds to the diagram in Fig. 3.2(a), where only the diagonal components of the Nambu–Gorkov propagator appear, while the second line corresponds to the diagram in Fig. 3.2(b), formed from the off-diagonal components. As we mentioned earlier, at small temperatures $T \sim \phi_0$ and in weak coupling, $\phi_0 \ll \mu$, contributions from gluon (or ghost) loops are suppressed by a factor of $T^2/\mu^2 \sim \phi_0^2/\mu^2$, and this is the reason that only the fermion loops are depicted in Fig. 3.2 as the dominant contribution to the gluon self-energy. In Eq. (3.46), three traces are still to be taken. Next we find the trace over color and flavor spaces.

3.4.2 Color and flavor space

In two-flavor CSC, the trace over color and flavor space can be performed individually [137]. However, in the CFL phase due to the locking of the color and flavor spaces, we cannot take the trace over the color and flavor spaces separately. Instead, we use the most convenient method introduced in Eq. (7) of Ref. [138]. Let us introduce projectors

$$
\mathcal{C}^{(1)ij}_{rs} \equiv \frac{1}{3}\,\delta^i_r\,\delta^j_s\;,
\tag{3.47a}
$$

$$
\mathcal{C}^{(2)ij}_{rs} \equiv \frac{1}{2}\left(\delta_{rs}\,\delta^{ij}-\delta^j_r\,\delta^i_s\right)\;,
\tag{3.47b}
$$

$$
\mathcal{C}^{(3)ij}_{rs} \equiv \frac{1}{2}\left(\delta_{rs}\,\delta^{ij}+\delta^j_r\,\delta^i_s\right)-\frac{1}{3}\,\delta^i_r\,\delta^j_s\;,
\tag{3.47c}
$$

which are symmetric under simultaneous exchange of color, i,j, and flavor, r,s, indices. $\mathcal{C}^{(1)}$ is the singlet projector $\mathbf{P_1}$ and $\mathcal{C}^{(2)}+\mathcal{C}^{(3)} \equiv \mathbf{1}-\mathbf{P_1} \equiv \mathbf{P_8}$ is the octet projector, cf. Eqs. (3.11)
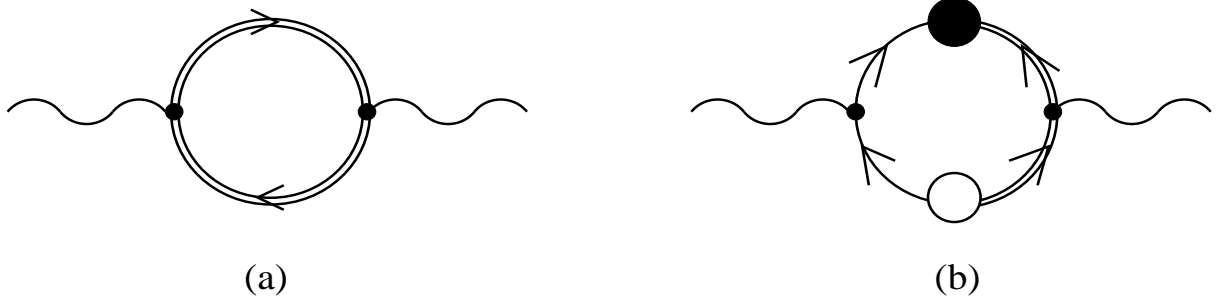
Figure 3.2: The contributions from (a) the diagonal and (b) the off-diagonal components of the Nambu–Gorkov propagator to the gluon self-energy. Double full lines stand for the full quasiparticle propagator $G^{\pm}$, single full lines for the free propagator $G_0^{\pm}$. The full blob represents Φ^-, the empty blob Φ^+. Vertices are represented by small blobs [149].

and (3.12) in Ref. [139]. We can write the gap matrices $\Phi^{\pm}$ in terms of these projectors (3.47) as follows

$$\Phi^{\pm} \equiv \sum_{n=1}^{3} \mathcal{C}^{(n)} \, \Phi_n^{\pm} \, , \tag{3.48}$$

where

$$\Phi_1^{\pm} \;\; \equiv \;\; 2\left(\Phi_{\mathbf{\bar{3}}}^{\pm} + 2\,\Phi_{\mathbf{6}}^{\pm}\right) \, , \tag{3.49a}$$

$$\Phi_2^{\pm} \;\; \equiv \;\; \Phi_{\mathbf{\bar{3}}}^{\pm} - \Phi_{\mathbf{6}}^{\pm} \, , \tag{3.49b}$$

$$\Phi_3^{\pm} \;\; \equiv \;\; -\Phi_2^{\pm} \, . \tag{3.49c}$$

Here $\Phi_{\mathbf{\bar{3}}}^{\pm}$ is the gap matrix in the antitriplet channel and $\Phi_{\mathbf{6}}^{\pm}$ is the gap matrix in the sextet channel,

$$\Phi^{\pm \, ij}_{rs} \equiv \Phi_{\mathbf{\bar{3}}}^{\pm}\left(\delta_r^i \, \delta_s^j - \delta_s^i \, \delta_r^j\right) + \Phi_{\mathbf{6}}^{\pm}\left(\delta_r^i \, \delta_s^j + \delta_s^i \, \delta_r^j\right) \, . \tag{3.50}$$

In order to avoid confusion, it must be noticed that the relation between antitriplet and sextet gaps with the gap function κ_1 and κ_2 of Ref. [66] is as follows,

$$\phi_{\mathbf{3}\ell}^+ = -\phi_{\mathbf{3}\mathbf{r}}^+ \equiv (\kappa_1 - \kappa_2) \, ,$$
$$\phi_{\mathbf{6}\ell}^+ = -\phi_{\mathbf{6}\mathbf{r}}^+ \equiv (\kappa_1 + \kappa_2) \, . \tag{3.51}$$

However, it was already shown in [78] that condensation mainly takes place only in the attractive channel where $\kappa_1 - \kappa_2 \neq 0$. This does not change the method which we use here and its effect will be only on the relative values of the gap functions $\Phi_1^{\pm}$ and $\Phi_2^{\pm}$. In Eq. (3.49), the gap matrices $\Phi_{1,2,3}^{\pm}$ are in spinor space,

$$\Phi_n^+(K) \equiv \sum_{h=r,\ell} \sum_{e=\pm} \phi_{n,h}^e(K)\, \mathcal{P}_h \, \Lambda_{\mathbf{k}}^e \quad , \quad \Phi_n^-(K) \equiv \sum_{h=r,\ell} \sum_{e=\pm} \left[\phi_{n,h}^e(K)\right]^* \mathcal{P}_{-h} \, \Lambda_{\mathbf{k}}^{-e} \, , \tag{3.52}$$

where $\mathcal{P}_{r,\ell} \equiv (1 \pm \gamma_5)/2$ are chirality projectors, $-h = \ell$ when $h = r$ and $-h = r$ when $h = \ell$, $\Lambda_{\mathbf{k}}^{\pm} \equiv (1 \pm \gamma_0 \gamma \cdot \hat{\mathbf{k}})/2$ are energy projectors, and $\phi_{n,h}^e(K)$ are simple functions of 4-momentum

K^μ. Employing the projectors introduced in (3.47), the quasiparticle propagators read

$$G^\pm(K) \equiv \sum_{n=1}^{3} \mathcal{C}^{(n)} G_n^\pm(K) \, , \tag{3.53}$$

where

$$G_n^\pm(K) = \sum_{h=r,\ell} \sum_{e=\pm} \mathcal{P}_{\pm h} \Lambda_{\mathbf{k}}^{\pm e} \frac{1}{k_0^2 - [\epsilon_{\mathbf{k}}^e(\phi_{n,h}^e)]^2} \left[G_0^\mp(K) \right]^{-1} \, . \tag{3.54}$$

The quasiparticle energies are defined as

$$\epsilon_{\mathbf{k}}^e(\phi_{n,h}^e) \equiv \sqrt{(\mu - ek)^2 + |\phi_{n,h}^e|^2} \, , \tag{3.55}$$

where $\phi_{n,h}^e$ is the gap function for pairing of quarks ($e = +1$) or antiquarks ($e = -1$) with chirality h. Here, we have used the quasiparticle propagators $G^\pm(K)$ and energies $\epsilon_{\mathbf{k}}^e(\phi_h^e)$ introduced in [105, 128]. For our purposes, it is convenient to define a singlet and an octet gap matrix according to

$$\Phi_{\mathbf{1}}^\pm \equiv \Phi_1^\pm \quad , \quad \Phi_{\mathbf{8}}^\pm \equiv \Phi_2^\pm \equiv -\Phi_3^\pm \, , \tag{3.56}$$

with which Eq. (3.53) can be explicitly written as

$$G^\pm(K) \equiv \mathbf{P_1} \, G_{\mathbf{1}}^\pm(K) + \mathbf{P_8} \, G_{\mathbf{8}}^\pm(K) \, . \tag{3.57}$$

Here $\mathbf{P_{1,8}}$ are the singlet and octet projectors introduced in [139] and we have $G_{\mathbf{1}}^\pm \equiv G_1^\pm$, $G_{\mathbf{8}}^\pm \equiv G_2^\pm = G_3^\pm$. Having this, we follow the same method to evaluate the off-diagonal components of the quasiparticle propagators,

$$\Xi^\pm(K) \equiv \sum_{n=1}^{3} \mathcal{C}^{(n)} \Xi_n^\pm(K) \, , \tag{3.58}$$

where

$$\Xi_n^+(K) \;\; = \;\; -\sum_{h=r,\ell} \sum_{e=\pm} \frac{\phi_{n,h}^e(K)}{k_0^2 - [\epsilon_{\mathbf{k}}^e(\phi_{n,h}^e)]^2} \, \mathcal{P}_{-h} \, \Lambda_{\mathbf{k}}^{-e} \, , \tag{3.59}$$

$$\Xi_n^-(K) \;\; = \;\; -\sum_{h=r,\ell} \sum_{e=\pm} \frac{\left[\phi_{n,h}^e(K)\right]^*}{k_0^2 - [\epsilon_{\mathbf{k}}^e(\phi_{n,h}^e)]^2} \, \mathcal{P}_h \, \Lambda_{\mathbf{k}}^e \, . \tag{3.60}$$

Since $\phi_{2,h}^e = -\phi_{3,h}^e$, we do not have an expression for the off-diagonal component similar to what we have for the propagators (3.57). Instead, we find that $\Xi_{\mathbf{1}}^\pm \equiv \Xi_1^\pm$, $\Xi_{\mathbf{8}}^\pm \equiv \Xi_2^\pm \equiv -\Xi_3^\pm$.

Inserting Eqs. (3.53) and (3.58) into Eq. (3.37), the traces over color and flavor space are taken,

$$\Pi_{ab}^{\mu\nu}(P) \;\; = \;\; \delta_{ab} \, \Pi^{\mu\nu}(P) \, , \tag{3.61a}$$

$$\Pi^{\mu\nu}(P) \;\; = \;\; \frac{g^2}{12} \frac{T}{V} \sum_K \mathrm{Tr}_s \left[\gamma^\mu \, G_{\mathbf{1}}^+(K) \, \gamma^\nu \, G_{\mathbf{8}}^+(K-P) + \gamma^\mu \, G_{\mathbf{8}}^+(K) \, \gamma^\nu \, G_{\mathbf{1}}^+(K-P) \right.$$

$$\left. + \gamma^\mu \, G_{\mathbf{1}}^-(K) \, \gamma^\nu \, G_{\mathbf{8}}^-(K-P) + \gamma^\mu \, G_{\mathbf{8}}^-(K) \, \gamma^\nu \, G_{\mathbf{1}}^-(K-P) \right.$$

$$\begin{aligned}
&+ 7\,\gamma^\mu\, G_{\mathbf{8}}^+(K)\,\gamma^\nu\, G_{\mathbf{8}}^+(K-P) + 7\,\gamma^\mu\, G_{\mathbf{8}}^-(K)\,\gamma^\nu\, G_{\mathbf{8}}^-(K-P) \\
&+ \gamma^\mu\, \Xi_{\mathbf{1}}^-(K)\,\gamma^\nu\, \Xi_{\mathbf{8}}^+(K-P) + \gamma^\mu\, \Xi_{\mathbf{8}}^-(K)\,\gamma^\nu\, \Xi_{\mathbf{1}}^+(K-P) \\
&+ \gamma^\mu\, \Xi_{\mathbf{1}}^+(K)\,\gamma^\nu\, \Xi_{\mathbf{8}}^-(K-P) + \gamma^\mu\, \Xi_{\mathbf{8}}^+(K)\,\gamma^\nu\, \Xi_{\mathbf{1}}^-(K-P) \\
&+ 2\,\gamma^\mu\, \Xi_{\mathbf{8}}^-(K)\,\gamma^\nu\, \Xi_{\mathbf{8}}^+(K-P) + 2\,\gamma^\mu\, \Xi_{\mathbf{8}}^+(K)\,\gamma^\nu\, \Xi_{\mathbf{8}}^-(K-P) \Big] \ .
\end{aligned}$$

(3.61b)

It is realised that, because $\mathrm{Tr}_c T_a \, \mathrm{Tr}_c T_b \equiv 0$, the gluon self-energy is diagonal in the adjoint colors a, b. Additionally, we see that there are no terms containing two quasiparticle propagators with singlet gaps $\Phi_{\mathbf{1}}^\pm$.

The evaluation the trace over the spinor space is absolutely analogous to the two-flavor case [137]. Nevertheless, in order to complete the procedure, we rewrite the calculations for our case, i.e. the CFL phase.

3.4.3   Mixed representations for quark propagators

In Ref. [105, 128] the quasiparticle propagators for $m = 0$ are calculated in terms of chirality and energy projectors. Here, we have the same form of the propagator obtained in [105, 128]. The only difference is that it contains different gap matrices introduced via Eqs.(3.49) and (3.54) in comparison to the previous result,

$$G_n^\pm(K) = \sum_{h=r,\ell} \sum_{e=\pm} \mathcal{P}_{\pm h}\, \Lambda_{\mathbf{k}}^{\pm e} \, \frac{1}{k_0^2 - [\epsilon_{\mathbf{k}}^e(\phi_{n,h}^e)]^2} \left[G_0^\mp(K) \right]^{-1} \ , \tag{3.62}$$

The chirality projectors, $\mathcal{P}_{r,\ell}$, were already introduced after Eq.(3.52). Besides, the quasiparticle energies assumed a different form than the one in [105, 128],

$$\epsilon_{\mathbf{k}}^e(\phi_{n,h}^e) \equiv \sqrt{(\mu - ek)^2 + |\phi_{n,h}^e|^2} \ , \tag{3.63}$$

where $\phi_{n,h}^e$ is the nth gap function for pairing of quarks ($e = +1$) or antiquarks ($e = -1$) with chirality h.

In [128], it is illustrated that the gap functions in mean-field approximation differ for left- and right-handed gap functions by a complex phase factor,

$$\phi_{n,r}^e = \phi_n^e \exp(i\,\theta^e) \quad , \quad \phi_{n,\ell}^e = -\phi_n^e \exp(-i\,\theta^e) \ , \tag{3.64}$$

where $\phi_n^e \in \mathbf{R}$ so that the phase factor is independent of the energy projection, $\theta^+ = \theta^- \equiv \theta$. The value of θ is fixed by condensation, but this breaks spontaneously the $U_A(1)$ symmetry restored at high densities. There are interesting results on condensation in different channels depending on the value of θ. For $\theta = 0$ or $\pi/2$, condensation happens in a spin-zero channel with parity $J^P = 0^+$ or $J^P = 0^-$, respectively. Furthermore, for $\theta \neq 0$, there is always a $J^P = 0^-$ admixture, thus in this case, condensation breaks parity too [127, 140]. In the following, for the sake of simplicity, we consider only the $\theta = 0$ case.

From Eq. (3.64) we have $|\phi^e_{n,r}| \equiv |\phi^e_{n,\ell}| \equiv \phi^e_n$. Hence the sum over chiralities in Eq. (3.62) is superfluous. Using

$$\left[G_0^{\mp}(K) \right]^{-1} = \left[k_0 \mp (\mu - ek) \mp 2\,ek\,\Lambda_{\mathbf{k}}^{\mp e} \right] \gamma_0 \,, \tag{3.65}$$

Eq. (3.62) reads

$$G_n^{\pm}(K) = \sum_{e=\pm} \frac{k_0 \mp (\mu - ek)}{k_0^2 - [\epsilon_{\mathbf{k}}^e]^2} \Lambda_{\mathbf{k}}^{\pm e} \gamma_0 \,. \tag{3.66}$$

In comparison with Eq. (3.26) we see that only the free quark excitation energies (3.27) have been replaced by the quasiparticle excitation energies (3.55), $\epsilon_{\mathbf{k}0}^e \to \epsilon_{\mathbf{k}}^e \equiv \epsilon_{\mathbf{k}}^e(\phi_n^e)$. Hence, we can precisely follow the procedure leading to Eqs. (3.29). We only have to change $\epsilon_{\mathbf{k}0}^e$ to $\epsilon_{\mathbf{k}}^e$,

$$\begin{aligned}
G_n^+(\tau, \mathbf{k}) &= -\sum_{e=\pm} \Lambda_{\mathbf{k}}^e \gamma_0 \left\{ (1 - n_{\mathbf{k}}^e)\, [\theta(\tau) - N(\epsilon_{\mathbf{k}}^e)] \exp(-\epsilon_{\mathbf{k}}^e \tau) \right. \\
&\quad - \left. n_{\mathbf{k}}^e\, [\theta(-\tau) - N(\epsilon_{\mathbf{k}}^e)] \exp(\epsilon_{\mathbf{k}}^e \tau) \right\}, \tag{3.67a} \\
G_n^-(\tau, \mathbf{k}) &= -\sum_{e=\pm} \gamma_0 \Lambda_{\mathbf{k}}^e \left\{ n_{\mathbf{k}}^e\, [\theta(\tau) - N(\epsilon_{\mathbf{k}}^e)] \exp(-\epsilon_{\mathbf{k}}^e \tau) \right. \\
&\quad - \left. (1 - n_{\mathbf{k}}^e)\, [\theta(-\tau) - N(\epsilon_{\mathbf{k}}^e)] \exp(\epsilon_{\mathbf{k}}^e \tau) \right\}. \tag{3.67b}
\end{aligned}$$

Here

$$n_{\mathbf{k}}^e \equiv \frac{\epsilon_{\mathbf{k}}^e + \mu - ek}{2\,\epsilon_{\mathbf{k}}^e} \tag{3.68}$$

is the occupation number for quasiparticles ($e = +1$) or quasi-antiparticles ($e = -1$) at zero temperature [105] and, therefore, $1 - n_{\mathbf{k}}^e$ for quasiparticle holes or quasi-antiparticle holes. Due to the presence of the gap ϕ_n^e in the quasiparticle excitation spectrum, the occupation numbers are no longer simple theta functions in momentum space, as they were in the noninteracting case; the theta functions become "smeared" over a range $\sim \phi_n^e$ around the Fermi surface (cf. Fig. 2 in [105]). Equations (3.31) and (3.33) are also fulfilled by $G_n^{\pm}(\tau, \mathbf{k})$.

Moreover, Eqs. (3.67) and (3.29) have the same structure except that the quasiparticle energies in Eq. (3.67) depend on the gap function. Consequently, the traces in Eq. (3.29) can be found with the following replacements,

$$\epsilon_i^0 \to \epsilon_i \equiv \epsilon_{\mathbf{k}_i}^{e_i} \quad, \quad n_i^0 \to n_i \equiv n_{\mathbf{k}_i}^{e_i} \quad, \quad N_i^0 \to N_i \equiv N(\epsilon_i)\,. \tag{3.69}$$

On the other hand, we have to use the same mixed representations for the off-diagonal components of $\mathcal{S}(K)$. From Eq. (3.59), we have

$$\Xi_n^+(K) = -\sum_{h=r,\ell} \sum_{e=\pm} \frac{\phi_h^e(K)}{k_0^2 - [\epsilon_{\mathbf{k}}^e]^2} \mathcal{P}_{-h}\, \Lambda_{\mathbf{k}}^{-e} \quad, \quad \Xi_n^-(K) = -\sum_{h=r,\ell} \sum_{e=\pm} \frac{[\phi_h^e(K)]^*}{k_0^2 - [\epsilon_{\mathbf{k}}^e]^2} \mathcal{P}_h\, \Lambda_{\mathbf{k}}^e \,. \tag{3.70}$$

Accepting the argument of [128] we also assume that $\phi_{n,h}^e(k_0)$ has no poles or cuts in the complex k_0-plane and that $\phi_{n,h}^e(k_0) = \phi_{n,h}^e(-k_0)$. This leads to the following expressions,

$$\Xi_n^+(\tau, \mathbf{k}) = \sum_{h=r,\ell} \sum_{e=\pm} \mathcal{P}_{-h}\, \Lambda_{\mathbf{k}}^{-e}\, \frac{\phi_{n,h}^e(\epsilon_{\mathbf{k}}^e, \mathbf{k})}{2\,\epsilon_{\mathbf{k}}^e} \left\{ [\theta(\tau) - N(\epsilon_{\mathbf{k}}^e)] \exp(-\epsilon_{\mathbf{k}}^e \tau) \right.$$

$$+ \quad [\theta(-\tau) - N(\epsilon_{\mathbf{k}}^e)] \exp(\epsilon_{\mathbf{k}}^e \tau) \} \ , \tag{3.71a}$$

$$\Xi_n^-(\tau, \mathbf{k}) = \sum_{h=r,\ell} \sum_{e=\pm} \mathcal{P}_h \, \Lambda_{\mathbf{k}}^e \, \frac{\left[\phi_{n,h}^e(\epsilon_{\mathbf{k}}^e, \mathbf{k})\right]^*}{2\,\epsilon_{\mathbf{k}}^e} \left\{ [\theta(\tau) - N(\epsilon_{\mathbf{k}}^e)] \exp(-\epsilon_{\mathbf{k}}^e \tau) \right.$$

$$+ \quad [\theta(-\tau) - N(\epsilon_{\mathbf{k}}^e)] \exp(\epsilon_{\mathbf{k}}^e \tau) \} \ , \tag{3.71b}$$

where the energy in the gap functions $\phi_{n,h}^e$ is on the quasiparticle mass shell, $k_0 \equiv \pm \epsilon_{\mathbf{k}}^e$. Now, we can straightforwardly compute the trace of the terms in Eqs. (3.61) related to $\Xi^\pm$,

$$T \sum_{k_0} \mathrm{Tr}_s \left[\gamma^\mu \, \Xi_n^\mp(K_1) \, \gamma^\nu \, \Xi_n^\pm(K_2)\right] = \sum_{e_1, e_2 = \pm} \mathcal{U}_\pm^{\mu\nu}(\mathbf{k}_1, \mathbf{k}_2) \frac{\phi_{n,1} \, \phi_{n,2}}{4\,\epsilon_1\,\epsilon_2}$$

$$\times \quad \left[\left(\frac{1}{p_0 + \epsilon_1 + \epsilon_2} - \frac{1}{p_0 - \epsilon_1 - \epsilon_2} \right) (1 - N_1 - N_2) \right.$$

$$- \quad \left. \left(\frac{1}{p_0 - \epsilon_1 + \epsilon_2} - \frac{1}{p_0 + \epsilon_1 - \epsilon_2} \right) (N_1 - N_2) \right] \ , \tag{3.72}$$

where we have applied again variables $K_1 \equiv K$, $K_2 \equiv K - P$. Also, we have used

$$\phi_{n,i} \equiv \phi_n^{e_i}(\epsilon_i, \mathbf{k}_i) \ , \tag{3.73}$$

together with

$$\mathcal{U}_\pm^{\mu\nu}(\mathbf{k}_1, \mathbf{k}_2) \equiv \mathrm{Tr}_s \left[\gamma^\mu \, \Lambda_{\mathbf{k}_1}^{\pm e_1} \, \gamma^\nu \, \Lambda_{\mathbf{k}_2}^{\mp e_2} \right] \ . \tag{3.74}$$

The sum over chiralities h_1 and h_2 could be performed trivially knowing that $\mathcal{P}_h \, \gamma^\mu = \gamma^\mu \, \mathcal{P}_{-h}$ and $\mathcal{P}_r \, \mathcal{P}_\ell = 0$.

Assuming $\phi_{n,r}^e = -\phi_{n,\ell}^e \equiv \phi_n^e \in \mathbf{R}$, the result is (cf. Refs. [137, 149])

$$\Pi^{\mu\nu}(P) = -\frac{g^2}{12} \int \frac{d^3\mathbf{k}}{(2\pi)^3} \sum_{e_1, e_2 = \pm} \left(\mathcal{T}_+^{\mu\nu}(\mathbf{k}_1, \mathbf{k}_2) \right.$$

$$\times \quad \left[\left(\frac{\hat{n}_1 \, (1 - n_2)}{p_0 + \hat{\epsilon}_1 + \epsilon_2} - \frac{(1 - \hat{n}_1) \, n_2}{p_0 - \hat{\epsilon}_1 - \epsilon_2} \right) (1 - \hat{N}_1 - N_2) \right.$$

$$+ \quad \left(\frac{(1 - \hat{n}_1) \, (1 - n_2)}{p_0 - \hat{\epsilon}_1 + \epsilon_2} - \frac{\hat{n}_1 \, n_2}{p_0 + \hat{\epsilon}_1 - \epsilon_2} \right) (\hat{N}_1 - N_2)$$

$$+ \quad \left(\frac{n_1 \, (1 - \hat{n}_2)}{p_0 + \epsilon_1 + \hat{\epsilon}_2} - \frac{(1 - n_1) \, \hat{n}_2}{p_0 - \epsilon_1 - \hat{\epsilon}_2} \right) (1 - N_1 - \hat{N}_2)$$

$$+ \quad \left(\frac{(1 - n_1) \, (1 - \hat{n}_2)}{p_0 - \epsilon_1 + \hat{\epsilon}_2} - \frac{n_1 \, \hat{n}_2}{p_0 + \epsilon_1 - \hat{\epsilon}_2} \right) (N_1 - \hat{N}_2)$$

$$+ \quad 7 \left(\frac{n_1 \, (1 - n_2)}{p_0 + \epsilon_1 + \epsilon_2} - \frac{(1 - n_1) \, n_2}{p_0 - \epsilon_1 - \epsilon_2} \right) (1 - N_1 - N_2)$$

$$+ \quad 7 \left(\frac{(1 - n_1) \, (1 - n_2)}{p_0 - \epsilon_1 + \epsilon_2} - \frac{n_1 \, n_2}{p_0 + \epsilon_1 - \epsilon_2} \right) (N_1 - N_2) \right] + \mathcal{T}_-^{\mu\nu}(\mathbf{k}_1, \mathbf{k}_2)$$

$$\times \quad \left[\left(\frac{(1 - \hat{n}_1) \, n_2)}{p_0 + \hat{\epsilon}_1 + \epsilon_2} - \frac{\hat{n}_1 \, (1 - n_2)}{p_0 - \hat{\epsilon}_1 - \epsilon_2} \right) (1 - \hat{N}_1 - N_2) \right.$$

$$+ \quad \left(\frac{\hat{n}_1\, n_2}{p_0 - \hat{\epsilon}_1 + \epsilon_2} - \frac{(1 - \hat{n}_1)\,(1 - n_2)}{p_0 + \hat{\epsilon}_1 - \epsilon_2} \right) (\hat{N}_1 - N_2)$$

$$+ \quad \left(\frac{(1 - n_1)\,\hat{n}_2}{p_0 + \epsilon_1 + \hat{\epsilon}_2} - \frac{n_1\,(1 - \hat{n}_2)}{p_0 - \epsilon_1 - \hat{\epsilon}_2} \right) (1 - N_1 - \hat{N}_2)$$

$$+ \quad \left(\frac{n_1\,\hat{n}_2}{p_0 - \epsilon_1 + \hat{\epsilon}_2} - \frac{(1 - n_1)\,(1 - \hat{n}_2)}{p_0 + \epsilon_1 - \hat{\epsilon}_2} \right) (N_1 - \hat{N}_2)$$

$$+ \quad 7 \left(\frac{(1 - n_1)\,n_2}{p_0 + \epsilon_1 + \epsilon_2} - \frac{n_1\,(1 - n_2)}{p_0 - \epsilon_1 - \epsilon_2} \right) (1 - N_1 - N_2)$$

$$+ \quad 7 \left(\frac{n_1\,n_2}{p_0 - \epsilon_1 + \epsilon_2} - \frac{(1 - n_1)\,(1 - n_2)}{p_0 + \epsilon_1 - \epsilon_2} \right) (N_1 - N_2) \Big] - \left[\mathcal{U}_+^{\mu\nu}(\mathbf{k}_1, \mathbf{k}_2) + \mathcal{U}_-^{\mu\nu}(\mathbf{k}_1, \mathbf{k}_2) \right]$$

$$\times \quad \left\{ \frac{\hat{\phi}_1\, \phi_2}{4\, \hat{\epsilon}_1\, \epsilon_2} \left[\left(\frac{1}{p_0 + \hat{\epsilon}_1 + \epsilon_2} - \frac{1}{p_0 - \hat{\epsilon}_1 - \epsilon_2} \right) (1 - \hat{N}_1 - N_2) \right. \right.$$

$$- \quad \left. \left(\frac{1}{p_0 - \hat{\epsilon}_1 + \epsilon_2} - \frac{1}{p_0 + \hat{\epsilon}_1 - \epsilon_2} \right) (\hat{N}_1 - N_2) \right]$$

$$+ \quad \frac{\phi_1\, \hat{\phi}_2}{4\, \epsilon_1\, \hat{\epsilon}_2} \left[\left(\frac{1}{p_0 + \epsilon_1 + \hat{\epsilon}_2} - \frac{1}{p_0 - \epsilon_1 - \hat{\epsilon}_2} \right) (1 - N_1 - \hat{N}_2) \right.$$

$$- \quad \left. \left(\frac{1}{p_0 - \epsilon_1 + \hat{\epsilon}_2} - \frac{1}{p_0 + \epsilon_1 - \hat{\epsilon}_2} \right) (N_1 - \hat{N}_2) \right]$$

$$+ \quad 2\, \frac{\phi_1\, \phi_2}{4\, \epsilon_1\, \epsilon_2} \left[\left(\frac{1}{p_0 + \epsilon_1 + \epsilon_2} - \frac{1}{p_0 - \epsilon_1 - \epsilon_2} \right) (1 - N_1 - N_2) \right.$$

$$- \quad \left. \left. \left(\frac{1}{p_0 - \epsilon_1 + \epsilon_2} - \frac{1}{p_0 + \epsilon_1 - \epsilon_2} \right) (N_1 - N_2) \right] \right\} \right) . \tag{3.75}$$

where

$$\phi_i \equiv \phi_{\mathbf{8}}^{e_i} \quad , \quad \hat{\phi}_i \equiv \phi_{\mathbf{1}}^{e_i} . \tag{3.76}$$

The excitation energies for quasiparticles with octet and singlet gaps are

$$\epsilon_i \equiv \epsilon_{\mathbf{k}_i}^{e_i}(\phi_i) \quad , \quad \hat{\epsilon}_i \equiv \epsilon_{\mathbf{k}_i}^{e_i}(\hat{\phi}_i) , \tag{3.77}$$

respectively and the occupation numbers for quasiparticles with octet and singlet gaps read

$$n_i \equiv n_{\mathbf{k}_i}^{e_i} \equiv \frac{\epsilon_i - \xi_i}{2\, \epsilon_i} \quad , \quad \hat{n}_i \equiv \hat{n}_{\mathbf{k}_i}^{e_i} \equiv \frac{\hat{\epsilon}_i - \xi_i}{2\, \hat{\epsilon}_i} \tag{3.78}$$

where $\xi_i \equiv e_i\, k_i - \mu$. The thermal occupation numbers are defined as

$$N_i \equiv N_{\mathbf{k}_i}^{e_i} \equiv \left[\exp\left(\frac{\epsilon_i}{T} \right) + 1 \right]^{-1} \quad , \quad \hat{N}_i \equiv \hat{N}_{\mathbf{k}_i}^{e_i} \equiv \left[\exp\left(\frac{\hat{\epsilon}_i}{T} \right) + 1 \right]^{-1} \tag{3.79}$$

Besides, we have used the following expressions

$$\mathcal{T}_\pm^{00} \quad = \quad \mathcal{U}_\pm^{00} = 1 + e_1 e_2\, \hat{\mathbf{k}}_1 \cdot \hat{\mathbf{k}}_2 , \tag{3.80a}$$

$$\mathcal{T}_\pm^{0i} \quad = \quad \mathcal{T}_\pm^{i0} = -\mathcal{U}_\pm^{0i} = \mathcal{U}_\pm^{i0} = \pm e_1\, \hat{k}_1^i \pm e_2\, \hat{k}_2^i \quad , \quad i = x, y, z , \tag{3.80b}$$

$$\mathcal{T}_\pm^{ij} \quad = \quad -\mathcal{U}_\pm^{ij} = \delta^{ij} \left(1 - e_1 e_2\, \hat{\mathbf{k}}_1 \cdot \hat{\mathbf{k}}_2 \right) + e_1 e_2 \left(\hat{k}_1^i\, \hat{k}_2^j + \hat{k}_1^j\, \hat{k}_2^i \right) , \quad i, j = x, y, z \tag{3.80c}$$

Having Eq.(3.75), we can start to evaluate the longitudinal $\Pi^{00}(P)$ and transverse $\Pi^t(P)$ components of the self-energy and plot the associated spectral densities. Before doing this, however, we must notice that, as already shown in [141], for the 2SC phase, where the $SU(3)_c$ gauge symmetry is spontaneously broken by diquark condensation, the Nambu-Goldstone excitations of the diquark condensate mix with the gluons associated with the broken generators of the original gauge group. It is shown that the mixing can be removed with a particular choice of 't Hooft gauge. The unmixing leads to a new form for the longitudinal component of the gluon self-energy $\hat{\Pi}^{00}(P)$ which is substantially different from the one we have obtained before the unmixing $\Pi^{00}(P)$. The same kind of mixing must happen in the CFL phase and the procedure for unmixing is as it is for the 2SC phase.

3.4.4 NG bosons and longitudinal gluon modes

In this section, we present the calculations which manifest the mixing between the Nambu-Goldstone bosons and the longitudinal gluon modes. Afterwards, we show how the decoupling takes place using a proper choice of the 't Hooft gauge.

To write the Lagrangian of color superconductivity, we have to add the term

$$\int_{x,y} \bar{\psi}_{Cr}(x)\, \Delta^+(x,y)\, \psi_r(y) \;, \tag{3.81}$$

and the corresponding charge-conjugate term

$$\int_{x,y} \bar{\psi}_r(x)\, \Delta^-(x,y)\, \psi_{Cr}(y) \;, \tag{3.82}$$

to the Lagrangian of the normal phase (3.8). Here, Δ^- is related to Δ^+ via

$$\Delta^- \equiv \gamma_0\, (\Delta^+)^\dagger\, \gamma_0 \;. \tag{3.83}$$

Hence, we have the quark (replica) partition function in the presence of the gluon field A_a^μ *and* the diquark source fields Δ^+, Δ^-:

$$
\begin{aligned}
\mathcal{Z}_M[A, \Delta^+, \Delta^-] \;\equiv\; & \int \prod_{r=1}^{M/2} \mathcal{D}\bar{\Psi}_r\, \mathcal{D}\Psi_r\, \exp\left\{ \sum_{r=1}^{M/2} \left[\int_{x,y} \bar{\Psi}_r(x)\, S^{-1}(x,y)\, \Psi_r(y) \right. \right. \\
& + \left. \left. \int_x \left(g\, \bar{\Psi}_r(x)\, A_\mu^a(x)\, \hat{\Gamma}_a^\mu\, \Psi_r(x) \right) \right] \right\} \;,
\end{aligned}
\tag{3.84}
$$

where

$$S^{-1}(x,y) \equiv \begin{pmatrix} [G_0^+]^{-1}(x,y) & \Delta^-(x,y) \\ \Delta^+(x,y) & [G_0^-]^{-1}(x,y) \end{pmatrix} \tag{3.85}$$

is the inverse quasiparticle propagator. One should notice that the diquark condensate is not an external field, but assumes a nonzero value because of an intrinsic property of the system. In addition, it is the Legendre-transformed functional which gives the effective action and the fluctuations for the diquark condensate, i.e., the proper functional which provides thermodynamic functions is a Legendre transform of $\ln \mathcal{Z}[\Delta^+, \Delta^-]$. Therefore, the functional dependence

on the diquark source term has to be replaced by that on the corresponding canonically conjugate variable, the diquark condensate. If the latter is *constant*, the effective action is, up to a factor of V/T, identical to the effective potential, cf. Ref. [142]. The pressure is obtained from the value of the effective potential at its maximum point. This maximum is determined by a Dyson-Schwinger equation for the diquark condensate, which is identical to the standard gap equation for the color-superconducting gap. In the mean-field approximation, the relevant calculations are done in Refs. [128, 130, 133]. In this approximation we have (from [105]),

$$\Delta^+(x,y) \sim \langle\, \psi_{Cr}(x)\,\bar{\psi}_r(y)\,\rangle \quad, \quad \Delta^-(x,y) \sim \langle\, \psi_r(x)\,\bar{\psi}_{Cr}(y)\,\rangle \; . \tag{3.86}$$

In the following, we consider the partition function in the presence of diquark source terms $\Delta^\pm$. Note, however, that the derivation of the pressure via the Legendre transformation $\ln\mathcal{Z}[\Delta^+,\Delta^-]$ does not concern us because we only want to calculate the gluon propagator. For this purpose, we use the same diquark sources for all quark species, $\Delta_r^\pm = \Delta^\pm$.

The fluctuations of the diquark condensate correspond physically to the Nambu-Goldstone excitations, meson fields, in a color superconductor. Here, instead of considering the physical meson fields, we consider the variables in $\mathcal{Z}[\Delta^+,\Delta^-]$ which correspond to these fields. We choose these fluctuations to be complex phase factors multiplying the magnitude of the source terms,

$$\Delta^+(x,y) = \mathcal{V}^*(x)\,\Phi^+(x,y)\,\mathcal{V}^\dagger(y) \; , \tag{3.87}$$
$$\Delta^-(x,y) = \mathcal{V}(x)\,\Phi^-(x,y)\,\mathcal{V}^T(y) \; , \tag{3.88}$$

where

$$\mathcal{V}(x) \equiv \exp\left(i\sum_{a=1}^{8} \varphi_a(x)T_a \right) \; . \tag{3.89}$$

The fields φ_a are external fields which, after a Legendre transformation of $\ln\mathcal{Z}[\Delta^+,\Delta^-]$, are replaced by the meson fields. Nevertheless, we refer to them as meson fields in the following. Besides, after explicitly introducing the fluctuations of the diquark source terms in terms of phase factors, the functions $\Phi^\pm$ are allowed to fluctuate only in magnitude.

To preserve the simple structure of the terms coupling the quark fields to the diquark sources, we have to express the quark fields ψ_r in terms of new fields χ_r,

$$\psi_r = \mathcal{V}\,\chi_r \quad, \quad \bar{\psi}_r = \bar{\chi}_r\,\mathcal{V}^\dagger \; . \tag{3.90}$$

Since the meson fields are real-valued and the generators $T_1,\ldots,T_8$ are hermitian, the (matrix-valued) operator $\mathcal{V}$ is unitary, $\mathcal{V}^{-1} = \mathcal{V}^\dagger$. The charge-conjugate fields are written as following

$$\psi_{Cr} = \mathcal{V}^*\,\chi_{Cr} \quad, \quad \bar{\psi}_{Cr} = \bar{\chi}_{Cr}\,\mathcal{V}^T \; , \tag{3.91}$$

and using them we have

$$\bar{\psi}_{Cr}(x)\,\Delta^+(x,y)\,\psi_r(y) \equiv \bar{\chi}_{Cr}(x)\,\Phi^+(x,y)\,\chi_r(y) \; , \tag{3.92}$$
$$\bar{\psi}_r(x)\,\Delta^-(x,y)\,\psi_{Cr}(y) \equiv \bar{\chi}_r(x)\,\Phi^-(x,y)\,\chi_{Cr}(y) \; . \tag{3.93}$$

In the mean-field approximation, the diquark source terms are proportional to

$$\Phi^+(x,y) \sim \langle\, \chi_{Cr}(x)\,\bar{\chi}_r(y)\,\rangle \quad, \quad \Phi^-(x,y) \sim \langle\, \chi_r(x)\,\bar{\chi}_{Cr}(y)\,\rangle \; . \tag{3.94}$$

In addition, the transformations (3.90) change the form of the kinetic terms of the quarks and the term coupling quarks to gluons,

$$
\bar{\psi}_r \left(i\,\gamma^\mu\partial_\mu + \mu\,\gamma_0 + g\,\gamma_\mu\,A_a^\mu T_a \right) \psi_r \;=\; \bar{\chi}_r \left(i\,\gamma^\mu\partial_\mu + \mu\,\gamma_0 + \gamma_\mu\,\omega^\mu \right) \chi_r \;, \tag{3.95a}
$$

$$
\bar{\psi}_{Cr} \left(i\,\gamma^\mu\partial_\mu - \mu\,\gamma_0 - g\,\gamma_\mu\,A_a^\mu T_a^T \right) \psi_{Cr} \;=\; \bar{\chi}_{Cr} \left(i\,\gamma^\mu\partial_\mu - \mu\,\gamma_0 + \gamma_\mu\,\omega_C^\mu \right) \chi_{Cr} \;, \tag{3.95b}
$$

where

$$
\omega^\mu \equiv \mathcal{V}^\dagger \left(i\,\partial^\mu + g\,A_a^\mu T_a \right) \mathcal{V} \tag{3.96a}
$$

is the $N_c N_f \times N_c N_f$-dimensional Maurer-Cartan one-form introduced in Ref. [143]. The charge-conjugate version of the previous formula is

$$
\omega_C^\mu \equiv \mathcal{V}^T \left(i\,\partial^\mu - g\,A_a^\mu T_a^T \right) \mathcal{V}^* \;. \tag{3.96b}
$$

The Nambu-Gorkov spinors

$$
X_r \equiv \begin{pmatrix} \chi_r \\ \chi_{Cr} \end{pmatrix} \;, \quad \bar{X}_r \equiv \left(\bar{\chi}_r \,, \, \bar{\chi}_{Cr} \right) \tag{3.97}
$$

together with the $2N_c N_f \times 2N_c N_f$-dimensional Maurer-Cartan one-form

$$
\Omega^\mu(x, y) \equiv -i \begin{pmatrix} \omega^\mu(x) & 0 \\ 0 & \omega_C^\mu(x) \end{pmatrix} \delta^{(4)}(x - y) \;, \tag{3.98}
$$

lead to the quark (replica) partition function

$$
\mathcal{Z}_M[\Omega, \Phi^+, \Phi^-] \equiv \int \prod_{r=1}^{M/2} \mathcal{D}\bar{X}_r\, \mathcal{D}X_r \; \exp\left\{ \sum_{r=1}^{M/2} \int_{x,y} \bar{X}_r(x) \left[\mathcal{S}^{-1}(x, y) + \gamma_\mu \Omega^\mu(x, y) \right] X_r(y) \right\} \;, \tag{3.99}
$$

where the inverse propagator has the following form

$$
\mathcal{S}^{-1} \equiv \begin{pmatrix} [G_0^+]^{-1} & \Phi^- \\ \Phi^+ & [G_0^-]^{-1} \end{pmatrix} \;. \tag{3.100}
$$

Since Eq. (3.99) features both gluons and fermions and we are interested only in the gluonic part, we have to integrate out the fermionic part. An analytical calculation yields

$$
\mathcal{Z}_M[\Omega, \Phi^+, \Phi^-] \equiv \left[\det\left(\mathcal{S}^{-1} + \gamma_\mu \Omega^\mu \right) \right]^{M/2} \;, \tag{3.101}
$$

where the determinant is over Nambu-Gorkov, color, flavor, spin, and space-time indices. Now it is the time to let $M \to 1$. Therefore, the QCD partition function changes into

$$
\mathcal{Z}[\varphi, \Phi^+, \Phi^-] = \int \mathcal{D}A \; \exp\left[S_A + \frac{1}{2} \operatorname{Tr} \ln\left(\mathcal{S}^{-1} + \gamma_\mu \Omega^\mu \right) \right] \;. \tag{3.102}
$$

which contains meson φ_a and diquark $\Phi^\pm$ source fields. Linearity of Ω^μ in A_a^μ (cf. Eq. (3.98) with (3.96a)) helps to expand the logarithm to the second order in Ω^μ,

$$\frac{1}{2}\operatorname{Tr}\ln\left(\mathcal{S}^{-1}+\gamma_\mu\Omega^\mu\right) \simeq \frac{1}{2}\operatorname{Tr}\ln\mathcal{S}^{-1}+\frac{1}{2}\operatorname{Tr}\left(\mathcal{S}\,\gamma_\mu\Omega^\mu\right)-\frac{1}{4}\operatorname{Tr}\left(\mathcal{S}\,\gamma_\mu\Omega^\mu\,\mathcal{S}\,\gamma_\nu\Omega^\nu\right)$$

$$\equiv S_0[\Phi^+,\Phi^-]+S_1[\Omega,\Phi^+,\Phi^-]+S_2[\Omega,\Phi^+,\Phi^-]\,. \qquad (3.103)$$

The term S_1 is a tadpole source term for the gluon fields and does not affect the gluon propagator. Thus, we ignore this term in the following. Furthermore, the quadratic term S_2 represents the contribution of a fermion loop to the gluon self-energy. First we take the trace over Nambu-Gorkov space,

$$\begin{aligned}
S_2 &= -\frac{1}{4}\int_{x,y}\operatorname{Tr}_{c,f,s}[G^+(x,y)\,\gamma_\mu\omega^\mu(y)\,G^+(y,x)\,\gamma_\nu\omega^\nu(x)\\
&\quad+\ G^-(x,y)\,\gamma_\mu\omega_C^\mu(y)\,G^-(y,x)\,\gamma_\nu\omega_C^\nu(x)\\
&\quad+\ \Xi^+(x,y)\,\gamma_\mu\omega^\mu(y)\,\Xi^-(y,x)\,\gamma_\nu\omega_C^\nu(x)\\
&\quad+\ \Xi^-(x,y)\,\gamma_\mu\omega_C^\mu(y)\,\Xi^+(y,x)\,\gamma_\nu\omega^\nu(x)]\,.
\end{aligned} \qquad (3.104)$$

To proceed, we have to find the trace over color, flavor, and spin indices. For simplicity, let us switch into Fourier space,

$$G^\pm(x,y) = \frac{T}{V}\sum_K e^{-iK\cdot(x-y)}\,G^\pm(K)\,, \qquad (3.105\text{a})$$

$$\Xi^\pm(x,y) = \frac{T}{V}\sum_K e^{-iK\cdot(x-y)}\,\Xi^\pm(K)\,, \qquad (3.105\text{b})$$

$$\omega^\mu(x) = \sum_P e^{-iP\cdot x}\,\omega^\mu(P)\,, \qquad (3.105\text{c})$$

$$\omega_C^\mu(x) = \sum_P e^{-iP\cdot x}\,\omega_C^\mu(P)\,. \qquad (3.105\text{d})$$

From (3.96a) and (3.89), we already know that ω^μ and ω_C^μ are functions of the meson fields φ_i. We expand ω^μ and ω_C^μ to the linear order in the meson fields,

$$\omega^\mu \simeq g\,A_a^\mu\,T_a-\sum_{a=1}^{8}(\partial^\mu\varphi_a)\,T_a\,, \qquad (3.106\text{a})$$

$$\omega_C^\mu \simeq -g\,A_a^\mu\,T_a^T+\sum_{a=1}^{8}(\partial^\mu\varphi_a)\,T_a^T\,. \qquad (3.106\text{b})$$

Using these expressions we find

$$\begin{aligned}
S_2 &= -\frac{1}{4}\sum_{K,P}\operatorname{Tr}_{c,f,s}\left[G^+(K)\,\gamma_\mu\omega^\mu(P)\,G^+(K-P)\,\gamma_\nu\omega^\nu(-P)\right.\\
&\quad+\ G^-(K)\,\gamma_\mu\omega_C^\mu(P)\,G^-(K-P)\,\gamma_\nu\omega_C^\nu(-P)\\
&\quad+\ \Xi^+(K)\,\gamma_\mu\omega^\mu(P)\,\Xi^-(K-P)\,\gamma_\nu\omega_C^\nu(-P)\\
&\quad+\left.\ \Xi^-(K)\,\gamma_\mu\omega_C^\mu(P)\,\Xi^+(K-P)\,\gamma_\nu\omega^\nu(-P)\right]\,.
\end{aligned} \qquad (3.107)$$

After inserting (3.96a) and using (3.46), the final result can be written in the compact form (cf. Eq. (C19) of Ref. [144])

$$S_2 = -\frac{1}{2}\frac{V}{T}\sum_P\sum_{a=1}^{8}\left[A_\mu^a(-P) - \frac{i}{g}\,P_\mu\,\varphi^a(-P)\right]\Pi_{aa}^{\mu\nu}(P)\left[A_\nu^a(P) + \frac{i}{g}\,P_\nu\,\varphi^a(P)\right]\,, \qquad (3.108)$$

where the transversality of the polarisation tensor in the normal-conducting phase, $\Pi^{\mu\nu}(P)\,P_\nu = P_\mu\,\Pi^{\mu\nu}(P) = 0$, has been used. Now we have to tensor-decompose $\Pi_{aa}^{\mu\nu}$ to make the mixing visible. There are different ways to do this [141, 144], but we follow the method used in [129]. First, we consider the parallel and orthogonal subspaces of P_μ. The projector onto the parallel subspace of P^μ is

$$\mathrm{E}^{\mu\nu} = \frac{P^\mu\,P^\nu}{P^2}\,, \qquad (3.109)$$

and a vector orthogonal to P^μ, for instance, is

$$N^\mu \equiv \left(\frac{p_0\,p^2}{P^2}, \frac{p_0^2\,\mathbf{p}}{P^2}\right) \equiv (g^{\mu\nu} - \mathrm{E}^{\mu\nu})\,f_\nu\,, \qquad (3.110)$$

where $f^\mu = (0, \mathbf{p})$. Second, we introduce the following projectors

$$\mathrm{B}^{\mu\nu} = \frac{N^\mu\,N^\nu}{N^2}\,,\quad \mathrm{C}^{\mu\nu} = N^\mu\,P^\nu + P^\mu\,N^\nu\,,\quad \mathrm{A}^{\mu\nu} = g^{\mu\nu} - \mathrm{B}^{\mu\nu} - \mathrm{E}^{\mu\nu}\,. \qquad (3.111)$$

The explicit form of the tensor $\mathrm{A}^{\mu\nu}$ shows that $\mathrm{A}^{\mu\nu}$ projects onto the spatially transverse subspace orthogonal to P^μ,

$$\mathrm{A}^{00} = \mathrm{A}^{0i} = 0\,,\quad \mathrm{A}^{ij} = -\left(\delta^{ij} - \hat{p}^i\,\hat{p}^j\right)\,, \qquad (3.112)$$

and in the same way, we see that the tensor $\mathrm{B}^{\mu\nu}$ projects onto the spatially longitudinal subspace orthogonal to P^μ,

$$\mathrm{B}^{00} = -\frac{p^2}{P^2}\,,\quad \mathrm{B}^{0i} = -\frac{p_0\,p^i}{P^2}\,,\quad \mathrm{B}^{ij} = -\frac{p_0^2}{P^2}\,\hat{p}^i\,\hat{p}^j\,. \qquad (3.113)$$

Now we can write the gluon self-energy in terms of the projectors,

$$\Pi_{aa}^{\mu\nu}(P) = \Pi_{aa}^{\mathrm{a}}(P)\,\mathrm{A}^{\mu\nu} + \Pi_{aa}^{\mathrm{b}}(P)\,\mathrm{B}^{\mu\nu} + \Pi_{aa}^{\mathrm{c}}(P)\,\mathrm{C}^{\mu\nu} + \Pi_{aa}^{\mathrm{e}}(P)\,\mathrm{E}^{\mu\nu}\,. \qquad (3.114)$$

Furthermore, if we introduce the transverse and longitudinal component of the self-energy as

$$\Pi_{aa}^{t}(P) \equiv \frac{1}{2}\left(\delta^{ij} - \hat{p}^i\,\hat{p}^j\right)\Pi_{aa}^{ij}(P)\,,\quad \Pi_{aa}^{\ell}(P) \equiv \hat{p}_i\,\Pi_{aa}^{ij}(P)\,\hat{p}_j\,, \qquad (3.115)$$

the polarisation functions Π_{aa}^{a}, Π_{aa}^{b}, Π_{aa}^{c}, and Π_{aa}^{e}, respectively, assumes the following form

$$\Pi_{aa}^{\mathrm{a}}(P) = \frac{1}{2}\,\Pi_{aa}^{\mu\nu}(P)\,\mathrm{A}_{\mu\nu} = -\Pi_{aa}^{t}(P)\,, \qquad (3.116a)$$

$$\Pi_{aa}^{\mathrm{b}}(P) = \Pi_{aa}^{\mu\nu}(P)\,\mathrm{B}_{\mu\nu} = -\frac{p^2}{P^2}\left[\Pi_{aa}^{00}(P) + 2\,\frac{p_0}{p}\,\Pi_{aa}^{0i}(P)\,\hat{p}_i + \frac{p_0^2}{p^2}\,\Pi_{aa}^{\ell}(P)\right]\,, \qquad (3.116b)$$

$$\Pi_{aa}^{\mathrm{c}}(P) = \frac{1}{2\,N^2\,P^2}\,\Pi_{aa}^{\mu\nu}(P)\,\mathrm{C}_{\mu\nu} = -\frac{1}{P^2}\left[\Pi_{aa}^{00}(P) + \frac{p_0^2 + p^2}{p_0\,p}\,\Pi_{aa}^{0i}(P)\,\hat{p}_i + \Pi_{aa}^{\ell}(P)\right] \qquad (3.116c)$$

$$\Pi_{aa}^{\mathrm{e}}(P) = \Pi_{aa}^{\mu\nu}(P)\,\mathrm{E}_{\mu\nu} = \frac{1}{P^2}\left[p_0^2\,\Pi_{aa}^{00}(P) + 2\,p_0\,p\,\Pi_{aa}^{0i}(P)\,\hat{p}_i + p^2\,\Pi_{aa}^{\ell}(P)\right]\,. \qquad (3.116d)$$

All these calculations are aiming to manifest the mixing between the excitations of the condensate with the gauge fields corresponding to the broken generators of the underlying gauge group. To achieve this goal, we define

$$A_{\perp\,\mu}^a(P) = \mathrm{A}_\mu^{\ \nu}\, A_\nu^a(P) \quad , \quad A_\parallel^a(P) = \frac{P^\mu\, A_\mu^a(P)}{P^2} \quad , \quad A_N^a(P) = \frac{N^\mu\, A_\mu^a(P)}{N^2} \,. \tag{3.117}$$

Since N^μ is odd under $P \to -P$, we find $A_\parallel^a(-P) = -P^\mu A_\mu^a(-P)/P^2$, and $A_N^a(-P) = -N^\mu A_\mu^a(-P)/N^2$. Consequently, Eq. (3.108) transforms into

$$
\begin{aligned}
S_2 \;=\; & -\frac{1}{2}\frac{V}{T}\sum_P\sum_{a=1}^8 \Bigg\{ A_{\perp\,\mu}^a(-P)\, \Pi_{aa}^{\mathrm{a}}(P)\, \mathrm{A}^{\mu\nu}\, A_{\perp\,\nu}^a(P) - A_N^a(-P)\, \Pi_{aa}^{\mathrm{b}}(P)\, N^2\, A_N^a(P) \\
& - \left[A_\parallel^a(-P) + \frac{i}{g}\,\varphi^a(-P) \right] \Pi_{aa}^{\mathrm{c}}(P)\, N^2 P^2\, A_N^a(P) \\
& - A_N^a(-P)\, \Pi_{aa}^{\mathrm{c}}(P)\, N^2 P^2 \left[A_\parallel^a(P) + \frac{i}{g}\,\varphi^a(P) \right] \\
& - \left[A_\parallel^a(-P) + \frac{i}{g}\,\varphi^a(-P) \right] \Pi_{aa}^{\mathrm{e}}(P)\, P^2 \left[A_\parallel^a(P) + \frac{i}{g}\,\varphi^a(P) \right] \Bigg\} \,.
\end{aligned}
\tag{3.118}
$$

The mixing occurs in the components orthogonal to the spatially transverse degrees of freedom, *i.e.*, for the spatially longitudinal fields, A_N^a, and the fields parallel to P^μ, $A_\parallel^a$. This is in fact a mixing of mesons and gluon fields. These terms can be eliminated by a suitable choice of the 't Hooft gauge. The unmixing is done in two steps. First we have to eliminate the terms which mix A_N^a and $A_\parallel^a$ using the following transformation,

$$\hat{A}_\parallel^a(P) = A_\parallel^a(P) + \frac{\Pi_{aa}^{\mathrm{c}}(P)\, N^2}{\Pi_{aa}^{\mathrm{e}}(P)}\, A_N^a(P) \,. \tag{3.119}$$

We must notice that, in the 2SC phase, due to the unbroken $SU(2)_c$, for $a = 1, 2, 3$ gluons Π_{aa}^{c} automatically vanishes and there are no terms to mix $A_\parallel^a$ and A_N^a. Thus, we do not have to perform the substitution (3.119) for those gluons. In contrast to this, in the CFL phase, the mixing happens for $a = 1, \dots 8$ and we have to substitute (3.119) into (3.118) for all gluons.

Notice that the shift in the fields P^μ, Eq. (3.119), does not change the physical observables. The reason is as follows. First, the Jacobian $\partial(\hat{A}_\parallel, A_N)/\partial(A_\parallel, A_N)$ is unity, so the measure of the functional integral over gauge fields is not affected. Second, since the remaining term in the gauge field action is quadratic in the gauge fields, it is relevant for the derivation of the gluon propagator. This term, however, is a free field action,

$$
\begin{aligned}
S_{F^2}^{(0)} \;\equiv\; & -\frac{1}{2}\frac{V}{T}\sum_P\sum_{a=1}^8 A_\mu^a(-P)\left(P^2\, g^{\mu\nu} - P^\mu P^\nu \right) A_\nu^a(P) \\
\equiv\; & -\frac{1}{2}\frac{V}{T}\sum_P\sum_{a=1}^8 A_\mu^a(-P)\, P^2\, (\mathrm{A}^{\mu\nu} + \mathrm{B}^{\mu\nu})\, A_\nu^a(P) \,,
\end{aligned}
\tag{3.120}
$$

meaning that it does not contain $A^a_\parallel(P)$. Therefore, it is not affected by the shift of variables (3.119) either. Renaming $\hat{A}^a_\parallel \to A^a_\parallel$, the final result for S_2 reads

$$
\begin{aligned}
S_2 \;\; = \;\; & -\frac{1}{2}\frac{V}{T}\sum_P\sum_{a=1}^8 \Big\{\, A^a_{\perp\,\mu}(-P)\,\Pi^{\mathrm{a}}_{aa}(P)\,A^{\mu\nu}\,A^a_{\perp\,\nu}(P) - A^a_N(-P)\,\hat{\Pi}^{\mathrm{b}}_{aa}(P)\,N^2\,A^a_N(P) \\
& \qquad -\left[A^a_\parallel(-P)+\frac{i}{g}\,\varphi^a(-P)\right]\Pi^{\mathrm{e}}_{aa}(P)\,P^2\left[A^a_\parallel(P)+\frac{i}{g}\,\varphi^a(P)\right]\Big\}\,,\quad (3.121)
\end{aligned}
$$

where

$$
\hat{\Pi}^{\mathrm{b}}_{aa}(P) \equiv \Pi^{\mathrm{b}}_{aa}(P) - \frac{[\Pi^{\mathrm{c}}_{aa}(P)]^2\,N^2 P^2}{\Pi^{\mathrm{e}}_{aa}(P)}\,. \tag{3.122}
$$

Now, we can choose the 't Hooft gauge fixing term to eliminate the mixing between $A^a_\parallel$ and φ^a with the following expression

$$
S_{\mathrm{gf}} = \frac{1}{2\,\lambda}\frac{V}{T}\sum_P\sum_{a=1}^8\left[P^2\,A^a_\parallel(-P)-\lambda\,\frac{i}{g}\,\Pi^{\mathrm{e}}_{aa}(P)\,\varphi^a(-P)\right]\left[P^2\,A^a_\parallel(P)-\lambda\,\frac{i}{g}\,\Pi^{\mathrm{e}}_{aa}(P)\,\varphi^a(P)\right]\,.
$$
$$
\tag{3.123}
$$

The non-locality of the 't Hooft gauge in coordinate space does not cause any problem in momentum space. Note that $P^2\,A^a_\parallel(P)\equiv P^\mu\,A^a_\mu(P)$. Therefore, in various limits the choice of gauge (3.123) corresponds to covariant gauge,

$$
S_{\mathrm{cg}} = \frac{1}{2\,\lambda}\frac{V}{T}\sum_P\sum_{a=1}^8 A^a_\mu(-P)\,P^\mu\,P^\nu\,A^a_\nu(P)\,. \tag{3.124}
$$

Adding (3.123) to (3.121) and (3.120), we find

$$
\begin{aligned}
S^{(0)}_{F^2}+S_2+S_{\mathrm{gf}} \;\;=\;\; & -\frac{1}{2}\frac{V}{T}\sum_P\sum_{a=1}^8\Big\{\, A^a_{\perp\,\mu}(-P)\left[P^2+\Pi^{\mathrm{a}}_{aa}(P)\right]\mathrm{A}^{\mu\nu}\,A^a_{\perp\,\nu}(P) \\
& -\;\; A^a_N(-P)\left[P^2+\hat{\Pi}^{\mathrm{b}}_{aa}(P)\right]N^2\,A^a_N(P) \\
& -\;\; A^a_\parallel(-P)\left[\frac{1}{\lambda}\,P^2+\Pi^{\mathrm{e}}_{aa}(P)\right]P^2\,A^a_\parallel(P) \\
& +\;\; \frac{\lambda}{g^2}\,\varphi^a(-P)\left[\frac{1}{\lambda}\,P^2+\Pi^{\mathrm{e}}_{aa}(P)\right]\Pi^{\mathrm{e}}_{aa}(P)\,\varphi^a(P)\Big\}\,. \tag{3.125}
\end{aligned}
$$

As we see the mesons and gluon fields are decoupled. In this case, the inverse gluon propagator is

$$
\Delta^{-1\,\mu\nu}_{aa}(P) = \left[P^2+\Pi^{\mathrm{a}}_{aa}(P)\right]\mathrm{A}^{\mu\nu}+\left[P^2+\hat{\Pi}^{\mathrm{b}}_{aa}(P)\right]\mathrm{B}^{\mu\nu}+\left[\frac{1}{\lambda}\,P^2+\Pi^{\mathrm{e}}_{aa}(P)\right]\mathrm{E}^{\mu\nu}\,,\quad (3.126)
$$

which gives the gluon propagator for gluons of color a

$$
\Delta^{\mu\nu}_{aa}(P) = \frac{1}{P^2+\Pi^{\mathrm{a}}_{aa}(P)}\,\mathrm{A}^{\mu\nu}+\frac{1}{P^2+\hat{\Pi}^{\mathrm{b}}_{aa}(P)}\,\mathrm{B}^{\mu\nu}+\frac{\lambda}{P^2+\lambda\,\Pi^{\mathrm{e}}_{aa}(P)}\,\mathrm{E}^{\mu\nu}\,. \tag{3.127}
$$

For $\lambda \neq 0$ this expression has nonphysical contributions parallel to P^μ. When we compute physical observables, these terms have to be cancelled by the corresponding Fadeev-Popov ghosts. For $\lambda = 0$, however, there are no nonphysical contributions and the gluon propagator is explicitly transverse, *i.e.*, $P_\mu \Delta_{aa}^{\mu\nu}(P) = \Delta_{aa}^{\mu\nu}(P) P_\nu = 0$. In this case the ghost propagator is independent of the chemical potential μ and the contribution of Fadeev-Popov ghosts to the polarisation tensor is $\sim g^2 T^2$, which is negligible at $T = 0$. For $\lambda = 0$, the inverse meson field propagator is

$$D_{aa}^{-1}(P) \equiv \Pi_{aa}^{\mathrm{e}}(P)\, P^2 = P_\mu\, \Pi_{aa}^{\mu\nu}(P)\, P_\nu \ , \tag{3.128}$$

and the dispersion relation for the mesons is determined from $D_{aa}^{-1}(P) = 0$, cf. Ref. [139]. From Eq. (3.127), the transverse mode of the gluon propagator can be read from the coefficient of $\mathrm{A}^{\mu\nu}$ as

$$\Delta_{aa}^{t}(P) \equiv \frac{1}{P^2 + \Pi_{aa}^{\mathrm{a}}(P)} = \frac{1}{P^2 - \Pi_{aa}^{t}(P)} \ , \tag{3.129}$$

with the definitions in Eq. (3.116a). Considering (3.113), we multiply the coefficient of $\mathrm{B}^{\mu\nu}$ in Eq. (3.127) with the standard factor $-P^2/p^2$, cf. [129], to obtain the longitudinal propagator

$$\hat{\Delta}_{aa}^{00}(P) \equiv -\frac{P^2}{p^2} \frac{1}{P^2 + \hat{\Pi}_{aa}^{\mathrm{b}}(P)} = -\frac{1}{p^2 - \hat{\Pi}_{aa}^{00}(P)} \ , \tag{3.130}$$

where the longitudinal gluon self-energy is

$$\hat{\Pi}_{aa}^{00}(P) \equiv p^2\, \frac{\Pi_{aa}^{00}(P)\, \Pi_{aa}^{\ell}(P) - \left[\Pi_{aa}^{0i}(P)\, \hat{p}_i\right]^2}{p_0^2\, \Pi_{aa}^{00}(P) + 2\, p_0\, p\, \Pi_{aa}^{0i}(P)\, \hat{p}_i + p^2\, \Pi_{aa}^{\ell}(P)} \ . \tag{3.131}$$

Here, we have used Eq.(3.122) and the relations (3.116). In the next subsection (3.5) we compute the self-energies and the relevant spectral densities.

3.5 Explicit calculation of the gluon self-energy

The Meissner mass is introduced via

$$m_M^2 \equiv \lim_{p \to 0} \Pi^{ii}(0, p) \ . \tag{3.132}$$

The explicit form of Π^{ij} was already shown in [149],

$$
\begin{aligned}
\Pi^{ij}(P) \ = \ & -\frac{g^2}{12} \int \frac{d^3\mathbf{k}}{(2\pi)^3} \sum_{e_1,e_2=\pm} \left[\delta^{ij} \left(1 - e_1 e_2\, \hat{\mathbf{k}}_1 \cdot \hat{\mathbf{k}}_2\right) + e_1 e_2 \left(\hat{k}_1^i\, \hat{k}_2^j + \hat{k}_1^j\, \hat{k}_2^i\right) \right] \\
& \times \left[\left(\frac{1}{p_0 + \hat{\epsilon}_1 + \epsilon_2} - \frac{1}{p_0 - \hat{\epsilon}_1 - \epsilon_2}\right) (1 - \hat{N}_1 - N_2)\, \frac{\hat{\epsilon}_1\, \epsilon_2 - \xi_1\, \xi_2 + \hat{\phi}_1\, \phi_2}{2\, \hat{\epsilon}_1\, \epsilon_2} \right. \\
& \ + \left(\frac{1}{p_0 + \epsilon_1 + \hat{\epsilon}_2} - \frac{1}{p_0 - \epsilon_1 - \hat{\epsilon}_2}\right) (1 - N_1 - \hat{N}_2)\, \frac{\epsilon_1\, \hat{\epsilon}_2 - \xi_1\, \xi_2 + \phi_1\, \hat{\phi}_2}{2\, \epsilon_1\, \hat{\epsilon}_2} \\
& \left. + 7 \left(\frac{1}{p_0 + \epsilon_1 + \epsilon_2} - \frac{1}{p_0 - \epsilon_1 - \epsilon_2}\right) (1 - N_1 - N_2)\, \frac{\epsilon_1\, \epsilon_2 - \xi_1\, \xi_2 + 2\, \phi_1\, \phi_2/7}{2\, \epsilon_1\, \epsilon_2} \right.
\end{aligned}
$$

$$+ \left(\frac{1}{p_0 - \hat{\epsilon}_1 + \epsilon_2} - \frac{1}{p_0 + \hat{\epsilon}_1 - \epsilon_2} \right) (\hat{N}_1 - N_2) \frac{\hat{\epsilon}_1 \epsilon_2 + \xi_1 \xi_2 - \hat{\phi}_1 \phi_2}{2 \, \hat{\epsilon}_1 \epsilon_2}$$

$$+ \left(\frac{1}{p_0 - \epsilon_1 + \hat{\epsilon}_2} - \frac{1}{p_0 + \epsilon_1 - \hat{\epsilon}_2} \right) (N_1 - \hat{N}_2) \frac{\epsilon_1 \hat{\epsilon}_2 + \xi_1 \xi_2 - \phi_1 \hat{\phi}_2}{2 \, \epsilon_1 \hat{\epsilon}_2}$$

$$+ 7 \left(\frac{1}{p_0 - \epsilon_1 + \epsilon_2} - \frac{1}{p_0 + \epsilon_1 - \epsilon_2} \right) (N_1 - N_2) \frac{\epsilon_1 \epsilon_2 + \xi_1 \xi_2 - 2 \, \phi_1 \phi_2/7}{2 \, \epsilon_1 \epsilon_2} \Bigg] \quad (3.133)$$

On the other hand, the Debye mass is defined as

$$m_D^2 \equiv - \lim_{p \to 0} \hat{\Pi}^{00}(0, p) \,, \qquad (3.134)$$

where $\hat{\Pi}^{00}$ is introduced in (3.131) and the minus sign is due to the choice of metric. Therefore, in order to evaluate the value of the Debye and Meissner masses we have to calculate the associated gluon self-energies.

In order to show $\hat{\Pi}^{00}_{aa}$ as a function of p_0, we need to calculate Π^{00}_{aa}, Π^{ℓ}_{aa}, and $\Pi^{0i}_{aa} \, \hat{p}_i$. For further purposes, we also have to calculate the transverse component of the gluon self-energy, Π^t_{aa}. According to Eq. (31a) of Ref. [149] we have,

$$\Pi^{00}(P) = - \frac{g^2}{12} \int \frac{d^3\mathbf{k}}{(2\pi)^3} \sum_{e_1, e_2 = \pm} (1 + e_1 e_2 \, \hat{\mathbf{k}}_1 \cdot \hat{\mathbf{k}}_2)$$

$$\times \ \Bigg[\left(\frac{1}{p_0 + \hat{\epsilon}_1 + \epsilon_2} - \frac{1}{p_0 - \hat{\epsilon}_1 - \epsilon_2} \right) (1 - \hat{N}_1 - N_2) \frac{\hat{\epsilon}_1 \epsilon_2 - \xi_1 \xi_2 - \hat{\phi}_1 \phi_2}{2 \hat{\epsilon}_1 \epsilon_2}$$

$$+ \ \left(\frac{1}{p_0 + \epsilon_1 + \hat{\epsilon}_2} - \frac{1}{p_0 - \epsilon_1 - \hat{\epsilon}_2} \right) (1 - N_1 - \hat{N}_2) \frac{\epsilon_1 \hat{\epsilon}_2 - \xi_1 \xi_2 - \phi_1 \hat{\phi}_2}{2 \epsilon_1 \hat{\epsilon}_2}$$

$$+ \ 7 \left(\frac{1}{p_0 + \epsilon_1 + \epsilon_2} - \frac{1}{p_0 - \epsilon_1 - \epsilon_2} \right) (1 - N_1 - N_2) \frac{\epsilon_1 \epsilon_2 - \xi_1 \xi_2 - 2\phi_1 \phi_2/7}{2 \epsilon_1 \epsilon_2}$$

$$+ \ \left(\frac{1}{p_0 + \hat{\epsilon}_1 + \epsilon_2} - \frac{1}{p_0 - \hat{\epsilon}_1 - \epsilon_2} \right) (\hat{N}_1 - N_2) \frac{\hat{\epsilon}_1 \epsilon_2 + \xi_1 \xi_2 + \hat{\phi}_1 \phi_2}{2 \hat{\epsilon}_1 \epsilon_2}$$

$$+ \ \left(\frac{1}{p_0 + \epsilon_1 + \hat{\epsilon}_2} - \frac{1}{p_0 - \epsilon_1 - \hat{\epsilon}_2} \right) (N_1 - \hat{N}_2) \frac{\epsilon_1 \hat{\epsilon}_2 + \xi_1 \xi_2 + \phi_1 \hat{\phi}_2}{2 \epsilon_1 \hat{\epsilon}_2}$$

$$+ \ 7 \left(\frac{1}{p_0 + \epsilon_1 + \epsilon_2} - \frac{1}{p_0 - \epsilon_1 - \epsilon_2} \right) (N_1 - N_2) \frac{\epsilon_1 \epsilon_2 + \xi_1 \xi_2 + 2\phi_1 \phi_2/7}{2 \epsilon_1 \epsilon_2} \Bigg] \quad (3.135\text{a})$$

and from Eq. (31b) of Ref. [149] we know that

$$\Pi^t(P) = - \frac{g^2}{12} \int \frac{d^3\mathbf{k}}{(2\pi)^3} \sum_{e_1, e_2 = \pm} (1 - e_1 e_2 \, \hat{\mathbf{k}}_1 \cdot \hat{\mathbf{p}} \, \hat{\mathbf{k}}_2 \cdot \hat{\mathbf{p}})$$

$$\times \ \Bigg[\left(\frac{1}{p_0 + \hat{\epsilon}_1 + \epsilon_2} - \frac{1}{p_0 - \hat{\epsilon}_1 - \epsilon_2} \right) (1 - \hat{N}_1 - N_2) \frac{\hat{\epsilon}_1 \epsilon_2 - \xi_1 \xi_2 + \hat{\phi}_1 \phi_2}{2 \hat{\epsilon}_1 \epsilon_2}$$

$$+ \ \left(\frac{1}{p_0 + \epsilon_1 + \hat{\epsilon}_2} - \frac{1}{p_0 - \epsilon_1 - \hat{\epsilon}_2} \right) (1 - N_1 - \hat{N}_2) \frac{\epsilon_1 \hat{\epsilon}_2 - \xi_1 \xi_2 + \phi_1 \hat{\phi}_2}{2 \epsilon_1 \hat{\epsilon}_2}$$

$$+ \quad 7 \left(\frac{1}{p_0 + \epsilon_1 + \epsilon_2} - \frac{1}{p_0 - \epsilon_1 - \epsilon_2} \right) (1 - N_1 - N_2) \, \frac{\epsilon_1 \epsilon_2 - \xi_1 \xi_2 + 2\phi_1 \phi_2/7}{2\,\epsilon_1 \epsilon_2}$$

$$+ \quad \left(\frac{1}{p_0 + \hat{\epsilon}_1 + \epsilon_2} - \frac{1}{p_0 - \hat{\epsilon}_1 - \epsilon_2} \right) (\hat{N}_1 - N_2) \, \frac{\hat{\epsilon}_1 \epsilon_2 + \xi_1 \xi_2 - \hat{\phi}_1 \phi_2}{2\,\hat{\epsilon}_1 \epsilon_2}$$

$$+ \quad \left(\frac{1}{p_0 + \epsilon_1 + \hat{\epsilon}_2} - \frac{1}{p_0 - \epsilon_1 - \hat{\epsilon}_2} \right) (N_1 - \hat{N}_2) \, \frac{\epsilon_1 \hat{\epsilon}_2 + \xi_1 \xi_2 - \phi_1 \hat{\phi}_2}{2\,\epsilon_1 \hat{\epsilon}_2}$$

$$+ \quad 7 \left(\frac{1}{p_0 + \epsilon_1 + \epsilon_2} - \frac{1}{p_0 - \epsilon_1 - \epsilon_2} \right) (N_1 - N_2) \, \frac{\epsilon_1 \epsilon_2 + \xi_1 \xi_2 - 2\phi_1 \phi_2/7}{2\,\epsilon_1 \epsilon_2} \Bigg] \quad (3.135\mathrm{b})$$

and

$$\Pi^\ell(P) \;=\; -\frac{g^2}{12} \int \frac{d^3 \mathbf{k}}{(2\pi)^3} \sum_{e_1, e_2 = \pm} (1 - e_1 e_2 \hat{\mathbf{k}}_1 \cdot \hat{\mathbf{k}}_2 + 2\, e_1 e_2 \, \hat{\mathbf{k}}_1 \cdot \hat{\mathbf{p}} \, \hat{\mathbf{k}}_2 \cdot \hat{\mathbf{p}})$$

$$\times \quad \Bigg[\left(\frac{1}{p_0 + \hat{\epsilon}_1 + \epsilon_2} - \frac{1}{p_0 - \hat{\epsilon}_1 - \epsilon_2} \right) (1 - \hat{N}_1 - N_2) \, \frac{\hat{\epsilon}_1 \epsilon_2 - \xi_1 \xi_2 + \hat{\phi}_1 \phi_2}{2\,\hat{\epsilon}_1 \epsilon_2}$$

$$+ \quad \left(\frac{1}{p_0 + \epsilon_1 + \hat{\epsilon}_2} - \frac{1}{p_0 - \epsilon_1 - \hat{\epsilon}_2} \right) (1 - N_1 - \hat{N}_2) \, \frac{\epsilon_1 \hat{\epsilon}_2 - \xi_1 \xi_2 + \phi_1 \hat{\phi}_2}{2\,\epsilon_1 \hat{\epsilon}_2}$$

$$+ \quad 7 \left(\frac{1}{p_0 + \epsilon_1 + \epsilon_2} - \frac{1}{p_0 - \epsilon_1 - \epsilon_2} \right) (1 - N_1 - N_2) \, \frac{\epsilon_1 \epsilon_2 - \xi_1 \xi_2 + 2\phi_1 \phi_2/7}{2\,\epsilon_1 \epsilon_2}$$

$$+ \quad \left(\frac{1}{p_0 + \hat{\epsilon}_1 + \epsilon_2} - \frac{1}{p_0 - \hat{\epsilon}_1 - \epsilon_2} \right) (\hat{N}_1 - N_2) \, \frac{\hat{\epsilon}_1 \epsilon_2 + \xi_1 \xi_2 - \hat{\phi}_1 \phi_2}{2\,\hat{\epsilon}_1 \epsilon_2}$$

$$+ \quad \left(\frac{1}{p_0 + \epsilon_1 + \hat{\epsilon}_2} - \frac{1}{p_0 - \epsilon_1 - \hat{\epsilon}_2} \right) (N_1 - \hat{N}_2) \, \frac{\epsilon_1 \hat{\epsilon}_2 + \xi_1 \xi_2 - \phi_1 \hat{\phi}_2}{2\,\epsilon_1 \hat{\epsilon}_2}$$

$$+ \quad 7 \left(\frac{1}{p_0 + \epsilon_1 + \epsilon_2} - \frac{1}{p_0 - \epsilon_1 - \epsilon_2} \right) (N_1 - N_2) \, \frac{\epsilon_1 \epsilon_2 + \xi_1 \xi_2 - 2\phi_1 \phi_2/7}{2\,\epsilon_1 \epsilon_2} \Bigg] \quad (3.135\mathrm{c})$$

The projection $\Pi^{0i}(P)\,\hat{p}_i$ was not explicitly given in Ref. [149]. Starting with Eq. (24) of Ref. [149] and following similar steps, we find

$$\Pi^{0i}(P)\,\hat{p}_i \;=\; \frac{g^2}{12} \int \frac{d^3 \mathbf{k}}{(2\pi)^3} \sum_{e_1, e_2 = \pm} (e_1 \hat{\mathbf{k}}_1 \cdot \hat{\mathbf{p}} + e_2 \, \hat{\mathbf{k}}_2 \cdot \hat{\mathbf{p}})$$

$$\times \quad \Bigg[\left(\frac{1}{p_0 + \hat{\epsilon}_1 + \epsilon_2} + \frac{1}{p_0 - \hat{\epsilon}_1 - \epsilon_2} \right) (1 - \hat{N}_1 - N_2) \, \frac{\hat{\epsilon}_1 \xi_2 - \xi_1 \epsilon_2}{2\,\hat{\epsilon}_1 \epsilon_2}$$

$$+ \quad \left(\frac{1}{p_0 + \epsilon_1 + \hat{\epsilon}_2} + \frac{1}{p_0 - \epsilon_1 - \hat{\epsilon}_2} \right) (1 - N_1 - \hat{N}_2) \, \frac{\epsilon_1 \xi_2 - \xi_1 \hat{\epsilon}_2}{2\,\epsilon_1 \hat{\epsilon}_2}$$

$$+ \quad 7 \left(\frac{1}{p_0 + \epsilon_1 + \epsilon_2} + \frac{1}{p_0 - \epsilon_1 - \epsilon_2} \right) (1 - N_1 - N_2) \, \frac{\epsilon_1 \xi_2 - \xi_1 \epsilon_2}{2\,\epsilon_1 \epsilon_2}$$

$$+ \quad \left(\frac{1}{p_0 + \hat{\epsilon}_1 + \epsilon_2} + \frac{1}{p_0 - \hat{\epsilon}_1 - \epsilon_2} \right) (\hat{N}_1 - N_2) \, \frac{\hat{\epsilon}_1 \xi_2 + \xi_1 \epsilon_2}{2\,\hat{\epsilon}_1 \epsilon_2}$$

$$+ \quad \left(\frac{1}{p_0 + \epsilon_1 + \hat{\epsilon}_2} + \frac{1}{p_0 - \epsilon_1 - \hat{\epsilon}_2} \right) (N_1 - \hat{N}_2) \, \frac{\epsilon_1 \xi_2 + \xi_1 \hat{\epsilon}_2}{2\,\epsilon_1 \hat{\epsilon}_2}$$

$$+ \quad 7 \left(\frac{1}{p_0 + \epsilon_1 + \epsilon_2} + \frac{1}{p_0 - \epsilon_1 - \epsilon_2} \right) (N_1 - N_2) \, \frac{\epsilon_1 \xi_2 + \xi_1 \epsilon_2}{2\,\epsilon_1 \epsilon_2} \Bigg] . \quad (3.135\mathrm{d})$$

Here $\xi_i \equiv e_i k_i - \mu$, $\mathbf{k}_1 \equiv \mathbf{k}$ and $\mathbf{k}_2 \equiv \mathbf{k} - \mathbf{p}$, where $\mathbf{k}$ is the quark three-momentum and $\mathbf{p}$ is the gluon three-momentum. The octet and singlet gap functions for quasiparticles ($e_i = +1$) and quasiantiparticles ($e_i = -1$) are $\phi_i \equiv \phi_{\mathbf{8}}^{e_i}$ and $\hat{\phi}_i \equiv \hat{\phi}_{\mathbf{1}}^{e_i}$, respectively, and the corresponding excitation energies are $\epsilon_i \equiv \sqrt{\xi_i^2 + \phi_i^2}$ and $\hat{\epsilon}_i \equiv \sqrt{\xi_i^2 + \hat{\phi}_i^2}$. The thermal distribution functions are $N_i \equiv [\exp(\epsilon_i/T) + 1]^{-1}$, and $\hat{N}_i \equiv [\exp(\hat{\epsilon}_i/T) + 1]^{-1}$, respectively. In the limit $T \to 0$, since $\epsilon_i, \hat{\epsilon}_i > 0$, the latter, N_i and $\hat{N}_i$, vanish. Then the expressions simplify to

$$
\begin{aligned}
\Pi^{00}(P) &= -\frac{g^2}{12} \int \frac{d^3\mathbf{k}}{(2\pi)^3} \sum_{e_1,e_2=\pm} (1 + e_1 e_2 \hat{\mathbf{k}}_1 \cdot \hat{\mathbf{k}}_2) \\
&\times \left[\left(\frac{1}{p_0 + \hat{\epsilon}_1 + \epsilon_2} - \frac{1}{p_0 - \hat{\epsilon}_1 - \epsilon_2} \right) \frac{\hat{\epsilon}_1 \epsilon_2 - \xi_1 \xi_2 - \hat{\phi}_1 \phi_2}{2\,\hat{\epsilon}_1 \epsilon_2} \right. \\
&+ \left(\frac{1}{p_0 + \epsilon_1 + \hat{\epsilon}_2} - \frac{1}{p_0 - \epsilon_1 - \hat{\epsilon}_2} \right) \frac{\epsilon_1 \hat{\epsilon}_2 - \xi_1 \xi_2 - \phi_1 \hat{\phi}_2}{2\,\epsilon_1 \hat{\epsilon}_2} \\
&+ \left. 7 \left(\frac{1}{p_0 + \epsilon_1 + \epsilon_2} - \frac{1}{p_0 - \epsilon_1 - \epsilon_2} \right) \frac{\epsilon_1 \epsilon_2 - \xi_1 \xi_2 - 2\phi_1 \phi_2/7}{2\,\epsilon_1 \epsilon_2} \right] , \quad (3.136a)
\end{aligned}
$$

$$
\begin{aligned}
\Pi^t(P) &= -\frac{g^2}{12} \int \frac{d^3\mathbf{k}}{(2\pi)^3} \sum_{e_1,e_2=\pm} (1 - e_1 e_2 \hat{\mathbf{k}}_1 \cdot \hat{\mathbf{p}}\, \hat{\mathbf{k}}_2 \cdot \hat{\mathbf{p}}) \\
&\times \left[\left(\frac{1}{p_0 + \hat{\epsilon}_1 + \epsilon_2} - \frac{1}{p_0 - \hat{\epsilon}_1 - \epsilon_2} \right) \frac{\hat{\epsilon}_1 \epsilon_2 - \xi_1 \xi_2 + \hat{\phi}_1 \phi_2}{2\,\hat{\epsilon}_1 \epsilon_2} \right. \\
&+ \left(\frac{1}{p_0 + \epsilon_1 + \hat{\epsilon}_2} - \frac{1}{p_0 - \epsilon_1 - \hat{\epsilon}_2} \right) \frac{\epsilon_1 \hat{\epsilon}_2 - \xi_1 \xi_2 + \phi_1 \hat{\phi}_2}{2\,\epsilon_1 \hat{\epsilon}_2} \\
&+ \left. 7 \left(\frac{1}{p_0 + \epsilon_1 + \epsilon_2} - \frac{1}{p_0 - \epsilon_1 - \epsilon_2} \right) \frac{\epsilon_1 \epsilon_2 - \xi_1 \xi_2 + 2\phi_1 \phi_2/7}{2\,\epsilon_1 \epsilon_2} \right] , \quad (3.136b)
\end{aligned}
$$

$$
\begin{aligned}
\Pi^{\ell}(P) &= -\frac{g^2}{12} \int \frac{d^3\mathbf{k}}{(2\pi)^3} \sum_{e_1,e_2=\pm} (1 - e_1 e_2 \hat{\mathbf{k}}_1 \cdot \hat{\mathbf{k}}_2 + 2\,e_1 e_2 \hat{\mathbf{k}}_1 \cdot \hat{\mathbf{p}}\, \hat{\mathbf{k}}_2 \cdot \hat{\mathbf{p}}) \\
&\times \left[\left(\frac{1}{p_0 + \hat{\epsilon}_1 + \epsilon_2} - \frac{1}{p_0 - \hat{\epsilon}_1 - \epsilon_2} \right) \frac{\hat{\epsilon}_1 \epsilon_2 - \xi_1 \xi_2 + \hat{\phi}_1 \phi_2}{2\,\hat{\epsilon}_1 \epsilon_2} \right. \\
&+ \left(\frac{1}{p_0 + \epsilon_1 + \hat{\epsilon}_2} - \frac{1}{p_0 - \epsilon_1 - \hat{\epsilon}_2} \right) \frac{\epsilon_1 \hat{\epsilon}_2 - \xi_1 \xi_2 + \phi_1 \hat{\phi}_2}{2\,\epsilon_1 \hat{\epsilon}_2} \\
&+ \left. 7 \left(\frac{1}{p_0 + \epsilon_1 + \epsilon_2} - \frac{1}{p_0 - \epsilon_1 - \epsilon_2} \right) \frac{\epsilon_1 \epsilon_2 - \xi_1 \xi_2 + 2\phi_1 \phi_2/7}{2\,\epsilon_1 \epsilon_2} \right] , \quad (3.136c)
\end{aligned}
$$

$$
\begin{aligned}
\Pi^{0i}(P)\,\hat{p}_i &= \frac{g^2}{12} \int \frac{d^3\mathbf{k}}{(2\pi)^3} \sum_{e_1,e_2=\pm} (e_1\,\hat{\mathbf{k}}_1 \cdot \hat{\mathbf{p}} + e_2\,\hat{\mathbf{k}}_2 \cdot \hat{\mathbf{p}}) \\
&\times \left[\left(\frac{1}{p_0 + \hat{\epsilon}_1 + \epsilon_2} + \frac{1}{p_0 - \hat{\epsilon}_1 - \epsilon_2} \right) \frac{\hat{\epsilon}_1 \xi_2 - \xi_1 \epsilon_2}{2\,\hat{\epsilon}_1 \epsilon_2} \right.
\end{aligned}
$$

$$+ \quad \left(\frac{1}{p_0 + \epsilon_1 + \hat{\epsilon}_2} + \frac{1}{p_0 - \epsilon_1 - \hat{\epsilon}_2} \right) \frac{\epsilon_1 \xi_2 - \xi_1 \hat{\epsilon}_2}{2 \, \epsilon_1 \hat{\epsilon}_2}$$

$$+ \quad 7 \left(\frac{1}{p_0 + \epsilon_1 + \epsilon_2} + \frac{1}{p_0 - \epsilon_1 - \epsilon_2} \right) \frac{\epsilon_1 \xi_2 - \xi_1 \epsilon_2}{2 \, \epsilon_1 \epsilon_2} \Bigg] \; . \tag{3.136d}$$

Having these relations, in the following, we evaluate the imaginary part of $\Pi^{00}(P)$ explicitly; the calculation of the other components is similar. Afterwards we compare the result with the associated HDL limit using (3.44).

3.5.1 Imaginary parts

We are interested in the retarded self-energy, so we analytically continue $p_0 \to p_0 + i\eta$. We use the Dirac identity

$$\frac{1}{x + i\eta} = \mathcal{P}\frac{1}{x} - i\pi\delta(x) \; , \tag{3.137}$$

where $\mathcal{P}$ stands for the principal-value prescription. For the HDL self-energies (3.44), the imaginary parts are calculated in [141]. The results are

$$\operatorname{Im}\Pi_0^t(P) \;\; = \;\; -\pi \, \frac{3}{4} \, m_g^2 \, \frac{p_0}{p} \left(1 - \frac{p_0^2}{p^2} \right) \theta(p - p_0) \; , \tag{3.138a}$$

$$\operatorname{Im}\Pi_0^{00}(P) \;\; = \;\; -\pi \, \frac{3}{2} \, m_g^2 \, \frac{p_0}{p} \, \theta(p - p_0) \; , \tag{3.138b}$$

$$\operatorname{Im}\Pi_0^{0i}(P) \, \hat{p}_i \;\; = \;\; +\pi \, \frac{3}{2} \, m_g^2 \, \frac{p_0^2}{p^2} \, \theta(p - p_0) \; , \tag{3.138c}$$

$$\operatorname{Im}\Pi_0^\ell(P) \;\; = \;\; -\pi \, \frac{3}{2} \, m_g^2 \, \frac{p_0^3}{p^3} \, \theta(p - p_0) \; , \tag{3.138d}$$

For the CFL phase, we calculate imaginary part of $\Pi^{00}(P)$. However, the method for the other components of the self-energy are to a large extent the same and we refrain from giving them explicitly here. From (3.136a) and using the Dirac identity (3.137) we have

$$\operatorname{Im}\Pi^{00}(P) \;\; = \;\; \pi \, \frac{g^2}{12} \int \frac{d^3\mathbf{k}}{(2\pi)^3} \sum_{e_1, e_2 = \pm} (1 + e_1 e_2 \hat{\mathbf{k}}_1 \cdot \hat{\mathbf{k}}_2)$$

$$\times \;\; \left\{ \left[\delta(p_0 + \hat{\epsilon}_1 + \epsilon_2) - \delta(p_0 - \hat{\epsilon}_1 - \epsilon_2) \right] \frac{\hat{\epsilon}_1 \epsilon_2 - \xi_1 \xi_2 - \hat{\phi}_1 \phi_2}{2 \, \hat{\epsilon}_1 \epsilon_2} \right.$$

$$+ \quad \left[\delta(p_0 + \epsilon_1 + \hat{\epsilon}_2) - \delta(p_0 - \epsilon_1 - \hat{\epsilon}_2) \right] \frac{\epsilon_1 \hat{\epsilon}_2 - \xi_1 \xi_2 - \phi_1 \hat{\phi}_2}{2 \, \epsilon_1 \hat{\epsilon}_2}$$

$$+ \quad \left. \left[\delta(p_0 + \epsilon_1 + \epsilon_2) - \delta(p_0 - \epsilon_1 - \epsilon_2) \right] \frac{7(\epsilon_1 \epsilon_2 - \xi_1 \xi_2) - 2\phi_1 \phi_2}{2 \, \epsilon_1 \epsilon_2} \right\} \; . \tag{3.139}$$

Since Eq. (3.139) is an odd function of p_0, $\operatorname{Im}\Pi(-p_0, \mathbf{p}) \equiv -\operatorname{Im}\Pi(p_0, \mathbf{p})$, the calculation can be restricted to positive values of the energy $p_0 \geq 0$. Hence, the first delta-function in each square bracket in Eq. (3.139) can be dropped. Moreover, we are interested in gluon energies and momenta $p_0, p \ll \mu$. Consequently, in order to have a vanishing argument of the remaining

delta-functions, the quasiparticle energies should not be too large either, $\epsilon_i, \hat{\epsilon}_i \ll \mu$. As a result of this, only the terms with $e_1 = e_2 = +1$ will contribute because when either e_1 or $e_2 = -1$, then $\epsilon_i \simeq \hat{\epsilon}_i \simeq |k_i + \mu| \sim \mu$, which is too far from the Fermi surface to make a contribution for $p_0 \ll \mu$. Shifting the integration variable so that $\mathbf{k}_1 = \mathbf{k} + \mathbf{p}/2$ and $\mathbf{k}_2 = \mathbf{k} - \mathbf{p}/2$, and using the fact that $p \ll \mu$, we find that

$$\hat{\mathbf{k}}_1 \cdot \hat{\mathbf{k}}_2 \simeq 1 \,, \quad \xi_{1,2} \simeq \xi \pm \frac{\mathbf{p} \cdot \hat{\mathbf{k}}}{2} \equiv \xi_\pm \,, \tag{3.140}$$

where we have defined $\xi \equiv k - \mu$. Furthermore, we denote

$$\epsilon_\pm \equiv \sqrt{\xi_\pm^2 + \phi^2} \,, \quad \hat{\epsilon}_\pm \equiv \sqrt{\xi_\pm^2 + \hat{\phi}^2} \,. \tag{3.141}$$

Setting $\phi_1 \simeq \phi_2 \equiv \phi$, $\hat{\phi}_1 \simeq \hat{\phi}_2 \equiv \hat{\phi} \simeq 2\phi$ in weak coupling, we obtain

$$\begin{aligned}
\operatorname{Im}\Pi^{00}(P) = -\frac{g^2\pi}{6} \int \frac{d^3\mathbf{k}}{(2\pi)^3} \quad & \Big[\delta(p_0 - \hat{\epsilon}_+ - \epsilon_-) \frac{\hat{\epsilon}_+\epsilon_- - \xi_+\xi_- - 2\phi^2}{2\hat{\epsilon}_+\epsilon_-} \\
+ \;& \delta(p_0 - \epsilon_+ - \hat{\epsilon}_-) \frac{\epsilon_+\hat{\epsilon}_- - \xi_+\xi_- - 2\phi^2}{2\epsilon_+\hat{\epsilon}_-} \\
+ \;& \delta(p_0 - \epsilon_+ - \epsilon_-) \frac{7(\epsilon_+\epsilon_- - \xi_+\xi_-) - 2\phi^2}{2\epsilon_+\epsilon_-} \Big] \,. \tag{3.142}
\end{aligned}$$

Now, in order to simplify the integration, we choose $\mathbf{p} = (0, 0, p)$, i.e we integrate only over the polar angle φ. In order to integrate over ξ we make use of the delta-functions in the expressions. Denoting $x = \cos\theta$, the roots of the arguments of the delta-functions in Eq. (3.142) are (in the order of appearance)

$$\xi_{1,2}^*(x) = \frac{-3px\phi^2 \pm p_0\sqrt{(p^2x^2 - p_0^2 + 9\phi^2)(p^2x^2 - p_0^2 + \phi^2)}}{2(p^2x^2 - p_0^2)} \,, \tag{3.143a}$$

$$\xi_{3,4}^*(x) = \frac{3px\phi^2 \pm p_0\sqrt{(p^2x^2 - p_0^2 + 9\phi^2)(p^2x^2 - p_0^2 + \phi^2)}}{2(p^2x^2 - p_0^2)} \,, \tag{3.143b}$$

$$\xi_{5,6}^*(x) = \pm \frac{p_0}{2}\sqrt{1 - \frac{4\phi^2}{p_0^2 - p^2x^2}} \,. \tag{3.143c}$$

Then,

$$\begin{aligned}
\operatorname{Im}\Pi^{00}(P) = \;& -\pi m_g^2 \frac{\phi^2}{3\, p\, p_0} \bigg\{ \Theta(p_0 - 3\phi) \int_0^{u_1} dy \Big[\frac{9}{\sqrt{(y^2 - 1 + 9\Phi^2)(y^2 - 1 + \Phi^2)}} \\
& - \frac{10 + 9\Phi^2}{(1 - y^2)\sqrt{(y^2 - 1 + 9\Phi^2)(y^2 - 1 + \Phi^2)}} \\
& + \frac{18\Phi^2}{(1 - y^2)^2\,\sqrt{(y^2 - 1 + 9\Phi^2)(y^2 - 1 + \Phi^2)}} \Big] \\
& + \Theta(p_0 - 2\phi) \int_0^{u_2} dy\, \frac{5 + 9y^2}{(y^2 - 1)^{3/2}\,\sqrt{y^2 - 1 + 4\Phi^2}} \bigg\} \,, \tag{3.144}
\end{aligned}$$

where $y \equiv p\,x/p_0$, $\Phi \equiv \phi/p_0$, $u_1 = \min(p/p_0, \sqrt{1 - 9\phi^2/p_0^2}\,)$, $u_2 = \min(p/p_0, \sqrt{1 - 4\phi^2/p_0^2}\,)$ and m_g is the gluon mass parameter (squared), $m_g^2 = N_f g^2 \mu^2/6\pi^2$, for $N_f = 3$.

Using the elliptic integrals of first, second, and third kind,

$$F(\varphi, k) = \int_0^\varphi \frac{d\alpha}{\sqrt{1 - k^2 \sin^2 \alpha}}\,, \tag{3.145a}$$

$$E(\varphi, k) = \int_0^\varphi d\alpha\,\sqrt{1 - k^2 \sin^2 \alpha}\,, \tag{3.145b}$$

$$\Pi(\varphi, l, k) = \int_0^\varphi \frac{d\alpha}{(1 + l\,\sin^2 \alpha)\sqrt{1 - k^2 \sin^2 \alpha}}\,, \tag{3.145c}$$

and the complete elliptic integrals of the first, $\mathbf{K}(k) = F(\pi/2, k)$, the second kind, $\mathbf{E}(k) = E(\pi/2, k)$, and the third kind $\mathbf{\Pi}(l, r) = \Pi(\pi/2, l, r)$ in Eq. (3.144), we obtain the final result

$$
\begin{aligned}
\mathrm{Im}\,\Pi^{00}(P) = {} & \frac{\pi m_g^2}{6}\frac{p_0}{p}\bigg(\Theta(p_0 - 3\phi)\,\frac{s^2}{\sqrt{4 - s^2}}\bigg\{ \Theta(E_p^{\mathbf{18}} - p_0)\bigg[9\,\mathbf{K}(t') - \Big(10 + \frac{9}{4}\,s^2\Big)\mathbf{\Pi}(l, t') \\
& - \frac{9}{2}\,s^2\,\frac{d}{dn}\frac{1}{n}\mathbf{\Pi}(\frac{l}{n}, t')\Big|_{n=1} \bigg] + \Theta(p_0 - E_p^{\mathbf{18}})\bigg[9\,F(\alpha', t') - \Big(10 + \frac{9}{4}\,s^2\Big)\Pi(\alpha', l, t') \\
& - \frac{9}{2}\,s^2\,\frac{d}{dn}\frac{1}{n}\,\Pi(\alpha', \frac{l}{n}, t')\Big|_{n=1} \bigg] \bigg\} - \Theta(p_0 - 2\phi)\bigg\{ \Theta(E_p^{\mathbf{88}} - p_0)\bigg[7\,\mathbf{E}(t) - \frac{9}{2}\,s^2\,\mathbf{K}(t) \bigg] \\
& + \Theta(p_0 - E_p^{\mathbf{88}})\bigg[7\,E(\alpha, t) - \frac{9}{2}\,s^2 F(\alpha, t) - 7\,\frac{p}{p_0}\sqrt{1 - \frac{4\phi^2}{p_0^2 - p^2}}\,\bigg] \bigg\} \bigg)\,,
\end{aligned} \tag{3.146}
$$

where $t' = \sqrt{(p_0^2 - 9\phi^2)/(p_0^2 - \phi^2)}$, $t = \sqrt{1 - 4\phi^2/p_0^2}$, and $\alpha' = \arcsin[p/\sqrt{p_0^2 - 9\phi^2}\,]$. Also $\alpha = \arcsin[p/(tp_0)]$, $l = -1 + 9\phi^2/p_0^2$ and $s = 2\phi/p_0$.

The imaginary parts of the other components of the gluon self-energy can be obtained analogously from Eqs. (3.136b), (3.136c), and (3.136d). In addition to Eq. (3.140) we employ the following approximations,

$$\hat{\mathbf{k}}_1 \cdot \hat{\mathbf{p}}\,\hat{\mathbf{k}}_2 \cdot \hat{\mathbf{p}} \simeq (\hat{\mathbf{k}} \cdot \hat{\mathbf{p}})^2\,, \quad \hat{\mathbf{k}}_1 \cdot \hat{\mathbf{p}} + \hat{\mathbf{k}}_2 \cdot \hat{\mathbf{p}} \simeq 2\,\hat{\mathbf{k}} \cdot \hat{\mathbf{p}}\,. \tag{3.147}$$

In consequence, we find the final results for the imaginary part of the gluon self-energies,

$$
\begin{aligned}
\mathrm{Im}\,\Pi^t(P) = {} & \frac{\pi m_g^2}{12}\frac{p_0}{p}\bigg[\frac{s^2}{\sqrt{4 - s^2}}\,\Theta(p_0 - 3\,\phi)\bigg(\Theta(E_p^{\mathbf{18}} - p_0)\Big\{ \frac{p_0^2}{p^2}\Big(1 - \frac{s^2}{4}\Big)\mathbf{E}(t') \\
& + \Big[1 - \frac{p_0^2}{p^2}(11 + 2s^2)\Big]\mathbf{K}(t') - \Big[10(1 - \frac{p_0^2}{p^2}) + \frac{9s^2}{4}\,(1 - 3\frac{p_0^2}{p^2})\Big]\mathbf{\Pi}(l, t') \\
& - \frac{9s^2}{2}\Big(1 - \frac{p_0^2}{p^2}\Big)\frac{d}{dn}\frac{1}{n}\mathbf{\Pi}\,(\frac{l}{n}, t')\Big|_{n=1} \Big\} + \Theta(p_0 - E_p^{\mathbf{18}})\Big\{ \frac{p_0^2}{p^2}\Big(1 - \frac{s^2}{4}\Big)E(\alpha', t') \\
& + \Big[1 - \frac{p_0^2}{p^2}(11 + 2s^2)\Big]F(\alpha', t') - \Big[10(1 - \frac{p_0^2}{p^2}) + \frac{9s^2}{4}\,(1 - 3\frac{p_0^2}{p^2})\Big]\Pi(\alpha', l, t') \\
& - \frac{9s^2}{2}\,\Big(1 - \frac{p_0^2}{p^2}\Big)\frac{d}{dn}\frac{1}{n}\Pi\,(\alpha', \frac{l}{n}, t')\Big|_{n=1} \Big\} \bigg)
\end{aligned}
$$

$$
+ \quad \Theta(p_0 - 2\phi)\Bigg(\Theta(E_p^{\mathbf{88}} - p_0)\Big\{\Big[\frac{5p_0^2}{2p^2}\,s^2 - 7(1 - \frac{p_0^2}{p^2})\Big]\mathbf{E}(t) + \frac{s^2}{2}\Big(5 - 19\frac{p_0^2}{p^2}\Big)\mathbf{K}(t)\Big\}
$$

$$
+ \quad \Theta(p_0 - E_p^{\mathbf{88}})\Big\{\Big[\frac{5p_0^2}{2p^2}\,s^2 - 7(1 - \frac{p_0^2}{p^2})\Big]E(\alpha, t) + \frac{s^2}{2}\Big(5 - 19\frac{p_0^2}{p^2}\Big)F(\alpha, t)
$$

$$
+ \quad 7\frac{p}{p_0}\Big(1 - \frac{p_0^2}{p^2}\Big)\sqrt{1 - \frac{4\phi^2}{p^2 - p_0^2}}\,\Big\}\,\Bigg)\Bigg]\,, \tag{3.148a}
$$

$$
\begin{aligned}
\mathrm{Im}\,\Pi^\ell(P) \;=\; & -\frac{\pi m_g^2}{6}\frac{p_0^3}{p^3}\Bigg(\frac{s^2}{\sqrt{4 - s^2}}\Theta(p_0 - 3\,\phi)\Big\{\Theta(E_p^{\mathbf{18}} - p_0)\Big[\Big(1 - \frac{s^2}{4}\Big)\mathbf{E}(t') \\
& + \quad \Big(10 + \frac{27}{4}\,s^2\Big)\mathbf{\Pi}(l, t') - \Big(11 + 2s^2\Big)\mathbf{K}(t') + \frac{9}{2}s^2\,\frac{d}{dn}\frac{1}{n}\,\mathbf{\Pi}(l, t')\Big|_{n=1}\Big] \\
& + \quad \Theta(p_0 - E_p^{\mathbf{18}})\Big[\Big(1 - \frac{s^2}{4}\Big)E(\alpha', t') + \Big(10 + \frac{27}{4}\,s^2\Big)\Pi(\alpha', l, t') \\
& - \quad \Big(11 + 2s^2\Big)F(\alpha', t') + \frac{9}{2}s^2\frac{d}{dn}\frac{1}{n}\,\Pi(\alpha', l, t')\Big|_{n=1}\Big]\Big\} \\
& + \quad \Theta(p_0 - 2\phi)\Big\{\Theta(E_p^{\mathbf{88}} - p_0)\Big[\Big(7 + \frac{5}{2}\,s^2\Big)\mathbf{E}(t) - \frac{19}{2}\,s^2\,\mathbf{K}(t)\Big] \\
& + \quad \Theta(p_0 - E_p^{\mathbf{88}})\Big[\Big(7 + \frac{5}{2}\,s^2\Big)E(\alpha, t) - \frac{19}{2}\,s^2\,F(\alpha, t) \\
& - \quad \frac{7\,p}{p_0}\sqrt{1 - \frac{4\,\phi^2}{p_0^2 - p^2}}\,\Big]\,\Big\}\,\Bigg)\,, \tag{3.148b}
\end{aligned}
$$

$$
\begin{aligned}
\mathrm{Im}\,\Pi^{0i}(P)\,\hat{p}_i \;=\; & -\frac{\pi m_g^2}{6}\frac{p_0^2}{p^2}\Bigg(\frac{2s^2}{\sqrt{4 - s^2}}\,\Theta(p_0 - 3\,\phi)\Big\{\Theta(E_p^{\mathbf{18}} - p_0)\Big[5\,\mathbf{K}(t') - (5 + \frac{9}{4}\,s^2)\,\mathbf{\Pi}(l, t') \\
& - \quad \frac{9}{4}\,s^2\,\frac{d}{dn}\frac{1}{n}\,\mathbf{\Pi}(l, t')\Big|_{n=1}\Big] + \Theta(p_0 - E_p^{\mathbf{18}})\Big[5\,F(\alpha', t') - (5 + \frac{9}{4}\,s^2)\,\Pi(\alpha', l, t') \\
& - \quad \frac{9}{4}\,s^2\,\frac{d}{dn}\frac{1}{n}\,\Pi(\alpha', l, t')\Big|_{n=1}\Big]\Big\} - 7\,\Theta(p_0 - 2\phi)\Big\{\Theta(E_p^{\mathbf{88}} - p_0)\Big[\mathbf{E}(t) - s^2\,\mathbf{K}(t)\Big] \\
& + \quad \Theta(p_0 - E_p^{\mathbf{88}})\Big[\mathbf{E}(\alpha, t) - \frac{p}{p_0}\sqrt{1 - \frac{4\,\phi^2}{p_0^2 - p^2}} - s^2\,F(\alpha, t)\Big]\,\Big\}\,\Bigg)\,. \tag{3.148c}
\end{aligned}
$$

As a matter of comparison, in the limit $\phi \to 0$, we reproduce the HDL limit,

$$
\lim_{\phi \to 0}\mathrm{Im}\,\Pi^{00}(P) \;\equiv\; \mathrm{Im}\,\Pi_0^{00}(P)\,, \tag{3.149a}
$$

$$
\lim_{\phi \to 0}\mathrm{Im}\,\Pi^{t}(P) \;\equiv\; \mathrm{Im}\,\Pi_0^{t}(P)\,, \tag{3.149b}
$$

$$
\lim_{\phi \to 0}\mathrm{Im}\,\Pi^{\ell}(P) \;\equiv\; \mathrm{Im}\,\Pi_0^{\ell}(P)\,, \tag{3.149c}
$$

$$
\lim_{\phi \to 0}\mathrm{Im}\,\Pi^{0i}(P)\,\hat{p}_i \;\equiv\; \mathrm{Im}\,\Pi_0^{0i}(P)\,\hat{p}_i\,. \tag{3.149d}
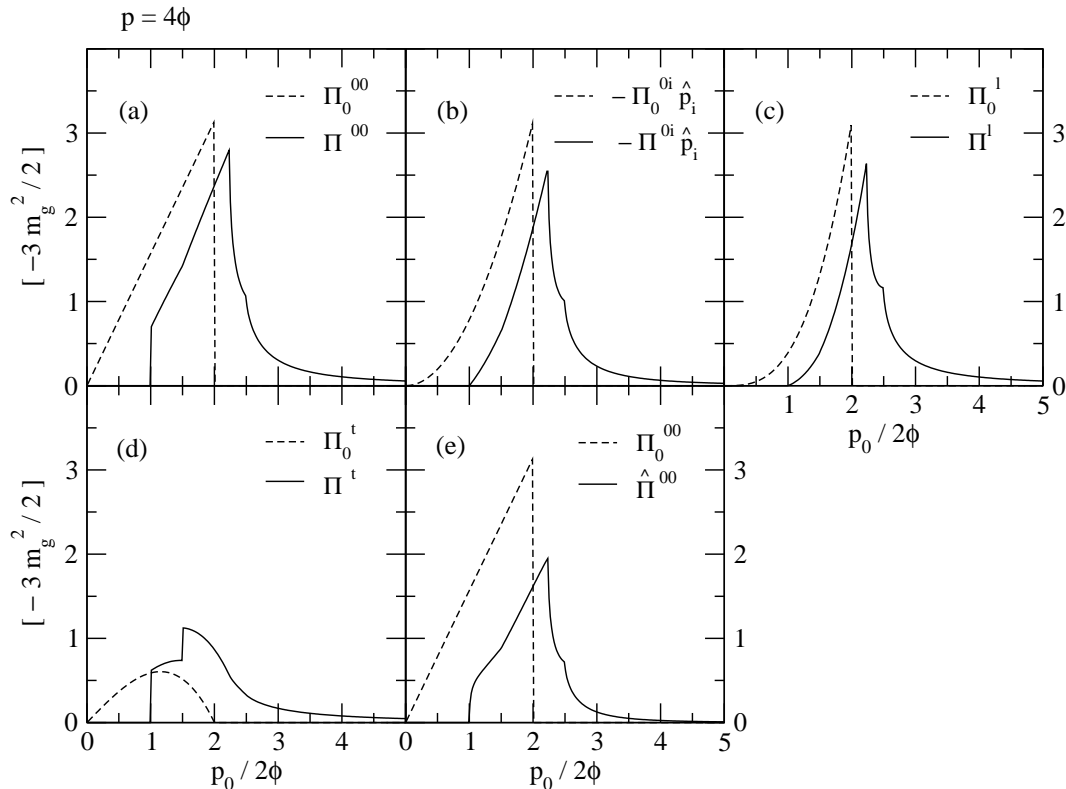$$

Figure 3.3: The imaginary parts of (a) Π^{00}, (b) $-\Pi^{0i}\hat{p}_i$, (c) Π^ℓ, (d) Π^t, and (e) $\hat{\Pi}^{00}$ as a function of energy p_0 for a gluon momentum $p = 4\phi$. The solid lines are for the CFL phase, the dotted lines correspond to the HDL self-energy.

In Fig. 3.3 we show the imaginary part of several components of the gluon self-energy for a gluon momentum $p = 4\phi$ as a function of the gluon energy p_0. We also show the corresponding results for the gluon self-energy in the "hard-dense loop" (HDL) limit, $\Pi_0^{\mu\nu}$, cf. Eqs. (63a), (65a), (69a) and (69b) of Ref. [141]. The imaginary parts are quite similar to those of the 2SC case, cf. Fig. 1 of Ref. [141]. There are subtle differences, though, due to the appearance of two kinds of gapped quark excitations, one so-called singlet excitation with a gap ϕ_1, and eight so-called octet excitations with a gap $\phi_8 \equiv \phi$ [66]. In weak coupling, the singlet gap is approximately twice as large as the octet gap, $\phi_1 \simeq 2\,\phi_8 \equiv 2\,\phi$ [138, 145]. The one-loop gluon self-energy in the CFL phase has two types of contributions, depending on whether the quarks in the loop correspond to singlet or octet excitations, cf. Eq. (23b) of Ref. [149]. For the first type, both quarks in the loop are octet excitations, and for the second, one is an octet and the other a singlet excitation. There is no contribution from singlet-singlet excitations.

Nonvanishing octet-octet excitations require gluon energies to be larger than $2\,\phi_8 \equiv 2\,\phi$, while octet-singlet excitations require a larger gluon energy, $p_0 \geq \phi_1 + \phi_8 \equiv 3\,\phi$. This introduces

some additional structure in the imaginary parts at $p_0 = 3\phi$, which can be seen particularly well in Figs. 3.3 (d) and (e).

Some imaginary parts exhibit a peak-like structure at a gluon energy

$$p_0 = E_p^{\mathbf{88}} \equiv \sqrt{p^2 + (\phi_{\mathbf{8}} + \phi_{\mathbf{8}})^2} = \sqrt{20}\,\phi \tag{3.150}$$

followed by a sharp drop for larger energies. The mathematical reason is seen in Eqs. (3.146) and (3.148), where the regions $p_0 > E_p^{\mathbf{88}}$ and $p_0 \leq E_p^{\mathbf{88}}$ are separated by Θ functions. In the normal phase, the imaginary parts of the gluon self-energies actually vanish above $p_0 = p$. In color-superconducting phases, the imaginary parts do not vanish but fall off rapidly. This has already been noted for the 2SC phase [141], and is confirmed here by the results for the CFL phase. If there is a peak-like structure at $p_0 = E_p^{\mathbf{88}}$, from Eqs. (3.146) and (3.148) we expect a similar peak to appear at

$$p_0 = E_p^{\mathbf{18}} \equiv \sqrt{p^2 + (\phi_{\mathbf{1}} + \phi_{\mathbf{8}})^2} = 5\,\phi \;. \tag{3.151}$$

One indeed sees an additional structure at this point, but it is much less pronounced since it is located on top of the sharp drop of the first peak.

3.5.2 Real parts

There are two possibilities to compute the real parts of the gluon self-energy. Either, one evaluates a principal-value integral, cf. Eq. (3.137), or one employs the dispersion integral

$$\operatorname{Re}\Pi(p_0, \mathbf{p}) \equiv \frac{1}{\pi}\mathcal{P}\int_{-\infty}^{\infty} d\omega\, \frac{\operatorname{Im}\Pi(\omega, \mathbf{p})}{\omega - p_0} + C \;, \tag{3.152}$$

where C is a (subtraction) constant. If $\operatorname{Im}\Pi(\omega, \mathbf{p})$ is an odd function of ω, $\operatorname{Im}\Pi(-\omega, \mathbf{p}) \equiv -\operatorname{Im}\Pi(\omega, \mathbf{p})$ the dispersion integral becomes

$$\operatorname{Re}\Pi(p_0, \mathbf{p}) \equiv \frac{1}{\pi}\mathcal{P}\int_{0}^{\infty} d\omega\, \operatorname{Im}\Pi_{\mathrm{odd}}(\omega, \mathbf{p})\Big(\frac{1}{\omega + p_0} + \frac{1}{\omega - p_0}\Big) + C \;, \tag{3.153}$$

and if it is an even function of ω, $\operatorname{Im}\Pi(-\omega, \mathbf{p}) \equiv +\operatorname{Im}\Pi(\omega, \mathbf{p})$ we have

$$\operatorname{Re}\Pi(p_0, \mathbf{p}) \equiv \frac{1}{\pi}\mathcal{P}\int_{0}^{\infty} d\omega\, \operatorname{Im}\Pi_{\mathrm{even}}(\omega, \mathbf{p})\Big(\frac{1}{\omega - p_0} - \frac{1}{\omega + p_0}\Big) + C \;, \tag{3.154}$$

where in both cases $\Pi(p_0, \mathbf{p})$ is assumed to be analytic in the upper complex p_0 plane.

For the electric gluons in the HDL limit, using Eq. (3.152) with the associated imaginary parts coming from (3.138), we have

$$\operatorname{Re}\Pi_0^{00}(p_0, \mathbf{p}) \simeq -3\, m_g^2 \left(1 - \frac{p_0}{2p}\ln\left|\frac{p_0 + p}{p_0 - p}\right|\right) + C_0^{00} \;, \tag{3.155a}$$

and for magnetic gluons

$$\operatorname{Re}\Pi_0^{t}(p_0, \mathbf{p}) \simeq \frac{3}{2}\, m_g^2 \left[\frac{p_0^2}{p^2} + \left(1 - \frac{p_0^2}{p^2}\right)\frac{p_0}{2p}\ln\left|\frac{p_0 + p}{p_0 - p}\right| - \frac{2}{3}\right] + C_0^{t} \;. \tag{3.155b}$$
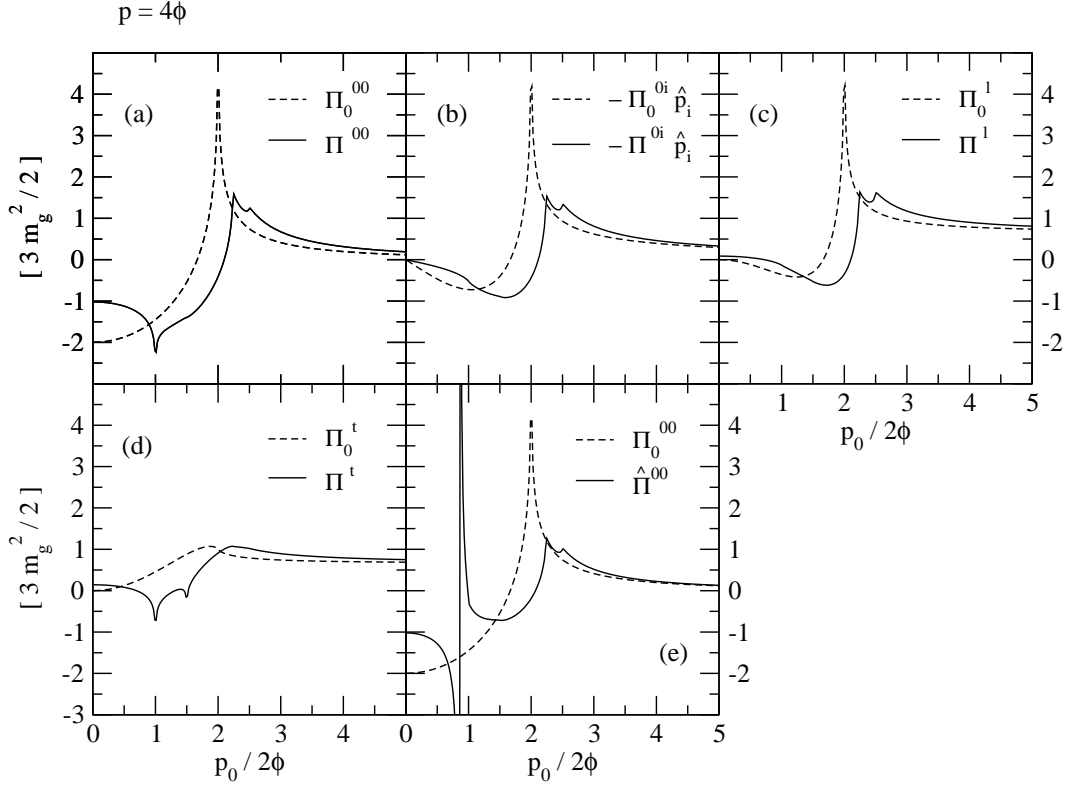
Figure 3.4: The real parts of (a) Π^{00}, (b) $-\Pi^{0i}\hat{p}_i$, (c) Π^{ℓ}, (d) Π^t, and (e) $\hat{\Pi}^{00}$ as a function of energy p_0 for a gluon momentum $p = 4\phi$. The solid lines are for the CFL phase, the dotted lines correspond to the HDL self-energy.

Comparison with a direct calculation via Eq. (3.44) determines

$$C_0^{00} \equiv 0 \quad , \quad C_0^t \equiv m_g^2 \, , \tag{3.156}$$

such that the term $-2/3$ in Eq. (3.155b) is cancelled by C_0^t and the magnetic self-energy has the correct zero-energy limit, $\operatorname{Re}\Pi_0^t(0, \mathbf{p}) = 0$, representing the absence of magnetic screening to one-loop order. Thus, the standard expressions for the real parts of the HDL self-energies are recovered [129, 136].

The values of the constants C^{00}, C^t, C^{ℓ}, and C^{0i} are determined by the large-p_0 dependence of the self-energy. Thus, it does not matter which color-superconducting phase we consider, and the constants assume the same values as for the 2SC phase, $C^{00} = C^{0i} = 0$, $C^t = C^{\ell} = m_g^2$, cf. Ref. [141].

In Fig. 3.4 we show the real parts of the gluon self-energy corresponding to the imaginary parts shown in Fig. 3.3. These are quite similar to the ones in the 2SC phase, cf. Fig. 2 of Ref. [141]. An explanation of the various structures can be given following arguments similar to those
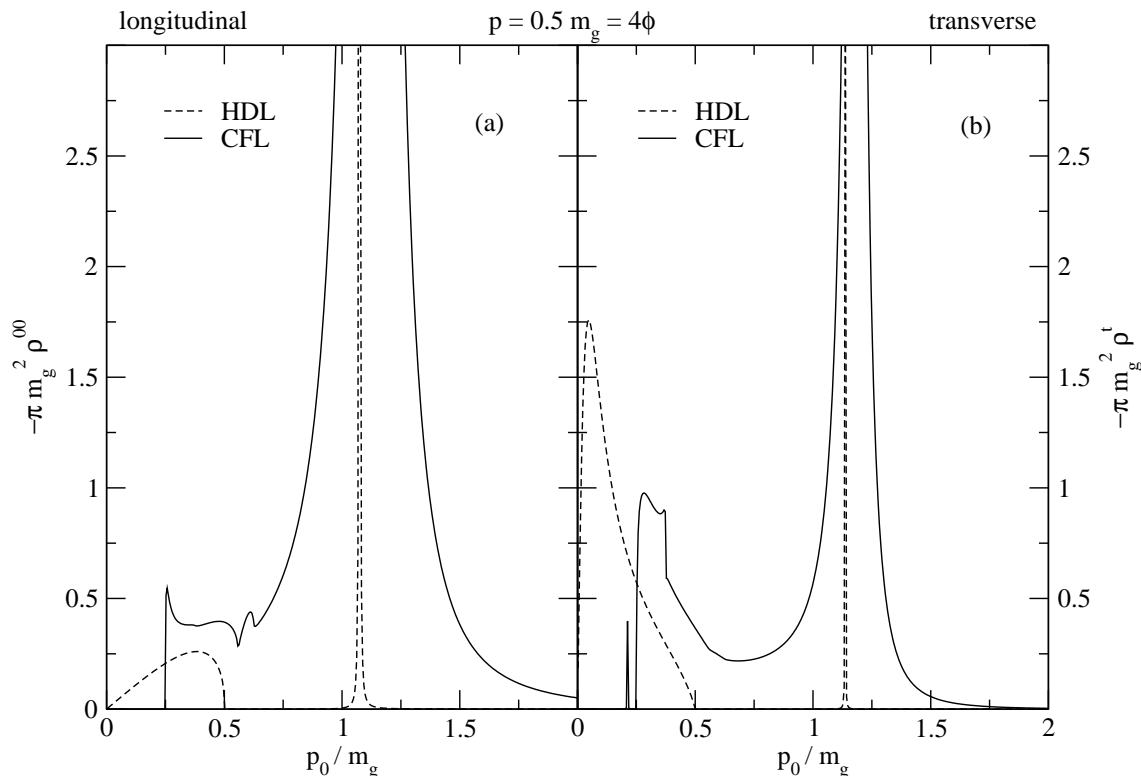
Figure 3.5: The spectral densities for (a) longitudinal and (b) transverse gluons for a gluon momentum $p = m_g/2$, with $m_g = 8\,\phi$. The dashed lines correspond to the HDL limit.

of Refs. [108, 141]. In essence, when computing the real part from a dispersion integral over the imaginary part, cf. Eq. (3.152), a change of gradient in the imaginary part leads to a cusp-like structure in the real part. The only function that does not fit this general rule is $\mathrm{Re}\,\hat{\Pi}^{00}$. The reason is that this function is computed from the real part of the right-hand side of Eq. (3.131). Note the singularity at $p_0 \simeq 1.6\,\phi$. This singularity is caused by a root of the denominator in Eq. (3.131), $P_\mu \Pi^{\mu\nu}(P)\, P_\nu = 0$. As shown in Ref. [139] (see also Ref. [141] for the 2SC case), this condition determines the dispersion relation of the Goldstone excitations. As one expects, for large energies $p_0 \gg \phi$ the real parts of the self-energies approach the corresponding HDL limit. Deviations from the HDL limit occur only for gluon energies $p_0 \sim \phi$.

3.5.3 Spectral densities

We now compute the spectral densities from the real and imaginary parts of the gluon self-energies. When $\mathrm{Im}\,\hat{\Pi}^{00}(p_0, \mathbf{p}), \mathrm{Im}\,\Pi^t(p_0, \mathbf{p}) \neq 0$, the spectral densities are regular and given by
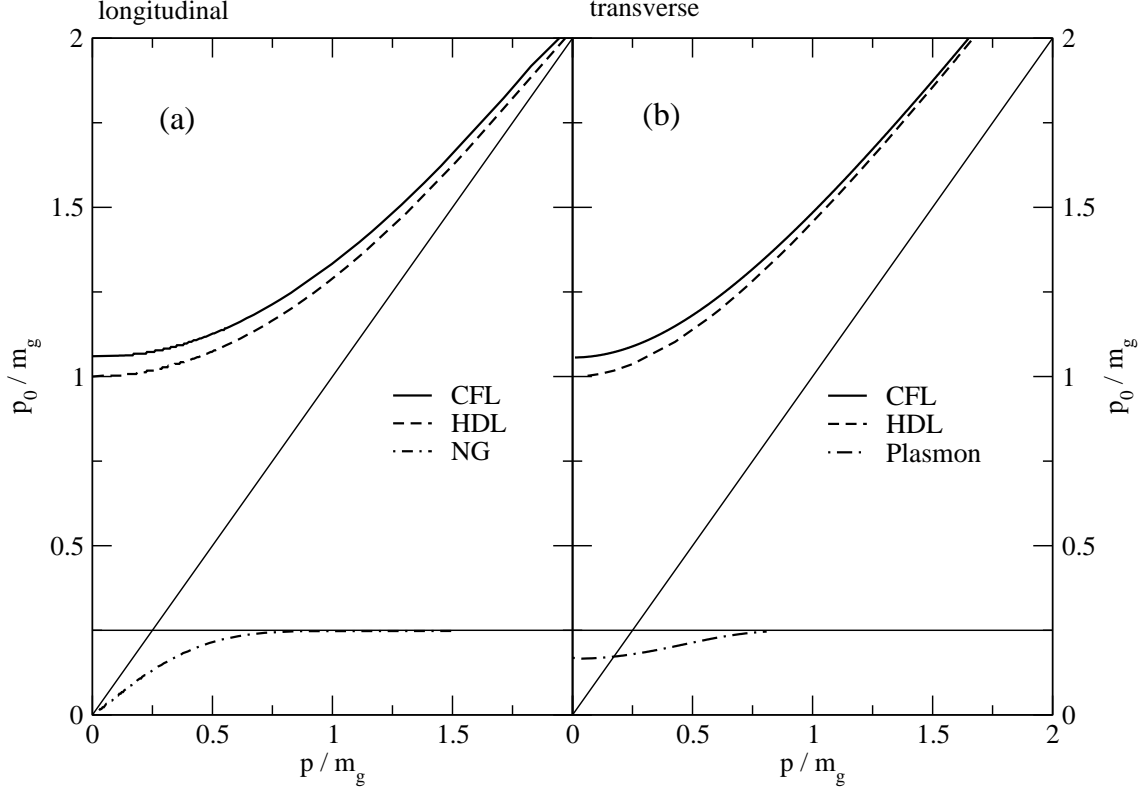
Figure 3.6: The dispersion relations for (a) longitudinal and (b) transverse excitations in the CFL phase. The full lines correspond to the regular longitudinal and transverse excitations. The dashed lines are for the HDL limit. The dash-dotted line in part (a) shows the dispersion relation for the Nambu-Goldstone excitation. The light plasmon dispersion relation is shown by the dash-dotted line in part (b). As in Fig. 3.5, the value of the gap is chosen such that $m_g = 8\,\phi$.

$$\hat{\rho}^{00}(p_0, \mathbf{p}) \;=\; \frac{1}{\pi} \frac{\mathrm{Im}\,\hat{\Pi}^{00}(p_0, \mathbf{p})}{[p^2 - \mathrm{Re}\,\hat{\Pi}^{00}(p_0, \mathbf{p})]^2 + [\mathrm{Im}\,\hat{\Pi}^{00}(p_0, \mathbf{p})]^2} \;, \tag{3.157a}$$

$$\rho^{t}(p_0, \mathbf{p}) \;=\; \frac{1}{\pi} \frac{\mathrm{Im}\,\Pi^{t}(p_0, \mathbf{p})}{[p_0^2 - p^2 - \mathrm{Re}\,\Pi^{t}(p_0, \mathbf{p})]^2 + [\mathrm{Im}\,\Pi^{t}(p_0, \mathbf{p})]^2} \;. \tag{3.157b}$$

If $\mathrm{Im}\,\hat{\Pi}^{00}(p_0, \mathbf{p})$ or $\mathrm{Im}\,\Pi^{t}(p_0, \mathbf{p})$ vanish, the corresponding spectral density has a simple pole given by

$$[p^2 - \mathrm{Re}\,\hat{\Pi}^{00}(p_0, \mathbf{p})]_{p_0 = \omega^{00}(\mathbf{p})} = 0 \tag{3.158}$$

for longitudinal gluons and

$$[p_0^2 - p^2 - \mathrm{Re}\,\Pi^{t}(p_0, \mathbf{p})]_{p_0 = \omega^{t}(\mathbf{p})} = 0 \tag{3.159}$$

for transverse gluons.

In Fig. 3.5 we show the spectral densities for longitudinal and transverse gluons in the CFL phase in comparison to the HDL limit. Note that there is a delta function-like peak in the transverse spectral density at an energy $p_0 \simeq 0.21 \, m_g$. This peak corresponds to a collective excitation, the so-called "light plasmon" predicted in Ref. [146] (see also [147]). We show the dispersion relation of this collective mode in Fig. 3.6 (b). The mass $m_{\mathrm{coll}} \simeq 1.35 \, \phi$ is roughly in agreement with the value $m_{\mathrm{coll}} \simeq 1.362 \, \phi$ of Ref. [146]. As the momentum increases, the energy of the light plasmon excitation approaches $2 \, \phi$ from below. For momenta larger than $\sim 8 \, \phi$, the location of this excitation branch becomes numerically indistinguishable from the continuum in the spectral density above $p_0 = 2 \, \phi$, cf. Fig. 3.5. Close inspection reveals that the dispersion relation of the light plasmon has a minimum at a nonzero value of $p \simeq 1.33 \, \phi$, indicating a van Hove singularity.

In Fig. 3.6 we also show the dispersion relations for the "regular" longitudinal and transverse excitations, as well as for the Nambu-Goldstone excitation defined by the root of $P^\mu \, \Pi_{\mu\nu}(P) \, P^\nu = 0$ [141, 139]. For our choice of gauge the gluon propagator is 4-transverse and this mode does not mix with the longitudinal component of the gauge field [141]. Therefore, the Nambu-Goldstone mode does not appear as a peak in the longitudinal spectral density, cf. Fig. 3.5. We finally note that other collective excitations have been investigated in Ref. [148].

Chapter 4

Summary and Outlook

The inert phases are the only experimentally observed phases of superfluid ^{3}He. In order to make use of them, one has to study their thermal properties. The equivalent phases in color-superconducting matter have already been studied in the case that matter is composed of one type of quark flavor in a spin-one state [100]. Since three-flavor spin-zero CSC has a larger gap (almost 100 times) than one-flavor spin-one CSC, it is more feasible to find the evidence of the former in the interior of compact stars. Hence, it is of crucial importance to know whether the ground state of quark matter is in any of the inert phases. Since each phase has a typical signature for detection, then, this study helps us to look for the right sign of CSC among the observational data received from compact stars.

Here, first we studied the inert phases of spin-zero three-flavor CSC for massless quarks. In analogy to Ref. [123] we used QCD to calculate the expression for the pressure of the phases in this state. we found that the pressure of the CFL phase is larger than the pressure of the rest of the inert phases. Surprisingly enough, we realised that the so-called sSC phase takes the second place in the ranking of the studied phases. This is a new result. In the sSC phase as well as the CFL phase, all quarks participate in Cooper pairing, i.e., the sSC phase is made of $(gd-bs), (gs-bd), (ru-bs)$, and $(rs-bu)$ pairings, and the CFL phase is composed of $(gd-bs), (gs-bd), (ru-bs), (rs-bu), (ru-gd)$, and $(rd-gu)$ pairings. On the other hand, the 2SC phase contains $(ru-gd)$ and $(rd-gu)$ pairings and its pressure is equal to that of the A and A* phases. Cooper pairs in the A phase are $(rd-gs), (rs-gd), (ru-gs)$, and $(rs-gu)$, and the A* phase contains $(gu-bd), (gd-bu), (ru-bd)$, and $(rd-bu)$ pairings. We see that there is not any trivial relation between the number and type of quarks participating in pairing in each phase and the pressure of that phase. The reason is two-fold. Firstly, in the massless case, there is not a real distinction between quarks flavor. The only difference between them is due to the different color charge of quarks. Secondly, the number of a specific Cooper pair in each phase might be different than that in another phase. This makes the analysis non-trivial.

In addition, It is very interesting to know which phase of CSC can be realised in nature. At the moment the most promising place for color superconductivity is the interior of compact stars. On the other hand, we know that compact stars should be color and electric charge neutral. Therefore, in order to study the behaviour of the CSC inert phases in compact stars we have to impose the color and charge neutrality conditions onto the system. This changes the

number and type of quarks participating in the pairing since the neutrality condition shifts the Fermi energy of quarks. In this case, the value of the gap for a particular pairing and the energy released of the paired quarks are the criteria which implies whether these chosen quarks pair or not. If the difference between the Fermi energy of two quarks is larger than the energy released from them being paired (gap energy), then, there will not take place any pairing between those quarks and vise verse. However, there might appear gapless pairs, cf. Ref [83, 150].

Since QCD calculations for the system with massive quarks and imposing the neutrality condition are very difficult we used the NJL model. However, there arises a problem as the cost of using a simplified calculation. In the NJL model, in contrast to QCD, tadpoles do not vanish. This destroys the neutrality of the system. To restore the symmetry, when we use the NJL model, we have to introduce a relevant chemical potential into the system so as to clean the effects of the tadpoles and to return the system to the neutral state. For this, in each phase, one has to look for tadpoles of that phase.

Detecting the tadpoles of the phase, here the A and A* phases, we introduced the relevant chemical potential to annihilate the tadpoles. After this, we calculated the pressure of the phases including the neutrality condition. For higher chemical potentials μ, we found the CFL phase as the ground state and at moderate μ the 2SC phase as the dominant phase. In addition, we realised that the A* phase is the color-transformed version of the 2SC phase. There was not, at least for some value of chemical potential μ, any chance for the A phase to win over the other phases and therefore to be the ground state of the matter in compact stars. However, the large magnetic field of compact stars can change the result and there is still a hope for the A phase to be realized at some point on the QCD phase diagram. Also, the magnetic field might destroy the degeneracy between the 2SC phase and the A* phase; this can lead to a new result for the A* phase.

On the other hand, since the CFL phase is so far the most important phase of CSC at large densities, it is very interesting to investigate the properties of the matter in the CFL phase. It is very fundamental to know the Meissner and Debye masses of gluons in the CFL phase as well as studying their spectral densities and dispersion relations. To achieve these purposes, we have to calculate the gluon self-energy in this phase. The calculations for the dispersion relation at zero momentum have been done in the literature [138, 147]. For nonzero momentum calculations are only done for the 2SC phase [108].

From Ref. [149] we calculated explicitly the imaginary and real part of the gluon self-energy for a given momentum at all energies. Using the self-energies, we calculated the relevant spectral densities. For the magnetic gluon, we found that for values of the energy less than twice of the gap there is a light plasmon mode. Our result is in good agreement with those of [138, 147] which were done only for zero momentum. Studying the dispersion relations for the self-energies reveals that there is a minimum in the spectrum of the light plasmon which stands for the van-Hove type singularities in condensed matter physics. Also, the value of Meissner and Debye masses found by our calculations are very close (5 percent) to those found in [149, 151].

There remains, however, much to be done. First of all one has to make sure that the 2SC and the CFL phases are the real ground states of the matter and there is not any other phase which can take over. For this, one has to impose magnetic field to the A and A* phase which have high possibilities to appear in the phase diagram. If they do not show up, then the chromomagnetic instability of the gapped and gapless 2SC phase together with that of the gapless CFL phase

must be resolved [91, 92, 93]. Via the chromomagnetic instability, the Meissner squared mass for gluons of the mentioned phases become negative. Among the others, one of the possibilities to solve the problem is the light plasmon condensation. If the light plasmon condenses, then the released energy of these collective excitations might remove the chromomagnetic instability. This project is in progress. At the same time one should find Meissner and Debye squared masses of gluons in the A and A* phases. If there is not any chromomagnetic instability for these phases and if there is not any solution for the instabilities of the gapped and gapless 2SC and the gapless CFL phases, then, one of the A and A* phases which has larger pressure can be the real ground state for the interior matter of compact stars.

Chapter 5

Zusammenfassung

Stark wechselwirkende Teilchen wie Protonen und Neutronen sowie alle Mesonen und Baryonen können in kondensierter Materie vorkommen. Ihre Eigenschaften und die Eigenschaften der baryonischen Dichte werden im Prinzip durch die mikroskopische Theorie der starken Wechselwirkungen (QCD) beschrieben.

Es ist bekannt, dass Baryonen keine punktförmigen Teilchen sind. Sie haben eine typische Größe von ungefähr $1\,\mathrm{fm} = 10^{-13}\,\mathrm{cm}$. In der hoch dichten Materie werden Baryonen zwangmäßig zusammen gehalten, so dass es zu einem Überlapp kommen kann. Bei diesen Dichten werden die einzelnen Quarks durch die benachbarten Baryonen geteilt. mit der weiteren Erhöhung der Dichte werden Quarks schließlich über große Entfernungen beweglich, d.h., das spalten. In diesem Fall wird die hadronische Materie in Quarks umgesetzt.

Heutzutage glaubt man, dass Quark-Materie sich im zentralen Bereich der Neutronensterne befindet [50, 51, 52, 53, 54, 55, 56, 57, 58]. Neutronensterne sind dichte, mit dem Neutron gepackte Reste von kompakten Sternen, die in Supernova-Explosionen auslösten, Abschnitt 1.7. Fast vor Jahrzehnten wurde vorgeschlagen, dass im Kern der Neutronensterne eine farbsupraleitende Phase existieren kann [59, 60, 61, 62]. Diese Möglichkeit hat enormes Interesse in der Physik und Astrophysik der Quark-Materie ausgelöst.

Der Kern eines Neutronensterns hat eine Dichte, die um ein Vielfaches größer ist als die Dichte des nuklearen Grundzustands. Bei diesen hohen Dichten zeigt die asymptotische Freiheit [16, 17], dass die Quarks sich fast wie freie Teilchen verhalten und deshalb, große Fermi Oberflächen bilden. Wenn die Wechselwirkungen zwischen Quarks betrachtet werden, dann realisiert man, dass die wichtisten interquark Streuungsprozesse erst durch Erhaltungssätze und Fermi-Statistik möglich werden und dass diese große Impulse tragen und bei asymptotisch hohen Dichten schwach erscheinen. Erst dadurch, dass die Wechselwirkungen zwischen Quarks völlig zu vernachlässigen sind, konnte man versuchen, die thermodynamischen Eigenschaften des entsprechenden Grundzustands zu verstehen. Folglich wird die Materie aus einem Fermi-See von im Wesentlichen freien Quarks gebildet, deren Verhalten durch die freien Quarks dominiert wird, und es sind diese Quarks mit hohem Impuls, die an der Fermi Oberfläche existieren.

Die Helmholtz-Energie ist gegeben durch, $F = E - \mu N$, wobei E die Gesamtenergie des Systems ist, μ ist das chemische Potenzial der Teilchen im System, und N ist die Anzahl der Teilchen. An der Fermi Oberfläche, $E_F = \mu N$, wird die freie Energie minimiert, so dass das

Hinzufügen oder die Entnahme einzelner Teilchen keine freie Energie kostet. In Anwesenheit einer schwach attraktiven Wechselwirkung, werden ein Teilchenpaar (oder Lochpaare) geschaffen ohne, dass hierfür extra freie Energie benötigt wird. Tatsächlich hat das System ein Tendenz für solche Wechselwirkungen. In der Folge werden viele solche Paare in allen Zustandsmoden, in der Nähe von der Fermi Oberfläche gebildet, und die Paare, die jetzt bosonisch erscheinen, bilden ein Kondensat.

In der kondensierten Materie Systeme, ist die repulsiv elektrostatische Kraft, die dominierende Wechselwirkung. Es gibt mehreren Fälle, wo das System attraktiv Phonon getriebene Wechselwirkungen enthält. Gemäß der BCS-Theorie, in Anwesenheit der attraktiven Wechselwirkungen, ist die Fermi Oberfläche nicht stabil. Dann wird der wahre Grundzustand des Systems ein komplizierter kohärenter Zustand der Teilchenpaare (Elektronen oder Löcher) sein, die Cooper-Paare genannt werden. Der Grundzustand wird eine Überlagerung der Zustände sein, mit aller möglichen Anzahl der Paare. Folglich wird die elektromagnetische Gauge-Symmetrie durch Elektron Cooper-Paare gebrochen, d.h. die Symmetrie der Fermionzahl wird gebrochen. Ähnlich zu jedem System, dass zu eine spontane Symmetriebrechung führen kann, ergibt sich einer Masse für das Photon und dies führt zu Meissner-Effekt.

In QCD, ist die dominierende Wechselwirkung zwischen Quarks, selbst attraktiv [61, 62, 63, 64, 65]. Gluons spielen die Rolle von Phononen im Gitter. Die relevanten Freiheitsgrade, sind denen, die Quarks mit ihrem Impuls, nah zu der Fermi Oberfläche halten. Deshalb, bei ausreichend niedriger Temperatur, spricht alles dafür, dass eine superleitende Phase der Quarks gebildet wird. Dieser Art der Supraleitung, wird "Farbsupraleitung" (FSL) genannt. In der Farbsupraleitung, werden die anziehenden Wechselwirkungen bereits aus der primären starken Wechselwirkung hervorgerufen. Folge dessen, kann die genaue Art dieser Wechselwirkungen aus der Grundsätze Berechnet werden. Hierfür wird asymptotische Freiheit verwendet. Außerdem bei Dichten, wo die starke Wechselwirkung viel größer ist als die elektromagnetischen Wechselwirkungen, erwartet man, dass die Farbsupraleiter sehr stabil sind, wenn das Verhältnis ihre Energielücke und die Kritische Temperatur zu Fermi-Energie ziemlich groß wird [59].

Farbsupraleitung führt zu spontane Brechung der Farbe und die chirale Symmetrie. Das Spektrum der elementaren Übergänge, unterscheidet sich sehr von der naiven Störungstheorie. Im Grunde, die massenlosen Gluonen und Quarks, wird via Higgs-Mechanisme erst massiv werden und dabei entstehen neue kollektiven Moden und viele Quanten Zahlen werden modifiziert. Alle elementaren Übergänge, tragen ganzzahlige elektrostatische Ladungen. Insgesamt, findet man eine unheimliche Ähnlichkeit, zwischen Eigenschaften, die sich aus mikroskopischem Lagrangian der asymptotischen Dichten berechnen lassen und die Eigenschaften bei den neidrige Dichten, die sich auf die Phänomenologie der Hadronen basieren. Insbesonder, die traditionelle "Geheimnisse" der Anziehung und chirale Symmetriebrechung sind in ein völlig mikroskopische-, schwache Kupplung andiskutiert worden, die ein genaue physikalische und intrinsiche regime beschreiben [66, 67].

Seit längerem Zeit, ist es bekannt, dass kondensierte Quarks Materie ein Farbsupraleiter sein könnte [63, 65, 68]. Diese Fakten, werden in viele Studien vernachlässigt. Im großen Ganzen war dies ausgelöst durch Beobachtungen in Ref. [61, 62] in dem der Wert für die farbsupraleitende Lücke ungefähr $100\,\mathrm{MeV}$ beträgt. Diese gilt beim Baryonische Dichten, die sich im Zentralen Bereich einer massiven Stern befindet, d.h. bei Dichten, die ein Vielfaches der normale nuklearem Dichte sind, $n_0 \simeq 0.15\,\mathrm{fm}^{-3}$. Dieser durchaus normale Abschätzung

für die Energie Lücke in QCD, wo die typische Energie Skala 2200 MeV beträgt, eröffnete viele neue Möglichkeiten für die Theoretiker dies zu untersuchen. Das Haupt Argument hierfür ist, dass die Entstehung solcher großen Energie Lücken in Quark-Spektrum ein klares Zeichen ist für existenz eines farbsupraleitender Zustands in der Materie.

So wie in elektrische Supraleiter, die folge der Farb-Supraleitung in kondesierte Quark Materie ist die Erscheinung einer Energie-Lücke die für ein Einzelteichen-Spektrum nicht Null ist,

$$\mathcal{E}_{\mathbf{k}} = \sqrt{(E_{\mathbf{k}} - \mu)^2 + \Delta^2}, \tag{5.1}$$

wobei Δ die Lücke darstellt. Das Erscheinen von einer Lücke im Spektrum soll der Transport beinflüssen. Die Anwesenheit einer Lücke in der Energie Spektrum sollte die Transport Eigenschaften (z.B. Leitfähigkeit und Vikosität) in Quark Materie beinflüssen. Dadurch, wenn die Quark Materie im inneren der massive Sterne existieren, dann reflektiert sich das zum Beispiel in Kühlungsrate und in der Rotationsträgheit der solche Sterne. Außerdem, eine Lücke die nicht Null wird, verändert die thermodynamische Eigenschaften, z.B. die spezifische Wärme und die Zustandsgleichung. Angewendet auf Sterne, könnte dies die theoretische Vorhersage für den Masse-Radius Verhältnis verändern, oder auch die Existenz einer neuen familien des massiven Sterns andeuten.

Im Algemeinen, ist es von großr Interesse ein systematisches studium aller mögliche Wirkungen der Farb-Supraleitung in massive Sterne durch zu führen. Bevor dies ermöglicht werden kann, sollte man zuerst die Struktur der QCD Phasendiagramm und die Eigenschaften der verschiedenen Farb-Supraleitungsphasen datailliert kennen müssen. Trotz die neusten Fortschritt in diesem Gebit, bleiben solche Kentnisse noch sehr Lückehaft. Während viele verschiedene Phasen der Quark Materie sind vorgeschlagen, jedoch besteht keine sichere Aussage, dass alle möglichkeiten schon ergriffen sind. Dies ist der Fall wenn zusätzliche Voraussetzungen der Ladungsneutralität und β Gleichgewicht erfüllt sind.

In manchen Fällen, könnte die Supraleitung gleichzeitig mit der Baryon Supraflüssigkeit und/oder die magnetische Meissner Effekt existieren. Falls die Materie einer Supraflüssigkeit ist, dann enstehen rotierende Vortizes inm Stellar-Kern und werden ein Teil von dem Drehimpuls des Sterns tragen. Durch den Meissner-Effekt, kann der innere des Sterns mit magnetischen Fluß-Kanäle eingefädelt werden. In beiden Fällen, konnte die Entwicklung den Sternen beinflusst werden [69].

Die inerten Phasen sind die einzigen experimentell beobachteten Phasen der ^{3}He. Um davon gebrauch machen zu können, sind die Kentnisse über ihre Thermische Eigenschaften notwendig. Die Ähnlichen Phasen in farbsupraleitende Materie sind bereits untersucht worden. Allerdings im Falle, dass die Materie aus eines Quarktyps in Spin 1 Zustand [100] besteht. Da die "Drei-Variant" der Spin-Null CSC ein größeren Energielücke (fast 100 mahl) hat als die "Ein-Variant" Spin-Eins CSC, ist es plausiblere um hier für Beweise im inneren des Sterns zu finden. Daher ist sehr wichtig um die inerte Phase der Quarks in Grundzustand zu kennen. Da jede Phase eine typische Signatur hat, hilft uns dies Studium sehr um nach die richtige Aspekte der CSC in massive Sterne zu suchen.

Hier haben wir erst die inerte Phasen der, Spin-Null Drei-Variant CSC für massenlose Quarks beobachtet. Analog zu Ref. [123], haben wir QCD benutzt um die Ausdruck für den Phasendruck des Zustands zu ermitteln. Wir fanden, dass CFL Phasendruck gößer ist als der Restdruck in

der inerten Phase. Überraschungsweise, haben wir bemerkt, dass die sogenannte sSC Phase den zweiten Platz einnimmt in der beobachteten Phase. Das ist ein neues Ergebnis. In die sSC Phase als auch CFL Phase, alle Quarks nehmen an das Cooper-Paar-Formen teil, d.h. dass, die sSC Phase aus, $(gd - bs), (gs - bd), (ru - bs)$, und $(rs - bu)$ Paaren bestedht. Die CFL Phase besteht aus, $(gd - bs), (gs - bd), (ru - bs), (rs - bu), (ru - gd)$, und $(rd - gu)$ Paaren. Anderzeits, die 2SC Phase enthält $(ru - gd)$ und $(rd - gu)$ Paaren und sein Druck ist gleich an die A und A* Phasen. Cooper Paare in der A Phase sind $(rd - gs), (rs - gd), (ru - gs)$, und $(rs - gu)$, und die, A* Phase enthält $(gu - bd), (gd - bu), (ru - bd)$, und $(rd - bu)$ Paaren. Wir sehen, dass da kein triviale Zusammenhang, zwischen der Zahl und der Typ des Quarks besteht, die als Paare in jede Phase und Druck vorkommen. Der Grund hierfür zweifältig. Erstens im Massenlosen Zustand besteht kein echter Unterschied zwischen Quark Varianten. Der einzige Unterschied zwischen ihnen sind die Farbänderungen. Zweitens, die Anzahl der Cooer Paare in jede Phase können sich mit denen aus der andere Phase sich unterscheiden. Dies macht die analyse nicht trivial. Dabei, es ist sehr interssant zu wissen welche Phase der CSC in der Natur erkannt werden kann.

Im Moment wird das viel versprechende Farbsupraleitung in der inneren des massiven Sterns gesucht. Andererseits wissen wir, dass massive Sterne, farb- und ladungsneutral sein sollten. Deshalb um das Verhalten der CSC inerte Phasen im massiven Sterne zu studieren, sollten wir das Kriterium der farb- und ladungsneutralität einführen müssen. Das ändert der Zahl und der Typ den Quarks Teilchen, die an die Paarung teilnehmen, dadurch verschiebt sich die Fermi Energie der Quarks Teilchen beim betrachten der Neutralitätsbedingung. In diesem Fall sind der Wert der Lücke für eine besondere Paarung, die paarweise angeordneten Quarks und die frei kommense Energie der Paare, die Kriterien, um diese Quark-Paare mit ins Brechnung einzubeziehen oder auch nicht. Wenn der Unterschied zwischen die Fermi Energie von zwei Quark Teilchen größer ist als die frei kommende Energie der Paarung (Energie der Lücke), dann wird dort keine Paarung zwischen jenen Quarks und umgekehrt stattfinden. Jedoch, können dort Paare ohne Lücke erscheinen [83, 150].

Da QCD Berechnungen für das System mit massiven Quarks und die Betrachtung der Neutralitätsbedingung sehr schwierig sind, verwendeten wir das NJL-Modell. Jedoch, dort entsteht ein Problem dass, wir eine vereinfachte Berechnung zum verwenden haben. Im NJL-Modell, im Gegensatz zu QCD, verschwinden die Fräcke nicht. Das zerstört die Neutralität des Systems. Um die Symmetrie beim verwenden des NJL-Modells wieder zu herstellen, müssen wir ein relevantes chemisches Potenzial im System einführen, um die Effekten der Fräcke zu beseitigen und das System im neutralen Zustand zurückführen. Dafür, in jeder Phase, muss man nach Fräcke dieser Phase suchen.

Wenn die Fräcke den Phasen (hier der A und A* Phasen) berechnet waren, führten wir das relevante chemische Potenzial ein, um die Fräcke zu vernichten. Danach berechneten wir den Phasendruck zusammen mit der Neutralitätsbedingung. Für das höhere chemische Potenzial μ fanden wir die CFL Phase als der Grundzustand und bei gemäßigtem μ, fanden wir 2SC Phase als die dominierende Phase. Außerdem realisierten wir, dass die A* Phase die farbenumgestaltete Version der 2SC Phase ist. Für ein mindest Wer des chemischen Potenzials μ, gab es keine Möglichkeit für eine Phase, um die anderen Phasen zu übermeistern und deshalb als Grundzustand der Materie bezeichnet zu werden. Jedoch kann das große magnetische Feld von den massiven sternen das Ergebnis ändern, und es gibt noch eine Hoffnung für die A Phase,

die irgendwie auf dem QCD Phasendiagramm zu realisieren ist. Außerdem könnte das abgelegte magnetische Feld, die Entartung zwischen 2SC Phase und die A* Phase zerstören; das kann zu einem neuen Ergebnis für die A* Phase führen.

Andererseits, da die CFL Phase bis jetzt die wichtigste Phase von CSC mit großen Dichten erscheint, istes sehr interesant, die Eigenschaften der Materie in der CFL Phase zu untersuchen. Es ist sehr fundamental, die Meissner und Debye Massen der Gluonen in der CFL Phase, sowie dem Studieren ihrer spektrale Dichten und Dispersion zu wissen. Um diese Ziele zu erreichen, müssen wir die Gluon Eigen-Energie in dieser Phase berechnen. Die Berechnungen für die Dipersion bei Impuls = 0, sind in der Literatur [138, 147] berichtet worden. Für den Impuls ungleich an Null, sind nur Berechnungen für 2SC Phase [108] berichtet worden.

Aus der Referenz [149], berechneten wir das imaginäre und reale Teil der Gluon Eigen-Energie für alle Energien bei einem gegebenen Impuls. Beim verwenden der Eigen-Energien, berechneten wir die relevante Spektrale Dichten. Für den magnetischen Gluon fanden wir ein Licht Plasmon Mode, für Energiewerte zweimal kleiner als der Lücke. Unser Ergebnis ist im guten Vergleich mit Ref. [138, 147], die wir nur für den Impuls = 0, ausgeführt haben. Der Dispersionszusammenhang für die Eigen-Energie zeigt, dass es ein Minimum im Spektrum des Lichtplasmons gibt, das für die van-Hove Singularität in Festkörper Pyhsik eintritt. Außerdem sind die Werte für Meissner und Debye Massen, die durch unsere Berechnungen gefunden sind sehr nah (5 Prozent abweichung) zu den Berechneten Werte in [149, 151].

Es bleibt noch viel, was noch gemacht werden soll. Vor allem muss man sicher sein, dass 2SC und die CFL Phasen die wirklichen Grundzustände der Materie darstellen und, dass es kein jede andere Phase gibt, die überhand nehmen kann. Dafür muss man magnetisches Feld zu den Phasen A und A* anwenden, die große Möglichkeit haben in Phasediagramm zu erscheinen. Wenn es sich nicht zeigt, dann muss die chromomagnetische Instabilität der 2SC Phase mit- und ohne Lücke, zusammen mit der CFL Phase ohne Lücken [91, 92, 93] aufgelöst werden. Via die chromomagnetische Instabilität, wird die Meissner quadratierte Masse für bisher erwähnte Gluonen, negativ. Zwischen alle andern, ist die Möglichkeit via das Lichtplasmon, dieses Problem zu lösen. Wenn das Lichtplasmon kondensiert, dann kann die freiwerdende Energie der kollektiven Anregungen, die chromomagnetische Instabilität entlassen. Dieses Projekt ist im Ablauf. Gleichzeitig, sollte man nach Meissner und Debye quadratierte Gluon Massen in der A und A* Phase suchen. Wenn da kein chromomagnetische Instabilität der Phasen vorliegt und dass, da keine Lösung gibt für die Instabilität der 2SC Phase mit und ohne Lücke und die CFL Phase ohne Lücke, dann sollte man die A und A* Phasen die größere Druck enthalten als die wirkliche Grundzustand für das innere der massiven Sterne betrachten.

Bibliography

[1] H. K. Onnes, Leiden Comm. B **122** 124 (1911).

[2] J. Bardeen, L. N. Cooper, and J. R. Schrieffer, Phys. Rev. **106** 162 (1957).

[3] J. Bardeen, L. N. Cooper, and J. R. Schrieffer, Phys. Rev. **108**, 1175 (1957).

[4] B. S. Deaver, Jr., W. M. Fairbank, Phys. Rev. Lett. **7** 43 (1961).

[5] R. Doll, M. Näbauer, Phys. Rev. Lett. **7** 51 (1961).

[6] V. V. Schmidt, *The Physics of Superconductors*, 1997 (Springer).

[7] F. London and H. London (1935), Proc. R. Soc. London **A149** (71).

[8] V. L. Ginzburg and L. D. Landau, Zh. Eksp. Teor. Fiz. **20** 1064 (1950) [Sov. Phys. JETP **20** 1064 (1950)].

[9] N. N. Bogoliubov, Sov. Phys. - JETP (Engl. Transl.) ; Vol/Issue: 7:1.

[10] D. Vollhardt and P. Wölfle, *The Superfluid Phases of Helium 3*, 1990 (Taylor & Francis, London).

[11] L. N. CooperPhys. Rev. **104** 1189 (1956).

[12] V. A. Miransky, *Dynamical Symmetry Breaking in Quantum Field Theories*, 1993 (World Scientific).

[13] M. L. E. Oliphant, B. B. Kinsey, and Lord Rutherford, Proc. R. Soc. London A **141** 722 (1933).

[14] F. London, *Superfluids* Vol. I, 1950 (Wiley, New York); *Superfluids* Vol. II, 1954 (Wiley, New York).

[15] L. D. Landau, Zh. Eksp. Teor. Fiz. **30** 1058 (1956) [Sov. Phys. JETP **3** 101 (1957)]; Zh. Eksp. Teor. Fiz. **32** 59 (1957) [Sov. Phys. JETP **5** 101 (1957)].

[16] H. D. Politzer, Phys. Rev. Lett. **30** 1346 (1973).

[17] D. J. Gross and F. Wilczek, Phys. Rev. D **8** 3633 (1973); Phys. Rev. D **9** 980 (1974).

[18] T. Schäfer, [hep-ph/0304281].

[19] T. D. Lee and C. N. Yang, Phys. Rev. **105** 1119 (1957).

[20] K. Huang, C. N. Yang, Phys. Rev. **105** 767 (1957).

[21] A. A. Abrikosov, L. P. Gorkov, and I. E. Dzyaloshinski, *Methods of Quantum Field Theory in Statistical Physics*, 1963 (Prentice-Hall, Englewood Cliffs, N.J.).

[22] L. Platter, H. W. Hammer, and U. G. Meissner, Nucl. Phys. A **714** 250 (2003) [nucl-th/0208057].

[23] P. W. Higgs, Phys. Lett. **12** 132 (1964), Phys. Rev. Lett. **13** 508 (1964)

[24] M. Gell-Mann, Phys. Rev. **125** 1067 (1961).

[25] Y. Ne'man, Nucl. Phys. **26** 165 (1961).

[26] F. J. Yndúrain, *The Theory of Quark and Gluon Interactions*, 1993 (Springer).

[27] S. Bethke, [hep-ex/0211012].

[28] S. B. Rüster, V. Werth, M. Buballa, I. A. Shovkovy, and D. H. Rischke, Phys. Rev. D **72** 034004 (2005) [hep-ph/0503184].

[29] R. D. Pisarski and F. Wilczek, Phys. Rev. D **29** 338 (1984).

[30] U. M. Heller, [hep-lat/0610114].

[31] Z. Fodor, C. Guse, S. Katz, and K. Szabo, [hel-lat/0511032]; [hel-lat/0511033].

[32] see, for instance: EOS collaboration, Phys. Rev. Lett. **85** 1194 (2000), Phys. Rev. C **64** 054602 (2001), Phys. Rev. C **65** 054617 (2002); INDRA Collaboration (J.D. Frankland et al.), Nucl. Phys. A **689**905, 940 (2001); S. Das Gupta, A. Z. Mekjian, and M. B. Tsang, [nucl-th/0009033].

[33] D. H. Rischke, Prog. Part. Nucl. Phys. **52** 197 (2004) [nucl-th/0305030].

[34] M. A. Stephanov, [hep-lat/0701002].

[35] Y. Nambu and G. Jona-Lasinio, Phys. Rev. **122** 345 (1961).

[36] Y. Nambu and G. Jona-Lasinio, Phys. Rev. **124** 246 (1961).

[37] M. Buballa, Phys. Rept. **407** 205 (2005) [hep-ph/0402234].

[38] H. Kleinert, *On the Hadronization of Quark Theories*, 1978 (Plenum Press, New York).

[39] M. K. Volkov, Ann. Phys. (NY) **157** 282 (1984).

[40] T. Hatsuda, T. Kunihiro, Phys. Lett. B **145** 7 (1984).

[41] M. L. Goldberger, S. B. Treiman, Phys. Rev. **110** 1178 (1958).

[42] M. Gell-Mann, R. J. Oakes, and B. Renner, Phys. Rev. **175** 2195 (1968).

[43] N. K. Glendenning, *Compact Stars, Nuclear Physics, Particle Physics, and General Relativity*, 2000 (Springer).

[44] W. Baade, and F. Zwicky, Phys. Rev. **45** 138 (1934).

[45] S. I. A. Garpman, N. K. Glendenning, and Y. J. Karant, Nucl. Phys. A **322** 382 (1979).

[46] N. K. Glendenning, Astrophys. J. **293** 470 (1985).

[47] N. K. Glendenning, Nucl. Phys. A **493** 521 (1989).

[48] N. K. Glendenning, Phys. Lett. B **114** 392 (1982); Z. Phys. A **326** 57 (1987); ibid **327** 295 (1987).

[49] L. Zhi-cheng, L. Shao-rong, and G. Shang-hui, Act. Astrophys. Sin **5** 310 (1986).

[50] D. Ivanenko and D. F. Kurdgelaidze, Astrofiz. **1** 479 (1965); Lett. Nuovo Cim. **2** 13 (1969).

[51] N. Itoh, Prog. Theor. Phys. **44** 291 (1970).

[52] F. Iachello, W. D. Langer, and A. Lande, Nucl. Phys. A **219** 612 (1974).

[53] D. D. Ivanenko and D. F. Kurdgelaidze, Astrophys. **1** 251 (1965).

[54] H. Fritzsch, M. Gell–Mann, H. Leutwyler, Phys. Lett. B **47** 365 (1973).

[55] G. Baym, S. Chin, Phys. Lett. B **62** 241 (1976).

[56] B. D. Keister and L. S. Kisslinger, Phys. Lett. B **64** 117 (1976).

[57] G. Chapline, M. Nauenberg, Phys. Rev. D **16** 450 (1977); Ann. New York Academy of Sci. **302** 191 (1977).

[58] W. B. Fechner, P. C. Joss, Nature **274** 347 (1978).

[59] K. Rajagopal, F. Wilczek, [hep-ph/0011333].

[60] M. G. Alford, Ann. Rev. Nucl. Part. Sci. **51** 131 (2001).

[61] M. G. Alford, K. Rajagopal, and F. Wilczek, Phys. Lett. B **422** 247 (1998) [hep-ph/9711395].

[62] R. Rapp, T. Schäfer, E. V. Shuryak, M. Velkovsky, Phys. Rev. Lett. **81** 53 (1998) [hep-ph/9711396]; Ann. Phys. **280** 35 (2000).

[63] B. Barrois, Nucl. Phys. B **129** 390 (1977).

[64] B. Barrois, *Nonperturbative Effects in Dense Quark Matter*, Cal Tech PhD thesis, UMI 79-04847-mc (1979).

[65] D. Bailin and A. Love, Nucl. Phys. B **190** 175 (1981); Nucl. Phys. B **205** 119 (1982); Phys. Rep. **107** 325 (1984).

[66] M. G. Alford, K. Rajagopal, and F. Wilczek, Nucl. Phys. B **537** 443 (1999) [hep-ph/9804403].

[67] T. Schäfer, F. Wilczek, Phys. Rev. Lett. **82** 3956 (1999) [hep-ph/9811473].

[68] S. C. Frautschi, *Hadronic Matter at Extreme Energy Density*, 1980 (Plenum Press).

[69] I. A. Shovkovy, Found. Phys. **35** 1309 (2005) [nucl-th/0410091]

[70] M. G. Alford, Ann. Rev. Nucl. Part. Sci. **51** 131 (2001) [hep-ph/0102047].

[71] K. Rajagopal, E. Shuster, Phys. Rev. D **62** 085007 (2000) [hep-ph/0004074].

[72] N. Agasian, B. Kerbikov, V. Shevchenko, Phys. Rept. **320** 131 (1999) [hep-ph/9902335].

[73] D. Ebert, K. Klimenko, H. Toki, Phys. Rev. D **64** 014038 (2001) [hep-ph/0011273].

[74] J. Berges and K. Rajagopal, Nucl. Phys. B **538** 215 (1999).

[75] G. W. Carter, D. Diakonov, Phys. Rev. D **60** 016004 (1999).

[76] M. Iwasaki, T. Iwado, Phys. Lett. B **350** 163 (1995); M. Iwasaki, Prog. Theor. Phys. Suppl. **120** 187 (1995).

[77] D. T. Son, Phys. Rev. D **59** 094019 (1999) [hep-ph/9812287].

[78] R. D. Pisarski, D. H. Rischke, Phys. Rev. D **61** 051501 (2000) [nucl-th/9907041].

[79] D. J. Gross, F. Wilczek, Phys. Rev. Lett **30** 1343 (1973).

[80] M. G. Alford, K. Rajagopal, JHEP **0206** 031 (2002) [hep-ph/0204001].

[81] A. W. Steiner, S. Reddy, and M. Prakash, Phys. Rev. D **66** 094007 (2002) [hep-ph/0205201].

[82] M. Huang, P. F. Zhuang, and W. Q. Chao, Phys. Rev. D **67** 065015 (2003) [hep-ph/0207008].

[83] I. A. Shovkovy, M. Huang, Phys. Lett. B **564** 205 (2003) [hep-ph/0302142]; Nucl. Phys. A **729** 835 (2003) [hep-ph/0307273].

[84] M. G. Alford, C. Kouvaris, and K. Rajagopal, Phys. Rev. Lett. **92** 222001 (2004) [hep-ph/0311286].

[85] P. Amore, M. C. Birse, J. A. McGovern, and N. R. Walet, Phys. Rev. D **65** 074005 (2002).

[86] M. Huang, I. A. Shovkovy, Nucl. Phys. A **729** 835 (2003).

[87] S. B. Rüster, I. A. Shovkovy, and D. H. Rischke, Nucl. Phys. A **743** 127 (2004) [hep-ph/0405170].

[88] A. I. Larkin, Y. N. Ovchinnikov, Zh. Eksp. Teor. Fiz. **47** 1136 (1964) [Sov. Phys. JETP. **20** 762 (1965)].

[89] P. Fulde, R. A. Ferrell, Phys. Rev. A **135** 550 (1964).

[90] K. Fukushima, C. Kouvaris, and K. Rajagopal, Phys. Rev. D **71** 034002 (2005) [hep-ph/0408322].

[91] M. Huang, I. A. Shovkovy, Phys. Rev. D **70** 051501(R) (2004) [hep-ph/0407049]; Phys. Rev. D **70** 094030 (2004), [hep-ph/0408268].

[92] R. Casalbuoni, R. Gatto, M. Mannarelli, G. Nardulli, and M. Ruggieri, Phys. Lett. B **605** 362 (2005) [hep-ph/0410401].

[93] M. G. Alford, Q. H. Wang, J. Phys. G **31** 719 (2005) [hep-ph/0501078].

[94] M. Kitazawa, D. H. Rischke, and Igor A. Shovkovy, Phys. Lett. B **637** 367 (2006) [hep-ph/0602065].

[95] T. Schäfer, Phys. Rev. Lett. **85** 5531 (2000) [nucl-th/0007021].

[96] P. F. Bedaque, T. Schäfer, Nucl. Phys. A **697** 802 (2002) [hep-ph/0105150].

[97] D. Kaplan, S. Reddy, Phys. Rev. D **65** 054042 (2002) [hep-ph/0107265].

[98] A. Kryjevski, Phys. Rev. D **68** 074008 (2003)[hep-ph/0305173].

[99] L. Michel, Rev. Mod. Phys. **52** 617 (1980).

[100] A. Schmitt, *Ph.D. thesis* [nucl-th/0405076].

[101] K. Rajagopal, A. Schmitt, Phys. Rev. D **73** 045003 (2006) [hep-ph/0512043].

[102] H. Malekzadeh, Phys. Rev. D **74** 065011 (2006) [hep-ph/0604260].

[103] J. M. Cornwall, R. Jackiw, and E. Tomboulis, Phys. Rev. D **10** 2428 (1974).

[104] T. Fugleberg, Phys. Rev. D **67** 034013 (2003).

[105] R. D. Pisarski, D. H. Rischke, Phys. Rev. D **60** 094013 (1999) [nucl-th/9903023].

[106] Q. Wang, D. H. Rischke, Phys. Rev. D **65** 054005 (2002).

[107] C. Manuel, Phys. Rev. D **62** 114008 (2000).

[108] D. H. Rischke, Phys. Rev. D **64** 094003 (2001) [nucl-th/0103050].

[109] A. Schmitt, Q. Wang, and D. H. Rischke, Phys. Rev. D **66** 114010 (2002) [nucl-th/0209050].

[110] S. B. Rüster, D. H. Rischke, Phys. Rev. D **69** 045011 (2004).

[111] H. Abuki, Prog. Theor. Phys. **110** 937 (2003).

[112] S. B. Rüster, V. Werth, M. Buballa, I. A. Shovkovy, and D. H. Rischke, Phys. Rev. D **73** 034025 (2006) [hep-ph/0509073].

[113] D. G. Dumm, D. B. Blaschke, A. G. Grunfeld, and N. N. Scoccola, Phys. Rev. D **73** 114019 (2006) [hep-ph/0512218].

[114] A. Gerhold, A. Rebhan, Phys. Rev. D **68** 011502 (2003) [hep-ph/0305108].

[115] R. Kobes, G. Kunstatter, and A. Rebhan, Phys. Rev. Lett. **64** 2992 (1990); Nucl. Phys. B **355** 1 (1991); A. Rebhan, Lect. Notes Phys. **583** 161 (2002).

[116] D. D. Dietrich, D. H. Rischke, Prog. Part. Nucl. Phys. **53** 305 (2004) [nucl-th/0312044].

[117] M. Buballa, I. A. Shovkovy, Phys. Rev. D **72** 097501 (2005) [hep-ph/0508197].

[118] J. Polchinski, [hep-th/9210046].

[119] M. Buballa, M. Oertel, Nucl. Phys. A **703** 770 (2002).

[120] F. Gastineau, R. Nebauer, and J. Aichelin, Phys. Rev. C **65** 045204 (2002).

[121] T. M. Schwarz, S. P. Klevansky, and G. Papp, Phys. Rev. C **60** 055205 (1999).

[122] P. Rehberg, S. P. Klevansky, and J. Hüfner, Phys. Rev. C **53** 410 (1996) [hep-ph/9506436].

[123] A. Schmitt, Phys. Rev. D **71** 054016 (2005) [nucl-th/0412033].

[124] H. Malekzadeh, D. H. Rischke, Phys.Rev. D **73** 114006 (2006) [hep-ph/0602082].

[125] J. R. Schrieffer, *Theory of Superconductivity* (New York, W.A. Benjamin, 1964).

[126] A. L. Fetter, J. D. Walecka, *Quantum Theory of Many-Particle Systems* 1971 (McGraw–Hill, New York).

[127] R. D. Pisarski, D. H. Rischke, Phys. Rev. Lett **83** 37 1999 [nucl-th/9811104].

[128] R. D. Pisarski, D. H. Rischke, Phys. Rev. D **61** 074017 (2000) [nucl-th/9910056].

[129] M. Le Bellac, *Thermal Field Theory* 1996 (Cambridge, Cambridge University Press).

[130] T. Schäfer, F. Wilczek, Phys. Rev. D **60** 114033 (1999) [hep-ph/9906512].

[131] N. Evans, S. Hsu, M. Schwetz, Phys. Lett. B **449** 281 (1999) [hep-ph/9810514]; Nucl. Phys. B **551** 275 (1999) [hep-ph/9808444].

[132] M. Huang, P. F. Zhuang, and W. Q. Chao, Phys. Rev. D **65** 076012 (2002).

[133] D. K. Hong, V. A. Miransky, I. A. Shovkovy, and L. C. R. Wijewardhana, Phys. Rev. D **61** 056001 (2000); Erratum-ibid. D **62** 059903 (2000).

[134] W. E. Brown, J. T. Liu, H. Ren, Phys. Rev. D **61** 114012 (2000); Phys. Rev. D **62** 054016 (2000); Phys. Rev. D **62** 054013 (2000).

[135] S. D. H. Hsu, M. Schwetz, Nucl. Phys. B **572** 211 (2000) [hep-ph/9908310].

[136] R. D. Pisarski, Physica A **158** 146 (1989).

[137] D. H. Rischke, Phys. Rev. D **62** 034007 (2000) [nucl-th/0001040].

[138] I. A. Shovkovy, L.C.R. Wijewardhana, Phys. Lett. B **470** 189 (1999) [hep-ph/9910225].

[139] K. Zarembo, Phys. Rev. D **62** 054003 (2000) [hep-ph/0002123].

[140] R. D. Pisarski, D. H. Rischke, Proc. of *QM'99 conference* [nucl-th/9906050].

[141] D. H. Rischke, I. A. Shovkovy, Phys. Rev. D **66** 054019 (2002) [nucl-th/0205080].

[142] V. A. Miransky, I. A. Shovkovy, and L. C. R. Wijewardhana, Phys. Lett. B **468** 270 (1999) [hep-ph/9908212].

[143] R. Casalbuoni, Z. Duan, and F. Sannino, Phys. Rev. D **62** 094004 (2000) [hep-ph/0004207].

[144] V. A. Miransky, I. A. Shovkovy, and L. C. R. Wijewardhana, Phys. Rev. D **64** 096002 (2001) [hep-ph/0104194].

[145] T. Schäfer, Nucl. Phys. B **575** 269 (2000) [hep-ph/9909574].

[146] V. P. Gusynin, I. A. Shovkovy, Nucl. Phys. A **700** 577 (2002) [hep-ph/0108175].

[147] R. Casalbuoni, R. Gatto, and G. Nardulli, Phys. Lett. B **498** 179 (2001); Erratum ibid. B **517** 483 (2001).

[148] K. Fukushima, K. Iida, Phys. Rev. D **71** 074011 (2005) [hep-ph/0501276].

[149] D. H. Rischke, Phys. Rev. D **62** 054017 (2000) [nucl-th/0003063].

[150] M. Alford, J. Berges, K. Rajagopal, Phys. Rev. Lett. **84** 598 (2000).

[151] D. T. Son, M. A. Stephanov, Phys. Rev. D **61** 074012 (2000).